MJHS Moldovan Journal of Health Sciences
REVISTA DE ȘTIINȚE ALE SĂNĂTĂȚII DIN MOLDOVA
Vol. 12
Issue 3,
Septembrie 2025
Category B

CONTENT HIGHLIGHTS:

Grigore Tinică, Mihail Enache, Andrei Țărus,
Silviu Stoleriu, Alberto Bacuşcă
The Tirone David procedure in acute type A aortic dissection – when, how, and why? The experience of Professor Dr. George I.M. Georgescu Institute of Cardiovascular Diseases

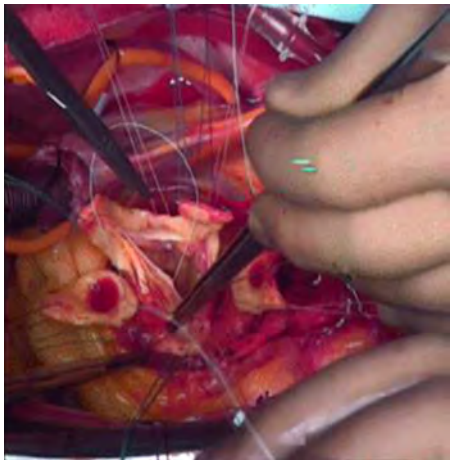

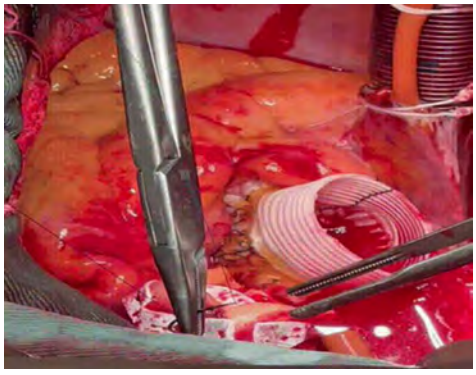

ISSN: 2345-1467
e-ISSN: 1857-4696

2.5 mg, N56 10mg, 15 mg, 20 mg, N28

KARDATUXAN®

RIVAROXABAN, COMPRIMATE FILMATE

Asigură un flux continuu

Opțiunea GEDEON RICHTER, KARDATUXAN este inhibitor direct, cu selectivitate crescută, al factorului Xa , cu biodisponibilitate orală.

- **debut rapid al acțiunii**
- **nivel scăzut al riscului de sângerare**
- **previne eficient accidentul vascular cerebral, embolia sistemică, tromboza venoasă profundă și trombembolismul pulmonar**

Denumirea comercială a medicamentului: KARDATUXAN 2,5 mg comprimate filmate. KARDATUXAN 10 mg comprimate filmate. KARDATUXAN 15 mg comprimate filmate. KARDATUXAN 20 mg comprimate filmate. **Compoziția calitativă și cantitativă:** KARDATUXAN 2,5 mg: fiecare comprimat filmat conține: rivaroxaban 2,5 mg. KARDATUXAN 10 mg: fiecare comprimat filmat conține: rivaroxaban 10 mg. KARDATUXAN 15 mg: fiecare comprimat filmat conține: rivaroxaban 15 mg. KARDATUXAN 20 mg: fiecare comprimat filmat conține: rivaroxaban 20 mg. **Indicații terapeutice:** KARDATUXAN 2,5 mg: Kardatuxan, administrat concomitent doar cu acid acetilsalicilic (AAS) sau cu AAS plus clopidogrel sau ticlopidină, este indicat pentru prevenirea evenimentelor aterotrombotice la pacienții adulți după un sindrom coronarian acut (SCA) cu valori crescute ale biomarkerilor cardiaci.Kardatuxan, administrat concomitent cu acid acetilsalicilic (AAS), este indicat pentru prevenirea evenimentelor aterotrombotice la pacientii adulți care prezintă boală arterială coronariană (BAC) sau boală arterială periferică simptomatică (BAP) cu risc crescut de evenimente ischemice. KARDATUXAN 10 mg: Prevenirea tromboemboliei venoase (TEV) la pacienții adulți care sunt supuși unei intervenții chirurgicale elective pentru substituția șoldului sau a genunchiului.Tratamentul trombozei venoase profunde (TVP) și al emboliei pulmonare (EP) și prevenirea recurenței TVP și a EP la adulți. KARDATUXAN 15 mg: *Adulți:* Prevenirea accidentului vascular cerebral și a emboliei sistemice la pacienții adulți cu fibrilație atrială non-valvulară cu unul sau mai mulți factori de risc, cum sunt insuficiența cardiacă congestivă, hipertensiunea arterială, vârsta ≥75 ani, diabetul zaharat, accidentul vascular cerebral sau atacul ischemic tranzitoriu în antecedente. Tratamentul trombozei venoase profunde (TVP) și al emboliei pulmonare (EP) și prevenirea recurenței TVP și a EP la adulți. *Copii și adolescenți:*Tratamentul tromboemboliei venoase (TEV) și prevenirea recurenței TEV la copii și adolescenți cu vârsta mai mică de 18 ani și cu greutatea cuprinsă între 30 kg și 50 kg după cel puțin 5 zile de la tratamentul anticoagulant parenteral inițial. KARDATUXAN 20 mg: *Adulți:* Prevenirea accidentului vascular cerebral și a emboliei sistemice la pacienții adulți cu fibrilație atrială non-valvulară cu unul sau mai mulți factori de risc, cum sunt insuficiența cardiacă congestivă, hipertensiunea arterială, vârsta ≥75 ani, diabetul zaharat, accidentul vascular cerebral sau atacul ischemic tranzitoriu în antecedente. Tratamentul trombozei venoase profunde (TVP) și al emboliei pulmonare (EP) și prevenirea recurenței TVP și a EP la adulți. *Copii și adolescenți:* Tratamentul tromboemboliei venoase (TEV) și prevenirea recurenței TEV la copii și adolescenți cu vârsta mai mică de 18 ani și cu greutatea peste 50 kg după cel puțin 5 zile de la tratamentul anticoagulant parenteral inițial. **Contraindicații:** KARDATUXAN 2,5 mg, 10 mg, 15 mg, 20 mg: Hipersensibilitate la substanța activă sau la oricare dintre excipienți; Hemoragie activă, semnificativă din punct de vedere clinic; Leziune sau afecțiune considerată a prezenta un risc semnificativ de sângerare majoră. Aceasta poate include ulcerația gastrointestinală curentă sau recentă, prezența neoplasmelor maligne cu risc crescut de sângerare, leziune recentă la nivelul creierului sau măduvei spinării, intervenție chirurgicală recentă cerebrală, spinală sau oftalmică, hemoragie intracraniană recentă, varice esofagiene cunoscute sau suspectate, malformații arterio-venoase, anevrism vascular sau anormalități vasculare intraspinale sau intracerebrale majore;Tratament concomitent cu orice alte anticoagulante, de exemplu, heparină nefracționată, heparină cu greutate moleculară mică (enoxaparina, dalteparina, etc.), derivate de heparină (fondaparina, etc.), anticoagulante orale (warfarina, dabigatran etexilat, apixaban etc.) exceptând situațiile specifice de schimbare a tratamentului anticoagulant sau când heparina nefracționată este administrată la dozele necesare pentru a menține deschis un cateter venos central sau arterial; Tratament concomitent al SCA cu terapie antiplachetară la pacienții cu accident vascular cerebral anterior sau accident ischemic tranzitoriu (AIT); Tratament concomitent al BAC/BAP cu AAS la pacienții cu accident vascular hemoragic sau lacunar în antecedente sau cu orice accident vascular cerebral în interval de o lună; Afecțiune hepatică asociată cu coagulopatie și risc hemoragic relevant din punct de vedere clinic, incluzând pacienții cu ciroză clasele B și C ale sistemului de clasificare Child Pugh; Sarcina și alăptarea.**Atenționări și precauții speciale pentru utilizare:** KARDATUXAN 2,5 mg: La pacienții cu SCA, eficacitatea și siguranța rivaroxaban 2,5 mg de două ori pe zi au fost investigate în administrare concomitentă cu medicamentele antiplachetare AAS în monoterapie sau AAS plus clopidogrel/ticlopidină.La pacienții cu BAC/BAP cu risc crescut de evenimente ischemice, eficacitatea și siguranța rivaroxaban 2,5 mg de două ori pe zi au fost investigate în asociere cu AAS. La pacienți după procedura recentă de revascularizare a membrului inferior din cauza BAP simptomatice, eficacitatea și siguranța rivaroxaban 2,5 mg de două ori pe zi au fost investigate în asociere cu medicamentul antiplachetar AAS în monoterapie sau AAS plus clopidogrel pe termen scurt. Dacă este necesar, tratamentul combinat antiplachetar cu clopidogrel trebuie să fie de scurtă durată; tratamentul combinat antiplachetar pe termen lung trebuie evitat. KARDATUXAN 10 mg, 15 mg, 20 mg: Se recomandă supravegherea din punct de vedere clinic pe toată durata perioadei de tratament. Risc hemoragic: pacienții trebuie monitorizați cu atenție pentru semnele de sângerare. Se recomandă să fie utilizat cu precauție în condiții cu risc crescut de hemoragie. Administrarea Kardatuxan trebuie întreruptă dacă apare hemoragie severă. Alți factori de risc hemoragic: rivaroxaban nu este recomandat la pacienți cu risc crescut de sângerare. Pacienți cu proteze valvulare:Rivaroxaban nu trebuie utilizat pentru tromboprofilaxie la pacienții care au trecut recent printr-o inlocuire percutanată de valvă aortică (TAVI).Pacienți cu sindrom antifosfolipidic: Rivaroxaban nu sunt recomandate la pacienții cu antecedente de tromboză, care sunt diagnosticați cu sindrom antifosfolipidic.Pacienții cu EP instabili hemodinamic sau pacienți care necesită tromboliză sau embolectomie pulmonară: Kardatuxan nu este recomandat ca alternativă la heparina nefracționată la pacienții cu embolie pulmonară care sunt instabili hemodinamic sau care pot beneficia de tromboliză sau embolectomie pulmonară, deoarece siguranța și eficacitatea rivaroxaban nu au fost stabilite în aceste situații clinice. KARDATUXAN 10 mg: Recomandări privind dozele înainte și după proceduri invazive și intervenții chirurgicale, altele decât intervențiile chirurgicale elective pentru substituția șoldului sau a genunchiului: Dacă este necesară o procedură invazivă sau o intervenție chirurgicală, trebuie oprită administrarea Kardatuxan 10 mg cu cel puțin 24 ore înainte de intervenție, dacă este posibil, precum și în funcție de opinia clinică a medicului. Dacă procedura nu poate fi amânată, trebuie evaluat riscul de sângerare comparativ cu gradul de urgență al intervenției. KARDATUXAN 15 mg, 20 mg: Recomandări privind dozele înainte și după proceduri invazive și intervenții chirurgicale: Dacă este necesară o procedură invazivă sau o intervenție chirurgicală, trebuie oprită administrarea Kardatuxan 15 mg sau Kardatuxan 20 mg cu cel puțin 24 ore înainte de intervenție, dacă este posibil, precum și în funcție de opinia clinică a medicului. Dacă procedura nu poate fi amânată, trebuie evaluat riscul de sângerare comparativ cu gradul de urgență al intervenției. **Reacții adverse:** KARDATUXAN 2,5 mg, 10 mg, 15 mg, 20 mg: Reacțiile adverse raportate cel mai frecvent la pacienții la care se administrează rivaroxaban au fost hemoragiile. Hemoragiile raportate cel mai frecvent au fost epistaxisul (4,5%) și hemoragia de tract gastrointestinal (3,8%). Frecvente (≥1/100 și <1/10): Anemie (inclusiv parametri de laborator corespunzători); Amețeli, cefalee; Hemoragie oculară (inclusiv hemoragie conjunctivală); Hipotensiune arterială, hematom; Epistaxis, hemoptizie; Sângerare gingivală, hemoragie la nivelul tractului gastrointestinal (inclusiv hemoragie rectală), dureri gastrointestinale și abdominale, dispepsie, greață, constipație, diaree, vărsături; Creștere a valorilor serice ale transaminazelor; Prurit (inclusiv cazuri mai puțin frecvente de prurit generalizat), erupție cutanată tranzitorie, echimoză, hemoragie cutanată și subcutanată; Dureri la nivelul extremităților; Hemoragie la nivelul tractului urogenital (inclusiv hematurie și menoragie), insuficiență renală (inclusiv creșterea creatininei serice, creșterea ureei serice); Febră, edem periferic, scădere a tonusului general și a energiei (inclusiv fatigabilitate și astenie); Hemoragie după o procedură (inclusiv anemie postoperatorie și hemoragie la nivelul plăgii), contuzie, secreții la nivelul plăgii. **Data și numărul autorizației de punere pe piață:** 2,5 mg - Nr.29430; 10 mg –Nr. 29431; 15 mg – Nr.29432; 20 mg – Nr.29433 din 30.11.2023. **Statutul legal:** cu prescripție medicală. **Data revizuirii textului:** Aprilie 2024. *Acest material publicitar este destinat persoanelor calificate să prescrie, să distribuie și/sau să elibereze medicamente. Pentru informații complete vă rugăm să consultați rezumatul caracteristicilor produsului. Informații detaliate privind acest medicament sunt disponibile pe site-ul Agenției Medicamentului și Dispozitivelor Medicale (AMDM) http://nomenclator.amdm.gov.md/*

GEDEON RICHTER

Societatea pe Acțiuni de Tip Deschis Fabrica de Produse Chimice "GEDEON RICHTER" Budapesta, Sucursala Chișinău, str. A. Pușkin, 47/1, bl. A, of.1; Tel.: (022) 22-14-49; (022) 22-26-71; www.gedeonrichter.md
Pentru mesaje de siguranță și informații medicale: e-mail: drugsafety.md@gedeonrichter.com sau tel.: (022) 20-21-90.

MJHS
Moldovan Journal of Health Sciences
Revista de Ştiinţe ale Sănătăţii din Moldova
2025;12(3)

CONTENT

RESEARCH ARTICLES

Moldovan Journal of Health Sciences
Revista de Ştiinţe ale Sănătăţii din Moldova

Ediţie în limba engleză

Fondator:
Instituţia Publică Universitatea de Stat de Medicină şi Farmacie „Nicolae Testemiţanu" din Republica Moldova

Redactor-şef:
Serghei Popa, dr. şt. med. conferenţiar universitar.

Colectivul redacţiei:
Dorian Sasu, redactor stilist
Sergiu Iacob, redactor stilist
Ana Orlic, redactor stilist
Irina Gangan, redactor

Adresa redacţiei:
biroul 303, blocul Administrativ, Universitatea de Stat de Medicină şi Farmacie „Nicolae Testemiţanu" bd. Ştefan cel Mare şi Sfânt, 165, Chişinău, Republica Moldova, MD-2004

Editat: Editura „Lexon-Prim"
Tiraj: 200 ex.

Înregistrată la Ministerul Justiţiei al Republicii Moldova (nr. 250 din 01.08.2014).

Categoria B acordată de Agenţia Naţională de Asigurare a Calităţii în Educaţie şi Cercetare (decizia nr. 2 din 04.11.2022)

English edition

Founder:
Public Institution *Nicolae Testemitanu* State University of Medicine and Pharmacy from Republic of Moldova

Editor-in-chief:
Serghei Popa, PhD.
university associate professor.

Editorial staff:
Dorian Sasu, editor
Sergiu Iacob, editor
Ana Orlic, editor
Irina Gangan, editor

Address of Editorial Office:
office 303; Administrative building, *Nicolae Testemitanu* State University of Medicine and Pharmacy
165, Ştefan cel Mare şi Sfânt blvd., Chisinau, Republic of Moldova, MD-2004

EDITORIAL BOARD

https://doi.org/10.52645/MJHS.2025.3.01

UDC: 616.132-089.843

RESEARCH ARTICLES

The Tirone David procedure in acute type A aortic dissection – when, how, and why? The experience of Professor Dr. George I.M. Georgescu Institute of Cardiovascular Diseases

Grigore Tinică[1,2,3], Mihail Enache[1,2], Andrei Țărus[1,2], Silviu Stoleriu[1,2], Alberto Bacuşcă[1,2]

[1]*Grigore T. Popa* University of Medicine and Pharmacy Iași, Romania

[2]*Professor Dr. George I.M. Georgescu* Institute of Cardiovascular Diseases, Iasi, Romania

[3]*Nicolae Testemițanu* State University of Medicine and Pharmacy, Chișinău, Republic of Moldova

ABSTRACT

Introduction. Acute type A aortic dissection represents a life-threatening cardiovascular emergency with catastrophic natural history and extremely high mortality in the absence of prompt surgical intervention. Over the last decades, surgical management has evolved from supracoronary replacement and composite root replacement (Bentall procedure) towards valve-sparing strategies, among which the Tirone David reimplantation procedure has gained increasing acceptance.

Material and methods. We performed a single-center, retrospective observational study at the *Professor Dr. George I.M. Georgescu* Institute of Cardiovascular Diseases, Iasi, Romania, reviewing all patients undergoing surgery for acute type A aortic dissection over a 25-year period (January 2000 – January 2025). According to intraoperative anatomy and hemodynamic status, patients were treated with one of the following strategies: supracoronary ascending aortic replacement (with or without valve replacement), composite root replacement (Bentall), or valve-sparing aortic root replacement (Tirone David).

Results. A total of 256 patients were operated for acute type A aortic dissection. Mean age was 55.8 years, with male predominance (69%). Hypertension was the most frequent risk factor (75%), and severe aortic regurgitation was present in 48% of cases. Valve-sparing root replacement was performed in 73% of patients (84% in the last 4 years), of which 16% were Tirone David procedures. Operative mortality was 13.7%, with a favorable downward trend over time. The most common complications were acute renal failure (21.5%, with hemodialysis in 16.8%), atrial fibrillation (18%), infectious complications (14-17%), neurological events (9.9%), and re-exploration for bleeding (11.3%). Median ICU stay was 9.8 days, and median hospital stay 17 days.

Conclusions. In carefully selected patients with repairable cusps and reconstructable aortic root, the Tirone David procedure is our operation of choice, providing preservation of physiological hemodynamics and avoidance of lifelong anticoagulation. The Bentall operation remains indicated for irreparable valves, severely fragile tissue, or critical hemodynamic instability, where procedural simplicity and predictability are paramount. Our institutional experience demonstrates that the Tirone David procedure is feasible and safe in the acute setting, with encouraging early outcomes and a trend toward improved survival.

Keywords: Tirone David procedure, valve-sparing aortic root replacement, type A acute aortic dissection, aortic root surgery, emergency cardiac surgery.

Cite this article: Tinică G, Enache M, Țărus A, Stoleriu S, Bacuşcă A. The Tirone David procedure in acute type A aortic dissection – when, how, and why? The experience of Professor Dr. George I.M. Georgescu Institute of Cardiovascular Diseases. Mold J Health Sci. 2025;12(3):3-11. https://doi.org/10.52645/MJHS.2025.3.01.

Manuscript received: 31.07.2025

Accepted for publication: 30.08.2025

Published: 15.09.2025

***Corresponding author**: **Grigore Tinică,** MD, PhD, university professor, academician

Key messages

What is not yet known on the issue addressed in the submitted manuscript

The optimal role and timing of the Tirone David procedure in the emergency setting of acute type A aortic dissection remain contro-

Professor Dr. George I.M. Georgescu Institute of Cardiovascular Diseases, Carol I 50 blvd, Iași 700503, Romania
e-mail: grigoretinica@yahoo.com

Authors' ORCID IDs
Grigore Tinică – https://orcid.org/0000-0002-1755-9674
Mihail Enache – https://orcid.org/0000-0003-3133-3900
Andrei Țărus – https://orcid.org/0000-0001-9428-0637
Silviu Stoleriu – https://orcid.org/0009-0003-3905-919X
Alberto Bacuşcă – https://orcid.org/0000-0002-8965-4072

versial. While elective series have demonstrated excellent long-term durability, evidence in acute dissections is still limited, particularly regarding patient selection and perioperative safety.

The research hypothesis

We hypothesized that in carefully selected patients with repairable cusps and reconstructable aortic roots, the Tirone David procedure can be performed safely in the acute setting, offering outcomes comparable to conventional root replacement while preserving valve function.

The novelty added by the manuscript to the already published scientific literature

This study reports one of the largest single-center experiences in Eastern Europe with valve sparing procedures for acute type A dissection, spanning 25 years. It demonstrates the feasibility and safety of valve-sparing root replacement in emergencies, highlights favorable early outcomes, and supports the trend toward wider adoption of this technique in appropriately selected patients.

Introduction

Acute type A aortic dissection is a major cardiovascular emergency characterized by separation of the aortic wall layers with the formation of a false lumen, leading to rapid compromise of perfusion to vital organs. This condition follows a fulminant course and carries an extremely high mortality in the absence of timely intervention. Studies have shown that mortality approaches 50% within the first 48 hours and may reach up to 90% at 30 days if surgery is not performed [1]. The natural history of type A aortic dissection is catastrophic, and the 2024 EACTS/STS guidelines recommend urgent surgical intervention in nearly all patients [2].

The etiology of acute aortic dissection is most often related to uncontrolled hypertension, responsible for approximately 70% of cases [3]. The remaining 30% are attributed to factors such as pre-existing aortic aneurysms, connective tissue disorders (e.g., Marfan syndrome, Ehlers–Danlos syndrome), or thoracic trauma [4]. Although traditionally considered a disease of the elderly, recent years have seen an increasing incidence in younger patients. Recent data indicate that nearly 45% of individuals diagnosed with acute aortic dissection are under 60 years of age [4, 5]. These findings highlight the importance of maintaining a high index of clinical suspicion, prompt use of diagnostic imaging, and rapid multidisciplinary intervention to reduce morbidity and mortality associated with this critical pathology.

Nevertheless, diagnosis of aortic dissection is often delayed, which negatively influences clinical outcomes and prognosis. Differential diagnosis is challenging, with nearly half of patients initially misdiagnosed and approximately one-third receiving inappropriate treatment, most often for acute coronary syndrome due to overlapping clinical presentations [6]. According to the IRAD registry, perioperative mortality has declined with the adoption of modern standardized strategies, including careful selection for root replacement and the use of valve-sparing techniques, decreasing from 25% to 18% [7].

Several surgical strategies are available for type A aortic dissection, ranging from valve preservation to valve replacement. The choice depends on valve status, the extent of root involvement, patient profile, and a careful balance between the risks of extensive repair and the potential need for complex reintervention. Proximal treatment has evolved from supracoronary replacement with or without valve replacement (Wheat) to composite graft replacement of both the root and valve (Bentall), and more recently to valve-sparing techniques, such as remodeling (Yacoub) and reimplantation (Tirone David) [8].

According to contemporary guidelines, complete root with valve replacement is recommended in acute type A aortic dissection when the intimal tear is located at the root, in the presence of significant tissue fragility, or when the aortic valve is irreparable, while valve-sparing root replacement remains a reasonable option in carefully selected patients, provided the surgery is performed in centers with appropriate expertise [9]. Similarly, the 2024 ACC/AHA guidelines emphasize that the decision between valve-sparing root replacement and the Bentall procedure should be individualized based on cusp integrity, the extent of root involvement, and the surgical expertise of the treating center [10].

Tirone David introduced the technique of aortic root reconstruction with valve preservation in the early 1990s. Initially applied in the elective surgery of ascending aortic aneurysms, the technique was subsequently extended to acute type A aortic dissection [11, 12]. The Tirone David procedure is indicated when the cusps are normal or repairable (without significant calcification or degeneration), and the root, although dissected or dilated, can be reconstructed within a prosthetic graft to restore geometry. It is preferred in younger patients, in those with connective tissue disorders, or with a repairable bicuspid valve; however, it requires sufficient hemodynamic stability and institutional expertise [12].

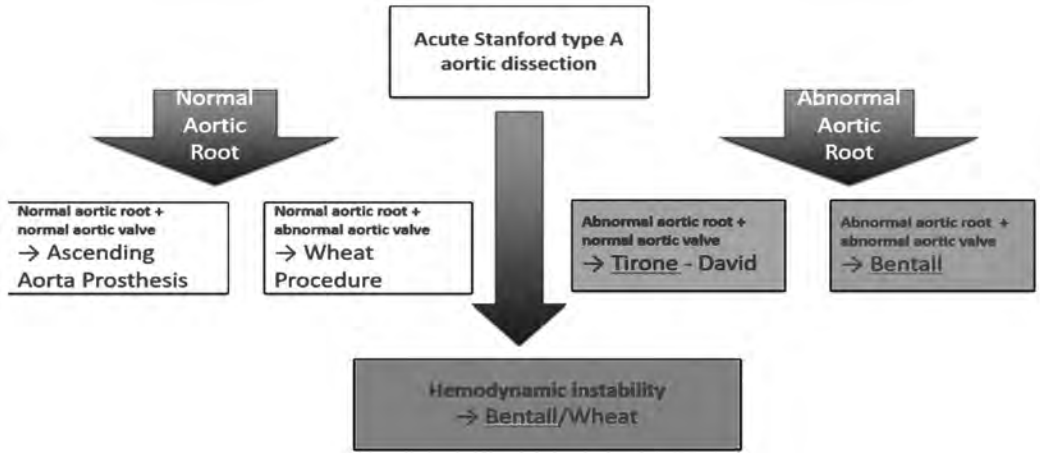

Fig. 1 Decisional algorithm.

The Bentall procedure is generally preferred when the aortic valve is deemed irreparable, such as in the presence of extensive calcification, cusp destruction, or severe prolapse. It is also indicated when the aortic root exhibits major structural loss or a dissecting extension that precludes reliable reconstruction, as well as in critically ill patients where operative simplicity and time efficiency are paramount [8].

In contrast, the Wheat procedure offers an alternative in situations where the valve must be replaced but the aortic root can be preserved. By maintaining the root, proximal anastomosis time is reduced, making this option particularly useful in unstable patients with favorable proximal anatomy, when the dissection is confined to the ascending aorta with an intact root and progressive dilatation is not anticipated [12].

Table 1. Comparative indications: Tirone David vs Bentall.

	Tirone David	Bentall
Aortic valve status	Anatomically normal valve or with minimal repairable lesions; no significant calcification/degeneration	Irreparable valve: calcified, severe stenosis, destroyed cusps, massive prolapse, or irreparable regurgitation
Root involvement in dissection	Affected/dilated root, but coaptation can be restored within a prosthetic graft (favorable geometry)	Root with major structural destruction or anatomically impossible to reconstruct
Patient profile	Young patient, long life expectancy; priority to avoid lifelong anticoagulation and preserve physiological hemodynamics	Critically ill patient where procedural simplicity and rapidity are essential, or where anticoagulation is not a concern
Connective tissue disorders (Marfan / Loeys–Dietz)	Preferred if valve is repairable; good results in experienced centers	Standard when the valve is compromised or anatomy unfavorable for reconstruction
Bicuspid aortic valve	Repairable bicuspid valve (favorable commissural/geometry relationships)	Irreparable or extensively calcified bicuspid valve
Perioperative priorities	Recommended when patient's condition allows a more complex procedure and expertise is available for Tirone David	Preferred when a rapid/standardized solution is required (shock, visceral/neurological ischemia) or the team lacks experience
Postoperative anticoagulation	Avoided (native valve preserved); advantageous in patients at risk of bleeding or with contraindications to anticoagulation	Required if a mechanical prosthesis is used; biological prosthesis possible but with lower durability
Surgeon's expertise	Requires high expertise in valve and root surgery; outcomes depend on center's volume and experience	Standardized technique, shorter learning curve, applicable in most centers

Material and methods

This is a single-center, retrospective observational study conducted at the *Prof. Dr. George I.M. Georgescu* Institute of Cardiovascular Diseases "" in Iași (IBCV Iași), a national reference center for cardiovascular surgery in Romania. The analysis included all cases of acute type A aortic dissection treated surgically at this institution over a 25-year period, from January 2000 to January 2025, providing a large and valuable dataset of clinical and operative information.

Depending on the anatomical and hemodynamic characteristics of each case, as well as the evolution of therapeutic protocols over time, patients were managed using one of the following surgical strategies:

- **Aortic root replacement with a valved conduit (Bentall procedure)**, the standard technique in cases where both the aortic valve and root were compromised by dissection or severe aneurysmal dilatation;
- **Valve-sparing aortic root replacement (Tirone David procedure)**, applied especially in younger patients or those with a competent tricuspid aortic valve, in order to preserve native valve function and avoid prosthetic valve implantation;

- **Segmental replacement of the ascending aorta**, indicated when the dissection was confined to this segment without root or valve involvement;
- **Ascending aortic and valve replacement with preservation of the aortic bulb (Wheat procedure)**.

Results

Preoperative Data. A total of 256 cases of acute type A aortic dissection were surgically treated at IBCV Iaşi over the 25-year study period. The number of cases operated in our institution followed an upward trend, with an average of 11 interventions per year, increasing in the last decade (2014-2024) to an annual mean of 15 cases, reflecting both increased referral and improved diagnostic and surgical capacity.

Most patients were male (69%), presenting at significantly younger ages compared to women (mean age 50.3 vs. 58.2 years). The overall mean age of the cohort was 55.8 years, lower than that reported in international literature, which may reflect a predisposition of the Romanian population to develop aortic dissections at younger ages, possibly associated with low adherence to antihypertensive therapy.

Regarding timing of presentation, the majority of patients arrived at our institution within 6-12 hours from symptom onset, a favorable factor for early surgical intervention. Arterial hypertension was the main identified risk factor, present in 75% of patients, followed by ascending aortic aneurysm associated with bicuspid aortic valve.

Table 2. Preoperative parameters.

Parameter	Value
Mean age (years)	55.8
Male sex	69%
Arterial hypertension	75%
Cardiogenic shock at presentation	18.3%
Pericardial effusion	20%
Oliguria	16.9%
Severe aortic regurgitation	48%
Ascending aorta diameter (mm)	45
Aortic annulus diameter (mm)	24.5
Symptom onset to admission interval	6–12 hours
Left ventricular ejection fraction (%)	51

Echocardiographic data. Preoperative evaluation revealed that 20% of patients presented with pericardial effusion, with or without signs of cardiac tamponade, 18.3% were in cardiogenic shock, and 16.9% had oliguria. The mean left ventricular ejection fraction was 51%, and 48% of patients exhibited grade III-IV aortic regurgitation. The mean diameter of the ascending aorta was 45 mm, while the aortic annulus measured an average of 24.5 mm.

Surgical technique. From a technical standpoint, most procedures aimed at preserving the native aortic valve (73%), while 10% of patients underwent the Bentall procedure and 17% the Wheat operation. A rising trend in valve-sparing procedures was observed, reaching 84% over the past four years.

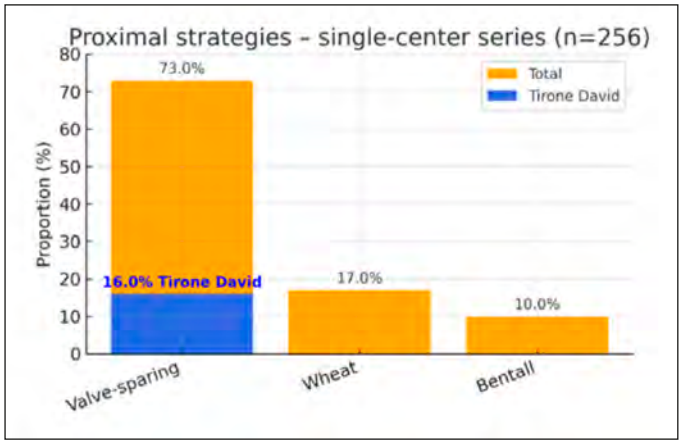

Fig. 2 Operative strategy.

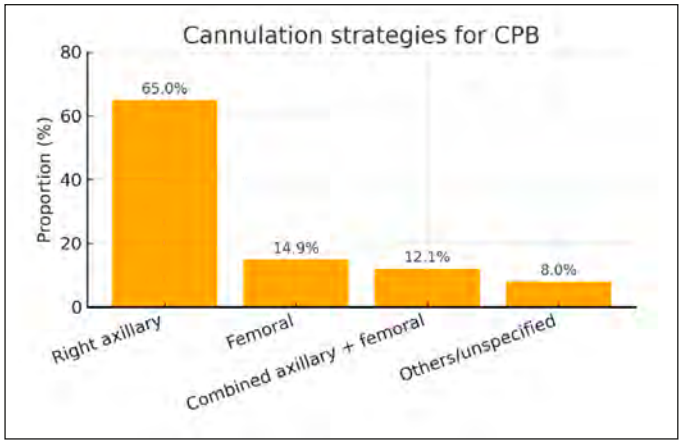

Fig. 3 Cannulation strategies

With regard to arterial cannulation strategy for cardiopulmonary bypass, the right axillary approach was considered the standard, employed in 65% of interventions, followed by femoral cannulation (14.9%) and combined axillary-femoral cannulation (12.1%). Myocardial protection was provided in most cases using combined antegrade and retrograde cardioplegia, with a mean cardiopulmonary bypass time of 264 minutes and a mean aortic cross-clamp time of 160 minutes.

The following summarizes the operative protocol for the Tirone David technique (Figure 4)

- **Aortic incision and evaluation of the aortic valve cusps**
  - The dilated ascending aorta is resected, leaving approximately 7-8 mm of aortic tissue at the base of the cusps.
  - The coronary buttons (left and right) are excised and mobilized, then retracted with stay sutures.
- **Isolation of the coronary buttons** (Figure 5)
  - The ostia of the coronary arteries are identified.
  - The coronary buttons are isolated with a margin of 4-5 mm of aortic tissue.
- **Dissection of the aortic root** (Figure 5)
  - The aortic root is carefully separated from the pulmonary artery.

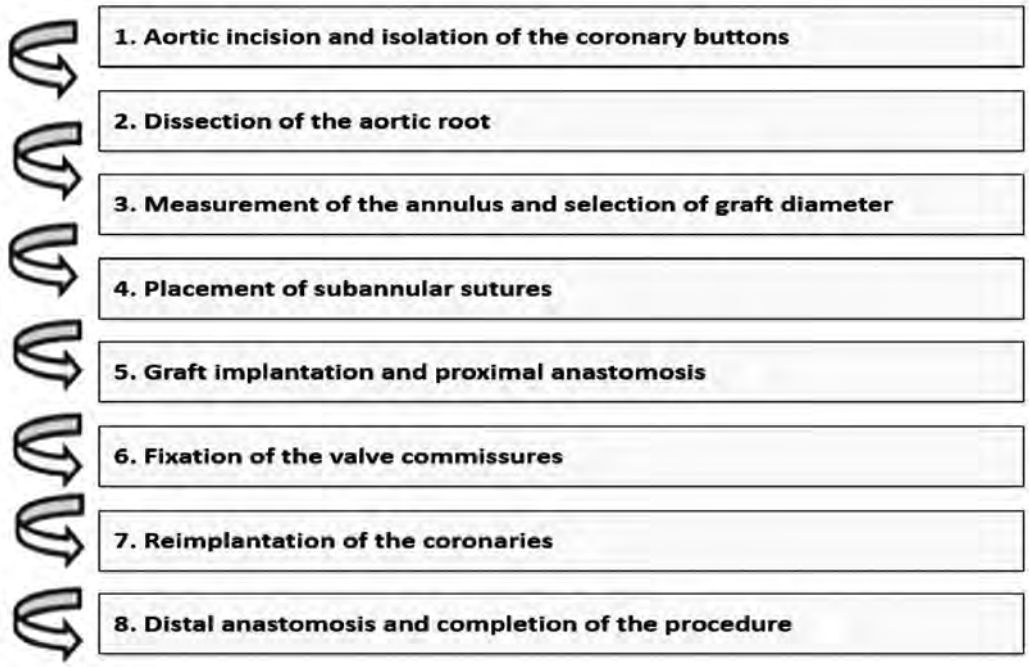

Fig. 4 Surgical Protocol Steps – Tirone David Procedure

Fig. 5 Aortic root dissection and isolation of the coronary buttons

Fig. 7 Subannular sutures placement

1. **Feindel–David:**
   Dgraft = (2 × H non-coronary cusp) × 32 + 2 × wall thickness
2. **Gleason:**
   Dgraft = 2 × H non-coronary cusp + (1–2 mm)
3. **El Khoury:**
   Dgraft = H interleaflet triangle (non-coronary/left-coronary)
4. **Fixed threshold:**
   Dgraft = D aortic annulus + 5 mm

Fig. 6 Methods for estimating the optimal prosthetic diameter

- Dissection is continued circumferentially down to the level of the aortic annulus, sometimes slightly below it.

Graft measurement and selection (Figure 6)

- A Hegar dilator is passed through the valve to determine the diameter of the left ventricular outflow tract.
- Several methods are available for estimating the optimal prosthetic diameter. The simplest approach is to select a Dacron graft whose size equals the dilator diameter plus approximately 11 mm.
- In practice, the final graft diameter usually ranges from 32 to 38 mm.

Placement of subannular sutures (Figure 7)

- Twelve to fifteen circumferential mattress sutures (2-0 Ethibond/Astralene) are placed beneath the aor-

tic annulus, with one suture positioned under each commissure.
- Care should be taken to avoid penetrating the endothelium, while ensuring even spacing of the sutures.

Graft implantation
- The graft is marked at 120° and the subannular sutures are passed through it. It is then lowered so that the annulus and valve are completely included within.
- The sutures are tied progressively, while maintaining the Hegar dilator in place to prevent narrowing of the outflow tract.

Resuspension of the valve commissures (Figure 8)
- The valve cusps are repositioned, and each commissure is anchored to the graft with 4-0 polypropylene sutures.
- Cusp coaptation is verified by irrigating with cold solution; if prolapse is present, the commissure position is adjusted or the affected cusp is suspended.

Reimplantation of the coronary arteries (Figure 9)
- Openings (neo-sinuses) are created in the graft for the coronary buttons.
- Coronary anastomoses are performed with fine sutures (5-0 polypropylene), ensuring uniform and watertight suture lines.
- If necessary, an external biological adhesive is applied for sealing.

Completion of the procedure (Figure 10)
- The integrity of the reconstruction, valve coaptation, and absence of regurgitation are verified.
- Continuity with the distal aorta is restored, usually by means of a hemi-arch or ascending aortic anastomosis.

Postoperative results. The presented data show that surgical intervention is associated with significant postoperative morbidity, with the most frequent complications being acute renal insufficiency (21.47%) and the need for hemodialysis (16.77%), highlighting the major impact on renal function and hemodynamic balance. Arrhythmias complicated the postoperative course in 18% of patients, the most common being atrial fibrillation. Infections, both respiratory (14.14%) and other types (17.17%), occurred in a substantial proportion of patients, reflecting postoperative vulnerability and prolonged hospitalization. Neurological (9.95%) and hemorrhagic (11.32%) complications were less frequent but potentially severe. The mean intensive care unit stay of 9.81 days and the total hospital stay of 17.09 days confirm the complexity of these cases and emphasize the need for dedicated preventive and management strategies to reduce renal, infectious, and arrhythmic risks in order to improve patient prognosis.

In the analyzed cohort, mortality was 13.7%, with a decreasing trend observed in recent years, reflecting progressive improvement in therapeutic outcomes achieved in our center.

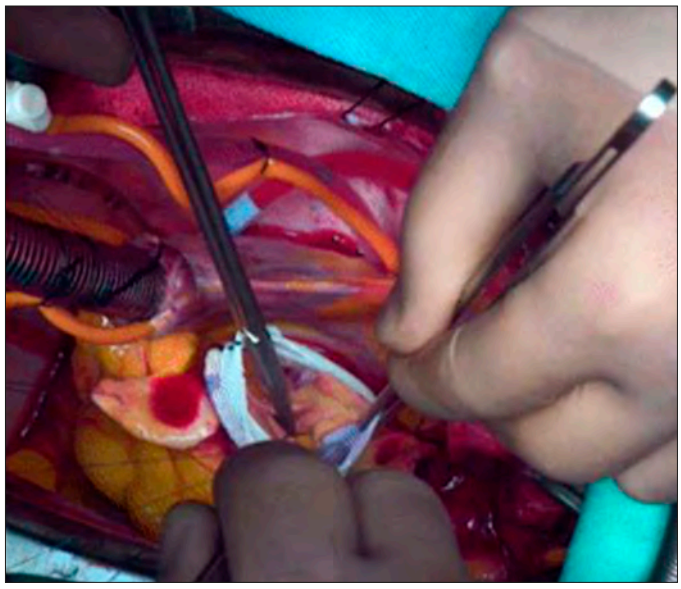

Fig. 8 Resuspension of the valve commissures

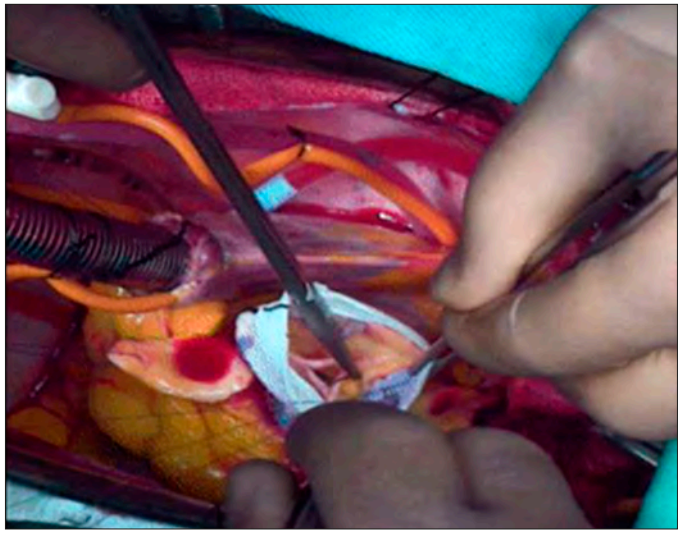

Fig. 9 Reimplantation of the coronary arteries

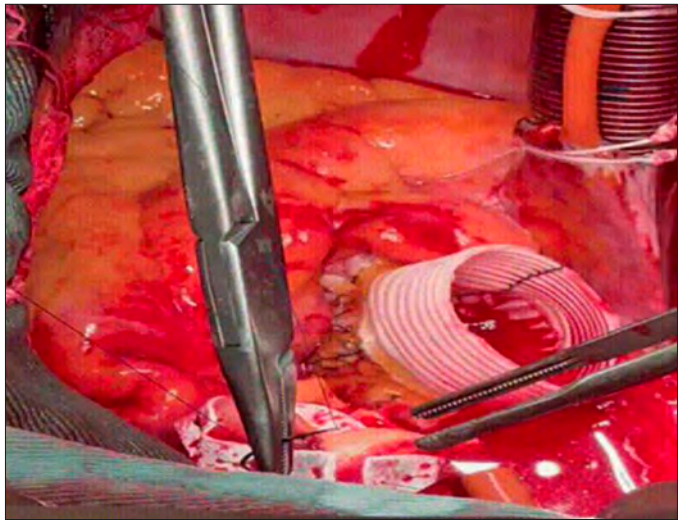

Fig. 10 Distal anastomosis

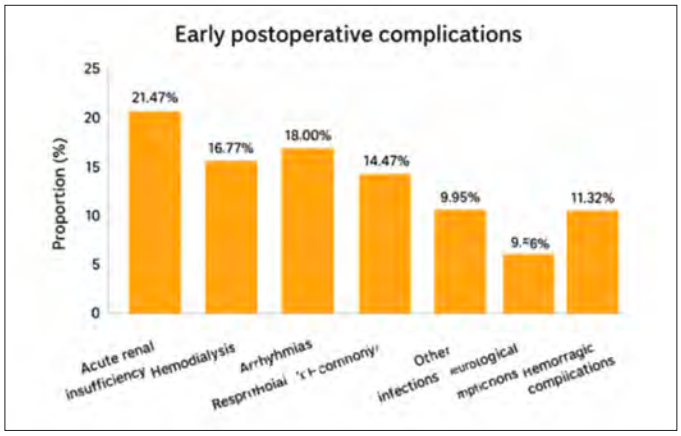

Fig. 11 Early postoperative complications

Table 3. Early postoperative complications

Parameter	Value
Perioperative mortality	13.7 %
Acute renal insufficiency	21.5 %
Hemodialysis	16.8 %
Atrial fibrillation	18 %
Respiratory infection	14.14 %
Other infections	17.17 %
Neurological complications	9.95 %
Bleeding requiring re-exploration	11.32 %
Length of intensive care stay (days)	9.81
Total hospital stay (days)	17.09

Discussions

The modern surgical treatment of aortic root pathology has evolved significantly over the past decades, beginning with the classic Bentall–De Bono procedure, which involves complete replacement of the aortic root and valve followed by reimplantation of the coronary ostia into a composite valved conduit [1]. Subsequently, techniques designed to preserve the native valve were developed, such as Robicsek aortoplasty, the Yacoub procedure (aortic root remodeling), and the David procedure (valve reimplantation into a tubular graft) [13]. In 2007, Hetzer proposed another technique – aortic valve relocation – further expanding the therapeutic armamentarium of the cardiovascular surgeon [14].

The choice of the most appropriate surgical technique in the setting of acute aortic root dissection has long been controversial. In this regard, Tirone David emphasized that dissections should be managed similarly to elective cases, advocating that aortic valves with normal or repairable cusps should be preserved, regardless of the degree of sinus involvement [14].

Over time, several variants of the David procedure have been developed, adapted to the patient's anatomic and clinical context. Its main advantage lies in the surgical flexibility it provides, allowing for a personalized approach in each case. In a retrospective analysis from the University of Michigan (Ann Arbor), comparing 307 David procedures with 184 Bentall procedures, both techniques showed good short- and long-term results, without significant differences in mortality or reintervention rates [15]. The authors emphasized that aortic root replacement should be reserved for cases with intimal tear at the root, aneurysm ≥ 45 mm, irreparable aortic valve disease, or connective tissue disorders [15]. Although the use of the David procedure in the emergency setting was initially controversial, data published by Beckmann et al. demonstrated that while immediate postoperative mortality is higher in acute dissection patients, long-term survival is comparable to that of electively operated patients [16]. Furthermore, freedom from valve reintervention at 1, 5, 10, and 15 years was excellent: 97%, 93%, 88%, and 85%, respectively [16].

Recent meta-analyses show equivalent survival between the Tirone David and Bentall procedures, with a higher risk of reintervention after Tirone David – a risk dependent on patient selection, aortic geometry, and the quality of reconstruction [17]. Contemporary series suggest excellent durability with a standardized and meticulous technique. Similarly, a comparative study from Leipzig concluded that, in the hands of experienced surgeons, the David procedure provides survival equivalent to Bentall when selectively applied according to patient-specific factors [18].

Patient subgroups

Young patients and those with connective tissue disorders – The Tirone David procedure is recommended when cusps are morphologically normal or repairable [2]. Avoidance of lifelong anticoagulation, preservation of physiologic root hemodynamics, and complete resection of diseased aortic wall are strong arguments for valve preservation, particularly in Marfan or Loeys–Dietz patients with intact cusps [11]. Modern studies show that, in emergency settings, the David procedure may be chosen as a first-line strategy in carefully selected patients with stable preoperative status; consecutive series report mortality comparable to alternative techniques and stable mid-term valve function, despite longer CPB times [11, 15]. Standardized cerebral protection and cannulation strategies (e.g., right axillary cannulation with selective antegrade cerebral perfusion) support extended approaches in young patients, reducing the neurological burden of more complex procedures. In our series, valve preservation was chosen in 73% of cases (84% in the past 4 years), especially in young patients and those with connective tissue disorders, provided that intraoperative evaluation confirmed repairable cusps and a sino-tubular junction that could be reliably reconstructed with a stable prosthetic graft.

Bicuspid aortic valve – The David procedure is feasible in bicuspid aortic valves if near-180° commissural symmetry and an effective cusp height of ~9-10 mm can be achieved, with targeted prolapse correction (central plication) as needed [19-21]. The literature highlights that success in bicuspid valves depends on reconstructed geometry (commissural angle, restoration of the base and sino-tubular junction). Once these are secured, residual insufficiency is reduced and durability is acceptable [21]. Conversely, extensive calcification, thickened cusps, or uncorrectable commissural ratios direct the choice toward Bentall, where

a standardized approach can be more easily applied [8]. For cases with fragile or dissected coronary buttons, modern reimplantation techniques and interposition options (Cabrol/Piehler) can prevent tension and stabilize root reconstruction when the David procedure is not indicated [22, 23]. In our practice, bicuspid patients were candidates only when intraoperative evaluation demonstrated proper commissural symmetry and cusp coaptation without regurgitation; otherwise, we favored Bentall to avoid early reintervention.

Hemodynamically unstable patients or those with malperfusion – In the presence of hemodynamic shock, preoperative resuscitation, tamponade with imminent collapse, or severe visceral/neurological malperfusion, the priority is rapid and secure proximal control using a standardized technique with predictable hemostasis. In these circumstances, Bentall (or, in strictly selected cases, Wheat) provides a shorter option, with robust proximal annular sutures and complete resection of dissected tissue, reducing the risk of proximal reintervention compared with partial root repairs [2]. Contemporary algorithms for acute type A dissection explicitly include "non-David bailout" strategies when critical status and/or complex distal anatomy jeopardize safety. In such situations, axillary cannulation (sometimes combined) and selective cerebral perfusion remain key to controlling neurological risk during circulatory arrest [24]. In our series, where right axillary cannulation was standard (65%), the same criterion was applied: David only for stabilized patients with repairable cusps; Bentall/Wheat when every minute saved and proximal hemostasis were paramount.

Profile of our series. The profile of our cohort (mean age 55.8 years; 69% male; presentation frequently within the first 6-12 hours; 48% severe aortic insufficiency; 73% David procedure; overall mortality 13.7% with a downward trend) is consistent with the literature, which demonstrates that careful selection allows extension of the David procedure to acute type A dissection without compromising safety, at the cost of a learning curve and longer cross-clamp/CPB times. In cases where the valve and/or root cannot be reconstructed within acceptable geometric parameters, systematic application of the Bentall technique (secure proximal hemostatic construction, appropriate graft/valve choice, tension-free coronary button reimplantation, interposition options) ensures robust outcomes and a reliable platform for high-risk emergencies.

Table 4. Major outcomes of the Tirone David procedure in acute type A aortic dissection

Study	Design/Center	n	Early mortality	Reintervention	Reference
Tanaka 2018, EJCTS	Observational	24 Tirone David	0%	7–10%	Tanaka H, et al. *Outcomes of VSRR in acute Type A dissection.* Eur J Cardiothorac Surg. 2018;53:1021–1026. doi:10.1093/ejcts/ezx463
Beckmann 2023, AnnalsCTS	Review	133	12.8%	Not specified	Beckmann E, Kaufeld T, Martens A, Rudolph L, Shrestha M, Krueger H, Haverich A, Shrestha ML. *Aortic valve-sparing root replacement (David-I) for acute aortic dissection type A.* Ann Cardiothorac Surg. 2023;12(3):276–278. doi:10.21037/acs-2022-avs1-168
Sá 2023, Int J Cardiol (meta)	Meta-analysis (7 studies)	367 Tirone David vs 491 Bentall	Similar between David vs Bentall	Higher risk after David vs Bentall	Sá MP, et al. *Long-term outcomes of VSRR vs composite valve graft in ATAAD: meta-analysis.* Int J Cardiol. 2023;382:12–19. doi:10.1016/j.ijcard.2023.03.062
Aubin/Kamiya 2019, Front Surg	Review	28	17.9%	0%	Aubin H, Kamiya H, et al. *Valve-Sparing Aortic Root Replacement as First-Choice Strategy in ATAAD.* Front Surg. 2019;6:1-9

Conclusions

In acute type A aortic dissection, the Tirone David procedure represents our operation of choice whenever the aortic cusps are intact or amenable to repair, the aortic root is not excessively fragile and allows for safe reconstruction, and the patient's clinical status tolerates the additional operative time. Conversely, the Bentall procedure remains the optimal option in the presence of irreparable cusps, markedly fragile tissue, or profound hemodynamic instability. Right axillary cannulation constitutes our institutional standard.

- When – The Tirone David procedure is favored when cusp repairability and root reconstructability are feasible; the Bentall operation is selected when the valve is irreparable, tissue integrity is compromised, or rapid operative completion is essential.
- How – Strict procedural standardization, including correct commissural orientation and accurate prosthesis sizing, is fundamental to ensure long-term durability.
- Why – Preservation of physiological hemodynamics and avoidance of lifelong anticoagulation justify the use of the Tirone David procedure in carefully selected patients. In contrast, the Bentall procedure provides greater simplicity and predictability in cases with unfavorable anatomy or hemodynamic compromise.

Our patient series supports the feasibility of the Tirone David operation in the setting of acute type A aortic dissection, with an operative mortality of 13.7% and a favorable downward trend over time.

Competing interests

None declared.

Authors' contributions

GT conceived the study, supervised the project, and critically revised the manuscript. ME contributed to study design, collected clinical data, and drafted parts of the manuscript. AȚ participated in surgical procedures, data acquisition, and interpretation. AB and SS contributed to perioperative data collection, analysis, and manuscript drafting. AB assisted in statistical analysis, data processing, and preparation of figures and tables. All authors reviewed the work critically, approved the final version of the manuscript, and agree to be accountable for all aspects of the work.

Patient consent

Obtained.

Ethics approval

The study was approved by the Research Ethics Committee of *Professor Dr. George I.M. Georgescu* Institute of Cardiovascular Diseases, Iasi, Romania (approval number 2185 / 2024-07-26).

Acknowledgements and funding

No external funding.

Provenance and peer review

Not commissioned, externally peer-reviewed.

References

1. Bentall H, De Bono A. A technique for complete replacement of the ascending aorta. Thorax. 1968;23(4):338-9. doi: 10.1136/thx.23.4.338.
2. Czerny M, Grabenwöger M, Berger T, Aboyans V, Della Corte A, Chen EP, et al. EACTS/STS Guidelines for diagnosing and treating acute and chronic syndromes of the aortic organ. Ann Thorac Surg. 2024;118(1):5-115. doi: 10.1016/j.athoracsur.2024.01.021.
3. David TE. Aortic valve sparing operations. Ann Thorac Surg. 2002;73(4):1029-30. doi: 10.1016/s0003-4975(02)03487-2.
4. Shi W, Keefe M, Matalanis G. Valve-sparing aortic root replacement and aortic valve repair [Internet]. In: Motomura N, ed. Aortic valve surgery. London: InTech; 2011 [cited 2025 Jun 14]. Available from: http://dx.doi.org/10.5772/21219.
5. David TE. Aortic valve sparing operations: a review. J Chest Surg. 2012;45(4):205-12. doi: 10.5090/kjtcs.2012.45.4.205.
6. Tian D, Rahnavardi M, Yan TD. Aortic valve sparing operations in aortic root aneurysms: remodeling or reimplantation? Ann Cardiothorac Surg. 2013;2(1):44-52. doi: 10.3978/j.issn.2225-319X.2013.01.14.
7. Pape LA, Awais M, Woznicki EM, Suzuki T, Trimarchi S, Evangelista A, et al. Presentation, diagnosis, and outcomes of acute aortic dissection: 17-year trends from the International Registry of Acute Aortic Dissection. J Am Coll Cardiol. 2015;66(4):350-8. doi: 10.1016/j.jacc.2015.05.029.
8. Ohira S, Cameron DE, Lansman SL, Spielvogel D. Complex Bentall operation: clinical pearls to standardize the procedure. Ann Thorac Surg. 2025;119(4):744-54. doi: 10.1016/j.athoracsur.2024.09.013.
9. Angelos P, Taylor LJ, Roggin K, Schwarze ML, Vaughan LM, Wightman SC, et al. Decision-making in surgery. Ann Thorac Surg. 2024;117(6):1087-94. doi: 10.1016/j.athoracsur.2024.01.001.
10. Isselbacher EM, Preventza O, Hamilton Black J, 3rd, Augoustides JG, Beck AW, Bolen MA, et al. 2022 ACC/AHA Guideline for the diagnosis and management of aortic disease: a report of the American Heart Association/American College of Cardiology Joint Committee on Clinical Practice Guidelines. Circulation. 2022;146(24):e334-e482. doi: 10.1161/cir.0000000000001106.
11. Aubin H, Akhyari P, Rellecke P, Pawlitza C, Petrov G, Lichtenberg A, et al. Valve-sparing aortic root replacement as first-choice strategy in acute type A aortic dissection. Front Surg. 2019;6:46. doi: 10.3389/fsurg.2019.00046.
12. Ahmed EM, Chen E. Valve sparing aortic root replacement for aortic valve insufficiency in type A aortic dissection. In: Sellke FW, et al., editors. Aortic dissection and acute aortic syndromes. Cham: Springer; 2021. p. 269-282. doi: 10.1007/978-3-030-66668-2_19.
13. Yacoub MH, Gehle P, Chandrasekaran V, Birks EJ, Child A, Radley-Smith R. Late results of a valve-preserving operation in patients with aneurysms of the ascending aorta and root. J Thorac Cardiovasc Surg. 1998;115(5):1080-90. doi: 10.1016/s0022-5223(98)70408-8.
14. David T. Reimplantation valve-sparing aortic root replacement is the most durable approach to facilitate aortic valve repair. JTCVS Techniques. 2021;7:72-8. doi: 10.1016/j.xjtc.2020.12.042.
15. Yang B, Norton EL, Hobbs R, Farhat L, Wu X, Hornsby WE, et al. Short- and long-term outcomes of aortic root repair and replacement in patients undergoing acute type A aortic dissection repair: twenty-year experience. J Thorac Cardiovasc Surg. 2019;157(6):2125-36. doi: 10.1016/j.jtcvs.2018.09.129.
16. Beckmann E, Kaufeld T, Martens A, Rudolph L, Shrestha M, Krueger H, et al. Aortic valve-sparing root replacement (David-I) for acute aortic dissection type A. Ann Cardiothorac Surg. 2023;12(3):276-8. doi: 10.21037/acs-2022-avs1-168.
17. Sá MP, Tasoudis P, Jacquemyn X, Van den Eynde J, Rad AA, Weymann A, et al. Long-term outcomes of valve-sparing root versus composite valve graft replacement for acute type A aortic dissection: meta-analysis of reconstructed time-to-event data. Int J Cardiol. 2023;382:12-9. doi: 10.1016/j.ijcard.2023.03.062.
18. Subramanian S, Leontyev S, Borger MA, Trommer C, Misfeld M, Mohr FW. Valve-sparing root reconstruction does not compromise survival in acute type A aortic dissection. Ann Thorac Surg. 2012;94(4):1230-4. doi: 10.1016/j.athoracsur.2012.04.094.
19. Jahanyar J, de Kerchove L, El Khoury G. Bicuspid aortic valve repair: the 180°-reimplantation technique. Ann Cardiothorac Surg. 2022;11(4):473-81. doi: 10.21037/acs-2022-bav-18.
20. Schäfers HJ, Bierbach B, Aicher D. A new approach to the assessment of aortic cusp geometry. J Thorac Cardiovasc Surg. 2006;132(2):436-8. doi: 10.1016/j.jtcvs.2006.04.032.
21. Bierbach BO, Aicher D, Issa OA, Bomberg H, Gräber S, Glombitza P, et al. Aortic root and cusp configuration determine aortic valve function. Eur J Cardiothorac Surg. 2010;38(4):400-6. doi: 10.1016/j.ejcts.2010.01.060.
22. Aphram G, Tamer S, Mastrobuoni S, El Khoury G, de Kerchove L. Valve sparing root replacement: reimplantation of the aortic valve. Ann Cardiothorac Surg. 2019;8(3):415-7. doi: 10.21037/acs.2019.04.05.
23. Piehler JM, Pluth JR. Replacement of the ascending aorta and aortic valve with a composite graft in patients with nondisplaced coronary ostia. Ann Thorac Surg. 1982;33(4):406-9. doi: 10.1016/s0003-4975(10)63239-0.
24. Leshnower BG, Myung RJ, Kilgo PD, Vassiliades TA, Vega JD, Thourani VH, et al. Moderate hypothermia and unilateral selective antegrade cerebral perfusion: a contemporary cerebral protection strategy for aortic arch surgery. Ann Thorac Surg. 2010;90(2):547-54. doi: 10.1016/j.athoracsur.2010.03.118.

https://doi.org/10.52645/MJHS.2025.3.02

UDC: 611.831.7

RESEARCH ARTICLES

Development of the facial nerve and its specific features

Angela Babuci[1*], Zinovia Zorina[1], Ilia Catereniuc[1], Nataliya Trushel[2], Anastasia Bendelic[1], Nadia Ostahi[1], Sofia Lehtman[3]

[1]Department of Anatomy and Clinical Anatomy, *Nicolae Testemițanu* State University of Medicine and Pharmacy, Republic of Moldova
[2]Department of Normal Anatomy, Belarusian State Medical University, Republic of Belarus
[3]*Arsenie Guțan* Department of Oral-Maxillofacial Surgery and Oral Implantology, *Nicolae Testemițanu* State University of Medicine and Pharmacy, Republic of Moldova

ABSTRACT

Background. The data reported in the specialty literature on the embryogenesis of the facial nerve mainly refer to the initial stages of its development. Nevertheless, the intrauterine development of the facial nerve is a complex and insightful process, characterized by a range of peculiarities. The goal of our study was to highlight the specific developmental features of the facial nerve for a better understanding of its morphology in adults.

Material and methods. Fifty-two groups of serially sectioned human embryos and fetuses from the embryo-fetal collection of the Department of Normal Anatomy at the Belarusian State Medical University in Minsk were investigated. The embryonic samples were classified according to Carnegie stages (day of gestation and crown-rump length). For protocols description, an OLYMPUS CX31 binocular microscope (eyepiece 10x, objectives 4x; 10x; 40x; 100x) and a Nikon DS-Fi1 camera were used.

Results. The primary and secondary divisions of the facial nerve trunk, the chorda tympani, the greater petrosal nerve, and the intracerebral and peripheral connections of the facial nerve were distinguished at Carnegie stage 15. The first appearance of intraplexal connections within the parotid plexus was identified at Carnegie stage 16. At stage 20, thin connections between the geniculate ganglion and the vestibular ganglion were revealed. Macro- and microstructural changes in the geniculate ganglion were noted throughout its development. The plexiform nature of the peripheral divisions of the facial nerve and the formation of the *pes anserinus minor* were observed at stage 21. At Carnegie stage 23, the motor nucleus was well developed, and the internal knee of the facial nerve was identified.

Conclusions. Early specific features of facial nerve development include: 1) intracerebral and peripheral connections with neighboring cranial nerves; 2) intraplexal connections between branches of the parotid plexus; 3) distinguishable intracerebral pathways; 4) connections between the geniculate and vestibular ganglia. Late developmental peculiarities include: 1) progressive macro- and microstructural changes in the geniculate ganglion; 2) appearance of the *pes anserinus minor*; 3) formation of the motor nucleus, internal knee, and intracerebral pathways. These specific developmental features of the facial nerve provide clear evidence of its complex morphology in adults.

Keywords: facial nerve, embryonic development, Carnegie stages, geniculate ganglion, nerve connections.

Cite this article: Babuci A, Zorina Z, Catereniuc I, Trushel A, Bendelic A, Ostahi N, Lehtman S. Development of the facial nerve and its specific features. Mold J Health Sci. 2025;12(3):12-19. https://doi.org/10.52645/MJHS.2025.3.02.

Manuscript received: 19.07.2025

Accepted for publication: 05.08.2025

Published: 15.09.2025

[*]**Corresponding author: Angela Babuci**, MD, PhD, associate professor
Department of Anatomy and Clinical Anatomy
Nicolae Testemițanu State University of Medicine and Pharmacy
165 Stefan cel Mare și Sfant blvd, Chisinau, Republic of Moldova, MD-2004
email: angela.babuci@usmf.md

Key messages

What is not yet known about the issue addressed in the submitted manuscript

In the specialty literature, the development of the facial nerve refers particularly to its initial embryological stages, but the complexity of its specific developmental features goes beyond the published data.

The research hypothesis

Knowledge about the peculiarities of facial nerve development is

Authors' ORCID IDs
Angela Babuci – https://orcid.org/0000-0003-0305-1279
Zinovia Zorina – https://orcid.org/0000-0002-0749-6083
Ilia Catereniuc – https://orcid.org/0000-0002-5479-4198
Nataliya Trushel – https://orcid.org/0000-0003-0865-2495
Anastasia Bendelic – https://orcid.org/0000-0002-2838-3168
Nadia Ostahi – https://orcid.org/0009-0003-7197-0178
Sofia Lehtman – https://orcid.org/0000-0003-4653-8589

significant for understanding its topographical relationships with adjacent anatomical structures and for better comprehension of its involvement in impairments of neighboring cranial nerves.

The novelty added by the manuscript to the already published scientific literature

The current study highlights certain specific features of facial nerve development that have not been described by other authors.

Introduction

The fascinating process of facial nerve embryogenesis and its high susceptibility to a wide range of harmful factors, including viruses, bacterial infections, and genetic mutations, have strengthened our belief that even the most sophisticated imaging methods cannot provide a better understanding of facial nerve formation and functionality than the investigation of its development in human embryos.

The rhombencephalon develops from an excessively segmented neuroepithelial area of the cephalic portion of the neural tube, giving rise to neuromeres [1]. Müller and O'Rahilly proposed the first classification of the neuromeres, according to their position and appearance in the brain [2]. Thus, at Carnegie stage 9, the scientists identified 6 primary neuromeres, but by stage 14, all the secondary neuromeres had formed. The neuromeres were detectable until Carnegie stage 17. Lumsden revealed a distinct position of the cranial nerve roots in relation to individual rhombomeres in chick embryos. Thus, the trigeminal nerve root lies in r2, the facial nerve root in r4, and the glossopharyngeal in r6 [3]. The roots of the nerves were distinguished in the central furrow of the rhombomere, and "a tight correspondence between the position of each branchial motor nucleus and the rhombomeric pattern was observed" [3]. In vertebrates, the development of the face is related to the neural crest and is regulated by a "code of HOX genes in a segment-restricted way" [4]. By stage 17, the "branchial motor nerves emerge from nuclei within consecutive pairs of rhombomeres, each pair lying in register with an adjacent branchial arch" [5, p. 331], and a two-segment periodicity is established [5-7]. Under normal conditions, the trigeminal nerve develops from r2 and r3, the facial nerve from r4 and r5, the glossopharyngeal nerve from r6 and r7, and the vagus and accessory nerves from r7 and r8 [1-5, 8, 9].

In chick and mouse embryos, a particular HOX gene–GHOX 2.9 in chicks and HOX 2.9 in mice–is highly expressed at the level of r4 and the hyoid arch, from which the facial nerve derives [10-12]. The expression of HOX genes in the neural tube and neural crest cells, as well as the combined expression of HOX genes in both the neurogenic neural crest and branchial arches, determines the development of the facial nerve [9].

According to Sataloff and Danilo, in the third week of gestation, the facio-acoustic primordium derives from the rhombomeres of the rhombencephalon, giving rise to the facial nerve [13, 14]. The trunk of the facial nerve passes through the mesenchyme towards the facial neurogenic placodes, contributing to the formation of the nerve ganglia associated with the pharyngeal arches. By the fourth week of embryonic development, the facial nerve nucleus is formed, and the motor fibers of the facial nerve extend from it [13-15], while Müller considers that the motor nucleus of the facial nerve is not definitely formed until the last stage of embryogenesis (Carnegie stage 23) [2]. The parasympathetic ganglia derive from neural crest cells, and the axons of those neurons form the facial nerve [16]. In the 4th week of development, the chorda tympani is distinguished [13, 14]. During the 5th–7th weeks of gestation, the geniculate ganglion, the intermediate nerve, and the greater petrosal nerve appear [16, 17].

The geniculate ganglion is of mixed embryological origin, with the majority of its neurons deriving from the hyomandibular epibranchial placode, while the supporting cells are derivatives of the neural crest [18, 19]. In relation to the vestibulocochlear complex, the geniculate ganglion is located at the level of r4, being in contact with the epipharyngeal placode of the 2nd visceral arch [20].

Development of the motor components of the cranial nerves derived from the first three visceral arches depends on HOX gene expression [1]. Development of the facial nerve and of the geniculate ganglion "involves neuronal survival, differentiation, and neuron-glia interaction", regulated by the gene-related family of neurotrophins–nerve growth factor–which determines the growth of sympathetic and some sensory neurons, as well as neuronal survival [18]. During the 7th and 8th weeks, the mimic muscles derive from the second branchial arch, and by the 11th week of development, the facial nerve, which supplies these muscles, is characterized by obvious arborization. In the newborn, the anatomy of the facial nerve shows many similarities to that of the adult, except in the mastoid region, where the nerve is located more superficially due to underdevelopment of the mastoid process.

Considering the above-mentioned facts, the goal of our study was to highlight the morphological specific features of facial nerve development for a better understanding of its branching patterns, connections, and functionality in adults.

Material and methods

This current study was conducted on the basis of the Bilateral Agreement between the Department of Anatomy and Clinical Anatomy of *Nicolae Testemițanu* State Univer-

sity of Medicine and Pharmacy of the Republic of Moldova and the Department of Normal Anatomy of the Belarusian State Medical University in Minsk.

Fifty-two groups of serially sectioned human embryos and fetuses from the embryo-fetal historical collection of the Department of Normal Anatomy of the Belarusian State Medical University in Minsk were investigated. The crown-rump length (CRL) of the examined embryos and fetuses ranged from 4 mm to 70 mm.

According to available data, prior to dissection, the embryos and fetuses were fixed in 10% formalin solution, after which they were dissected by a microtome in sagittal, frontal, and transverse planes. The histological samples were subsequently stained using hematoxylin-eosin and Bielschowsky-Bücke silver impregnation methods. All the samples used in the current study were fixed and stained by the staff of the Department of Normal Anatomy of the Belarusian State Medical University in Minsk, at the time of the collection's creation. The descriptive and morphometric parameters of the embryos and fetuses were stored in an Excel database, maintaining the coding of the original collection. The embryonic samples were classified according to Carnegie stages (day of gestation and CRL), as proposed by Robinson [21]. For description of the protocols, the OLYMPUS CX31 binocular microscope (eyepiece 10x, objectives 4x; 10x; 40x; 100x) and Nikon DS-Fi1 camera were used.

Results

At the end of Carnegie stage 13, a narrow furrow splits the facio-acoustic primordium into the facial and acoustic ganglia. At stage 15, the facial nerve exits the rhombencephalon as a straight, well-impregnated trunk, consisting of loosely arranged nerve fibers (Fig. 1A). The geniculate ganglion, chorda tympani, and greater petrosal nerves were also identified at stage 15.

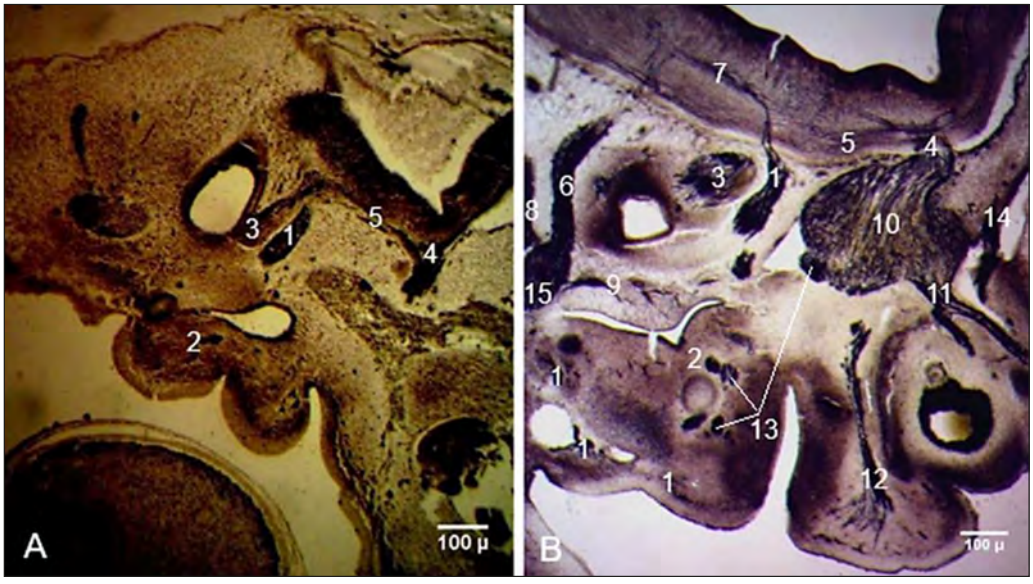

Fig. 1 Development and connections of the facial nerve in human embryos.

A. Carnegie stage 15 (CRL 9 mm). B. Carnegie stage 19 (CRL 17 mm). Sagittal sections. Staining (Bielschowsky-Bücke and hematoxylin-eosin). Microphotographs. 1 – facial nerve; 2 – chorda tympani; 3 – acoustic ganglion (future vestibular and spiral ganglia); 4 – trigeminal nerve; 5 – intracerebral connections between the facial nerve and trigeminal nerve; 6 – glossopharyngeal nerve; 7 – intracerebral connections between the facial nerve and glossopharyngeal nerve; 8 – vagus nerve; 9 – tympanic nerve; 10 – trigeminal ganglion; 11 – ophthalmic nerve; 12 – maxillary nerve; 13 – mandibular nerve; 14 – trochlear nerve; 15 – inferior ganglion of the glossopharyngeal nerve.

On deeper planes of the sagittal sections, the roots formed by the facial and trigeminal nerves faded, while those of the glossopharyngeal and vagus nerves were well distinguishable. The intracerebral connections between the facial and glossopharyngeal nerves were also identified. The connections between the vagus and hypoglossal nerves were highlighted. The neuronal groups that give rise to the facio-vestibulo-cochlear complex were detected in the region of the internal acoustic meatus at Carnegie stages 15-16 (CRL 9-11 mm).

At Carnegie stage 16, two roots of the facial nerve–an anterior and a posterior one–were highlighted on transverse cross-sections. The definitive formation of the intracerebral roots of the facial nerve and their fusion into a common trunk were established at Carnegie stage 18 (Fig. 2).

At Carnegie stage 19, the intracerebral connections of the facial nerve with the trigeminal and glossopharyngeal nerves became thicker, and a clear fibrillar character of these connections was observed. The peripheral branches

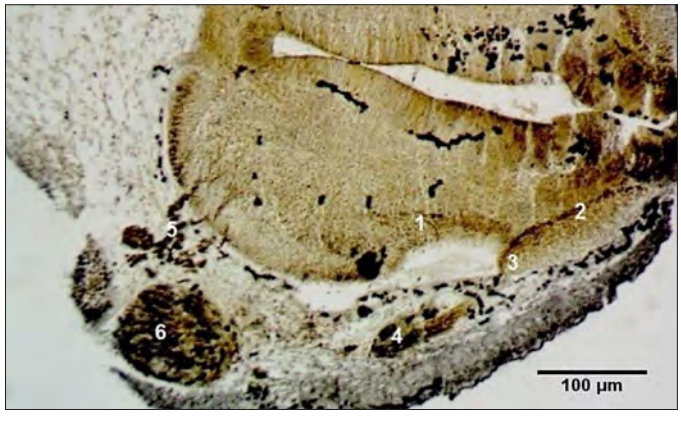

Fig. 2 Formation of the intracerebral roots of the facial nerve. Transverse cross-section through the hindbrain. Carnegie stage 18 (CRL 15 mm).

Staining (Bielschowsky-Bücke). Microphotograph. 1 – anterior root of the facial nerve; 2 – posterior root of the facial nerve; 3 – facial nerve; 4 – geniculate ganglion; 5 – roots of the trigeminal nerve; 6 – trigeminal ganglion.

of the facial nerve were better distinguished, and their connections with the peripheral branches of the trigeminal and glossopharyngeal nerves became more obvious. The course of the tympanic nerve through the mesenchyme of the developing petrous part of the temporal bone was clearly identified. The trochlear nerve and all the primary branches of the trigeminal nerve were well distinguished (Fig. 1B).

The biotaxis of the neuroblasts from the depth of the rhombencephalon towards the external surface of the brain appeared as fibrocellular cords at Carnegie stage 16 (Fig. 3A). At the cranial end of the hindbrain, the roots of the trigeminal nerve were highlighted. Medial to the trigeminal nerve, the intracerebral path of the facial nerve was identified. The internal knee of the facial nerve was observed on frontal sections of embryos at Carnegie stage 23, which is the last stage of embryonic development (Fig. 3B). The fibers of the facial nerve entered the internal acoustic meatus, close to the vestibular ganglion, continuing their course within the facial canal, and, upon exiting the stylomastoid foramen, the nerve appeared as a thick fibrous cord.

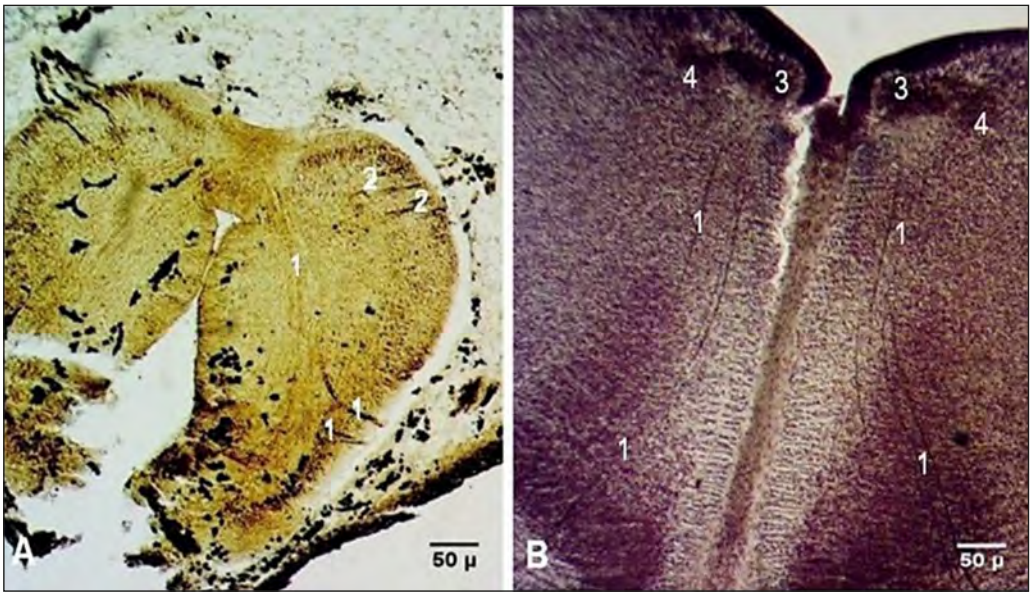

Fig. 3 Intracerebral course of the facial nerve in human embryos.

A. Transverse cross-section. Carnegie stage 16 (CRL 11 mm). B. Frontal section. Carnegie stage 23 (CRL 27 mm). Staining (Bielschowsky-Bücke and hematoxylin-eosin). Microphotographs. 1 – fibers of the facial nerve; 2 – fibers of the trigeminal nerve; 3 – motor nucleus of the facial nerve; 4 – internal knee of the facial nerve.

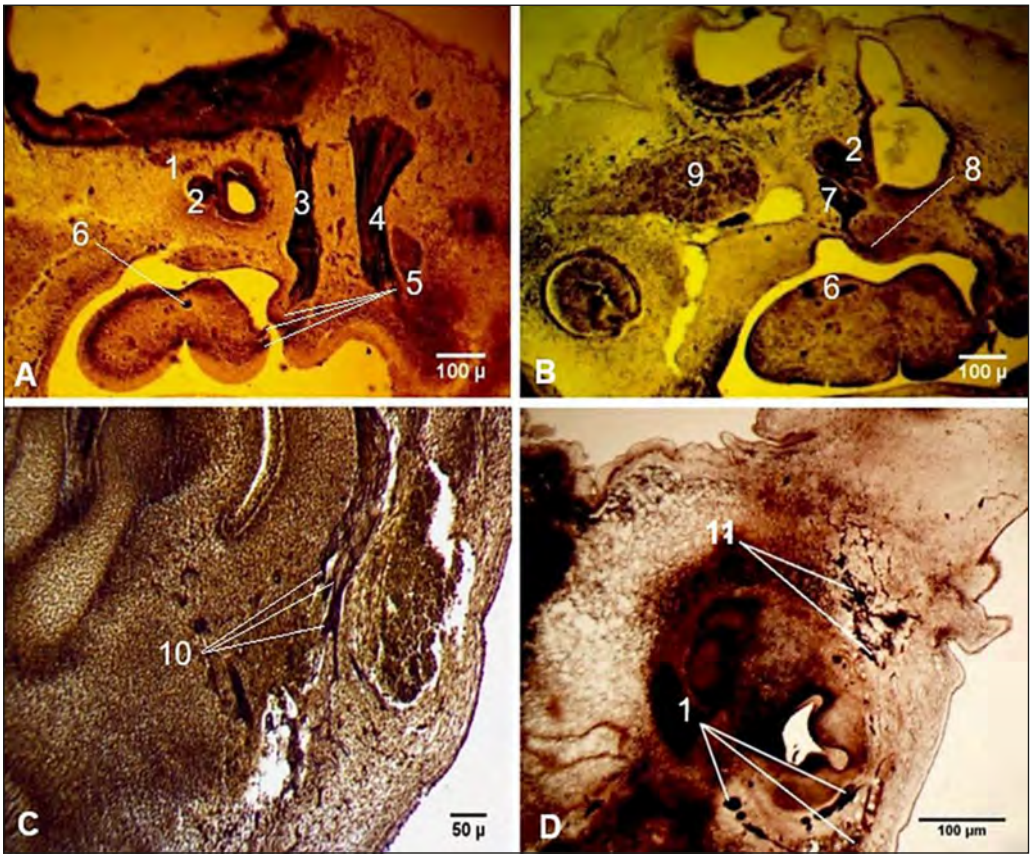

Fig. 4 Peculiarities of the peripheral connections of the facial nerve.

A. Connections of the facial nerve with the lingual branches of the glossopharyngeal nerve. Carnegie stage 15 (CRL 9 mm). B. Communicating branch of the facial nerve with the tympanic plexus. Carnegie stage 16 (CRL 11 mm). C. Intraplexal connections between the branches of the parotid plexus. Carnegie stage 17 (CRL 14 mm). D. A plexiform structure in the infraorbital region. Carnegie stage 21 (CRL 23 mm). Sagittal sections. Staining (Bielschowsky-Bücke). Microphotographs. 1 – facial nerve; 2 – acoustic ganglion; 3 – glossopharyngeal nerve; 4 – vagus nerve; 5 – connections of the facial nerve with the lingual branches of the glossopharyngeal nerve; 6 – chorda tympani; 7 – geniculate ganglion; 8 – communicating branch of the facial nerve with the tympanic plexus; 9 – trigeminal ganglion; 10 – intraplexal connections between the branches of the parotid plexus; 11 – plexiform structure in the infraorbital region, formed by connections between the facial and trigeminal nerves (pes anserinus minor).

Peripheral connections of the facial nerve were distinguished starting from Carnegie stage 15 (CRL 9 mm). Among the earliest revealed connections were those of the chorda tympani with the lingual branches of the glossopharyngeal nerve (Fig. 4A). At Carnegie stage 16 (CRL 11 mm), a communicating branch of the facial nerve with the tympanic plexus was highlighted (Fig. 4B). The first appearance of the parotid plexus was observed at Carnegie stage 17 (CRL 14 mm), and multiple thin intraplexal connections between the main divisions of the future parotid plexus were distinguished (Fig. 4C). At Carnegie stage 21 (CRL 23 mm), the extracranial branches of the facial nerve were represented by multiple distal arborizations. A plexiform structure, formed by connections between the distal ramifications of the temporofacial division of the facial nerve and the infraorbital branch of the maxillary nerve, was marked out in the infraorbital region. The infraorbital plexiform structure consisted of a well-defined fibrillar component with highly complex connections, known as the *pes anserinus minor* (Fig. 4 D).

As a specific feature of the geniculate ganglion during its embryonic and fetal development, continuous modifications in its shape–from oval to triangular and ovoid-triangular–were noted. A series of microscopic morphological changes were also observed. At Carnegie stage 18, the geniculate ganglion had an ovoid shape and was predominantly formed by nerve fibers, among which growing neuroblasts were distinguished. An hourglass-shaped narrowing was revealed on the medial side of the ganglion. The neuroblasts were randomly distributed within the geniculate ganglion; nevertheless, their concentration was clearly higher along its margins and in the core of the ganglion (Fig. 5A).

In fetuses with a CRL of 55 mm, the geniculate ganglion was oval, and the hourglass-shaped narrowing had disappeared. A neuronal redistribution within the geniculate ganglion occurred: the neuroblasts surrounded the external margin of the ganglion as a thick collar, while the central part consisted predominantly of nerve fibers, with only a few thin cords of neuroblasts highlighted in its core (Fig. 5B).

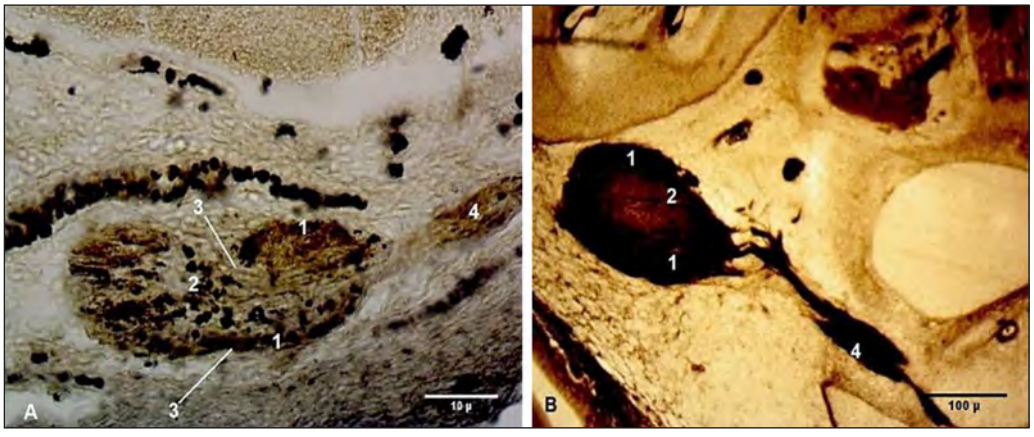

Fig. 5 Developmental peculiarities of the geniculate ganglion in embryos and fetuses.

Transverse cross-sections. A. Embryo at Carnegie stage 18 (CRL 15 mm). B. Fetus (CRL 55 mm). Staining (Bielschowsky-Bücke). Microphotographs. 1 – neuroblasts located at the periphery of the geniculate ganglion; 2 (A) – central cluster of neuroblasts; 2 (B) – thin cords of neuroblasts in the core of the ganglion; 3 – hourglass-shaped narrowing of the ganglion; 4 – facial nerve.

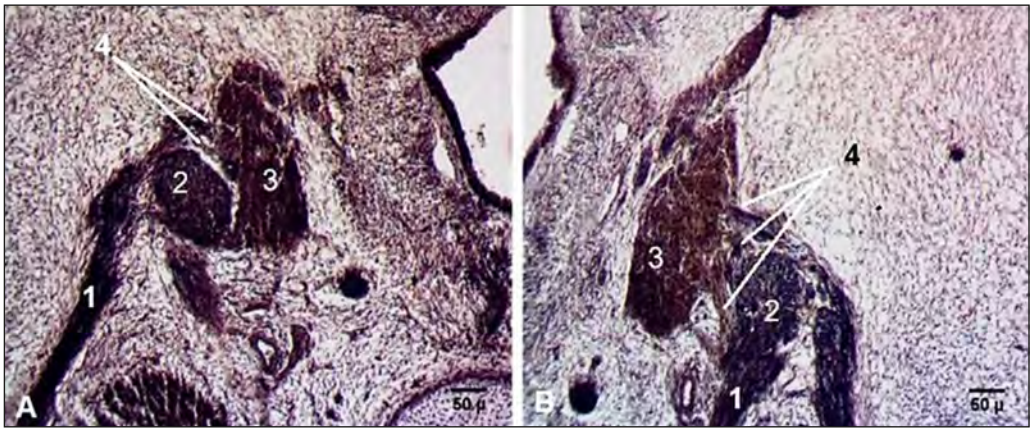

Fig. 6 Connections between the geniculate and vestibular ganglia.

Transverse cross-sections. Fetus (CRL 57 mm). A. Left side. B. Right side. Staining (hematoxylin-eosin). Microphotographs. 1 – facial nerve; 2 – geniculate ganglion; 3 – vestibular ganglion; 4 – connections between the geniculate and vestibular ganglia.

Among the specific features of the geniculate ganglion were its connections with the vestibular ganglion. At Carnegie stage 20, a thin connection between the geniculate and vestibular ganglia was highlighted. In fetuses, those connections became thicker and stronger (Fig 6).

Two abnormalities of the facial nerve were found among the examined embryos and fetuses. On a sagittal section of an embryo at Carnegie stage 19 (CRL 17 mm), a double, overlapping enlargement of the geniculate ganglion, from which two separate facial trunks derived, was detected (Fig.

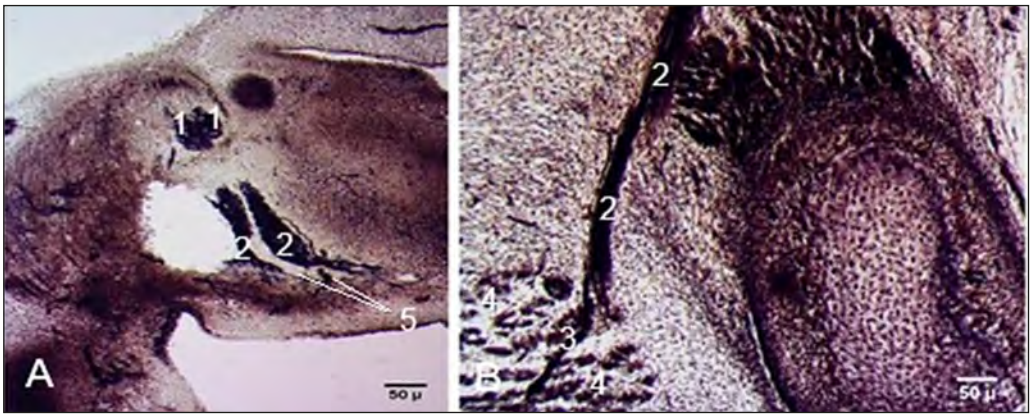

Fig. 7 Abnormal development of the facial nerve.

A. Double facial nerve trunk. Sagittal section. Embryo at Carnegie stage 19 (CRL 17 mm). B. Aberrant branch from the facial nerve to the sternocleidomastoid muscle. Transverse cross-section. Fetus (CRL 57 mm). Staining (hematoxylin-eosin). Microphotographs. 1 – geniculate ganglion; 2 – facial nerve; 3 – aberrant branch to the sternocleidomastoid muscle; 4 – sternocleidomastoid muscle; 5 – connections between the facial nerve trunks.

7A). Each facial trunk distally divided into multiple branches, giving rise to the parotid plexus. The peripheral branches of the anterior trunk were directed anteriorly, while those of the posterior trunk were spread both anteriorly and posteriorly, and a connection between these two trunks was revealed. In a fetus (CRL 57 mm), an aberrant branch to the sternocleidomastoid muscle, considered casuistic, was found (Fig. 7B).

Discussion

In the third week of embryonic development, no branches of the facial nerve or ganglia are distinguished; however, the facio-acoustic primordium is already formed [13, 14, 22].

At Carnegie stage 13, the facial nerve forms "a complex structure with the vestibulocochlear ganglion", which, by stage 14, divides into separate ganglia [20]. In the current study, the facio-acoustic primordium in the third week of embryonic life appeared as a triangular structure, separated by a narrow furrow into the facial nerve and acoustic ganglion.

A "fan-shaped pattern" of the facial nerve exit from the hindbrain nuclei located at the level of r4 and r5 was described in mice [23]. The fibers exiting the brain from the nuclei at the level of r4 entirely contributed to the formation of the facial nerve trunk. Two groups of nuclei were identified at the level of r5–a medial and a lateral one–and only the axons of the medial nuclear group participated in the formation of the motor root of the facial nerve. The axons of the lateral group of nuclei were considered to be preganglionic parasympathetic fibers [23].

Bruska et al. noted that, at stage 13, the geniculate ganglion consisted of vertical rows of cells running parallel to the facial nerve fibers, and the ganglion appeared as a separate morphological structure [24, 25]. According to Gasser, "the geniculate ganglion is well defined in 11.0-13.5 mm embryos" [26]. In our series of embryos, the geniculate ganglion appeared as a separate structure in embryos with a CRL of 11 mm. A specific feature of the geniculate ganglion was its tendency to change shape–from ovoid to fusiform and triangular–although the oval shape was generally characteristic of the ganglion. In the investigated samples, the central part of the geniculate ganglion consisted of nerve fibers, laterally bounded by two nerve cords of neuroblasts. In the core of the ganglion, parallel rows of neuroblasts were identified. At stage 18, the neuroblasts were large, and many more nerve fibers were present in the geniculate ganglion compared with the acoustic ganglion.

Danilo emphasized that the external knee of the facial nerve begins its formation during the sixth week of development [14]. In the current study, changes in the course of the facial nerve and its bending around the otic capsule were observed during the same period of gestation. The facial nerve emerged from the brain as many thin fibers that continued into the facial nerve trunk, from which the chorda tympani nerve at stage 14 and the greater petrosal nerve at stage 15 originated. Similar results were reported by Lobko [27].

According to Gasser, the peripheral divisions of the facial nerve began the parotid plexus formation in 18 mm embryos, while in our investigations the secondary divisions of the facial nerve were observed in embryos with a CRL of 14 mm, and some of those branches spread distally in a network fashion [26].

It is considered that migration of the pharyngeal efferent neurons influences the formation of the facial nerve internal knee, which appears at Carnegie stage 23 [25]. In our study, the internal knee of the facial nerve was also observed at Carnegie stage 23.

Experimental studies have proved that the zinc finger gene Krox-20 is a segment-specific regulator of HOX gene expression [9]. A similar regulatory effect on HOX gene expression is exerted by retinoic acid [28]. Under the influence of retinoic acid and the zinc finger Krox-20 gene, a transformation of the motor portion of the trigeminal nerve into the facial nerve was observed. The r2/3 transformed into r4/5, and subsequently the entire portion of the trigeminal area transformed into the facial-vestibuloacoustic area. Changes in HOXB1 gene expression resulted in duplications of r2/3 into r4/5, but no changes were noted in the normal r4/5 segments [9, 28].

Neural crest cells are multipotent and highly migratory. They are influenced by a range of cell signaling factors such as Fibrobrlast Growth Factor, Bone Morphogenetic Proteins,

retinoic acid, Notch ligands, Receptor Tyrosine Kinases, and Wnt proteins. These signaling pathways are active in the neural placodes and neural cells precursors that give rise to the cranial nerves. Disturbances in neural cell migration and differentiation can lead to various malformations and aberrant neurogenesis of the cranial nerves [29], including variations in the number and course of the facial nerve trunk [30]. The aberrant branch of the facial nerve to the sternocleidomastoid muscle could result from fusion of the posterior belly of the digastric muscle with the sternocleidomastoid muscle [31].

Conclusions

The development of the facial nerve is influenced by a range of factors, among which are HOX genes, neural crest cell migration and differentiation, signaling molecules, and viral and bacterial infections during the first 8 weeks of pregnancy. Early specific features of facial nerve development include: 1) intracerebral and peripheral connections with the neighboring cranial nerves; 2) intraplexal connections of the parotid plexus branches; 3) distinguishable intracerebral pathways; 4) connections of the geniculate ganglion with the vestibular ganglion. As late developmental peculiarities, the following were identified: 1) changeable macro- and microstructure of the geniculate ganglion; 2) appearance of the *pes anserinus minor*; 3) formation of the motor nucleus, internal knee, and intracerebral pathways. The developmental specific features of the facial nerve are obvious evidence of its complex morphology in adults.

Competing interests

None declared.

Authors' contributions

AB – conception and design of the work. AB, NT – contribution to acquisition of data. AB, ZZ, IC, NT – contribution to analysis and interpretation of data. AB, ZZ, IC, NT, ABend, NO, SL – drafting the article. All authors reviewed the work and approved the final version of the manuscript.

Acknowledgements and funding

No external funding.

Ethics approval

This research project was approved by the Research Ethics Committee of *Nicolae Testemițanu* State University of Medicine and Pharmacy of the Republic of Moldova (Minutes no. 1 of 19.09.2014) and complies with the 1964 Helsinki Declaration and its later amendments.

Provenance and peer review

Not commissioned, externally peer-reviewed.

References

1. Trainor PA, Krumlauf R. Patterning the cranial neural crest: hindbrain segmentation and Hox gene plasticity. Nat Rev Neurosci. 2000;1(2):116-124. doi: 10.1038/35039056.
2. Müller F, O'Rahilly R. The timing and sequence of appearance of neuromeres and their derivatives in staged human embryos. Acta Anatomica. 1997;158(2):83-99. doi: 10.1159/000147917.
3. Lumsden A, Keynes R. Segmental patterns of neuronal development in the chick hindbrain. Nature. 1989;337(6206):424-428. doi: 10.1038/337424a0.
4. Hunt P, Wilkinson D, Krumlauf R. Patterning the vertebrate head: murine Hox 2 genes mark distinct subpopulations of premigratory and migrating cranial neural crest. Development. 1991;112(1):43-50. doi: 10.1242/dev.112.1.43.
5. Lumsden A. The cellular basis of segmentation in the developing hindbrain. Trends Neurosci. 1990;13(8):329-335. doi: 10.1016/0166-2236(90)90144-Y.
6. Kuratani SC, Eichele G. Rhombomere transplantation repatterns the segmental organization of cranial nerves and reveals cell-autonomous expression of a homeodomain protein. Development. 1993;117(1):105-117. doi: 10.1242/dev.117.1.105.
7. Carpenter EM, Goddard JM, Chisaka O, Manley NR, Capecchi MR. Loss of Hox-A1 (Hox-1.6) function results in the reorganization of the murine hindbrain. Development. 1993;118(4):1063-1075. doi: 10.1242/dev.118.4.1063.
8. Clarke JD, Lumsden A. Segmental repetition of neuronal phenotype sets in the chick embryo hindbrain. Development. 1993;118(1):151-162. doi: 10.1242/dev.118.1.151.
9. Wilkinson DG. Molecular mechanisms of segmental patterning in the vertebrate hindbrain and neural crest. Bioessay. 1993;15(8):499-505. doi: 10.1002/bies.950150802.
10. Frohman MA, Boyle M, Martin GR. Isolation of the mouse Hox-2.9 gene; analysis of embryonic expression suggests that positional information along the anterior-posterior axis is specified by mesoderm. Development. 1990;110(2):589-607. doi: 10.1242/dev.110.2.589.
11. Maden M, Hunt P, Eriksson U, Kuroiwa A, Krumlauf R, Summerbell D. Retinoic acid-binding protein, rhombomeres and the neural crest. Development. 1991;111(1):35-43. doi: 10.1242/dev.111.1.35.
12. Guthrie S, Muchamore I, Kuroiwa A, Marshall H, Krumlauf R, Lumsden A. Neuroectodermal autonomy of Hox-2.9 expression revealed by rhombomere transpositions. Nature. 1992;356(6365):157-159. doi: 10.1038/356157a0.
13. Sataloff RT. Embryology of the facial nerve and its clinical applications. Laryngoscope. 1990;100(9):969-84. doi: 10.1288/00005537-199009000-00011.
14. Danilo AGO. Facial nerve: embryology and anatomy of its nucleus. MOJ Anat Physiol. 2018;5(3):164-166. doi: 10.15406/mojap.2018.05.00183.
15. Babuci A, Catereniuc I, Zorina Z, Botnari T, Lehtman S, Nastas L. Peculiarities of the facial nerve development. In: Trushel' N, editor. Innovatsii i aktual'nye problemy morfologii: Sbornik nauchnykh statei, posviashchennye 100-letiiu kafedry normal'noi anatomii

Belorusskogo gosudarstvennogo meditsinskogo universiteta [Innovations and current problems of morphology: Collection of scientific articles dedicated to the 100th anniversary of the Department of Normal Anatomy of the Belarusian State Medical University], Oct 2021. Minsk: BGMU; 2021, p. 361-365.
16. Sadler TW. Langman's medical embryology. 12th ed. Philadelphia: Lippincott William &Wilkins; 2012; 384 p.
17. Babuci A. Development of the facial nerve in human embryos. In: MedEspera: the 8th International Medical Congress for Students and Young Doctors; 2020 Sep 24-26; Chisinau, Republic of Moldova: Abstract book. Chișinău; 2020. p. 231-232.
18. D'Amico-Martel A, Noden DM. Contributions of placodal and neural crest cells to avian cranial peripheral ganglia. Am J Anat. 1983;166(4):445-468. doi: 10.1002/aja.1001660406.
19. Vazquez E, Calzada B, Naves J, Garnacho SS, del Valle M, Vega JA, Represa J. Developmental changes in nerve growth factor (NGF) binding and NGF receptor proteins trkA and p75 in the facial nerve. Anat Embryol (Berl). 1994;190(1):73-85. doi: 10.1007/BF00185848.
20. Weglowski M, Wozniak W, Piotrowski A, Bruska M, Weglowska J, Sobanski J, Grzymislawska M, Lupicka J. Early development of the facial nerve in human embryos at stages 13-15. Folia Morphol. 2015;74(2):252-257. doi: 10.5603/FM.2015.0039.
21. Robinson HP. Sonar measurement of fetal crown-rump length as means of assessing maturity in first trimester of pregnancy. Br Med J. 1973;4(5883):28-31. doi: 10.1136/bmj.4.5883.28.
22. Sataloff RT, Selber JC. Phylogeny and embryology of the facial nerve and related structures. Part I: Phylogeny. Ear Nose Throat J. 2003;82(9):704, 707-710.
23. Goddard JM, Rossel M, Manley NR, Capecchi MR. Mice with targeted disruption of Hoxb-1 fail to form the motor nucleus of the VIIth nerve. Development. 1996;122(10):3217-3228. doi: 10.1242/dev.122.10.3217.
24. Bruska M, Ulatowska-Błaszyk K, Węgłowski M, Woźniak W, Piotrowski A. Differentiation of the facial-vestibulocochlear ganglionic complex in human embryos of developmental stages 13-15. Folia Morphol (Warsz). 2009;68(3):167-173.
25. Müller F, O'Rahilly R. The initial appearance of the cranial nerves and related neuronal migration in staged human embryos. Cells Tissues Organs. 2011;193(4):215-38. doi: 10.1159/000320026.
26. Gasser RF. The development of the facial nerve in man. Ann Otol Rhinol Laryngol. 1967;76(1):37-56. doi: 10.1177/000348946707600103.
27. Lobko PI, Khil'kevich SI. Promezhutochnyi nerv i ego mesto v sisteme cherepnykh nervov [The intermediate nerve and its place in the system of cranial nerves]. Arkh Anat Gistol Embriol. 1989;97(9):37-46. Russian.
28. Marshall H, Nonchev S, Sham MH, Muchamore I, Lumsden A, Krumlauf R. Retinoic acid alters hindbrain Hox code and induces transformation of rhombomeres 2/3 into a 4/5 identity. Nature. 1992;360(6406):737-741. doi: 10.1038/360737a0.
29. Méndez-Maldonado K, Vega-López GA, Aybar MJ, Velasco I. Neurogenesis from neural crest cells: molecular mechanisms in the formation of cranial nerves and ganglia. Front Cell Dev Biol. 2020;8:635. doi: 10.3389/fcell.2020.00635.
30. Babuci A, Catereniuc I, Zorina Z, Bendelic A, Botnari T, Stepco E, Lehtman S, Strisca S, Nastas L, Motelica G, Procopenco O. Morphology and variability of the facial nerve trunk depending on the branching pattern, gender, anthropometric type and side of the head in Moldovan population. Folia Morphol (Warsz). 2023;82(4):791-797. doi: 10.5603/FM.a2022.0088.
31. Cvetko E. Sternocleidomastoid muscle additionally innervated by the facial nerve: case report and review of the literature. Anat Sci Int. 2015;90(1):54-6. doi: 10.1007/s12565-013-0224-8.

https://doi.org/10.52645/MJHS.2025.3.03

UDC: 611.133

RESEARCH ARTICLE

Variants of the common carotid artery branching patterns

Nadia Ostahi*, Angela Babuci, Ilia Catereniuc, Anastasia Bendelic, Zinovia Zorina

Department of Anatomy and Clinical Anatomy, *Nicolae Testemiţanu* State University of Medicine and Pharmacy, Chisinau, Republic of Moldova

ABSTRACT

Introduction. The common carotid artery is the main source of blood supply to the head and neck regions. Its branching patterns are of great interest in terms of both anatomical and clinical significance. Variability of the common carotid artery can influence the planning of vascular, endovascular and oncological interventions in the head and neck regions, to avoid vessel injuries as well as intra-operative and postoperative complications.

Material and methods. Variants of branching patterns of the common carotid artery were studied retrospectively on a sample size of 210 patients (118 males and 92 females). The mean age of patients was 63.6±13.44 years for males and 65.1±14.32 years for females (p = 0.444). Patients were examined by CT angiography, during the period 2020-2024, within the Institute of Emergency Medicine and Republican Center for Medical Diagnostics. The purpose of this article was to identify anatomical variations in the branching pattern of the CCA based on gender and laterality.

Results. The most frequent variant of the CCA branching pattern, considered a normal variant, was its bifurcation, identified on the right side in 70% of cases (n = 147) and on the left side in 54% (n = 113). The trifurcation of the CCA was more common on the left side (33.3%), compared to the right side (25.7%). The origin of the superior thyroid artery from the CCA trunk was observed in 12.8% of cases on the right side and in 3.8% on the left one. A rare variant revealed in the current study was the origin of the lingual artery from the CCA trunk (0.4%).

Conclusions. The branching variants of the common carotid artery are of clinical significance, particularly in surgical interventions on the neck. Knowledge of the topographic relationships of the CCA with the neighboring anatomical landmarks is essential to prevent intra-operative complications and improve the quality of surgical management.

Keywords: common carotid artery, carotid bifurcation, superior thyroid artery, lingual artery.

Cite this article: Ostahi N, Babuci A, Catereniuc I, Bendelic A, Zorin Z. Variants of the common carotid artery branching patterns. Mold J Health Sci. 2025;12(3):20-26. https://doi.org/10.52645/MJHS.2025.3.03.

Manuscript received: 09.07.2025

Accepted for publication: 15.08.2025

Published: 15.09.2025

***Corresponding author**: Nadia Ostahi, MD, PhD fellow,
Department of Anatomy and Clinical Anatomy,
Nicolae Testemiţanu State University of Medicine and Pharmacy,
Chisinau, Republic of Moldova
165, Stefan cel Mare si Sfânt blvd., Chisinau, Republic of Moldova, MD2004
e-mail: nadia.ostahi@usmf.md

Authors's ORCID IDs
Nadia Ostahi – https://orcid.org/0009-0003-7197-0178
Angela Babuci – https://orcid.org/0000-0003-0305-1279
Ilia Catereniuc – https://orcid.org/0000-0002-5479-4198,
Anastasia Bendelic – https://orcid.org/0000-0002-2838-3168
Zinovia Zorina – https://orcid.org/0000-0002-0749-6083

Key messages

What is not yet known on the issue addressed in the submitted manuscript

Considering that variants of the common carotid artery branching patterns are mainly studied based on a single or two criteria, our study was designed to provide comprehensive additional information by analyzing these patterns in relation to gender, laterality, and their topographical relationships with the neighboring anatomical structures and some landmarks, that could be useful for surgical access of the neck region.

The research hypothesis

The increasing number of head and neck surgeries requires detailed knowledge of common carotid artery variations, including its branching patterns variants and the topographical relationships of its branches with the adjacent anatomical structures.

The novelty added by the manuscript to the already published scientific literature

The identified arterial variants highlight the necessity of anatomical revision of the common carotid artery branching patterns, which are infrequently described in the specialized literature. Knowledge of these variations is clinically important for vascular head and neck surgery, oncology and interventional procedures, as it helps prevent iatrogenic injuries.

Introduction

The common carotid artery (CCA) is the main source of blood supply to the head and neck regions. At the superior border of the thyroid cartilage, it bifurcates into its primary branches: the internal carotid artery (ICA) and the external carotid artery (ECA). However, anatomical and imaging studies have revealed significant variability in the origin, level and angle of its bifurcation and branching patterns of the CCA [1-3].

Disturbances of the embryonic development at any Carnegie stage can result in abnormal development of the arterial system components, which can be caused by the regression or disappearance of some blood vessels, or due to their incomplete development [4]. In cases of arterial variants, they are detected during routine examinations by imaging methods or postmortem by anatomical dissection [5, 6].

According to bibliographic sources, about 10% of malpractice was recorded in surgical patients with anatomical variants [5]. The contemporary methods of imaging such as computed tomography, nuclear magnetic resonance, and three-dimensional reconstructions, offer the possibility of preoperative visualization of the blood vessels, decreasing the rate of iatrogenic injures [7].

Among the clinically important, anatomical branching pattern variants of CCA, is the origin of the superior thyroid artery directly from the common carotid artery, or its deviation from the main trunk of the CCA at the level of its bifurcation, with a variation rate of 2.2% - 61% [1, 8-10].

According to the results obtained by Esen et al. in 2018, who performed a large study on 1280 angiographies, the origin of the right superior thyroid artery from the CCA bifurcation was found in 20.5% of cases and of the left artery in 23.1% [11]. The origin of the superior thyroid artery directly from the CCA was reported in 14.1% of cases on the right and 35.3% on the left, respectively.

Bhardwaj et al. analyzed the origin of the superior thyroid artery on a sample size of 210 subjects [12]. The obtained result showed that in 14.3% of cases the superior thyroid artery derived at the level of the CCA bifurcation, while in 8.6% it originated directly from the CCA trunk.

The variability of the superior thyroid artery origin and its relationships to the superior laryngeal nerve are of particular importance in thyroidectomy [13]. In surgical interventions on the thyroid gland, injuries to the superior laryngeal nerve can occur at rates as high as 58% [14, 15].

Quadri- and pentafurcation of the CCA have been reported in the specialized literature as rare anatomical variants. Zaccheo et al. described a rare case of pentafurcation in which the CCA divided into the superior thyroid artery, lingual artery, facial artery, external carotid artery and internal carotid artery [16]. Kaneko et al. described another very rare case, when the superior thyroid artery, lingual artery and facial artery derived directly from the CCA, while the posterior auricular, maxillary and superficial temporal arteries arose from a common trunk. The internal carotid artery also originated from the CCA, and the occipital and ascending pharyngeal arteries arose from it [17].

Knowledge of anatomical variants related to CCA branching patterns is important both an anatomical and a clinical perspective. These variations can influence the planning of vascular, endovascular and oncological interventions in the head and neck regions, and are extremely important for avoiding vascular injuries and improving intraoperative and postoperative management [13, 18].

The purpose of our study was to identify anatomical variations in the CCA branching patterns depending on gender and laterality.

Material and methods

Variants of the CCA branching patterns were studied retrospectively on a sample size of 210 patients who underwent CT angiography of the carotid artery during the period 2020-2024, at the Institute of Emergency Medicine and the Republican Center for Medical Diagnostics. The study was approved by the Research Ethics Committee of *Nicolae Testemitanu* State University of Medicine and Pharmacy, based on decision No.3 dated 27.01.2025. The representative sample size was calculated using the EpiInfo7.2.2.6 program, under the "StatCalc – Sample Size and Power" module, based on the following parameters: confidence interval – 95.0% for statistical significance, statistical power – 80.0%, an expected outcome difference of 20.0% in patients with anatomical variants of the common carotid artery, PR = 2, and an equal group ratio of 1:1. The calculated value was 182, after adjusting for an estimated non-response rate of 10.0%, the final required sample size was 200.

The study group included 118 males and 92 females. The mean age of male patients was 63.6±13.44 years and the mean age of female patients was 65.1±14.32 years, (p = 0.444). To achieve the proposed aim and objectives, angiographic images of 400 carotid arteries were analyzed and processed. Based on this analysis, the absolute and relative values of the incidence of common carotid artery branching patterns were determined, depending on sex, laterality and neighboring anatomical landmarks. For CT angiographies of the carotid artery, the Canon Aquilion 320 slices computed tomography, which provides high-resolution images, was used. Subsequently, the angio-CT images were analyzed and interpreted using the RadiAnt DICOM Viewer 2024.1 software, with capacity of multiplanar and three-dimensional

reconstructions and maximum intensity projections, which allowed us to visualize in detail the branching variants of the CCA and to perform their morphometry. The data were stored in an Excel database, and statistical analysis was performed using predefined statistical functions in Excel. The frequency of anatomical variants according to sex, laterality, and neighboring anatomical landmarks was estimated by calculating the confidence interval at a 95% confidence interval.

To enhance the accuracy of the study, clear inclusion and exclusion criteria were established, allowing for the selection of a representative and homogeneous group of participants.

Inclusion criteria:

- Patients examined by CT angiography of the carotid artery >18 years old;
- Patients with clear and visible angiographic images.

Exclusion criteria:

- Patients examined by CT angiography of the carotid artery <18 years old;
- Patients with unclear or poor-quality angiographic images;
- Patients who have undergone surgical interventions involving the carotid arteries;
- Patients in flexion, retroflexion or laterally tilted head.

Results

In the current study, 420 CCAs were examined. The most frequent branching pattern of the CCA, considered a normal variant, was its bifurcation into ICA and ECA, being identified on the right side in 70% of cases (n = 147) and on the left side in 54% (n = 113). This variant was more frequently found in males (55.3%).

Another branching pattern variant of the CCA was its trifurcation into the ICA, ECA and superior thyroid artery (Fig. 1). The CCA trifurcation was more prevalent on the left side (33.3%) than on the right side (25.7%). The bilateral distribution of the CCA trifurcation was observed in 16.9% (n = 21), predominating in males (57.1%), compared to females (42.8%).

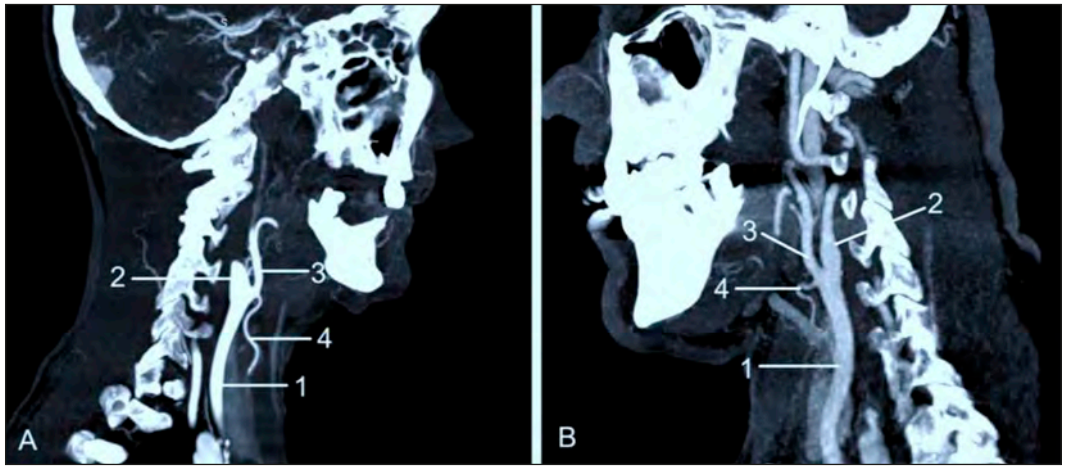

Fig. 1 Trifurcation of the common carotid artery.

A. Lateral view (right side). B. Lateral view (left side). 1 – common carotid artery; 2 – internal carotid artery; 3 – external carotid artery; 4 – superior thyroid artery.

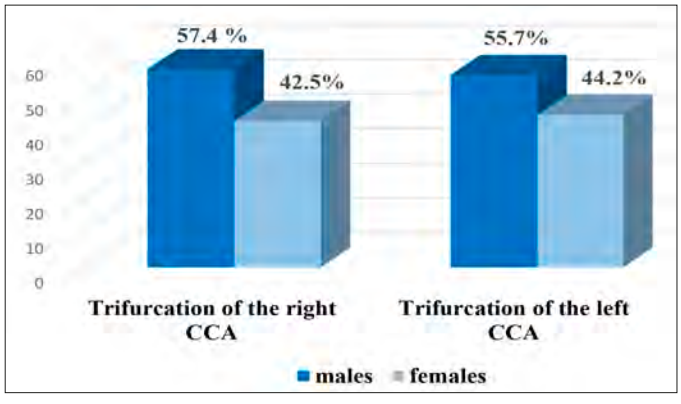

Fig. 2 Sex-based distribution of the common carotid trifurcation

Note: *CCA – common carotid artery*

On the right side, the trifurcation of the CCA was found in 57.4% of males (n = 31), while in females, the rate was 42.5% (n = 23). The left CCA trifurcation was found in 55.7% (n = 39) of males, and in 44.2% (n = 31). Our results showed a slight bilateral predominance of CCA trifurcation in males. The distribution of this variant depending on gender and laterality is presented in figure 2.

In 16.6% of cases, the common carotid artery divided into three branches ICA, ECA and superior thyroid artery (STA). The STA originated directly from the CCA below its bifurcation (Fig. 3). This variant was observed on the right side in 12.8% of cases and on the left side in 3.8%.

Similar to the CCA trifurcation, this variant (a high-origin superior thyroid artery) was more prevalent in males. In the male cohort, its distribution was nearly equal bilaterally, occurring on the right side in 62.5% of cases and on the left in 62.6%.In females, the distribution was also nearly equal between the left and right sides (37.5% and 37.0%, respectively).. The bilateral distribution of the origin of the superior thyroid artery below the bifurcation level per study group reached a rate of 11.4%.

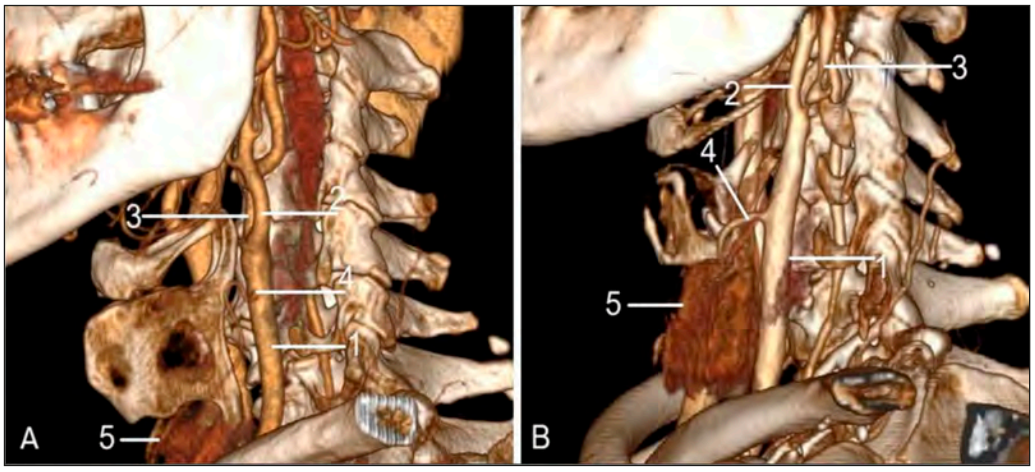

Fig. 3 Origin of the superior thyroid artery directly from the common carotid artery.

A, B. Anterolateral view (left side). 1 – common carotid artery; 2 – external carotid artery; 3 – internal carotid artery; 4 – superior thyroid artery; 5 – thyroid gland.

As a result of the morphometry of the distance between the CCA bifurcation (CCAB) and the origin of the superior thyroid artery (OSTA), four groups of variables were established (Fig.4).

- Group I included patients with the distance between OSTA and CCAB < 0.5 cm;
- Group II – patients with the distance between OSTA and CCAB 0.51 cm – 1 cm;
- Group III – patients with the distance between OSTA and CCAB 1.1 cm – 1.5 cm;
- Group IV – patients with the distance between OSTA and CCAB > 1.51 cm.

The obtained results demonstrate a higher frequency of the origin of the superior thyroid artery at a distance < 0.5 cm in relation to the level of the CCA bifurcation. This proximity may create uncertainty when identifying the STA during surgical interventions on the thyroid gland.

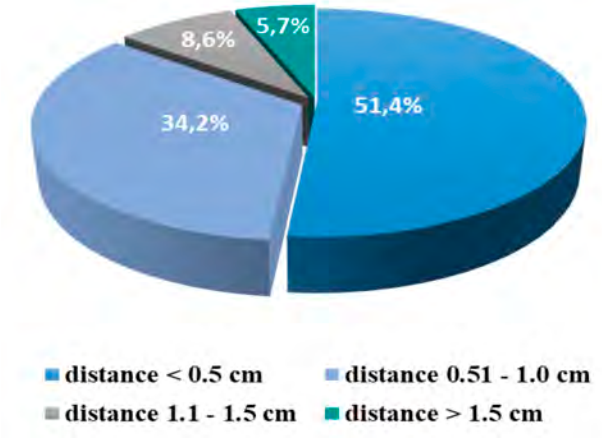

Fig. 4 Range-based analysis of superior thyroid artery origin relative to the common carotid artery bifurcation.

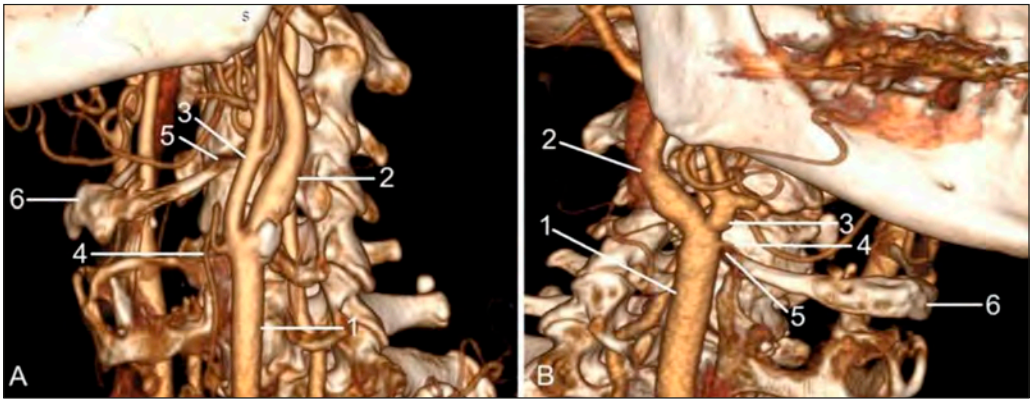

Fig. 5 Origin of the superior thyroid artery in relation to the hyoid bone.

A. Anterolateral view (left side). Origin of the superior thyroid artery, below the hyoid bone.
B. Anterolateral view (right side). Origin of the superior thyroid artery, above the hyoid bone.
1 – common carotid artery; 2 – internal carotid artery; 3 – external carotid artery; 4 – superior thyroid artery; 5 – greater horn of the hyoid bone

The origin of the superior thyroid artery from the level of the CCA bifurcation and directly from its trunk was analyzed in relation to the greater horn of the hyoid bone, which is an important anatomical landmark in the cervical region (Fig. 5).

Our results showed that in 20.1% of cases, the origin of the STA was above the greater horn of the hyoid bone, and in 14.5% of cases, it was at the level of the greater horn of the hyoid bone, and in 65.4% of cases it was below it.

When analyzed by laterality, the most common location for the superior thyroid artery's origin was below the greater horn of the hyoid bone. This pattern was observed in 64.5% of cases on the right side and 66.0% on the left. On the left side, the artery originated superior to the greater horn in 21.6% of cases and at the same level as the horn in 12.3%. On the right side, the artery's origin was superior to the horn in 17.7% of cases and at the same level as the horn in another 17.7%. Among the anatomical variants

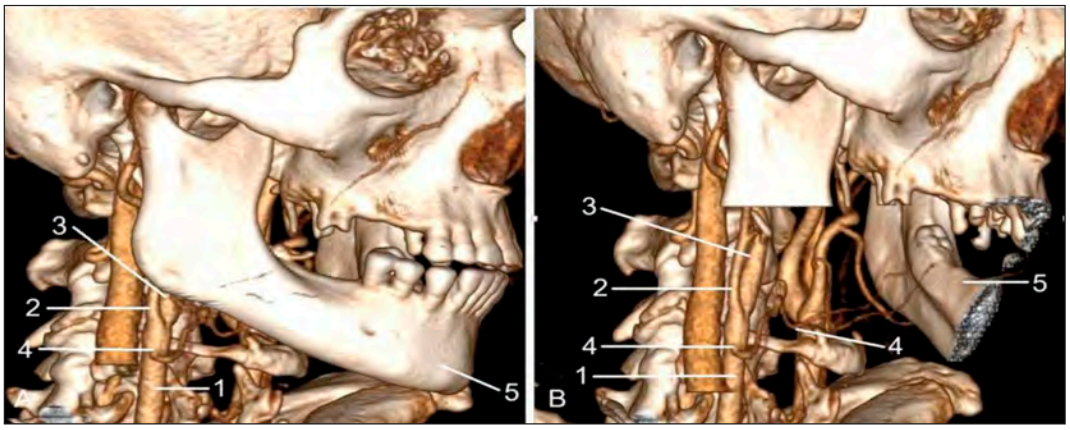

Fig. 6 Origin of the lingual artery directly from the common carotid artery.

A, B. anterolateral view, right side. 1 – common carotid artery; 2 – external carotid artery; 3 – internal carotid artery; 4 – superior thyroid artery.

highlighted in the study group, a rare branching pattern of the CCA, from which derived the ICA, ECA and lingual artery was identified (Fig. 6).

This variant was detected in a single female patient, constituting 0.4%. In this case, the lingual artery originated directly from the lateral semicircumference of the CCA, 0.91 cm below the main bifurcation. The artery then followed a semi-arcuate path, oriented anteromedially to the CCA, before continuing toward the tongue.

Discussion

According to bibliographic sources, there is evidence of increased variability of the common carotid artery branching patterns [2, 8, 15, 18, 19]. The most common variant, considered a normal variant, is the bifurcation of the common carotid artery into the internal carotid artery and the external carotid artery, reported in 61.5% [19]. In our study, the bifurcation of the CCA was found in 70% of cases on the right side and in 54% on the left side.

Other anatomical variants described in the specialty literature are the trifurcation, quadrifurcation and pentafurcation of the CCA. Ogeng's et al. conducted a study on 208 cadavers, reporting trifurcation of the CCA into the ICA, ECA and superior thyroid artery in 31.7% of cases [19]. Quadrifurcation of the CCA into the ICA, ECA, superior thyroid artery and ascending pharyngeal artery was found in 5.4%, and pentafurcation of the CCA into the ICA, ECA, superior thyroid artery, posterior auricular artery and occipital artery was revealed in 1.4%.

Some authors pointed out that CCA trifurcation, when the third branch is the superior thyroid artery, is the most common variant. Gupta et al. reported this variant in 21.5% of cases on the right side and 18.5% on the left [20], while Vazquez et al. observed a twice higher frequency of that variant, up to 49% [21].

Our results are in line with the data reported in the literature, but with a slight predominance of trifurcation on the left side with a ratio left/right of 33.3%/25.7%. Quadrifurcation and pentafurcation of the CCA were not identified in our sample size.

The direct origin of the superior thyroid artery from the CCA trunk, or from its bifurcation level has been studied by several authors. Calotă et al. found direct origin of the STA from the CCA in 8.8% and from the level of the CCA bifurcation in 28.8% [22]. Poutoglidis et al. conducted a meta-analysis study of the superior thyroid artery origin on 5488 cases, reported in the literature [23]. Their results showed that in 55% of cases the superior thyroid artery derived from the ECA. The STA origin from the level of the CCA bifurcation was marked out in 27.5%, from the CCA trunk in 15% and, very rarely, from the ICA with a rate of 0.05%, while Herrera-Núñez et al. found the origin of the superior thyroid artery at the CCA bifurcation in 20.4% of cases, and the direct from the CCA was reported in 17.1% [24].

In our study, the origin of the superior thyroid artery from the bifurcation level of the CCA was observed in 29.5% and in 8.3% from its trunk. Our results are consistent with data reported in the literature.

Knowledge about the origin of the superior thyroid artery is essential in planning surgical interventions. According to Tzortziset et al. in thyroid surgery, the superior thyroid artery should be ligated as close as possible to its origin, to avoid injury to the superior laryngeal nerve [25].

The origin of the superior thyroid artery from the CCA trunk, or from its bifurcation has been studied in relation to the hyoid bone. Calotă et al. classified the detected variants into three groups: infrahyoid origin (47%), origin at the level of the greater horn of the hyoid bone (25.8%), and suprahyoid origin (24.7%) [22].

Our data demonstrated the prevalence of the origin of the superior thyroid artery inferior to the greater horn of the hyoid bone in 65.4%. The suprahyoid origin was identified in 20.1% of cases, and its origin at the level of the greater horn of the hyoid bone was found in 14.5%.

The direct origin of the thyrolingual trunk from the CCA represents a rare variant of the CCA branching pattern, with a rate of 0.3%-1% [26]. Kapre et al. reported a case of the thyrolingual trunk origin from the level of the CCA bifurcation and in another case, the thyrolingual trunk was noted at 17 mm below the CCA bifurcation [27].

In rare cases the lingual artery derives directly from the CCA. Jadhov et al. reported a clinical case, when the lingual artery originated from the medial circumference of the CCA, at 6 mm below the CCA bifurcation [28].

Our results confirmed the data reported in the specialty literature, thus, in 0.4% of cases, the lingual artery derived directly from the CCA, at 9.1 mm below its bifurcation.

Conclusions

Knowledge of the common carotid artery branching pattern variation and its topographic relationships with the neighboring anatomical landmarks is of high clinical significance, playing an essential role in preventing intraoperative complications and improving the quality of surgical management.

Competing interests

None declared.

Authors' contributions

Conception and design of the work – NO, AB, IC. Contribution to acquisition of data NO. Contribution to analysis and interpretation of data NO, AB. Drafting the article NO, AB, IC, AB, ZZ. All authors critically reviewed the work and approved the final version of the manuscript.

Ethics approval

The research project was approved by the Research Ethics Committee of *Nicolae Testemițanu* State University of Medicine and Pharmacy (Minutes no. 3 from 27.01.2025).

Patient consent

Obtained.

Acknowledgements and funding

No external funding.

Provenance and peer review

Not commissioned, externally peer reviewed.

References

1. Biskupski M, Homzar S, Dąbrowska Z, Buczek J, Daniluk A, Iwaniuk K, et al. Clinical implications of variations of common carotid artery trifurcation. J Pre Clin Clin Res. 2024;18(1):83-7. https://doi.org/10.26444/jpccr/186029.
2. Abdalla M, Mohammed N, Abdallah R, Ahmed MK, Abdelrahim M, Salih A, et al. Anatomical variations of the bifurcation levels of the common carotid artery and superior thyroid artery. Cureus. 2024;16(10):e71120. doi: 10.7759/cureus.71120.
3. Kumar M, Kumar A, Ahuja CK, Khurana D. (Un) common carotid trifurcation. Neurol India. 2025;73(2):349-351. doi: 10.4103/neuroindia.NI_370_19.
4. Zorina Z, Catereniuc I, Babuci A, Botnari T, Certan G. Variants of branching of the upper limb arteries. Mold Med J. 2017;60(4):33-38. doi: 10.5281/zenodo.1106127.
5. Alraddadi A. Literature review of anatomical variations: clinical significance, identification approach, and teaching strategies. Cureus. 2021;13(4):e14451. doi: 10.7759/cureus.14451.
6. Rodriguez A, Cobeñas R, Gallo JC, Salamida A, Larrañaga N, Kozima S. Variantes anatómicas vasculares halladas de manera incidental en estudios de tomografía computada [Incidental findings of vascular anatomic variants on computed tomography]. Rev Argent Radiol. 2013;77(1):19-25. Spanish. doi: 10.7811/rarv77n1a03.
7. Sharma R, Nishan S, Yadav SK, Choudhary D. A comprehensive review of anatomical variations and their clinical significance in surgical procedures . J Ayurveda Integr Med Sci. 2025;10(5). https://doi.org/10.21760/jaims.10.5.20.
8. Thenmozhi A, Subadha C, Aruna K, Prabavathi P. Variations in the origin of superior thyroid artery-a cadaveric study in the south indian population. Int J Acad Med Pharm, 2024;6(4):526-529. doi: 10.47009/jamp.2024.6.4.103.
9. Triantafyllou G, Paschopoulos I, Duparc F, Tsakotos G, Tsiouris C, Olewnik Ł, Georgiev G, Zielinska N, Piagkou M. The superior thyroid artery origin pattern: a systematic review with meta-analysis. Surg Radiol Anat. 2024;46(9):1549-1560. doi: 10.1007/s00276-024-03438-2.
10. Borges A, Ramalho S, Ferreira L. Common carotid artery trifurcation: a potentially dangerous anatomical variant. BMJ Case Rep. 2021;14(2):e241104. doi: 10.1136/bcr-2020-241104.
11. Esen K, Ozgur A, Balci Y, Tok S, Kara E. Variations in the origins of the thyroid arteries on CT angiography. Jpn J Radiol. 2018;36(2):96-102. doi: 10.1007/s11604-017-0710-3.
12. Bhardwaj Y, Singh B, Bhadoria P, Malhotra R, Tarafdar S, Bisht K. Computed tomography angiographic study of surgical anatomy of thyroid arteries: clinical implications in neck dissection. World J Radiol. 2023;15(6):182-190. doi: 10.4329/wjr.v15.i6.182.
13. Dessie MA. Variations of the origin of superior thyroid artery and its relationship with the external branch of superior laryngeal nerve. PLoS One. 2018;13(5):e0197075. https://doi.org/10.1371/journal.pone.0197075.
14. Kowalczyk KA, Majewski A. Analysis of surgical errors associated with anatomical variations clinically relevant in general surgery. Review of the literature. Transl Res Anat. 2021;23:100107. https://doi.org/10.1016/j.tria.2020.100107.
15. Bednarz M, Gromaszek M, Daniluk A, Iwaniuk K, Samczuk M, Białkowska Z, et al. Superior thyroid artery – variations of origin and clinical significance. J Pre Clin Clin Res. 2024;18(2):168-74. https://doi.org/10.26444/jpccr/188620.
16. Zaccheo F, Mariotti F, Guttadauro A, Passaretti A, Campogrande ME, et al. A rare configuration origin of the superior thyroid, lingual and facial arteries in a pentafurcated common carotid artery. Anatomia. 2022;1(2):204-209. https://doi.org/10.3390/anatomia102002016.
17. Kaneko K, Akita M, Murata E, Imai M, Sowa K. Unilateral anomalous left common carotid artery; a case re-

port. Ann Anat. 1996;178(5):477-80. doi: 10.1016/S0940-9602(96)80147-6.
18. Lo A, Oehley M, Bartlett A, Adams D, Blyth P, Al-Ali S. Anatomical variations of the common carotid artery bifurcation. ANZ J Surg. 2006;76(11):970-2. doi: 10.1111/j.1445-2197.2006.03913.x.
19. Ogeng'o JA, Misiani MK, Loyal P, Ongeti KW, Gimongo J, Inyimili MI, et al. Variant termination of the common carotid artery: cases of quadrifurcation and pentafurcation. Anat J Af. 2014;3(3 Suppl):386-392.
20. Gupta P, Bhalla AS, Thulkar S, Kumar A, Mohanti BK, Thakar A, Sharma A. Variations in superior thyroid artery: a selective angiographic study. Indian J Radiol Imaging. 2014;24(1):66-71. doi: 10.4103/0971-3026.130701.
21. Vázquez T, Cobiella R, Maranillo E, Valderrama FJ, McHanwell S, Parkin I, Sañudo JR. Anatomical variations of the superior thyroid and superior laryngeal arteries. Head Neck. 2009;31(8):1078-85. doi: 10.1002/hed.21077.
22. Calotă RN, Rusu MC, Rusu MI, Dumitru CC, Vrapciu AD. Anatomical variables of the superior thyroid artery on computed tomography angiograms. Medicina (Kaunas). 2025;61(5):775. doi: 10.3390/medicina61050775.
23. Poutoglidis A, Savvakis S, Karamitsou P, Forozidou E, Paraskevas G, Lazaridis N, Fyrmpas G, Karamitsou A, Skalias A. Is the origin of the superior thyroid artery consistent? A systematic review of 5488 specimens. Am J Otolaryngol. 2023;44(2):103823. doi: 10.1016/j.amjoto.2023.103823.
24. Herrera-Núñez M, Menchaca-Gutiérrez JL, Pinales-Razo R, Elizondo-Riojas G, Quiroga-Garza A, Fernandez-Rodarte BA, Elizondo-Omaña RE, Guzmán-López S. Origin variations of the superior thyroid, lingual, and facial arteries: a computed tomography angiography study. Surg Radiol Anat. 2020;42(9):1085-1093. doi: 10.1007/s00276-020-02507-6.
25. Tzortzis AS, Antonopoulos I, Pechlivanidou E, Chrysikos D, Pappas N, Troupis T. Anatomical variations of the superior thyroid artery: a systematic review. Morphologie. 2023;107(358):100597. doi: 10.1016/j.morpho.2023.03.002.
26. Tsakotos G, Triantafyllou G, Vlychou M, Vassiou K, Kalamatianos T, Piagkou M. An ectopic thyrolingual trunk arising from the common carotid artery: a rare variant. Surg Radiol Anat. 2024;46(8):1301-1303. doi: 10.1007/s00276-024-03426-6.
27. Kapre M, Mangalgiri AS, Mahore D. Study of thyro-lingual trunk and its clinical relevance. Indian J Otolaryngol Head Neck Surg. 2013;65(2):102-4. doi: 10.1007/s12070-011-0411-7.
28. Jadhav SD, Ambali MP, Patil RJ. Anatomical variation of the origin of the right lingual artery. Int J Anat Var. 2011;4:75-8.

https://doi.org/10.52645/MJHS.2025.3.04

UDC: 616.127-005.4

RESEARCH ARTICLE

Diastolic dysfunction and myocardial ischemia in TAVI patients

Marcel Abraş[1,2*], Ecaterina Pasat[2], Maria-Magdalena Vicol[2], Cătălina Ciorici[1], Daniela Bursacovschi[2]

[1]Discipline of Cardiology, Department of Internal Medicine, *Nicolae Testemițanu* State University of Medicine and Pharmacy, Chisinau, Republic of Moldova
[2]Institute of Cardiology, Chisinau, Republic of Moldova

ABSTRACT

Introduction. Severe aortic stenosis and ischemic coronary artery disease are frequently associated in elderly patients, adding complexity to interventional management. Diastolic dysfunction, a marker of myocardial impairment and elevated filling pressures, may influence prognosis after transcatheter aortic valve implantation (TAVI), particularly in the presence of concomitant coronary pathology. The aim of the study was to analyze the interaction between severe aortic valve stenosis, left ventricular diastolic dysfunction, and coronary ischemia in elderly patients with complex cardiovascular disease.

Material and methods. This was a prospective analytical cohort study including 85 patients treated between 2019 and 2023, divided into two groups: Group I – TAVI without coronary intervention (n = 56), and Group II – TAVI associated with percutaneous coronary intervention (PCI) (n = 29), consisting of patients with significant coronary lesions. Echocardiography was performed according to the ESC/EACVI 2016 guideline standards, with detailed assessment of diastolic function.

Results. The prevalence of left ventricular diastolic dysfunction of varying severity showed a statistically significant difference between groups (p = 0.04): Group I – 35 patients (62.5%) versus Group II – 24 patients (82.7%). The E-wave velocity was lower in Group II: 152.4 cm/sec (IQR = 43.0) compared to 173.0 cm/sec (IQR = 32.0), p = 0.01. The E/A ratio and the incidence of E/A ≥2 showed a borderline significant difference (p = 0.04). Median E/e′ was higher in Group II – 9.2 (IQR = 5.4) compared to 6.4 (IQR = 4.2), p = 0.003. E/Vp was 1.2 (IQR = 0.4) versus 0.8 (IQR = 0.5), p < 0.001. Diastolic dysfunction was more frequent in Group II, with significantly different echocardiographic parameters, including decreased E-wave velocity, increased E/e′ and E/Vp ratios, and a higher incidence of E/A ≥2.

Conclusions. Patients undergoing both PCI and TAVI more frequently exhibited left ventricular diastolic dysfunction. The echocardiographic parameters E, E/e′, and E/Vp showed statistically significant differences, suggesting an additive impact of coronary artery disease on diastolic function impairment in the setting of severe aortic stenosis.

Keywords: aortic stenosis, diastolic dysfunction, TAVI, coronary artery disease.

Cite this article: Abraş M, Pasat E, Vicol MM, Ciorici C, Bursacovschi D. Diastolic dysfunction and myocardial ischemia in TAVI patients. Mold J Health Sci. 2025;12(3):27-33. https://doi.org/10.52645/MJHS.2025.3.04

Manuscript received: 31.07.2025

Accepted for publication: 30.08.2025

Published: 15.09.2025

***Corresponding author**: **Marcel Abraş**, MD, PhD, associate professor
Discipline of Cardiology, Department of Internal Medicine
Nicolae Testemițanu State University of Medicine and Pharmacy
165 Stefan cel Mare și Sfant blvd, Chișinău, Republic of Moldova, MD-2004
e-mail: marcel.abras@usmf.md

Authors's ORCID IDs
Marcel Abraș – https://orcid.org/0000-0003-2640-978X
Ecaterina Pasat - https://orcid.org/0000-0002-7737-9077
Maria-Magdalena Vicol - https://orcid.org/0009-0007-8126-6140
Cătălina Ciorici - https://orcid.org/0009-0003-7022-6857
Daniela Bursacovscihi - https://orcid.org/0000-0001-7530-3012

Key messages

What is not yet known on the issue addressed in the submitted manuscript

While the individual effects of aortic stenosis (AS) and coronary artery disease (CAD) on left ventricular diastolic dysfunction (LVDD) have been studied, the additive or synergistic impact of concomitant percutaneous coronary intervention (PCI) and transcatheter aortic valve implantation (TAVI) on diastolic function remains unclear. It is not yet established whether CAD independently exacerbates LVDD in patients undergoing TAVI.

The research hypothesis

The study hypothesizes that the presence of significant coronary artery disease requiring PCI in patients undergoing TAVI is associ-

ated with more pronounced left ventricular diastolic dysfunction, as reflected by echocardiographic parameters.

The novelty added by the manuscript to the already published scientific literature

This study provides new evidence suggesting that patients undergoing both TAVI and PCI exhibit more severe diastolic dysfunction compared to those receiving TAVI alone. It highlights significant differences in key echocardiographic markers (E, E/e′, E/Vp) between the groups, underscoring the potential additive role of CAD in diastolic impairment in the context of severe AS. These findings may inform risk stratification and tailored management strategies in this high-risk population.

Introduction

Aortic stenosis is the most common severe degenerative valvular disease requiring interventional or surgical treatment, characterized by a progressive reduction in the aortic valve area below 1 cm^2 from the normal values of 2–3 cm^2 [1, 2]. The prevalence of aortic stenosis is estimated at approximately 0.4% in the general population; however, this figure underestimates the reality in older age groups, where the incidence is significantly higher [3]. For the population over 60 years of age, studies report the following prevalence rates: 1.3% in the sixth decade of life, 3.9% in the seventh decade, and 9.8% among patients aged 80–89 years [4]. Another important epidemiological aspect is the frequent coexistence of ischemic heart disease (IHD) with aortic stenosis. Data on the prevalence of coronary artery disease among patients undergoing TAVI vary considerably, ranging from 15% to 82% [5–8]. Nevertheless, coronary revascularization is performed in only 10–20% of patients undergoing TAVI [5].

Coronary blood flow dynamics depends on a balance between ventricular, arterial, and neurohumoral mechanisms, in which the aortic valve plays a key role. In aortic stenosis, impaired valvular function reduces coronary flow reserve (CFR) and promotes myocardial ischemia [6]. Coronary blood flow is affected both proximally, by factors such as hypotension, left ventricular dysfunction, and aortic pathology, and distally, through microcirculatory dysfunction, ventricular hypertrophy, and diastolic dysfunction. In aortic stenosis, perfusion is reduced due to decreased perfusion pressure and microcirculatory remodeling associated with hypertrophy [6-8].

Coronary perfusion is regulated by the interaction between diastolic backward expansion waves (dBEW) and systolic forward compression waves (sFCW) [6]. The dynamics of these waves ensure adequate myocardial blood flow, particularly under the altered hemodynamic conditions associated with aortic stenosis. The reduction in stroke volume through the narrowed aortic valve leads to a decrease in mean arterial pressure. As a result, the pressure gradient between the aorta and the coronary arteries, as well as coronary perfusion pressure, decreases, thereby reducing oxygen delivery to the myocardium [9].

Left ventricular hypertrophy, although initially compensatory by reducing wall stress, decreases myocardial capillary density, increasing oxygen diffusion distance and creating an imbalance between increased oxygen demand and reduced coronary supply [9]. Under conditions of increased metabolic demand, coronary blood flow becomes dependent on the relative duration of diastole, which shortens as heart rate increases—a frequent finding in aortic stenosis. Consequently, tachycardia reduces subendocardial perfusion time, exacerbating the risk of ischemia [1,6]. In addition, diffuse fibrosis and left ventricular diastolic dysfunction—present in approximately 62% of patients with aortic stenosis [10], further contribute to symptom burden. Studies have demonstrated a strong correlation between the severity of dyspnea and the presence of myocardial fibrosis associated with diastolic dysfunction [10,11].

In patients with severe aortic stenosis and coronary artery disease, valve selection must consider coronary anatomy, post-implantation access, and the possibility of future coronary interventions, as the design of the transcatheter valve influences coronary ostia accessibility. [12].

Our study aims to contribute to the understanding of the complex interplay between severe aortic stenosis, diastolic dysfunction, and ischemic coronary artery disease, with the goal of identifying the implications of this triple impact on preprocedural assessment and post-TAVI prognosis in elderly patients with advanced cardiac pathology.

Material and methods

The observational analytical cohort study (both retrospective and prospective) included 85 elderly patients with severe aortic stenosis who underwent transcatheter aortic valve implantation (TAVI) between 2019 and 2023. The patients were selected from the interventional cardiology database of the Institute of Cardiology in Chisinau, Republic of Moldova. The inclusion criteria were: age ≥70 years, severe or pseudo-severe "low-flow, low-gradient" aortic stenosis, coronary artery disease eligible for percutaneous coronary intervention (PCI), and a minimum follow-up period of 1 year. The exclusion criteria were: age <70 years, mild or moderate aortic stenosis, non-PCI-eligible coronary lesions, myocardial infarction within the previous 90 days, previous coronary artery bypass grafting, and lack of informed consent. All patients included in the study met the eligibility criteria and signed informed consent forms. The study was approved by the Ethics Committee of the State University of Medicine and Pharmacy "Nicolae Testemitanu" (approval number 3/4.3/2024-03-19). Subsequently, patients were divided into two groups based on the myocardial revascularization strategy adopted before TAVI:

1. **TAVI group (n = 56)** – patients who underwent TAVI alone, without percutaneous coronary intervention.

2. TAVI+PCI group (n = 29) – patients who underwent both TAVI and PCI for the revascularization of significant coronary lesions.

The decision regarding the management of coronary artery disease (medical therapy versus coronary angioplasty) was made by the Heart Team based on national and international guideline recommendations, as well as individual patient characteristics. The primary indication for performing PCI was the presence of at least one stenosis ≥50% of the left main coronary artery trunk or a stenosis ≥70% of major coronary branches.

Diastolic function was evaluated echocardiographically according to the 2016 guidelines of the European Association of Cardiovascular Imaging (EACVI) [13], using a standardized multiparametric algorithm. Key parameters obtained from pulsed-wave Doppler included the transmitral inflow velocities: the E wave, representing early diastolic filling, and the A wave, corresponding to atrial contraction. The E/A ratio was analyzed for initial insight into the filling pattern. Tissue Doppler imaging (TDI) of the septal and lateral mitral annulus was used to measure early diastolic myocardial velocities (e'), providing information on active myocardial relaxation. The E/e' ratio was calculated as a surrogate marker of left ventricular filling pressures, with values >14 generally indicating elevated filling pressures. Additional structural parameters included the left atrial volume index (LAVI), measured by the biplane area-length method, which serves as a chronic marker of diastolic burden. A LAVI >34 mL/m^2 was considered abnormal. The peak tricuspid regurgitation velocity was assessed using continuous-wave Doppler to estimate pulmonary artery systolic pressure, a secondary indicator of increased left-sided filling pressures. Where image quality permitted, pulmonary venous flow and mitral deceleration time were also evaluated. Diastolic dysfunction was classified as: grade I (impaired relaxation with normal filling pressures), grade II (pseudonormal pattern indicating moderate elevation of filling pressures), and grade III (restrictive filling, associated with severe elevation of left atrial pressure and poor prognosis). All echocardiographic measurements were performed at end-expiration, with the patient in left lateral decubitus, using apical four-chamber views. To ensure reproducibility, each value was averaged over at least three cardiac cycles in sinus rhythm and five in the presence of atrial fibrillation. The classification of diastolic dysfunction required concordance between at least three out of four principal parameters, as per guideline recommendations. Cases with discordant or borderline values were categorized as "indeterminate diastolic function."

Statistical analyses were performed using SPSS version 25.0 (2017). Due to non-normal data distribution, non-parametric tests were applied. Continuous variables were presented as median and interquartile range (IQR) and compared using the Mann–Whitney U test. Categorical variables were analyzed with Chi-square or Fisher's exact test, as appropriate. A p-value <0.05 was considered statistically significant.

Results

To assess the impact of coronary revascularization on postprocedural outcomes following TAVI, the preprocedural characteristics of the two patient groups were compared, as presented in Table 1.

Table 1. Preprocedural characteristics of the "TAVI" and "TAVI+PCI" groups.

Parameter	TAVI (n = 56)	TAVI+ PCI (n = 29)	p
Age (years, mean ± SD)	77.2 ± 4.6	76.9 ± 5.0	0.82
Male sex, n (%)	15 (26.3%)	14 (48.2%)	0.04
BMI (kg/m^2, mean ± SD)	30.7 ± 5.1	28.9 ± 4.7	0.14
Hypertension, n (%)	56 (100%)	28 (96.5%)	0.33
Diabetes mellitus, n (%)	18 (31.5%)	12 (41.3%)	0.40
Atrial fibrillation, n (%)	22 (38.6%)	5 (20.58%)	0.04
Dyslipidemia, n (%)	44 (77.2%)	27 (93.1%)	0.07
AVA (cm^2, mean ± SD)	0.55 ± 0.17	0.69 ± 0.16	0.57
Mean gradient (mm Hg, mean ± DS)	55.1 ± 14.8	53.4 ± 14.5	0.53
Peak gradient (mm Hg, mean ± DS)	89.1 ± 21.8	85.1 ± 22.2	0.43
V_{max} (m/s, mean ± DS)	4.6 ± 0.6	4.64 ± 0.7	0.54
LVEF (%, mean ± DS)	59.2 ± 7.6	57.4 ± 7.9	0.10
Pulmonary hypertension, n (%)	47 (82.4%)	21 (72.4%)	0.58
Angina pectoris (FC II-III), n (%)	38 (66.6%)	27 (93.1%)	0.008
NYHA III-IV, n (%)	43 (75.4%)	24 (88.8%)	0.24
EuroSCORE II (%, mean ± DS)	4.4 ± 2.6	3.7 ± 2.5	0.17
STS score (%, valoarea medie ± SD)	4.5 ± 1.8	3.1 ± 3.6	0.96

Note: *BMI – body mass index, AVA – aortic valve area, V_{max} – maximum velocity across the aortic valve, LVEF – left ventricle ejection fraction, STS score - the Society of Thoracic Surgeons risk score.*

n – number of patients; mean (SD), Wilcoxon rank-sum test, Pearson Chi-Square test with estimated p-value.

In the study, among the 85 evaluated patients, 80% (n = 68) reported retrosternal pain, confirming the high frequency of anginal symptoms in severe aortic stenosis. In 12.9% of patients (n = 11), chest pain was the dominant symptom and the primary reason for cardiologic evaluation. Regarding triggering factors, chest pain was induced by physical exertion in 71.7% of patients (n = 61). Only one patient (1.17%) attributed the pain onset to emotional factors, and 2.35% (n = 2) reported an association with exposure to low temperatures. In 4.7% of cases (n = 4), chest pain could not be correlated with any evident trigger. According to the functional class (FC) of angina pectoris based on the Canadian Cardiovascular Society (CCS) classification, symptom severity was distributed as follows: 3 patients (4.4%) were classified as FC I, presenting occasional pain episodes during strenuous exertion; 33 patients (48.5%) were in FC II, reporting chest pain during moderate effort; and 32 patients (47.1%) were in FC III, experiencing pain during minimal effort. This distribution indicates a predominance of effort angina with moderate to severe severity.

Following the correlation of angina pectoris with ischemic coronary artery disease, an uneven distribution of symptoms was observed according to the severity of coronary lesions. Among the 32 patients with severe angina (FC III), 62.5% (n = 20) presented coronary lesions with

>50% stenosis, while 37.5% (n = 12) had minimal coronary lesions, suggesting a non-atherosclerotic ischemic mechanism of chest pain, likely due to impaired coronary flow secondary to severe aortic stenosis. In patients with moderate angina (FC II), 33.3% (n = 11) had coronary artery disease, whereas 66.7% (n = 22) did not exhibit significant coronary lesions. All patients with FC I (n = 3) had patent coronary arteries (Table 2).

Table 2. Association between angina severity and coronary artery disease CAD.

CCS Functional Class of Angina Pectoris	Patients with CAD	Patients without CAD	Total Patients
Class I, 3 (4.41%)	0 (0%)	3 (100%)	3
Class II, 33 (48.53%)	11 (33.33%)	22 (66.67%)	33
Class III, 32 (47.06%)	20 (62.5%)	12 (37.5%)	32
Total	31	37	68

Note: *CCS – Canadian Cardiovascular Society; CAD –* Coronary Artery Disease;*. n – number of patients; mean (SD), Wilcoxon rank-sum test, Pearson Chi-Square test with estimated p-value.*

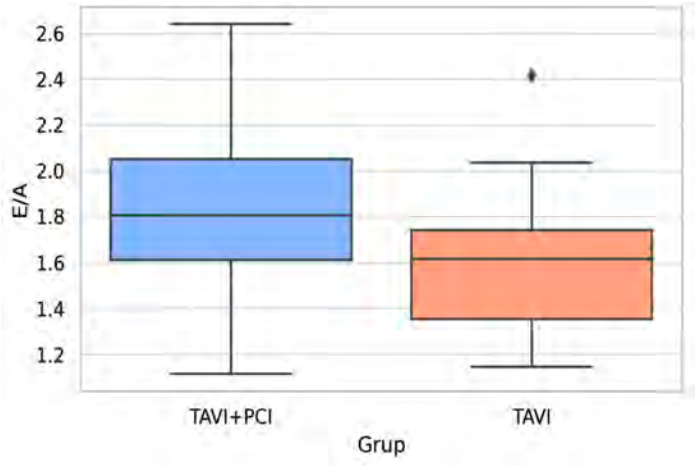

Fig. 1 Distribution of the E/A ratio in the both groups

Note: *The blue box represents patients TAVI+PCI, while the orange box represents patients undergoing TAVI alone.*

Although there are some differences between the groups, the overall patient profile is similar in terms of comorbidities, aortic stenosis severity, preoperative surgical risk, and left ventricular function.

Left ventricular diastolic dysfunction (LVDD) was significantly more frequent in Group II—patients undergoing concomitant TAVI and PCI. This difference supports the hypothesis that significant coronary artery disease, even when treated percutaneously, is frequently associated with persistent diastolic dysfunction, reflecting pre-existing myocardial remodeling. From a clinical perspective, Group II patients may represent a subgroup with greater functional vulnerability after TAVI, requiring closer echocardiographic monitoring during follow-up.

The distribution of LVDD grades according to the 2016 EACVI guidelines was as follows: Grade I (impaired relaxation) – 17.5% in Group I vs. 24.1% in Group II; Grade II (pseudonormal) – 47.4% in Group I vs. 41.3% in Group II; Grade III (restrictive) – 35.1% in Group I vs. 13.8% in Group II. Although the overall differences did not reach statistical significance (p = 0.063), the presence of a restrictive pattern in more than one-third of Group II patients has major clinical implications. These patients may have an increased risk of post-TAVI decompensation and could benefit from more aggressive diuretic optimization and serial echocardiographic follow-up.

In our study, the median values of the E/A ratio were significantly different between the group of patients treated with TAVI+PCI and the group undergoing TAVI alone, suggesting more severe diastolic dysfunction in the former group. The median E/A in Group II (TAVI+PCI) was 1.9 (IQR = 0.4), indicating a trend toward a restrictive filling pattern, compared to 1.6 (IQR = 0.3) in group I (TAVI only) , reflecting more preserved diastolic function with a less severe dysfunction pattern (Fig. 1).

The velocity of the E wave was significantly lower in Group II: 152.4 cm/s (IQR = 43.0) compared to 173.0 cm/s (IQR = 32.0) in Group I (p = 0.014), suggesting more pronounced impairment of active myocardial relaxation. This finding is frequently observed in the presence of chronic ischemia or fibrodegenerative infiltration—both common features in TAVI-eligible patients with concomitant coronary artery disease. An E/A ratio ≥2, indicative of a restrictive filling pattern, was more frequently observed in Group II. This difference reached statistical significance (p = 0.04) and, clinically, is often associated with severe heart failure symptoms and reduced tolerance to hemodynamic changes after the procedure.

The velocity of the A wave was slightly lower in Group II—70.3 cm/s (IQR = 18.6) compared to 75.9 cm/s (IQR = 21.2) in Group I, without statistical significance (p = 0.13). However, this contributes to the picture of passive ventricular filling dominated by elevated pressures, especially when correlated with increased E wave velocity and decreased e' wave velocity.

The E/e' ratio, used to estimate left ventricular filling pressure, was significantly higher in Group II—9.2 (IQR = 5.4) compared to 6.4 (IQR = 4.2) in Group I (p = 0.003). Values close to or exceeding 10 in the TAVI+PCI subset suggest elevated end-diastolic pressure, which may clinically manifest as residual pulmonary congestion post-procedure despite correction of the stenosis (Fig. 2). Additionally, 42.1% of patients in Group II had an E/e' ≥10, compared to only 13.8% in Group I (p = 0.012). This observation may indicate the need for early reassessment of diuretic therapy post-TAVI in patients undergoing concomitant revascularization.

The E/Vp ratio was significantly higher in Group II: 1.2 (IQR = 0.4) versus 0.8 (IQR = 0.5) in Group I (p < 0.001). E/Vp is a robust parameter for estimating filling pressure, independent of sinus rhythm, making it especially valuable in the context of the frequent atrial fibrillation observed in these patients.

The median isovolumetric relaxation time (IVRT) was

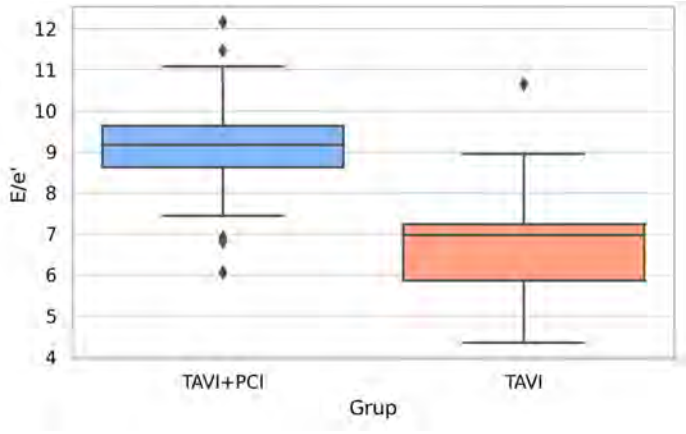

Fig. 2. Comparison of the E/e′ ratio

Note: *The blue box represents patients TAVI+PCI, while the orange box represents patients undergoing TAVI alone.*

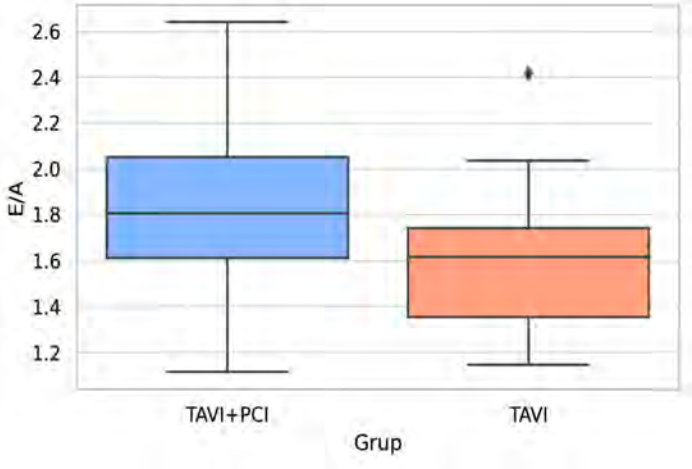

Fig. 3. Distribution of the E/Vp ratio

Note: *The blue box represents patients TAVI+PCI, while the orange box represents patients undergoing TAVI alone.*

shorter in Group II—72 ms (IQR = 14) compared to 78 ms (IQR = 17) in Group I (p = 0.082). A reduced IVRT reflects a stiff left ventricle that rapidly enters passive filling—typical for pseudo normal or restrictive filling patterns.

The deceleration time of the E wave (DTE) was significantly shorter in Group II—184 ms (IQR = 38) versus 207 ms (IQR = 41) in Group I (p = 0.033). A DTE <160 ms is considered an indirect marker of elevated end-diastolic pressure and decreased left ventricular compliance. In Group II, over one-third of patients had a DTE <160 ms.

Discussion

Aortic stenosis is the leading cause of valvular heart disease in the Western world and is associated with increased morbidity and mortality [14]. Progressive narrowing of the valve results in pressure overload of the left ventricle (LV), leading to hypertrophy and fibrosis, which can ultimately cause systolic and/or diastolic dysfunction of the LV [15]. The severity of diastolic dysfunction correlates with the severity of postprocedural hemodynamic parameters and the clinical course of the patient.

Percutaneous coronary revascularization (PCI) before TAVI is traditionally recommended to optimize coronary blood flow and reduce the risk of ischemic events during the hemodynamic stress generated by transcatheter aortic valve implantation [16]. This approach is consistent with current guidelines, which recommend prioritizing PCI for coronary artery lesions with >70% stenosis in proximal segments or >50% in the left main coronary artery, in order to ensure adequate myocardial perfusion, thereby reducing the risk of perioperative myocardial infarction and improving overall outcomes [2]. However, our results show that patients undergoing concomitant TAVI and PCI exhibit a more severe degree of diastolic dysfunction despite revascularization, compared with those treated with TAVI alone. Echocardiographic parameters (E, E/A, E/e′, E/Vp, DTE) indicated elevated end-diastolic pressures and a predominant restrictive diastolic pattern in the TAVI+PCI group, suggesting persistent subendocardial myocardial impairment, likely reflecting fibrotic remodeling or residual microvascular dysfunction.

This observation supports the hypothesis of a bidirectional mechanism between chronic myocardial ischemia and diastolic dysfunction: on one hand, coronary artery disease contributes to impaired ventricular filling through subendocardial ischemia, while on the other hand, elevated filling pressures and reduced ventricular compliance further compromise subendocardial coronary flow, especially in the context of reduced coronary flow reserve in severe aortic stenosis [17-19].

The presence of a restrictive diastolic pattern in one-third of revascularized patients highlights the importance of diastolic function assessment as a prognostic parameter. Moreover, the higher E/e′ and E/Vp ratios in the TAVI+PCI group are correlated with elevated filling pressures and more fragile hemodynamic tolerance, suggesting the need for rigorous postprocedural echocardiographic monitoring [20-21].

Recent literature supports the use of diastolic echocardiography not only as a diagnostic tool but also for guiding post-TAVI therapy. Studies such as PARTNER 3 and subanalyses from the TVT registry have shown that diastolic dysfunction correlates with cardiovascular mortality and rehospitalizations for heart failure [22]. In this context, patients undergoing TAVI+PCI may represent a functionally vulnerable subgroup requiring a personalized therapeutic strategy, including optimization of volume status, BNP/NT-proBNP assessment, and serial echocardiographic follow-up.

Our data support integrating diastolic dysfunction assessment into the pre-TAVI evaluation algorithm and postprocedural monitoring, particularly in patients with concomitant coronary artery disease. Evaluating diastolic function can guide patient selection and therapeutic adjustments, with potential independent prognostic value. In an increasingly complex clinical setting marked by comorbid-

ities and multidimensional therapeutic decisions, a thorough understanding of the interplay between ischemia and diastolic function becomes essential for treatment individualization and optimization of post-TAVI outcomes.

The main limitation of our study is the relatively small sample size, explained by the limited number of procedures performed and the low prevalence of significant coronary stenoses; however, the findings remain clinically relevant and provide valuable hypothesis-generating insights.

Conclusion

Left ventricular diastolic dysfunction was more frequent and more severe in patients undergoing concomitant TAVI and PCI compared to those treated with TAVI alone. Echocardiographic parameters (E/A, E/e′, E/Vp, DTE, IVRT) demonstrated a more impaired diastolic profile, with elevated end-diastolic pressures and a prevalent restrictive pattern in the TAVI+PCI group. These results suggest that significant coronary artery disease, even when treated, is associated with persistent myocardial remodeling and compromised diastolic function. Clinically, patients undergoing TAVI+PCI represent a vulnerable subgroup requiring more frequent echocardiographic follow-up and careful adjustment of postprocedural therapy.

Competing interests

None declared.

Authors' contributions

Substantial contribution to conception and design of the work, MA; substantial contribution to acquisition of data, DB, EP, CC; substantial contribution to analysis and interpretation of data, DB; drafting the article, M-MV, EP; critically reviewing the article for important intellectual content; MA; final approval of the version to be published, MA; taking responsibility and being accountable for all aspects of the work, MA, EP, M-MV. All the authors have read and agreed with the final version of the article.

Patient consent

Obtained.

Ethics approval

The study was approved by the Research Ethics Committee of *Nicolae Testemițanu* State University of Medicine and Pharmacy (approval number 3/4.3/2024-03-19).

Acknowledgements and funding

No external funding.

Provenance and peer review

Not commissioned, externally peer-reviewed.

References

1. McConkey HZR, Marber M, Chiribiri A, Pibarot P, Redwood SR, Prendergast BD. Coronary microcirculation in aortic stenosis: a physiological hornets' nest. Circ Cardiovasc Interv. 2019;12(8):e007470. doi: 10.1161/CIRCINTERVENTIONS.118.007547.
2. Vahanian A, Beyersdorf F, Praz F, Milojevic M, Baldus S, Bauersachs J, et al. 2021 ESC/EACTS guidelines for the management of valvular heart disease. Eur Heart J. 2022;43(7):561-632. doi: 10.1093/eurheartj/ehab395.
3. Bottaro G, Zappulla P, Deste W, Famà F, Agnello F, Trovato D, et al. Severe aortic valve stenosis: symptoms, biochemical markers, and global longitudinal strain. J Cardiovasc Echogr. 2020;30(3):154-61. doi: 10.4103/jcecho.jcecho_13_20.
4. Ancona R, Comenale Pinto S. Epidemiology of aortic valve stenosis (AS) and of aortic valve incompetence (AI): is the prevalence of AS/AI similar in different parts of the world? e-J Cardiol Pract. [Internet] 2020;18(10) [cited 2025 May 23]. Available from: https://www.escardio.org/Journals/E-Journal-of-Cardiology-Practice/Volume-18/epidemiology-of-aortic-valve-stenosis-as-and-of-aortic-valve-incompetence-ai#
5. Lønborg J, Jabbari R, Sabbah M, Veien KT, Niemelä M, Freeman P, et al. PCI in patients undergoing transcatheter aortic-valve implantation. N Engl J Med. 2024;391(23):2189-200. doi: 10.1056/NEJMoa2401513.
6. Michail M, Davies JE, Cameron JD, Parker KH, Brown AJ. Pathophysiological coronary and microcirculatory flow alterations in aortic stenosis. Nat Rev Cardiol. 2018;15(7):420-31. doi: 10.1038/s41569-018-0011-2.
7. Ahn JH, Kim SM, Park SJ, Jeong DS, Woo MA, Jung SH, et al. Coronary microvascular dysfunction as a mechanism of angina in severe aortic stenosis. J Am Coll Cardiol. 2016;67(12):1412-22. doi: 10.1016/j.jacc.2016.01.013
8. Zelis JM, Tonino PAL, Pijls NHJ, De Bruyne B, Kirkeeide RL, Gould KL, et al. Coronary microcirculation in aortic stenosis: pathophysiology, invasive assessment, and future directions. J Interv Cardiol. 2020;2020:1-13. doi: 10.1155/2020/4603169.
9. Libby P, Bonow RO. Braunwald's heart disease: a textbook of cardiovascular medicine. 11th ed. Philadelphia: Elsevier; 2022.
10. Lee HJ, Lee H, Kim SM, Park JB, Kim EK, Chang SA, et al. Diffuse myocardial fibrosis and diastolic function in aortic stenosis. JACC Cardiovasc Imaging. 2020;13(12):2561-72. doi: 10.1016/j.jcmg.2020.07.007.
11. Canty JM, Weil BR. Interstitial fibrosis and diastolic dysfunction in aortic stenosis. JACC Basic Transl Sci. 2020;5(5):481-3. doi: 10.1016/j.jacbts.2020.03.014.
12. Valvo R, Costa G, Tamburino C, Barbanti M. Coronary artery cannulation after transcatheter aortic valve implantation. EuroIntervention. 2021;17(10):835-47. doi: 10.4244/EIJ-D-21-00158.
13. Nagueh SF, Smiseth OA, Appleton CP, Byrd BF, Dokainish H, Edvardsen T, et al. Recommendations for the evaluation of left ventricular diastolic function by echocardiography: an update. J Am Soc Echocardiogr. 2016;29(4):277-314. doi: 10.1016/j.echo.2016.01.011.

14. Otto CM, Prendergast B. Aortic-valve stenosis: from patients at risk to severe valve obstruction. N Engl J Med. 2014;371(8):744-56. doi: 10.1056/NEJMra1313875.
15. Klein AL, Ramchand J, Nagueh SF. Aortic stenosis and diastolic dysfunction: partners in crime. J Am Coll Cardiol. 2020;76(24):2952-5. doi: 10.1016/j.jacc.2020.10.034.
16. Wenaweser P, Pilgrim T, Guerios E, Stortecky S, Huber C, Khattab AA, et al. Impact of coronary artery disease and PCI on outcomes in patients with severe aortic stenosis undergoing TAVI. EuroIntervention. 2011;7(5):541-8. doi: 10.4244/EIJV7I5A89.
17. Hong D, Lee SH, Shin D, Choi KH, Kim HK, Ha SJ, et al. Prognostic impact of cardiac diastolic function and coronary microvascular function on cardiovascular death. J Am Heart Assoc. 2023;12(3):e027690. doi: 10.1161/JAHA.122.027690.
18. Wada T, Shiono Y, Honda K, Higashioka D, Taruya A, Takahata M, et al. Serial changes of coronary flow reserve over one year after transcatheter aortic valve implantation in patients with severe aortic stenosis. Int J Cardiol Heart Vasc. 2022;42:101090. doi: 10.1016/j.ijcha.2022.101090.
19. Suzuki W, Nakano Y, Ando H, Fujimoto M, Sakurai H, Suzuki M, et al. Association between coronary flow and aortic stenosis during transcatheter aortic valve implantation. ESC Heart Fail. 2023;10(3):2031-41. doi: 10.1002/ehf2.14316.
20. Takagi H, Hari Y, Nakashima K, Yokoyama Y, Ueyama H, Kuno T, et al. Baseline left ventricular diastolic dysfunction affects midterm mortality after transcatheter aortic valve implantation. J Card Surg. 2020;35(3):536-43. doi: 10.1111/jocs.14409.
21. Angellotti D, Manzo R, Castiello DS, Immobile Molaro M, Mariani A, Iapicca C, et al. Echocardiographic evaluation after transcatheter aortic valve implantation: a comprehensive review. Life (Basel). 2023;13(5):1079. doi: 10.3390/life13051079.
22. ElGuindy A. PARTNER 2A & SAPIEN 3: TAVI for intermediate-risk patients. Glob Cardiol Sci Pract. 2016;2016(4):e201633. doi: 10.21542/gcsp.2016.33.

https://doi.org/10.52645/MJHS.2025.3.05

UDC: 616.329-007.43-072.1-089

RESEARCH ARTICLE

Hiatal surface area measurement – a useful tool during laparoscopic antireflux surgery

Serghei Cumpătă[1*], Vasile Guzun[2], Vladimir Iacub[1], Evghenii Guțu[1]

[1]Department of General Surgery and Semiology no. 3, *Nicolae Testemițanu* State University of Medicine and Pharmacy, Chisinau, Republic of Moldova
[2]*Gheorghe Paladi* Municipal Hospital, Chisinau, Republic of Moldova

ABSTRACT

Introduction. Accurate measurement of the esophageal hiatus is essential during laparoscopic repair of hiatal hernia, especially in patients with gastroesophageal reflux disease. Traditional intraoperative assessments are often subjective and inconsistent. This study proposes a novel, objective method for measuring the hiatal surface area using digital photography and open-source image analysis software.

Material and methods. Our study included 25 consecutive patients with hiatal hernia and gastroesophageal reflux disease undergoing laparoscopic fundoplication. During surgery, standardized digital photographs of the hiatal defect were captured with a fixed-size benchmark (1.0×1.0 cm). Images were analyzed postoperatively using ImageJ software to determine the hiatal surface area. Preoperative and 12-month postoperative symptom severity was measured using the Gastroesophageal Reflux Disease-Health Related Quality of Life score. Correlations between hiatal surface area, symptoms, and hernia recurrence were evaluated statistically.

Results. The mean hiatal surface area was 5.4 ± 1.8 cm^2. A strong positive correlation was observed between hiatal surface area and preoperative symptoms severity (r = 0.69), as well as postoperative improvement (r = 0.74). At 12 months, 88% of patients achieved significant symptoms reduction (≥50% reduction in Gastroesophageal Reflux Disease-Health Related Quality of Life score). Recurrence of symptoms was noted in 12% of patients, all of whom had a hiatal surface area greater than 6.0 cm^2. Therefore, patients with a hiatal surface area ≥6.0 cm^2 showed a higher risk of recurrence and less symptoms improvement compared to those with smaller defects.

Conclusions. The proposed intraoperative measurement technique is a simple, cost-effective, and reproducible tool for quantifying hiatal defects. It provides clinically meaningful information that can assist in surgical planning, predict postoperative outcomes, and identify patients who may benefit from reinforced crural repair.

Keywords: hiatal hernia, gastroesophageal reflux, laparoscopic fundoplication, esophageal hiatus, computer-assisted image interpretation.

Cite this article: Cumpătă S, Guzun V, Iacub V, Guțu E. Hiatal surface aria measurement – a useful tool during laparoscopic antireflux surgery. Mold J Health Sci. 2025;12(3):34-39. https://doi.org/10.52645/MJHS.2025.3.05.

Manuscript received: 13.06.2025

Accepted for publication: 15.08.2025

Published: 15.09.2025

[*]**Corresponding author**: **Serghei Cumpătă**, MD, assistant professor
Department of General Surgery and Semiology no. 3,
Nicolae Testemițanu State University of Medicine and Pharmacy
165, Stefan cel Mare si Sfânt blvd., Chisinau, Republic of Moldova, MD2004
e-mail: serghei.cumpata@usmf.md

Authors' ORCID IDs
Serghei Cumpătă – https://orcid.org/0000-0003-3472-6152
Vasile Guzun – https://orcid.org/0009-0001-1545-3470
Vladimir Iacub – https://orcid.org/0000-0002-1865-0787
Evghenii Guțu – https://orcid.org/0000-0003-4590-4735

Key messages

What is not yet known on the issue addressed in the submitted manuscript

Although the size of the hiatal defect is known to influence the complexity of the surgical procedure and postoperative outcomes, there is no standardized method for its intraoperative measurement. The clinical utility of hiatal surface area as a predictive parameter remains underexplored, and optimal thresholds for surgical decision-making are not clearly established. Furthermore, image-based techniques for real-time quantification during surgery are insufficiently validated in the current literature.

The research hypothesis

Intraoperative quantification of the hiatal surface area using calibrated digital photography offers a reliable, objective predictor of both clinical outcomes and surgical recurrence risk in patients with hiatal hernia and GERD.

The novelty added by the manuscript to the already published scientific literature

The manuscript introduces a simple, low-cost, and reproducible intraoperative method for quantifying the hiatal surface area using digital photography and open-source image analysis software. Unlike existing techniques based on direct physical measurement or subjective estimation, this approach allows real-time measurement without specialized equipment, offering practical applicability in routine surgical settings.

Introduction

The accurate measurement and understanding of the esophageal hiatus's anatomical and functional characteristics are crucial in the context of hiatal hernia (HH) diagnosis and surgical treatment. Disorders associated with the esophageal hiatus, particularly HHs, have become increasingly relevant in clinical practice due to their association with gastroesophageal reflux disease (GERD) and their impact on patient quality of life. HHs occur when the stomach protrudes through the enlarged esophageal hiatus into the thoracic cavity, often leading to significant clinical symptoms such as heartburn, regurgitation, and chest pain. HHs and GERD present significant clinical challenges due to their complex anatomy and the risk of postoperative complications such as dysphagia, gas-bloat syndrome and recurrent herniation. The prevalence of HHs and GERD is estimated to range from 10% to 50% in the adult population, with higher rates observed in older adults [1].

Historically, the management of HHs and GERD has focused on both conservative treatments, such as lifestyle modifications and pharmacotherapy, and surgical interventions, particularly in cases where conservative measures fail or complications occur. Currently, laparoscopic fundoplication (LF) remains the gold standard in antireflux surgery for HH and GERD, with excellent symptomatic results in 90% to 95% of cases [2, 3]. The surgical approach to HHs, however, has been a topic of ongoing debate, particularly regarding the best methods to ensure effective and durable repairs. The recurrence of HHs post-surgery, which has been reported in up to 10-30% of cases [4, 5], underscores the need for precise and individualized surgical techniques.

The integration of these advanced methodologies into the surgical workflow is particularly crucial in the context of an aging population, where the incidence of HHs is expected to increase. With the prevalence of GERD also on the rise, estimated to affect up to 20% of the adult population in Western countries [1], the need for effective and durable surgical solutions is more pressing than ever. The adoption of standardized measurement techniques, such as those proposed by Granderath and validated by Moten and Ouyang [6, 7], is likely to play a key role in addressing this challenge, providing surgeons with the tools they need to deliver optimal care.

The accurate assessment of the esophageal hiatus is a critical determinant of the success of HH and GERD surgery. The evolution of measurement techniques, from subjective intraoperative assessments to advanced imaging-based methods, represents a significant improvement in this field. As the surgical community continues to refine these approaches, the combination of intraoperative and imaging-based assessments will likely become a cornerstone of HH management, ultimately leading to improved patient outcomes and reduced rates of postoperative adverse events.

Material and methods

The study was conducted within the Department of General surgery and semiology no. 3 at *Nicolae Testemițanu* State University of Medicine and Pharmacy, at the General Surgery Clinic of the *Gheorghe Paladi* Municipal Hospital, Chisinau, Republic of Moldova. It involved 25 adult patients diagnosed with GERD with/or HH, all of whom underwent LF. The research was designed as a prospective, descriptive, observational and cross-sectional study aimed at assessing a novel intraoperative method for quantifying the HSA and its correlation with symptom severity and hernia recurrence. The study was conducted in accordance with the Declaration of Helsinki and approved by the Research Ethics Committee of *Nicolae Testemițanu* State University of Medicine and Pharmacy (Protocol No. 84, 20.06.2017). Informed consent was obtained from all participants.

Patient selection and surgical procedure. This study included 25 consecutive patients diagnosed with GERD and HH who were scheduled for elective LF. Patient inclusion criteria consisted of adults with a confirmed diagnosis of HH, and with preoperative symptoms of GERD. Patients with gross adhesions due to previous surgical interventions on the upper abdomen were excluded from this study.

To ensure uniformity and reproducibility of intraoperative measurements, all procedures were performed under general anesthesia using a laparoscopic approach with pneumoperitoneum established at 12–14 mmHg. During each surgery, standard laparoscopic techniques were employed, and exposure of the esophageal hiatus was achieved by systematic division of the phrenoesophageal ligament, hepatogastric ligament and atraumatic mobilization of the gastroesophageal junction, thereby facilitating clear identification of both diaphragmatic crura and optimal visualization for cruroplasty and fundoplication. After complete dissection and visualization of the esophageal hiatus, we proceeded with digital intraoperative imaging to assess the surface area of the defect.

Intraoperative imaging and analysis

To obtain accurate measurements of the hiatal defect, intraoperative digital photographs were taken. A digital camera mounted on a laparoscopic instrument with an adjustable lens (Olympus, Tokyo, Japan) was used to capture images under consistent lighting and focal distance settings to maintain measurement accuracy. A standardized "benchmark" reference object of known size (1.0 cm x 1.0 cm square) was placed within the operative field adjacent to the hiatal defect for calibration purposes. This benchmark was positioned in the same plane as the hiatal defect to avoid distortions from depth or angle, and all images were taken perpendicular to the plane of the defect to ensure consistency across measurements.

After obtaining the images, they were analyzed using ImageJ graphic software (National Institute of Mental Health, Bethesda, Maryland, USA), a free, open-source and commonly used tool for quantitative image analysis. The images were first converted to grayscale for enhanced contrast and ease of boundary definition. Each image was calibrated using the benchmark object, with the known area (1 cm^2) used to set a pixel-to-square centimeter ratio. This ratio was critical in accurately quantifying the hiatal defect area. Each image was independently assessed by two experienced surgeons to assess inter-observer reliability, and each observer repeated the measurements twice at different time points to assess intra-observer reliability.

Measurement procedure

1. **Calibration**: In each image, the benchmark square was manually selected and designed as a standard reference using the ImageJ calibration function. The software calculated the pixel-to-centimeter ratio based on the 1.0 cm x 1.0 cm benchmark area.
2. **Hiatal defect contouring**: The hiatal defect was then contoured manually using the "Freehand Selection" tool in ImageJ, which allowed precise outlining of the defect's irregular shape (Figure 1). Care was taken to include the full visible boundary of the defect while excluding surrounding tissues.

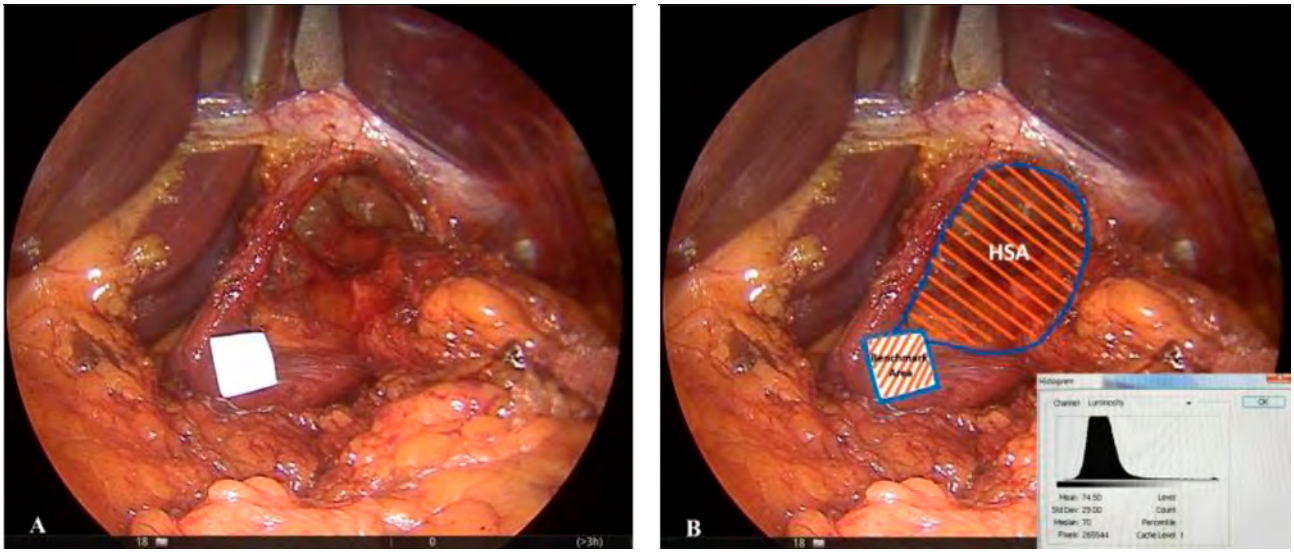

Fig. 1 Intraoperative method of HSA measurement.

A - Intraoperative view of the esophageal hiatus, with a 1.0 × 1.0 cm square-shaped calibration benchmark placed adjacent to the defect for surface area measurement. B - Intraoperative analysis in ImageJ software: the hiatal contour is manually delineated, and the calculated area (in cm^2) is based on pixel-to-size conversion using the internal calibration marker.

Note: HSA – hiatal surface aria

3. **Area calculation**: After contouring, the software calculated the total pixel area of the defect. Using the previously established pixel-to-centimeter ratio, the area of the hiatal defect was calculated in square centimeters. This calculation was based on the proportional relationship between the number of pixels in the benchmark and the contoured defect area, expressed as:

$$\text{Hiatal Defect Area } (cm^2) = \frac{HSA}{(\text{Benchmark area Pixels})} \times 1.0\ cm^2$$

Additional data. In addition to surface area quantification, we recorded demographic data, BMI, hernia type, and preoperative GERD-HRQL scores. All patients underwent fundoplication and posterior crural closure using nonabsorbable sutures, with or without mesh reinforcement, based on intraoperative judgment. Postoperative follow-up was performed at 3 and 12 months. At 12 months, patients were re-evaluated using the same GERD-HRQL instrument to assess clinical evolution. A reduction of ≥50% in the HRQL score was defined as significant symptomatic relief. Recurrence was defined clinically by symptoms returning or by characteristic endoscopic and/or radiologic abnormalities.

Statistical analysis

Data were recorded and analyzed using SPSS software (IBM Corp., Armonk, NY, USA). Continuous variables were expressed as mean ± standard deviation. Interobserver and intraobserver agreement for HSA measurements were assessed using the intraclass correlation coefficient (ICC). Correlation between HSA and GERD-HRQL score (pre- and postoperative) was evaluated using Pearson's coefficient. Statistical significance was defined as $p < 0.05$.

Results

Patient characteristics

A total of 25 patients with HH and GERD were included in this study. The mean age of the patients was 57.8 ± 12.3 years, with a range from 34 to 75 years. Of the 25 patients, 15 (60%) were female, and 10 (40%) were male. The mean body mass index (BMI) was 28.5 ± 3.7 kg/m^2.

Hiatal surface area (HSA) measurements

Using the new intraoperative imaging method with ImageJ software, the mean HSA of the hiatal defect was calculated to be 5.4 ± 1.8 cm^2, with individual measurements ranging from 2.8 to 9.2 cm^2. Table 1 summarizes the HSA measurements and provides additional demographic and clinical data.

The preoperative GERD-HRQL score averaged 27.7 ± 5.6, indicating moderate to severe symptoms burden. At 12-month follow-up, the postoperative GERD-HRQL score was 11.5 ± 4.9, reflecting significant symptomatic improvement ($p < 0.001$). The proportion of patients achieving a ≥50% reduction in HRQL score was 80% (n=20).

Table 1. Patient Demographics, HSA Measurements, and GERD-HRQL Scores (n = 25)

Variable Mean ± SD		Range
Age (years)	57.8 ± 12.3	34 – 75
BMI (kg/m^2)	28.5 ± 3.7	24.1 – 34.3
HSA (cm^2)	5.4 ± 1.8	2.8 – 9.2
Preoperative GERD-HRQL Score	27.7 ± 5.6	10 – 30
Postoperative GERD-HRQL Score	11.5 ± 4.9	6-13

***Note**:* Data are presented as mean ± standard deviation (SD) and range. *Abbreviations: HSA – hiatal surface area; GERD-HRQL – Gastroesophageal Reflux Disease Health-Related Quality of Life; BMI – body mass index.HSA – Hiatal surface aria*

Interobserver and intraobserver reliability

Two independent reviewers analyzed each patient's images to assess reliability. The interobserver intraclass correlation coefficient (ICC) was 0.92 (95% CI: 0.86–0.97), indicating high reliability between reviewers. The intraobserver ICC for repeat measurements was 0.94 (95% CI: 0.89–0.98) demonstrated in Table 2, confirming excellent measurement consistency.

Table 2. Interobserver and intraobserver reliability metrics

Reliability metric	ICC	95% Confidence interval
Interobserver ICC	0.92	0.86 – 0.97
Intraobserver ICC	0.94	0.89 – 0.98

***Note**:* Data are expressed as intraclass correlation coefficients (ICC) with corresponding 95% confidence intervals. Measurements were performed independently by two observers using the same digital image analysis protocol. *Abbreviations: ICC – intraclass correlation coefficient.*

Correlation between HSA and clinical outcomes

The HSA measurements were analyzed for potential correlations with preoperative symptoms, clinical outcomes, including postoperative symptom resolution and hernia recurrence at a 12-month follow-up (Figure 2). A strong positive correlation was identified between preoperative GERD-HRQL score and measured HSA (r = 0.69), suggesting that patients with larger hiatal defects experienced more severe symptoms (Table 3).

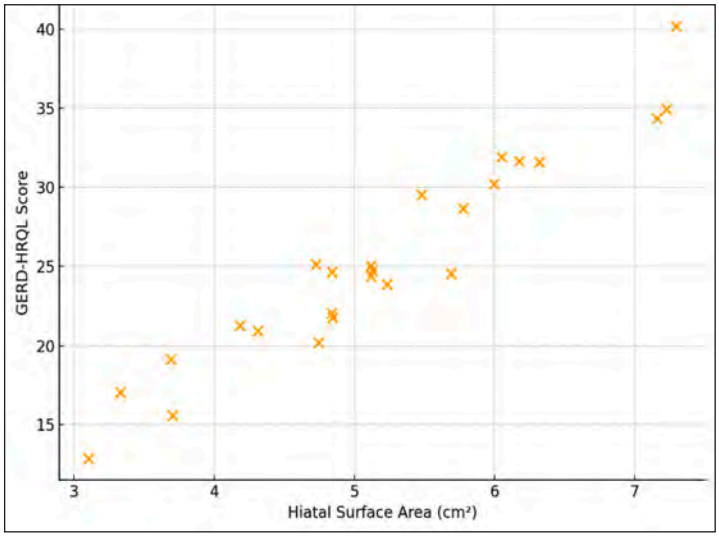

Fig. 2 Correlation between HSA and Preoperative GERD-HRQL

Note: The scatter plot illustrates a positive linear relationship between HSA and symptom severity, as measured by the preoperative GERD-HRQL score. Each dot represents one patient. *Abbreviations: HSA – hiatal surface area; GERD-HRQL – Gastroesophageal Reflux Disease Health-Related Quality of Life.*

Furthermore, a strong correlation was observed between HSA and postoperative symptoms improvement (r = 0.74), indicating the relevance of anatomical defect quantification in predicting surgical outcomes.

Table 3. HSA correlation analysis

Variable pair	Correlation coefficient (r)
HSA vs preoperative GERD-HRQL	0.69
HSA vs symptoms improvement (%)	0.74
HSA >6 cm^2 vs recurrence	Strong association

Note: Data include Pearson correlation coefficients (r) for continuous variables and descriptive association for binary outcomes. "Strong association" indicates a statistically significant relationship observed in all cases with HSA >6 cm^2. *Abbreviations: HSA – hiatal surface area; GERD-HRQL – Gastroesophageal Reflux Disease Health-Related Quality of Life.*

Patients with a larger HSA (≥6 cm^2) exhibited a higher recurrence rate (20%) compared to those with a smaller HSA (<6 cm^2), who had a recurrence rate of 6.6%. Table 4 provides a summary of postoperative outcomes in relation to HSA size.

Table 4. Postoperative outcomes based on HSA measurements

HSA Group	No. of Patients	Mean HSA (cm^2)	Recurrence Rate (%)	Symptom Resolution (%)
HSA <6 cm^2	15	4.2 ± 0.7	6.6	93.3
HSA ≥6 cm^2	10	7.3 ± 1.1	20	80
Overall	25	5.4 ± 1.8	12	88

Note: Data are presented as means ± standard deviations and percentages. Recurrence was defined as radiologically or endoscopically confirmed reappearance of hiatal hernia at 12-month follow-up. Symptom resolution was defined as ≥50% improvement in GERD-HRQL scores compared to baseline. *Abbreviations: HSA – hiatal surface area; GERD-HRQL – Gastroesophageal Reflux Disease Health-Related Quality of Life.*

A positive correlation ($r = 0.58$, $p < 0.05$) was observed between HSA size and postoperative symptom severity, with larger defects being associated with higher postoperative symptom scores. Additionally, a higher BMI was weakly associated with an increased HSA size ($r = 0.34$, $p = 0.07$), though this was not statistically significant in this sample.

Discussion

Surgical treatment of HH and GERD remains challenging due to technical complexity, anatomical variability, including esophageal hiatus size, and associated risk of recurrence. Thus, the accurate measurement of the diaphragmatic hiatal surface area (HSA) is a decisive factor in selecting a reliable and safe modality for hiatus repair, i.e. simple suturing or mesh reinforcement. Traditional surgical methods have often relied on attempts of real measurement or subjective intraoperative assessments, which can lead to variability in outcomes. Granderath et al. [6] have been at the forefront of addressing this issue, proposing a standardized method for calculating the HSA using geometric principles applied intraoperatively. Their studies have shown that tailoring the crural closure based on the calculated HSA significantly reduces the risk of postoperative complications, such as dysphagia and recurrent herniation. In a study involving 55 patients who underwent LF, Granderath and colleagues reported a recurrence rate of less than 5% when the HSA was used to guide surgical decisions.

The limitations of intraoperative measurements, which can be influenced by factors such as patient positioning and the extent of surgical dissection, have prompted the exploration of more objective and reproducible methods. Moten et al. [7] developed a novel technique using multi-detector computed tomography (MDCT) combined with multi-planar reconstruction (MPR) to measure the HSA in vivo. This method offers a significant advancement over traditional techniques by allowing for a non-invasive, preoperative assessment of the hiatus. In their study, which included 30 patients scheduled for HH repair, Moten and colleagues demonstrated a strong correlation between the HSA measurements obtained via MDCT-MPR and those obtained intraoperatively (Pearson correlation coefficient = 0.83, $p<0.001$). The study also highlighted the high reproducibility of the MDCT-MPR technique, with intra-class correlation coefficients for intra- and inter-observer agreement both exceeding 0.97 ($p <0.001$), indicating excellent consistency.

Further reinforcing the importance of accurate HSA measurement, Koch et al. [8] explored the relationship between the size of the esophageal hiatus and the outcomes of surgical repairs. Their research, involving a cohort of patients undergoing laparoscopic fundoplication, found that patients with larger hiatal defects (HSA >8 cm^2) were more likely to experience postoperative complications, including herniation and persistent reflux symptoms, compared to those with smaller defects. Specifically, they reported a herniation rate of approximately 15% in patients with HSA >8 cm^2, compared to just 3% in those with HSA ≤4 cm^2. This study underscores the need for precise preoperative assessment of the hiatal defect to tailor the surgical approach, particularly in determining whether to use mesh reinforcement during the repair. The role of advanced imaging techniques in enhancing surgical outcomes has also been highlighted by Ouyang et al. [7], who validated the use of MDCT-MPR for preoperative planning and postoperative assessment. Their findings suggest that MDCT-MPR not only provides accurate measurements of the HSA but also aids in identifying anatomical variations that could impact surgical decision-making, such as the presence of large hernias that might require more complex repairs. The incorporation of such imaging techniques into clinical practice represents a paradigm shift, moving away from subjective assessments to more objective, data-driven approaches that can improve patient outcomes.

The integration of these advanced methodologies into the surgical workflow is particularly crucial in the context of an aging population, where the incidence of HHs is expected to increase. With the prevalence of GERD also on the rise, estimated to affect up to 20% of the adult population in Western countries, the need for effective and durable surgical solutions is more pressing than ever. The adoption of standardized measurement techniques, such as those proposed by Granderath and validated by Moten and Ouyang [6, 7], is likely to play a key role in addressing this challenge, providing surgeons with the tools they need to deliver optimal care.

In our study, we proposed a novel intraoperative method for measuring the HSA based on calibrated digital photography and analysis with freely available software. The results obtained confirm that this technique is simple, reliable, and correlates strongly with the clinical severity of gastroesophageal reflux symptoms, as well as with the recurrence rate observed at 12 months postoperatively. A major strength of this method lies in its ability to overcome limitations of traditional intraoperative assessment, which often relies on subjective visual estimation or linear crural measurements. By introducing a fixed-size benchmark and analyzing the captured image through digital software, the surface area can be determined with high precision, regardless of the surgeon's experience or the degree of laparoscopic distortion. This objectivity adds reproducibility, which is critical when planning the extent of cruroplasty or the need for mesh reinforcement.

Furthermore, our findings showed a strong correlation between preoperative HSA and GERD-HRQL scores, reinforcing the anatomical-functional relationship between the size of the diaphragmatic defect and the severity of reflux

symptoms. Larger defects appear to facilitate more pronounced disruption of the antireflux barrier, leading to increased symptom burden. From a therapeutic perspective, this observation supports the need for individualized surgical planning, particularly in high-HSA patients.

The recurrence rate of 12% observed at 12 months is consistent with previously reported data. Importantly, all patients with recurrence had an HSA greater than 6 cm^2. This suggests a potential threshold above which standard suture cruroplasty may be insufficient, regardless of technique and suture material. Stratification of patients based on HSA could, therefore, be used intraoperatively to decide on additional interventions such as mesh hiatoplasty or anterior crural buttressing. While controversy persists regarding mesh use, particularly due to complications like erosion or fibrosis, a risk-based approach guided by anatomical quantification could lead to better outcomes and personalized therapy.

Compared to imaging-based techniques (e.g., CT volumetry, EUS, or intraoperative 3D scanning), our approach is markedly more accessible and inexpensive, not requiring specialized equipment or extended training. The only requisites are a sterile scale reference, a digital camera (standard laparoscopic systems suffice), and access to basic image processing software. Its simplicity makes it suitable for both tertiary centers and lower-resource surgical settings.

The reproducibility of the method was confirmed by strong inter- and intra-observer reliability scores. The protocol's minimal learning curve also allows it to be implemented across surgical teams with varying levels of experience, facilitating standardization in clinical practice and possibly in future multicentric research.

Nevertheless, several limitations must be acknowledged. First, although images were standardized as much as possible, subtle differences in camera angle or distance may still introduce minor variation in surface area estimation. Second, the study used GERD-HRQL score as a subjective symptom marker; objective measures such as 24-hour pH monitoring or manometry were not systematically incorporated. Lastly, follow-up was limited to 12 months, and long-term recurrence data remain to be assessed.

Conclusions

In conclusion, the proposed measurement technique offers a clinically useful, practical, and reproducible solution for quantifying the hiatal defect. Its potential impact includes improved intraoperative decision-making, more personalized surgical techniques, and better prediction of recurrence risk. However, patients with a HSA over 6 cm^2 exhibited a statistically significant higher recurrence rate compared to those with a smaller HSA (20% vs 6.6%, r = 0.58). Future research may focus on refining calibration protocols, integrating this method with other intraoperative tools, and validating it in prospective multicenter trials.

Competing interests

None declared.

Authors' contributions

SC and VG interpreted the data and performed the analytical part of the work, SC drafted the first manuscript; VI and EG conceptualized the project, designed the research and revised the manuscript critically.

Ethics approval

The research project was approved by the Research Ethics Committee of *Nicolae Testemiţanu* State University of Medicine and Pharmacy (Minutes no. 84, 20.06.2017).

Patient consent

Obtained.

Acknowledgements and funding

No external funding.

Declaration of generative AI and AI-assisted technologies in the writing process

The authors (SC) used OpenAI's ChatGPT in order to assist with reference formatting in Vancouver style and language refinement. After using this tool, the authors (EG, VI and VG) thoroughly reviewed and edited all content and take full responsibility for the scientific accuracy, originality, and integrity of the publication.

Provenance and peer review

Not commissioned, externally peer reviewed.

References

1. El-Serag HB, Sweet S, Winchester CC, Dent J. Update on the epidemiology of gastro-oesophageal reflux disease: a systematic review. Gut. 2014;63(6):871-80. doi: 10.1136/gutjnl-2012-304269.
2. Schlottmann F, Herbella FA, Allaix ME, Rebecchi F, Patti MG. Surgical treatment of gastroesophageal reflux disease. World J Surg. 2017;41(7):1685-1690. doi: 10.1007/s00268-017-3955-1.
3. Robinson B, Dunst CM, Cassera MA, Reavis KM, Sharata A, Swanstrom LL. 20 years later: laparoscopic fundoplication durability. Surg Endosc. 2015;29(9):2520-4. doi: 10.1007/s00464-014-4012-x.
4. Dallemagne B, Arenas Sanchez M, Francart D, et al. Long-term results after laparoscopic reoperation for failed antireflux procedures. Br J Surg. 2011;98(11):1581-7. doi: 10.1002/bjs.7590.
5. Turkcapar A, Kepenekci I, Mahmoud H, et al. Laparoscopic fundoplication with prosthetic hiatal closure. World J Surg. 2007;31(11):2169-76. doi: 10.1007/s00268-007-9066-7.
6. Granderath FA, Schweiger UM, Pointner R. Laparoscopic antireflux surgery: tailoring the hiatal closure to the size of hiatal surface area. Surg Endosc. 2007;21(4):542-8. doi: 10.1007/s00464-006-9041-7.
7. Moten AS, Ouyang W, Hava S, Zhao H, Caroline D, Abbas A. In vivo measurement of esophageal hiatus surface area using MDCT: description of the methodology and clinical validation. Abdom Radiol (NY). 2020 Sep;45(9):2656-2662. doi: 10.1007/s00261-019-02279-7.
8. Koch OO, Asche KU, Berger J, Weber E, Granderath FA. Influence of the esophageal hiatus size on the rate of reherniation after laparoscopic fundoplication and refundopilication with mesh hiatoplasty. Surg Endosc. 2013;25(4):1024-30. doi: 10.1007/s00464-010-1308-3.

https://doi.org/10.52645/MJHS.2025.3.06

UDC: 616.62-008.22-085.372-055.2

RESEARCH ARTICLE

Age related detrusor overactivity and symptoms perception in women: role of Botulinum toxin A injection for refractory overactive bladder

Mihaela Ivanov*, Emil Ceban

Department of Urology and Surgical Nephrology, *Nicolae Testemițanu* State University of Medicine and Pharmacy, Chisinau, Republic of Moldova

ABSTRACT

Introduction. Detrusor overactivity has been detected in approximately 50% of women with overactive bladder symptoms. According to the NICE guidelines, urodynamic testing is mandatory confirm the diagnosis of detrusor overactivity before performing minimally invasive treatment.

Material and methods. This study retrospectively analyzes 76 women, categorized into two groups based on age: reproductive age (n = 49) and climacteric period (n = 27), referred to the *Timofei Moșneaga* Republican Clinical Hospital between 2022 and 2024 for symptoms of overactive bladder. The research focused on physical examination, questionnaires, bladder diary, urinalysis, and urodynamic measurements before and after botulinum toxin type A injections in 30 patients with overactive bladder refractory to first-line therapy.

Results. In women with overactive bladder, the reproductive group was as follows: moderate problems (51%) > very severe problems (31%), severe problems (18%) (p = 0.02); in the group of women in the climacteric period: severe problems (48%) > very severe problems (37%) > moderate problems (15%) (p = 0.10). Based on urodynamics data, the diagnosis of overactive bladder with detrusor overactivity was confirmed by establishing the presence of phasic contractions of the detrusor (3.9 ± 1.15), increased values of detrusor pressure (45.9 ± 23.9 cmH_2O) and reduced bladder compliance (10.4 ± 11.4 ml/cmH_2O). In 100% of cases, these findings predicted an effective botulinum toxin type A injection. Daytime urinary frequency, nocturia, and urinary urgency scores improved significantly after botulinum toxin type A injection by 41.7%, 26.1% and 34.1%, respectively.

Conclusion. The study revealed age differences in overactive bladder symptom severity between the women in both groups. The reproductive period group experienced moderate complications, while the climacteric period group had more severe complications. Administration of botulinum toxin type A through detrusor injection has been shown to be efficacious in the management of overactive bladder.

Keywords: overactive bladder, botulinum toxin, detrusor overactivity, urodynamics.

Cite this article: Ivanov M, Ceban E. Age related detrusor overactivity and symptoms perception in women: role of Botulinum toxin A injection for refractory overactive bladder. Mold J Health Sci. 2025;12(3):40-45. https://doi.org/10.52645/MJHS.2025.3.06.

Manuscript received: 08.07.2025

Accepted for publication: 01.09.2025

Published: 15.09.2025

***Corresponding author:** Mihaela Ivanov, MD, PhD, assistant professor
Department of Urology and Surgical Nephrology
Nicolae Testemitanu State University of Medicine and Pharmacy
165 Stefan cel Mare și Sfant blvd, Chisinau, Republic of Moldova, MD-2004
e-mail: mihaella.litovcenco@gmail.com

Authors' ORCID IDs
Mihaela Ivanov – https://orcid.org/0000-0002-5990-320X
Emil Ceban – https://orcid.org/0000-0002-1583-2884

Key messages

What is not yet known on the issue addressed in the submitted manuscript

Although intradetrusor Botulinum toxin A is widely accepted for treating refractory overactive bladder, its age-related efficacy and perception of symptom improvement in women with detrusor overactivity remain insufficiently understood. Furthermore, data are scarce regarding the influence of aging on treatment response, urodynamic changes, and quality-of-life outcomes after Botulinum toxin A injection. There is also limited evidence on how symptom

perception differs between younger and older women, and whether these differences impact clinical decision-making or long-term management strategies.

The research hypothesis

Intradetrusor Botulinum toxin A injection improves overactive bladder symptoms in women with detrusor overactivity, regardless of age, but age-related differences may exist in symptom perception, urodynamic response, and treatment satisfaction.

The novelty added by the manuscript to the already published scientific literature

This study brings novel insight by stratifying women with refractory overactive bladder by age and evaluating the impact of Botulinum toxin A injection on both objective urodynamic parameters and subjective symptom perception. It is among the first to highlight age as a potential moderator of treatment response and perception, offering new data on how different age groups experience symptom relief after Botulinum toxin A.

Introduction

Overactive bladder (OAB) is a prevalent disorder impacting a significant segment of the population, especially women, and its prevalence increases with age. The main symptoms are urgency, frequent urination, nocturia, and urge incontinence [1, 2]. OAB may be characterized as a hypersensitivity condition in which patients manifest increased urge sensations at lower volumes of bladder filling compared to normal healthy individuals. In a study of 45 women and cystometric testing, all those who reported OAB symptoms gave significantly greater sensation of bladder filling at 25%, 50%, and 75% of the bladder's full capacity irrespective of the frequency of their urgency episodes [3].

Postmenopausal women have a higher probability to suffer from OAB symptoms due to physiological alterations like the reduced amount of estrogen or the weakened pelvic floor muscles [1, 4]. Estrogen receptors within the urogenital tract are sensitive to the hormonal fluctuations that accompany menopause [5].

The intradetrusor injection of botulinum toxin (BoNT-A) in patients with refractory OAB has been commonly documented. Leong's review found that approximately 80% of participants achieve a positive response to this treatment regimen, this treatment reduces the frequency of urination by 12-53% and the amount of urinary incontinence by 35-87% [6, 7]. Clinical efficacy of the therapy with 100 U BoNT-A was the same in older and younger women [8].

Material and methods

During the period 2022–2024, 76 women presenting with overactive bladder symptoms and referred to the *Timofei Moşneaga* Republican Clinical Hospital were retrospectively analyzed. Patients were categorized into two groups based on age: - reproductive age (RP, n = 49) and climacteric period (CP, n = 27). The study included an analysis of the clinical and urodynamic data from 30 patients with OAB resistant to conservative treatment, performed before and after the injection of BoNT-A. The inclusion criteria included: women older than 18 years, diagnosed with OAB, according to the International Continence Society (ICS) criteria. Exclusion criteria: post-void residual volume >10 ml assessed via USG, acute urinary tract infections, neurological diseases.

All enrolled patients completed 3-day voiding diary, the ICIQ-OAB questionnaire before and after injection. The urodynamic testing was performed to confirm detrusor overactivity (DO) using Medica SpA (Memphis Division, Medolla, Italy). and included: uroflowmetry, cystometry, pressure flow study, and ultrasound of the urinary bladder to evaluate the post-micturition urine volume.

BoNT-A intradetrusor injections were performed under intravenous anesthesia, following antibiotic prophylaxis with Ciprofloxacin 500 mg (KRKA, Slovenia). A dose of 100U BoNT-A (Neuronox®, Medytox Inc., Korea), diluted in 10 ml of 0.9% NaCl, was administered using rigid cystoscop (Karl Storz 19Fr rigid cystoscope). After bladder filling with ~150 ml NaCl 0.9%, injections were delivered supratrigonally using a 5Fr, 4 mm rigid needle, inserting ~2–3 mm into the detrusor. Twenty injections (10 U/mL, 0.5 ml/site) were distributed ~1 cm apart. The trigone, ventral wall, and dome were avoided. The bladder was emptied post-procedure.

Ethical considerations. Prior to enrollment, informed consent was obtained from all patients. The study was approved by the Research Ethics Committee of *Nicolae Testemițanu* State University of Medicine and Pharmacy of Republic of Moldova (Approval No. 24/05.03.2021). Patients who underwent the surgical procedure were required to confirm their understanding of its nature before consenting to the operation by signing an informed consent form.

Statistical methods. Statistical analysis of the data was processed using programs IBM SPSS v.27, RStudio and MedCalc. The comparison of frequencies observed in discrete categories between two or more independent groups was performed using the $\chi 2$ test (with the application of continuity correction for adjustment), with probability reporting (p). In the Kruskal-Wallis test, the values of the test ($\chi 2$), degrees of freedom (df), effect size (ε^2 – epsilon square), and probability (p) were reported. Continuous variables were presented using descriptive statistics (median, mean, standard deviation, standard mean error, intervariable interval, and coefficients of variation – CFV). The comparison of the coefficients of variation (CVC) in the independent groups was performed based on the Forkman method, with the reporting of probability (p), the value of the statistical test (F), and the confidence interval (95% CI). Statistical significance was set atp < 0.05.

Results

The total ICIQ-OAB score showed a statistically significant difference in the distribution of OAB symptom severity between the age groups (RP/CP). In the group of

women with a climacteric period, 100% of cases (n = 27) had increased severity (ICIQ-OAB$_{ST}$ ≥ 8), and in women of reproductive age, moderate severity level predominated in 55.10% of cases (n = 27); those with increased severity followed next, at 44.90% (n = 22).

Significant differences in bladder sensitivity indices were observed between the age groups (Table 1). The reproductive age (RP) group had higher average values for the urine retention duration index (SRBD$_{Duration}$) ($p < 0.001$; $d > 0.8$). Conversely, the climacteric period (CP) group had higher mean scores for the patient's perception of the intensity of voiding urgency (PPIUS) ($p < 0.001$ $d > 0.8$).

A Chi-square test revealed a statistically significant difference in PPIUS levels between the RP and CP groups ($\chi^2(3) = 71.79$, $p < 0.001$), with a large effect size (Cramér's V = 0.972).

Table 1. Self-reported indices of bladder sensitivity (voiding diary) in women with OAB

	Group	Average	SD	SE	t_{Welch}	*p*	MD	SED	$CI_{95\%}$ Lower limit.	$CI_{95\%}$ Upper limit	d_{Cohen}
PPIUS	RP (n = 49)	1.551	0.503	0.072	-13.965	< .001	-1.819	0.130	-2.08	-1.557	-3.40
	CP (n = 27)	3.370	0.565	0.109							
SRBD $_{duration}$	RP (n = 49)	22.653	7.576	1.082	8.793	< .001	12.838	1.460	9.92	15.749	1.98
	CP (n = 27)	9.815	5.092	0.980							
PPBC	RP (n = 49)	4.796	0.889	0.127	-2.306	0.024	-0.426	0.185	-0.79	-0.057	-0.53
	CP (n = 27)	**5.222**	0.698	0.134							

***Note**: RP – reproductive period; CP – climacteric period; PPIUS – patient's perception of the intensity of the voiding emergency; $SRBD_{duration}$ – duration of urine retention; PPBC – the patient's perception of the condition of the bladder; SD – standard deviation; SE – standard error; t_{Welch} – test t (Welch); p – probability; MD – average difference; SED – standard error difference; $CI_{95\%}$ – confidence interval 95%; d_{Cohen} – Effect Size (coefficient d according to Cohen).*

Patient perception about bladder condition, measured by the PPBC questionnaire, was significantly different between groups ($p = 0.024$). The mean score was higher in the climacteric period group (5.22 ± 0.70) compared to the reproductive age group (4.80 ± 0.89).

In the assessment of the total cohort of women with OAB, disregarding the age group factor, an almost analogous distribution regarding the various levels of severity of the PPBC index was noted (moderate problems, 38%; severe problems, 29%; and very severe problems, 33%). This distribution was not statistically significant ($\chi 2 = 0.974$; $p = 0.615$).

In females with OAB during the menopausal transition (Fig. 1), mean values of urodynamic indices tended to be lower (Table 2), with statistical significance for the following parameters (in decreasing order of probability): $p < 0.001$, urinary index IU (large effect size $d > 0.8$), strong urge to urinate SDV (large effect size $d > 0.8$), estimated isovolumetric pressure – modified PIP1 (moderate effect size $d > 0.5$).

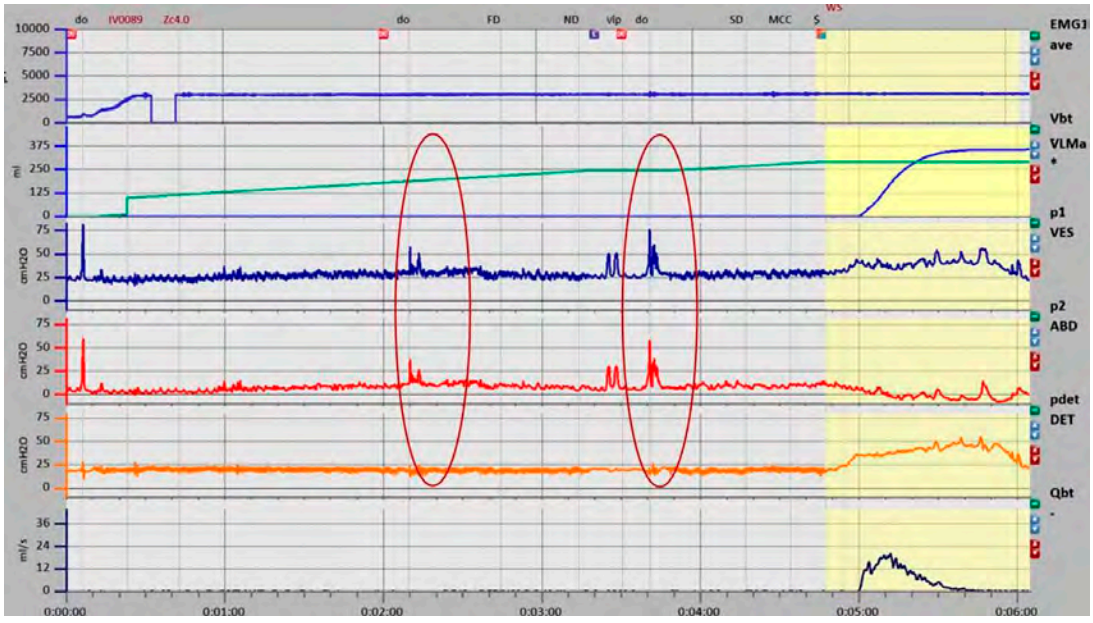

Fig. 1 Urodynamic test in women with refractory OAB before BoNT-A injection. Phasic detrusor contractions.

***Note:** DO – detrusor overactivity; FD – first desire to void; ND – normal desire to void; SD – strong desire to void; MCC – maxim cystometric capacity; Vlp – Valsalva leak point; EMG – electromyography; Vbt – infused volume; P_1ves – intravesical pressure; P_2abd – intraabdominal pressure; Pdet – detrusor pressure; Qbt – flow rate of urine.*

Table 2. Urodynamic indices in women with OAB in reproductive and climacteric period group

UDS	Group	Average	SD	SE	t_{Welch}	*p*	MD	SED	$CI_{95\%}$		d_{Cohen}
									Lower limit	Upper limit	
FSV	RP (n = 49)	64.735	17.379	2.483	50.908	0.452	3.290	4.341	-5.425	12.00	0.183
	CP (n = 27)	61.444	18.502	3.561							
FDV	RP (n = 49)	92.612	14.283	2.040	36.894	0.162	7.057	4.950	-2.975	17.08	0.364
	CP (n = 27)	85.556	23.436	4.510							
SDV	RP (n = 49)	117.633	15.837	2.262	40.923	< .001	17.188	4.830	7.434	26.94	0.892
	CP (n = 27)	100.444	22.171	4.267							
MCC	RP (n = 49)	150.245	24.868	3.553	36.071	0.841	1.800	8.906	-16.26	19.86	0.052
	CP (n = 27)	148.444	42.436	8.167							
PIP1	RP (n = 49)	68.218	12.744	1.821	62.350	0.007	5.481	1.969	1.56	9.417	0.582
	CP (n = 27)	62.737	3.896	0.750							

***Note**: RP – reproductive period; CP – climacteric period; FSV – first sensation of urination (ml); FDV – first desire of voiding (ml); SDV – strong desire of voiding (ml); MCC – maximum cystometric capacity of the bladder (ml); PIP1 – Estimated isovolumetric pressure – modified; SD – standard deviation; SE – standard error; t_{Welch} – test t (Welch); p – probability; MD – average difference; SED – standard error difference; $CI_{95\%}$–confidence interval 95%; d_{Cohen} – Effect Size (coefficient d according to Cohen).*

In the study, all patients who received drug treatment were managed for 6 months with combined conservative treatment: anticholinergic medication (66.6%) and selective β3-adrenoceptor agonists (43.3%). This treatment resulted in symptom improvement in 52.6% of the cases. The remaining 47.3% of the cases (19 patients in the reproductive period and 11 patients in the climacteric period) were non-responders to the treatment and thus invited for third-line therapy (intradetrusor injection of botulinum toxin type A).

Intravenous anesthesia was used during the surgical intervention. All subjects undergoing the procedure were administered prophylactic antibiotics (Ciprofloxacin 500 mg). The dosage utilized was 100 IU of BoNT-A (Neuronox®, Medytox Inc., Korea) and this dosage was diluted in 10 ml of 0.9% saline solution. The bladder was dilated under Karl Storz 19Fr rigid cystoscope guidance by infusing approximately 150-200 ml of NaCl at a concentration of 0.9%. A 5 Fr, 4 mm long rigid injection needle and was used to inject BoNT-A supratrigonally into the detrusor muscle (2-3 mm), in twenty separate locations with each injection site receiving 10 units/mL in 0.5 ml, spaced about 1 cm apart. Care was taken to avoid the bladder trigone, ventral wall, and dome due to their proximity to the peritoneal cavity. Post-injection, the bladder was drained using Foley an 18 Fr urethral catheter [9].

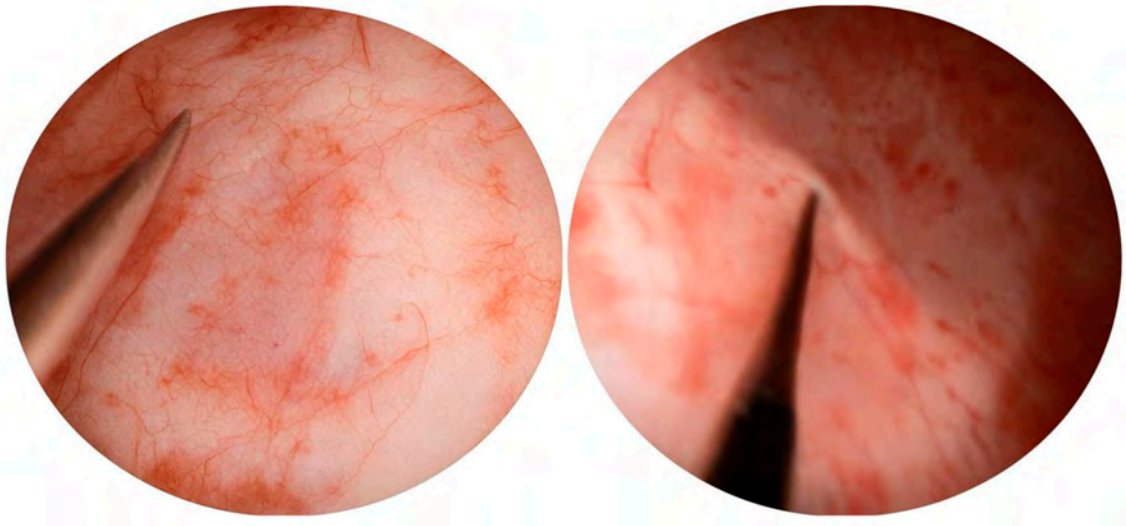

Fig. 2 Intradetrusor BoNT-A injections in women with refractory OAB.

The OAB symptoms were present in all cases in patients prior to BoNT-A injection (Fig. 2). Botulinum toxin improved urinary symptoms, with daytime frequency decreasing in 40% of patients and urinary urgency decreasing in 71%. After detrusor BoNT-A injection, 73.9% of patients reported the resolution of nocturia symptoms.

Two weeks after the BoNT-A injections, patients showed improvements in urinary frequency (41.7%), nocturia (26.1%), and urinary urgency scores (34.1%) compared to baseline measurements.

Table 3. Injection efficacy according to the degree of impairment of symptoms from ICIQ-OAB questionnaire

Severity of ICIQ-OAB	BoNT-A pre-injection (n = 30)	BoNT-A post-injection (after 2 weeks) (n = 30)
Absence of symptoms	0	21 (70%)
Mild	18 (60%)	9 (30%)
Severe	12 (40%)	0

***Note**: ICIQ-OAB – overactive bladder symptoms questionnaire; BoNT-A – botulinum toxin type A.*

The severity of LUTS/OAB, measured by the ICIQ-OAB questionnaire, showed a statistically significant reduction (Table 3).

Table 4. Refractory OAB before and after surgery

Urodynamic parameters		BoNT-A pre-injection (n = 30)	BoNT-A post-injection (after 2 weeks) (n = 30)
Cystometry	FS (ml)	82.7 ± 61.22	290.03 ± 29.33
	FDV (ml)	123.5 ± 112.3	313.3 ± 33.6
	SDV (ml)	170 ± 135	315 ± 28.2
	MCC (ml)	194.57 ± 150.93	333.56 ± 37.7
PIP1		119.4 ± 39.2	54.9 ± 7.52

***Note**: FS – first sensation of bladder filling; FDV – first desire to void; SDV – strong desire to void; MCC – maximum cytometric bladder capacity; **PIP1** – Estimated isovolumetric pressure-modified; BoNT-A – botulinum toxin type A.*

UDS performed after 2 weeks of injections (fig. 3) demonstrated an enhancement in bladder capacity/sensation, the complete absence of phasic detrusor contractions, and a normalization of detrusor pressure levels (Table 4).

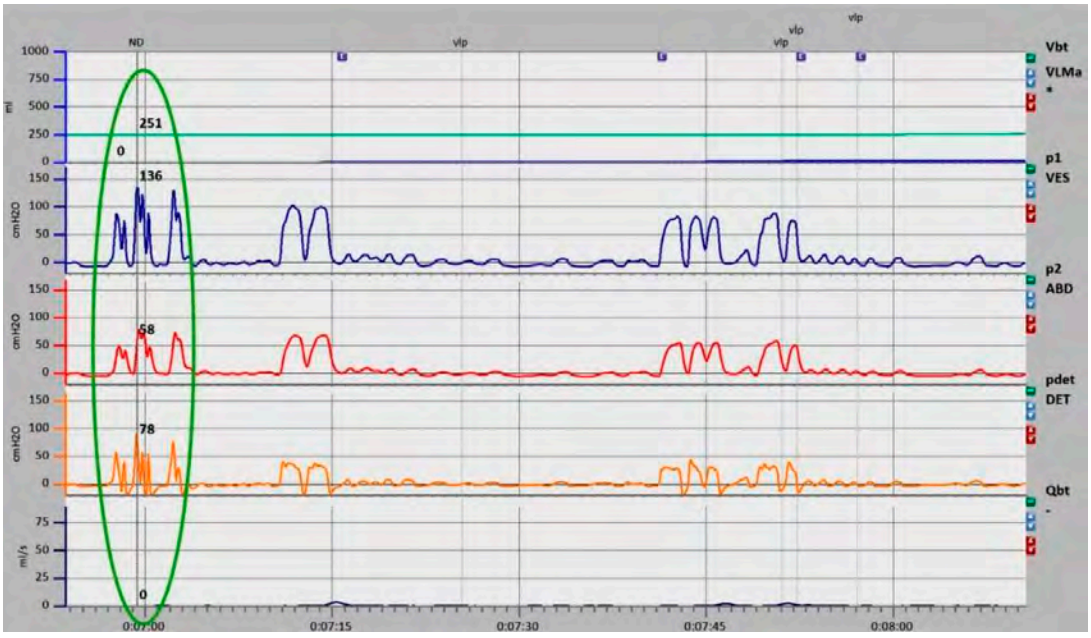

Fig. 3 Urodynamic test in women with refractory OAB after BoNT-A injection.

***Note:** ND – normal desire to void; Vlp – Valsalva leak point; EMG – electromyography; Vbt – infused volume; P_1ves – intravesical pressure; P_2abd – intraabdominal pressure; Pdet – detrusor pressure; Qbt – flow rate of urine.*

In the current cohort of 27 patients undergoing intravesical therapy with BoNT-A, 4 instances of urinary tract infection were identified, representing 14.8% of the cases, confirmed by positive urine cultures. The average of PVR was 3.9 ml, indicating the absence of postinjection acute urinary retention and the low urinary flow rate.

Discussion

Patients with overactive bladder (OAB) exhibit heightened sensitivity to bodily signals, which can evoke somatic or psychological symptoms. Younger and older OAB patients void with similar frequency, mean voided volume, and urge severity, with no differences noted in nocturia or bladder fullness sensation between the age groups. Perceptions of bladder fullness in asymptomatic older adults were compared to OAB patients at different ages and the result showed that age-related changes are a contributing factor in the development of overactive bladder. To confirm storage dysfunction signs aligning with the ICS-established OAB criteria the Sensation-related bladder diaries can be used [10].

In our qualitative evaluation of the PPIUS index, we observed that the perception of voiding urgency intensity was most often of moderate severity in women with OAB, with

variations depending on age group. In the reproductive age (RP) group, moderate severity was the most common (55%, n = 27), followed by the mild variant (45%, n = 22), and no other levels of severity were recorded. In the climacteric period (CP), severe cases were the most common (56%, n = 15), followed by the highest degree (PPIUS = 4), urinary incontinence (41%, n = 11), and moderate severity was the most common (4%, n = 1), with no instances of mild severity recorded.

According to the literature, the age did not appear to significantly influence the voided volume associated with bladder feelings, as assessed through sensation-related bladder diaries [10], but the indices of the clinical questionnaires in OAB patients (total scores) showed significant differences in the mean values between the groups of OAB patients of different age groups (RP/PC), with higher values in women in the climacteric period than in those of reproductive age ($p < 0.001$). In patients of climacteric age, the clinical manifestations assessed according to the questionnaires were characterized by a narrower range of responses regarding frequency, intensity, and severity compared to patients of reproductive age.

The assessment of bladder sensitivity in patients with OAB also showed significant differences. In the reproductive age (RP), 51% of the patients had moderate problems, 31% had severe problems, and 18% had very severe problems. The differences in proportions were significant ($p = 0.02$). In the group of women in the climacteric period (CP), the following order of magnitude was observed: 15% of the patients had severe problems, and the differences in proportions were not significant ($p = 0.10$).

Conclusions

The study showed that the women from both groups had different levels of symptoms. Women in the reproductive period had some moderate symptoms, whereas women in the climacteric period had more severe symptoms. The intradetrusor injections of 100U BoNT-A were proven effective in the management of hard-to-manage OAB with a DO established on UDS.

Competing interests

None declared.

Authors' contributions

Both authors participated in the study design and contributed to drafting the manuscript. The authors critically reviewed the work and approved the final version of the manuscript.

Ethics approval

The research project was approved by the Research Ethics Committee of *Nicolae Testemițanu* State University of Medicine and Pharmacy (Minutes no. 24 from 05.03.2021).

Patient consent

Obtained.

Acknowledgements and funding

No external funding.

Provenance and peer review

Not commissioned, externally peer reviewed.

References

1. Choi SJ, Lee H, Kim DI. Thread embedding acupuncture in postmenopausal women with overactive bladder: a prospective, single-arm, before-after study. Int J Womens Health. 2024;16:2287-2296. doi: 10.2147/IJWH.S494135.
2. Palmer MH, Willis-Gray MG. Overactive bladder in women. An evidence-based review of screening, assessment, and management. Am J Nurs. 2017;117(4):34-41. doi: 10.1097/01.NAJ.0000515207.69721.94.
3. Yamaguchi O, Honda K, Nomiya M, Shishido K, Kakizaki H, Tanaka H, et al. Defining overactive bladder as hypersensitivity. Neurourol Urodyn. 2007;26(6 Suppl):904-907. doi: 10.1002/nau.20482.
4. Blümel JE, Chedraui P, Baron G, Belzares E, Bencosme A, Calle A, et al. Menopausal symptoms appear before the menopause and persist 5 years beyond: a detailed analysis of a multinational study. Climacteric. 2012;15(6):542-551. doi: 10.3109/13697137.2012.658462.
5. Chen Y, Yu W, Yang Y, Duan J, Xiao Y, Zhang X, et al. Association between overactive bladder and peri-menopause syndrome: a cross-sectional study of female physicians in China. Int Urol Nephrol. 2015;47(5):743-749. doi: 10.1007/s11255-015-0948-6.
6. Gotoh D, Torimoto K, Takamatsu N, Onishi K, Morizawa Y, Hori S, et al. Intravesical injection of onabotulinumtoxina (Botulinum toxin type A) in Japanese patients with refractory overactive bladder. In Vivo (Brooklyn). 2024;38(3):1332-1337. doi: 10.21873/invivo.13573.
7. Grishin A., Spaska A., Kayumova L. Correction of overactive bladder with botulinum toxin type A (BONT-A). Toxicon, 2021; 200: 96–101.
8. Nurkkala M, Salo H, Piltonen T, Sova H, Rossi HR. Efficacy of 100-U Onabotulinumtoxin A treatment in female idiopathic overactive bladder – a prospective follow-up study. Int Urogynecol J. 2025;36(3):685-693. doi: 10.1007/s00192-025-06047-8.
9. Ivanov M, Ceban E. Role of Botulinum toxin A injections as a salvage therapy for refractory overactive bladder: insights from urodynamic studies. In: Sontea V, Tiginyanu I, Railean S, editors. 6th International Conference on Nanotechnologies and Biomedical Engineering: Proceedings of IFMBE-2023, Sep 20-23, 2023, Chisinau, Moldova. Cham: Springer; 2024. Vol. 2: Biomedical engineering and new technologies for diagnosis, treatment, and rehabilitation. p. 267-277.
10. Herrewegh A, Marcelissen T, van Koeveringe G, Vrijens D. Overactive bladder 'symptoms' or 'complaints' in young and elderly patients or healthy volunteers? Continence. 2024;9:101068. https://doi.org/10.1016/j.cont.2024.101068.

https://doi.org/10.52645/MJHS.2025.3.07

UDC: 617.735-007.23-053.9-07

RESEARCH ARTICLE

Targeting the biochemical signature of age-related macular degeneration: a preliminary study of potential diagnostic and prognostic biomarkers

Ecaterina Pavlovschi*, Angela Untila, Svetlana Protopop, Ala Ambros, Olga Tagadiuc

Department of Biochemistry and Clinical Biochemistry, *Nicolae Testemițanu* State University of Medicine and Pharmacy, Chisinau, Republic of Moldova

ABSTRACT

Introduction. Age-related macular degeneration is a multifactorial, polyetiological condition, affecting individuals over the age of 50, primarily characterized by progressive and irreversible loss of central vision. In the pursuit of a deeper understanding of its etiopathogenesis, risk factors, associated biomarkers, and diagnostic metabolites, the omics approach plays an essential role. The primary objective of this study was to evaluate selected omics biomarkers along with hematological and clinical data and to establish their correlations with macular degeneration.

Material and methods A pilot retrospective study was conducted, analyzing medical records of 80 patients admitted to the Ophthalmology Department of the *Timofei Moșneaga* Republican Clinical Hospital. Laboratory parameters were assessed and statistically analyzed using the Statistical Package for the Social Sciences. Statistical methods included binomial tests, Wilcoxon Signed-Rank tests, and One-sample tests. The data obtained were compared with the results of a comprehensive analysis of the latest scientific literature on age-related macular degeneration.

Results. Omics approach analysis, particularly proteomic and metabolomic analyses, has contributed significantly to the identification of metabolic pathways involved in age-related macular degeneration pathogenesis, facilitating the investigation of novel biomarkers for early diagnosis and potential therapeutic targets. In our pilot study, we evaluated clinical and biochemical data, including age, sex, laboratory values, and comorbidities, and compared them with currently published research data. Statistically significant biomarkers identified included glucose, triglycerides, prothrombin, fibrinogen, platelet count, and leukocyte count. Partially significant (dual) biomarkers included total cholesterol, erythrocyte sedimentation rate, and lymphocyte count. No statistical significance was observed for HDL-cholesterol, LDL-cholesterol, and international normalized ratio.

Conclusions. Omics approach represents a promising avenue for monitoring, diagnosing, and potentially treating age-related macular degeneration. By identifying key biomarkers, this approach supports early detection and opens the path for advanced therapeutic strategies such as gene therapy, cell-based treatments, complement pathway inhibitors, and nanotechnology-based interventions.

Keywords: age-related macular degeneration, drusen, retina, metabolism, biomarkers.

Cite this article: Pavlovschi E, Untila A, Protopop S, Ambros A, Tagadiuc O. Targeting the biochemical signature of age-related macular degeneration: a preliminary study of potential diagnostic and prognostic biomarkers. Mold J Health Sci. 2025;12(3):46-52. https://doi.org/10.52645/MJHS.2025.3.07.

Manuscript received: 15.07.2025

Accepted for publication: 12.08.2025

Published: 15.09.2025

***Corresponding author: Ecaterina Pavlovschi**, MD, PhD, associate professor, senior researcher
Chair of Biochemistry and Clinical Biochemistry
Nicolae Testemițanu State University of Medicine and Pharmacy.
27 Nicolae Testemițanu str, Chisinau, Republic of Moldova, MD-2025
e-mail: ecaterina.pavlovschi@usmf.md

Key messages

What is not yet known about the issue addressed in the submitted manuscript

The precise clinical significance and consistency of omics biomarkers in differentiating age-related macular degeneration subtypes and stages, particularly in underrepresented populations, remain unclear.

The research hypothesis

Specific biomarkers are significantly altered in age-related macu-

Authors' ORCID IDs
Ecaterina Pavlovschi – https://orcid.org/0000-0003-0385-4805
Angela Untila – https://orcid.org/0000-0002-3835-3341
Svetlana Protopop – https://orcid.org/0000-0003-1660-3343
Ala Ambros – https://orcid.org/0000-0001-8545-8501
Olga Tagadiuc – https://orcid.org/0000-0002-5503-8052

lar degeneration and may serve as both early diagnostic markers and therapeutic targets.

The novelty added by manuscript to the already published scientific literature

This study introduces new data, categorizes biomarkers by statistical relevance, and links them to the pathogenesis of age-related macular degeneration through a multi-test validation approach.

Introduction

According to studies and research conducted since the beginning of 2025, this year marks a significant milestone in medical advancements across various disciplines, with notable progress in ophthalmology. A particular focus has been directed toward neurodegenerative ocular diseases. Stargardt disease, for instance, is caused by loss-of-function mutations in the ABCA4 gene, leading to progressive macular degeneration and eventual vision loss. As an incurable condition, it has posed a major therapeutic challenge. However, recent breakthroughs in 2025 have brought promising developments in gene therapy, particularly through the identification of novel therapeutic vectors capable of precisely editing ABCA4 mutations. These advancements pave the way for potential vision restoration and represent a critical step forward in the management of inherited retinal dystrophies [1].

Additional innovations published throughout the year have highlighted the role of gene therapy in the treatment of age-related macular degeneration (AMD). Notably, studies have demonstrated that a single gene therapy intervention targeting retinal pigment epithelium (RPE) cells can induce sustained production of anti-angiogenic proteins, offering a promising long-term strategy for controlling neovascularization in AMD [2].

AMD is one of the leading causes of vision loss globally among individuals over 50 years of age. This research is of significant importance, as AMD has emerged as a major public health concern. In 2020, approximately 10 million individuals were diagnosed with AMD, and current projections estimate that this number will double by 2040, emphasizing the urgent need for effective diagnostic and therapeutic strategies [3].

AMD is a polyetiological condition influenced by both modifiable and non-modifiable risk factors. According to recent studies, modifiable factors such as smoking, hypertension, diabetes mellitus, and cardiovascular diseases are significantly associated with an increased risk of AMD. Non-modifiable factors, including advanced age and male sex, also show a strong statistical correlation with disease onset. However, findings regarding body mass index (BMI), total cholesterol, and triglyceride levels remain controversial, as these variables have not demonstrated statistically significant associations [4, 5].

According to the latest research, AMD is classified into several stages: subclinical AMD, characterized by the absence of retinal pigment epithelium (RPE) depigmentation and the presence of small drusen; early AMD, which involves small to medium drusen, focal depigmentation, and impaired dark adaptation; intermediate AMD, associated with the accumulation of large drusen and more pronounced RPE changes; and advanced AMD, which is currently divided into two forms: dry AMD, also known as geographic atrophy (GA), and wet AMD, referred to as choroidal neovascularization (CNV) [6-8].

Currently, omics-based approaches – particularly the metabolomic one – are increasingly applied in the study of AMD, with a focus on the early detection of the disease through specific biomarkers and the development of personalized therapeutic targets tailored to the individual pathophysiological profile of each patient. In parallel, efforts are being made to implement efficient and early screening strategies by integrating artificial intelligence (AI) technologies into diagnostic workflows [9].

The scientific relevance of this work also lies in its analysis of existing therapeutic approaches for AMD, particularly its advanced wet form, which is associated with severe, often irreversible, vision loss. While anti-VEGF agents remain the standard of care, recent advancements have introduced complement system inhibition therapies targeting components such as C3 (pegcetacoplan) and C5 (avacincaptad pegol), the latter approved by the U.S. Food and Drug Administration in 2023 [10]. However, these treatments remain insufficient for achieving definitive disease control, and there is still no effective pharmacological therapy available for the dry (atrophic) form of AMD.

To elucidate the etiopathogenesis of AMD, enable early diagnosis through biomarkers, and identify innovative therapeutic targets, the application of omics-based approaches, particularly metabolomics and proteomics, has proven essential. Metabolomics involves the comprehensive analysis of low-molecular-weight metabolites (typically < 1500 Da), while proteomics focuses on the study of proteins involved in biochemical reactions, cellular processes, and metabolic pathways [4]. Together, these approaches provide powerful tools for the quantitative and qualitative assessment of specific biomarkers, offering insights into the pathogenetic mechanisms underlying AMD and supporting the development of targeted, personalized interventions.

The aim of this study was to identify characteristic biomarkers in patients diagnosed with age-related macular degeneration and to interpret their alterations.

Material and methods

The research was based on a pilot retrospective study involving the analysis of 80 medical records of patients admitted to the Ophthalmology Department of the "Timofei Moşneaga" Republican Clinical Hospital between 2019 and 2023. Among the 80 patients diagnosed with age-related

macular degeneration (AMD), 42 were men (52.5%) and 38 were women (47.5%), with a mean age of 71.21 ± 8.81 years. Relevant data, including metabolic indices and biomarkers, were analyzed using SPSS version 23 (Statistical Package for the Social Sciences) for Windows XP. To assess statistical correlations with AMD, binomial tests, Wilcoxon Signed-Rank tests, and One-sample tests were applied.

The data obtained were compared with the results of a comprehensive analysis of the latest scientific literature on AMD. A systematic search of PubMed, MEDLINE, Web of Science, and Google Scholar was conducted to identify relevant studies published in English up to June 2025. Keywords included "age-related macular degeneration," "retinal degeneration," "metabolomics," "proteomics," "biomarkers," "oxidative stress," and "lipid metabolism."

Inclusion criteria were original research articles, reviews, and meta-analyses focusing on the AMD pathobiochemical mechanisms of ocular damage and potential marker identification by omics approaches. Data extraction and quality assessment were performed independently by two reviewers.

Results

Among the most researched etiopathogenetic mechanisms of AMD are oxidative stress (OS), nitrosative stress (NS), the complement system, lipid peroxidation (LPO), mitophagy, and mitochondrial DNA disorders [7].

The retina functions as a highly active metabolic center, with a substantial daily oxygen demand. However, exposure to various risk factors, such as psychological stress, aging, smoking, sleep deprivation, poor hygiene, and a nutritionally inadequate diet, can disturb the equilibrium between the antioxidant defense system and OS. This imbalance leads to the accumulation of reactive oxygen species (ROS), which cause oxidative damage at the level of the RPE, disrupt retinal metabolism, and contribute to progressive degeneration [9].

Additionally, with aging, lipofuscin (LF) – a cytotoxic and phototoxic component – accumulates. It contributes to the activation of drusogenesis and, upon exposure to blue light, has the property of releasing H_2O_2 and O_2^- (superoxide anion radical). Transformed into N-retinylidene-N-retinylethanolamine (A2E), it influences homeostasis and interferes with cholesterol metabolism by inducing OS, accompanied by LPO [11-13].

The hyperoxidative state within LPO initiates a vicious circle, which consequently damages DNA, proteins, and lipids, disrupting cellular functionality, survival, and proliferation, and additionally favoring the accumulation of LF [7].

Microvascular dysfunction is also involved in the deterioration of RPE function, leading to the dysregulation of nutrition and vascularization, setting up ischemia and activating angiogenesis by increasing the production of vascular endothelial growth factor (VEGF). Additionally, OS and vascular inflammation are associated, which worsen visual deficiencies, leading to pathological neovascularization, vascular damage, and disruption of the blood-retinal barrier.

Excessive production of ROS impairs the activation capacity of the antioxidant defense system and limits its ability to undergo repair. Consequently, this dysfunction leads to an energy crisis, primarily driven by damage to mitochondrial DNA [14, 15].

OS is one of the main causes of degeneration. Through pathological changes produced at the DNA level, it causes the activation of the STING (Stimulator of Interferon Genes) pathway, a cell signaling pathway located at the endoplasmic reticulum, which plays a role in detecting cytoplasmic/foreign DNA. This activation promotes chronic inflammation and, ultimately, the degeneration of RPE cells [16].

Moreover, OS triggers the activation of the PINK1/Parkin-mediated mitophagy pathway, leading to damage of the outer blood-retinal barrier. This impairment contributes to reduced choriocapillaris perfusion, resulting in ischemia and increased expression of VEGF. These events, in turn, activate the p62/Nrf2 signaling pathway, promoting dysregulated mitophagy and accumulation of dysfunctional mitochondria, thereby disrupting cellular homeostasis. Concurrently, the accumulation of PINK1 on the outer mitochondrial membrane and the subsequent recruitment of Parkin initiate the degradation of impaired mitochondria [17-19].

Similar to oxidative stress, nitrosative stress also contributes to the development of AMD through the release of peroxynitrite – a cytotoxic byproduct of nitric oxide (NO) dysregulation. This leads to disturbances in choroidal microcirculation and degeneration of the retinal pigment epithelium (RPE), ultimately promoting neovascularization via upregulation of vascular endothelial growth factor (VEGF) synthesis [20].

The enhanced risk of developing degeneration is also marked by aberrant activation of the complement system, with the alternative pathway being the primary one involved. These processes lead to the dysregulation of cellular turnover. This hypothesis was supported by research on donor eyes, where the presence of C3b deposits and membrane attack complex (MAC) accumulations in the choriocapillaris and RPE was confirmed, and components of this system were detected within drusen structures [21].

Along with etiopathogenetic mechanisms, significant changes are also observed at the level of cellular metabolism. Approximately 80%-89% of metabolic alterations involve lipids, for which the following biomarkers are characteristic: total cholesterol, HDL-cholesterol, LDL-cholesterol, triglycerides, ApoA1, and ApoB. Very low-density lipoproteins (VLDL) show reduced values, in contrast to HDL, whose levels are elevated [22]. In the literature, increased activity of the complement system alongside reduced cholesterol level and a quantitative reduction of glycerophospholipids, which promotes the risk of developing AMD as well as other degenerative pathologies. Some epidemiological studies have concluded that increased HDL levels and reduced triglycerides (TAG) are more characteristic of patients diagnosed with AMD [23-25].

In addition to changes in lipid metabolism, there are also changes in amino acid metabolism. Thee EF *et al.* (2023), in the conducted studies, concluded that the following amino acids had lower levels: histidine, citrate, alanine, phenylalanine, tyrosine, leucine, and valine, and, conversely, the ketone bodies, acetoacetate and 3-hydroxybutyrate, were elevated [22]. Also, hyperhomocysteinemia considerably increases the risk of AMD development via the inflammatory processes caused, OS, cell apoptosis, and epigenetic changes, which

lead to degeneration [26]. Additionally, it increases the level of glutamate, which induces neurotoxicity, promoting mitochondrial dysfunction and OS, resulting in cell death [27]. Mitochondrial dysfunction has also been found in the case of disorders of alanine, glycine, and serine metabolism [28].

As previously mentioned, the retina is an active metabolic center, and relies on glucose as an energy substrate, meaning that glucose metabolism cannot be overlooked in the case of AMD. Thus, the following changes in glucose metabolism have been observed: elevation of citrate and isocitrate, and a decrease in succinate, glutamine, and α-ketoglutarate, which promote the secretion of VEGF, responsible for macular neovascularization in AMD [29]. Hyperglycemia promotes the accumulation of advanced glycation end products (AGEs) which in turn trigger OS and pro-inflammatory pathways, ultimately leading to RPE dysfunction. At the same time, hyperglycemia stimulates VEGF expression and favors the development of the wet form of AMD [30].

Although there are multiple and varied controversies regarding the disorders detected in hemostatic metabolism, researchers support the idea that elevated fibrinogen concentrations may increase the risk of developing AMD, particularly its wet form. A few studies suggest that plasminogen activator inhibitor-1 is correlated with the occurrence of AMD. However, due to disputes in this area, the factors involved in hemostatic metabolism cannot yet be considered potential biomarkers for AMD [31].

In this study, the pilot retrospective analysis was considered relevant for comparing the data obtained from a selected patient cohort with findings reported in clinical studies. The investigation involved the review and evaluation of 80 medical records of patients admitted to the Ophthalmology Department of the "Timofei Moşneaga" Republican Clinical Hospital between 2019 and 2023. All patients included in the study were diagnosed with AMD, comprising 42 males (52.5%) and 38 females (47.5%), with a mean age of 71.21 ± 8.81 years. Relevant available data were extracted from the patients' medical records, including age, sex, laboratory indices, primary diagnosis, and comorbidities. These variables were analyzed using binomial tests, One-sample tests, and Wilcoxon Signed-Rank tests in SPSS to determine their statistically significant correlations with AMD. The binomial test, One-sample test, and Wilcoxon Signed-Rank test were applied to assess the statistical significance of categorical and continuous variables, allowing for the comparison of observed data with theoretical or clinical reference values, particularly where normal distribution could not be assumed.

Application of the binomial test identified the presence of statistically significant biomarkers with values of p<0.05, as outlined below: glucose (p=0.022); prothrombin (p<0.001); fibrinogen (p<0.001); triglycerides (p=0.031); platelet count (p=0.000); leukocyte count (p<0.001); and ESR (p=0.017). Statistically insignificant were the values of INR (p=0.203), total cholesterol (p=0.458), HDL-cholesterol (p=1.000), LDL-cholesterol (p=0.289), and lymphocyte count (p=0.110) (Table 1).

Table 1. Results obtained from the analysis of various biomarkers using the binomial and Wilcoxon Signed-Rank tests.

Parameter	Binomial test	Wilcoxon Signed-Rank test
Glucose	p<0.022 *	p=0.004 **
Prothrombin	p<0.001 ***	p=<0.001 ***
Fibrinogen	p<0.001 ***	p<0.001 ***
INR	p=0.203 ns	p<0.001 ***
Triglycerides	p=0.031 *	p=0.009 **
Total cholesterol	p=0.458 ns	p=0.041 *
HDL-cholesterol	p=1.000 ns	p=0.541 ns
LDL-cholesterol	p=0.289 ns	p=0.208 ns
Platelet count	p=<0.001 ***	p<0.001 ***
Leukocyte count	p<0.001 ***	p<0.001 ***
Lymphocyte count	p=0.110 ns	p=0.003 **
ESR	p=0.017 *	p=0.309 ns

Note: *Statistical significance compared to the control group: * – p < 0,05; ** – p < 0.01; *** – p < 0.001; ns – not significant. ESR – erythrocyte sedimentation rate; INR – international normalized ratio.*

Compared to the results of the Wilcoxon Signed-Rank test, some discrepancies were observed. Statistically significant laboratory indices in this test included fibrinogen, prothrombin, INR, platelet count, and leukocyte count, all with p-values < 0.001. Total cholesterol was also significant with p=0.041, though close to the significance threshold. Additionally, triglycerides (p=0.009), glucose (p=0.004), and lymphocyte count (p=0.003) showed statistical significance. The biomarkers found to be statistically insignificant in this test were ESR (p=0.309), HDL-cholesterol (p=0.541), and LDL-cholesterol (p=0.208) (Table 1).

These deviations may be due to study limitations, such as the relatively small number of patients involved, given that the pathology is not very common in the Republic of Moldova, incomplete laboratory data, lacunar diagnosis, and the lack of stratification according to the wet or dry form of AMD.

Another test used to investigate biomarkers associated with AMD is the One-sample test (Fig. 1). Regarding this test, it was observed that glucose has a lower mean value of 1.7053 and an upper mean of -0.2755, indicating asymmetry in the data and suggesting that it is statistically significant, thus showing a moderate but meaningful deviation. Prothrombin has a lower mean value of 22.0073 and an upper mean of -37.5641, both significant as they lie outside the reference range, indicating major deviations from the mean. For fibrinogen, the lower mean is 1.2843 (positive), and the upper mean is -0.7249 (negative); these data suggest asymmetry and a potential imbalance in data distribution. Additionally, deviations were noted for ESR, with a lower mean of 11.3533 and an upper mean of -0.3133, not necessarily significant on both sides, indicating slight asymmetry. A comparable pattern was observed for triglycerides, with a lower mean of 1.3061 and an upper mean of -0.4189, suggesting a slight deviation from reference values. In this test, insignificant deviations were found for total cholesterol and LDL-cholesterol, as presented in Fig.1.

As a result of the comprehensive investigation of the obtained data, we can conclude that acquired biomarkers can be divided into 3 categories: statistically significant biomarkers, dual biomarkers, and statistically insignificant biomarkers.

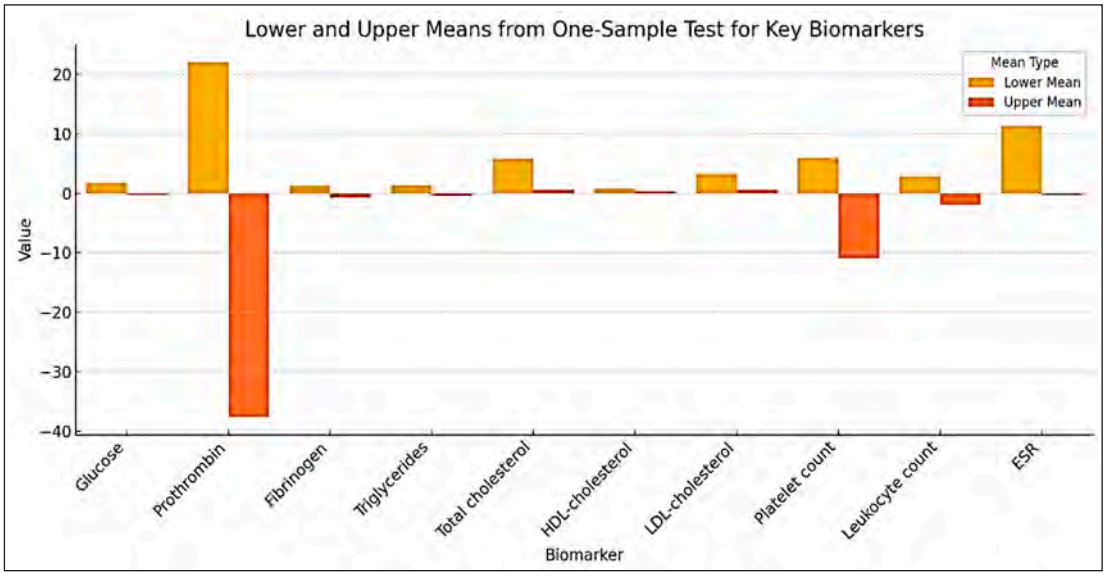

Fig. 1 Lower and upper mean estimates of key biomarkers in AMD patients as identified by the One-sample test

Note: a) Data are expressed as estimated mean differences. b) The One-sample test was used to assess whether the sample mean significantly deviates from the clinical reference value for each biomarker. Positive or negative mean values indicate the direction and magnitude of deviation from the reference mean. c) ESR – erythrocyte sedimentation rate.

Among the statistically significant biomarkers are glucose, triglycerides, prothrombin, fibrinogen, platelet count, and leukocyte count. These data confirm the involvement of glucose and lipid metabolism disorders–represented by triglycerides–in the etiopathogenesis of AMD; hemostatic metabolism imbalances, evidenced by changes in fibrinogen and prothrombin levels, indicating possible coagulation disorders along with platelet count; and last but not least, systemic inflammatory process, chronically represented by leukocyte count, which suggest an association with the risk of progression of macular lesions. These biomarkers thus become pathognomonic factors for AMD.

Among the dual biomarkers are total cholesterol, ESR, and lymphocyte count. ESR is statistically significant in the binomial test (p=0.017) and the One-sample test but is insignificant in Wilcoxon Signed-Rank test (p=0.309), likely due to differences in sensitivity to data distribution. Total cholesterol is insignificant (p=0.458) in the binomial test and significant, but close to the threshold (p=0.041) in Wilcoxon Signed-Rank test, indicating unclear deviations from the proportion. Additionally, lymphocyte count is insignificant (p=0.110) in the binomial test, but significant (p=0.003) in Wilcoxon Signed-Rank test, suggesting that the proportion does not differ from the clinical reference range, while the median level shows discrepancies.

Representatives of the subgroup of statistically insignificant biomarkers are HDL-cholesterol, LDL-cholesterol, and INR. Despite studies indicating the active involvement of hyperlipidemia in the etiopathogenesis of the disease and vascular risk at the ocular level, in the studied population we observe the opposite. The possible reason is that these biomarkers are not directly correlated with AMD.

Thus, to minimize the discrepancies observed in the study, it is necessary to apply several statistical methods to avoid presenting erroneous data. At the same time, we conclude that the study detected significant biomarkers correlated with AMD, such as glucose, triglycerides, and fibrinogen, indicating that these indices could be promising for assessing AMD risk, as they are associated with metabolic and inflammatory disorders specific to degeneration. However, to confirm these results, paraclinical imaging data of the patients involved in the study are also necessary, in particular those obtained by optical coherence tomography, as well as their medical history (diabetes mellitus, hypertension).

Discussions

In recent years, degeneration has gained momentum practically on all continents, with research demonstrating inevitable, progressive, and irreversible damage to the visual system, resulting in an unfavorable prognosis for this pathology.

As a result of this study, as well as those researched in scientific databases, we conclude the importance of modifiable and non-modifiable risk factors, environmental influences, lifestyle, and genetic factors in the evolution and manifestation of degeneration. These data are necessary for identifying potential effective therapeutic targets. We have presented their impact on health and the devastating consequences that lead to disability [5].

The burden imposed by this condition on individual health and societal systems has led the medical community to recognize AMD as a public health priority, for which early diagnosis and effective treatment are critically needed [3].

The integration of omics technologies, particularly metabolomics and proteomics, has significantly advanced our understanding of AMD pathogenesis. Metabolomics enables the identification of small-molecule metabolic signatures associated with disease progression, while proteomics allows characterization of changes in protein expression, structure, and interactions within retinal tissues. These approaches have uncovered new biomarkers and potential therapeutic targets, emphasizing their importance in both early diagnosis and personalized medicine strategies for AMD [4].

After understanding the etiopathogenetic mechanisms of AMD, researchers have identified that restoring the compromised antioxidant system can be achieved through sup-

plementation with exogenous antioxidants, such as β-carotene, vitamins C and E, copper, and zinc. The consumption of these antioxidants results in approximately a 25% decrease in the progression of the neovascular form of AMD over 5 years. Additionally, administration of lutein and zeaxanthin reduces the risk of progression to late AMD. Furthermore, consumption of acetyl L-carnitine, ω-3 fatty acids, and coenzyme Q10 has demonstrated considerable improvement in visual function in patients diagnosed with AMD [32].

Future research directions focus on gene and cell therapy, AI, and the development of targeted, individualized treatments aimed at monitoring, exploring, and managing the disease. For example, one promising therapy is intravitreal gene therapy with ADVM-022, which enables continuous production of aflibercept in retinal cells through a single injection, effectively inhibiting neovascularization [33].

Anti-VEGF therapy remains the standard treatment for wet AMD but has limitations in cases with macular fibrosis and carries side effects, including treatment resistance. Additionally, complement system inhibitors (pegcetacoplan, avacincaptad pegol) have shown promising results in AMD therapy but pose a risk of intraocular inflammation, particularly in geographic atrophy cases [34].

Thus, the omics approach opens new perspectives for the identification of AMD biomarkers and the development of effective therapies, but further studies are needed to optimize treatments and prevent disease progression.

In conclusion, we support the idea that, as a result of this pilot retrospective study, we identified some omics-derived indices as potential biomarkers for AMD risk assessment and monitoring. However, given the complexity of this pathology, a multidisciplinary approach that includes targeted metabolomic and proteomic investigations is essential. Additionally, to reduce the limitations encountered during the study, it is recommended to increase the sample size and extend the spectrum of monitored and analyzed parameters to avoid deficiencies.

Conclusions

The study highlighted the involvement of several biomarkers in the pathogenesis and progression of age-related macular degeneration (AMD), particularly those related to lipid metabolism (e.g., total cholesterol, LDL-cholesterol, HDL-cholesterol, triglycerides, apolipoprotein B, apolipoprotein A1), glucose metabolism, and hemostatic imbalance (e.g., fibrinogen, prothrombin). Among these, our pilot retrospective study confirmed the statistical significance of glucose, triglycerides, fibrinogen, prothrombin, platelet count, and leukocyte count, supporting their potential role as biomarkers for AMD risk assessment and disease monitoring.

These findings suggest that omics-derived indices, particularly from metabolomics and proteomics, could help in identifying personalized diagnostic and therapeutic targets. However, further large-scale, stratified studies are required to validate these associations, integrate imaging findings, and address current limitations related to data completeness and AMD subtype differentiation.

Competing interests

None declared.

Authors' contributions

EP and AU collected and analyzed the data and drafted the manuscript. AU and EP conceived the study, participated in study design, statistical analysis, and assisted in drafting the manuscript. SP and AA analyzed the data and critically revised the manuscript. OT critically evaluated the results, assessed their applicability, and critically revised the manuscript. All authors reviewed the work critically and approved the final version of the manuscript.

Informed consent for publication

Obtained.

Acknowledgements and funding

No external funding

Ethics approval

The study protocol was approved by the Research Ethics Committee of *Nicolae Testemițanu* State University of Medicine and Pharmacy (approval no. 58, dated June 20, 2024).

Provenance and peer review

Not commissioned, externally peer-reviewed.

References

1. Muller A, Sullivan J, Schwarzer W, et al. High-efficiency base editing in the retina in primates and human tissues. Nat Med. 2025;31(2):490-501. doi: 10.1038/s41591-024-03422-8.
2. Hushmandi K, Lam HY, Wong WM, et al. Gene therapy for age-related macular degeneration: a promising frontier in vision preservation. Cell Commun Signal. 2025;23(1):233. doi: 10.1186/s12964-025-02246-4.
3. Thomas CJ, Mirza RG, Gill MK. Age-related macular degeneration. Med Clin North Am. 2021;105(3):473-491. doi: 10.1016/j.mcna.2021.01.003.
4. Laíns I, Gantner M, Murinello S, et al. Metabolomics in the study of retinal health and disease. Prog Retin Eye Res. 2019;69:57-79. doi: 10.1016/j.preteyeres.2018.11.002.
5. Babaker R, Alzimami L, Al Ameer A, et al. Risk factors for age-related macular degeneration: updated systematic review and meta-analysis. Medicine (Baltimore). 2025;104(8):e41599. doi: 10.1097/MD.0000000000041599.
6. Spaide RF, Jaffe GJ, Sarraf D, et al. Consensus Nomenclature for Reporting Neovascular Age-Related Macular Degeneration Data: Consensus on Neovascular Age-Related Macular Degeneration Nomenclature Study Group. Ophthalmology. 2020;127(5):616-636. doi: 10.1016/j.ophtha.2019.11.004. Eratum in: Ophthalmology 2020 Oct;127(10):1434-1435. doi: 10.1016/j.ophtha.2020.07.019.
7. Bondy S, Maiese K, editors. Aging and age-related disorders. New York: Humana Press; 2010. 472 p. doi: 10.1007/978-1-60761-602-3. (Oxidative stress in applied basic research and clinical practice).
8. Li X, Cai S, He Z, et al. Metabolomics in retinal diseases: an update. Biology (Basel). 2021;10(10):944. doi: 10.3390/biology10100944.
9. Deng Y, Qiao L, Du M, et al. Age-related macular de-

generation: epidemiology, genetics, pathophysiology, diagnosis, and targeted therapy. Genes Dis. 2021;9(1):62-79. doi: 10.1016/j.gendis.2021.02.009.
10. Trincão-Marques J, Ayton LN, Hickey DG, et al. Gene and cell therapy for age-related macular degeneration: a review. Surv Ophthalmol. 2024;69(5):665-676. doi: 10.1016/j.survophthal.2024.05.002.
11. Pugazhendhi A, Hubbell M, Jairam P, Ambati B. Neovascular macular degeneration: a review of etiology, risk factors, and recent advances in research and therapy. Int J Mol Sci. 2021;22(3):1170. doi: 10.3390/ijms22031170.
12. Brown CN, Green BD, Thompson RB, den Hollander AI, Lengyel I; EYE-RISK consortium. Metabolomics and age-related macular degeneration. Metabolites. 2018;9(1):4. doi: 10.3390/metabo9010004.
13. Rajanala K, Dotiwala F, Upadhyay A. Geographic atrophy: pathophysiology and current therapeutic strategies. Front Ophthalmol (Lausanne). 2023;3:1327883. doi: 10.3389/fopht.2023.1327883.
14. Kaarniranta K, Uusitalo H, Blasiak J, et al. Mechanisms of mitochondrial dysfunction and their impact on age-related macular degeneration. Prog Retin Eye Res. 2020;79:100858. doi: 10.1016/j.preteyeres.2020.100858.
15. Hyttinen JMT, Blasiak J, Kaarniranta K. Non-coding RNAs regulating mitochondrial functions and the oxidative stress response as putative targets against age-related macular degeneration (AMD). Int J Mol Sci. 2023;24(3):2636. doi: 10.3390/ijms24032636.
16. Zou M, Ke Q, Nie Q, et al. Inhibition of cGAS-STING by JQ1 alleviates oxidative stress-induced retina inflammation and degeneration. Cell Death Differ. 2022;29(9):1816-1833. doi: 10.1038/s41418-022-00967-4.
17. Tisi A, Feligioni M, Passacantando M, Ciancaglini M, Maccarone R. The impact of oxidative stress on blood-retinal barrier physiology in age-related macular degeneration. Cells. 2021;10(1):64. doi: 10.3390/cells10010064.
18. Zhao B, Zhu L, Ye M, et al. Oxidative stress and epigenetics in ocular vascular aging: an updated review. Mol Med. 2023;29(1):28. doi: 10.1186/s10020-023-00624-7.
19. Zhang SM, Fan B, Li YL, Zuo ZY, Li GY. Oxidative stress-involved mitophagy of retinal pigment epithelium and retinal degenerative diseases. Cell Mol Neurobiol. 2023;43(7):3265-3276. doi: 10.1007/s10571-023-01383-z.
20. Toma C, De Cillà S, Palumbo A, Garhwal DP, Grossini E. Oxidative and nitrosative stress in age-related macular degeneration: a review of their role in different stages of disease. Antioxidants (Basel). 2021;10(5):653. doi: 10.3390/antiox10050653.
21. Maugeri A, Barchitta M, Mazzone MG, Giuliano F, Agodi A. Complement system and age-related macular degeneration: implications of gene-environment interaction for preventive and personalized medicine. Biomed Res Int. 2018;2018:7532507. doi: 10.1155/2018/7532507.
22. Thee EF, Acar İE, Colijn JM, et al. Systemic metabolomics in a framework of genetics and lifestyle in age-related macular degeneration. Metabolites. 2023;13(6):701. doi: 10.3390/metabo13060701.
23. Acar İE, Lores-Motta L, Colijn JM, et al. Integrating metabolomics, genomics, and disease pathways in age-related macular degeneration: the EYE-RISK Consortium. Ophthalmology. 2020;127(12):1693-1709. doi: 10.1016/j.ophtha.2020.06.020.
24. Lo Faro V. Answer to the Hamlet-like dilemma of lipid metabolites causing senile macular degeneration. Cell Rep Med. 2023;4(7):101077. doi: 10.1016/j.xcrm.2023.101077.
25. Tan LX, Germer CJ, La Cunza N, Lakkaraju A. Complement activation, lipid metabolism, and mitochondrial injury: converging pathways in age-related macular degeneration. Redox Biol. 2020;37:101781. doi: 10.1016/j.redox.2020.101781.
26. Tawfik A, Samra YA, Elsherbiny NM, Al-Shabrawey M. Implication of hyperhomocysteinemia in blood retinal barrier (BRB) dysfunction. Biomolecules. 2020;10(8):1119. doi: 10.3390/biom10081119.
27. Xia M, Zhang F. Amino acids metabolism in retinopathy: from clinical and basic research perspective. Metabolites. 2022;12(12):1244. doi: 10.3390/metabo12121244.
28. Mitchell SL, Ma C, Scott WK, et al. Plasma metabolomics of intermediate and neovascular age-related macular degeneration patients. Cells. 2021;10(11):3141. doi: 10.3390/cells10113141.
29. Han G, Wei P, He M, Teng H. Glucose metabolic characterization of human aqueous humor in relation to wet age-related macular degeneration. Invest Ophthalmol Vis Sci. 2020;61(3):49. doi: 10.1167/iovs.61.3.49.
30. Lee H, Han KD, Shin J. Association between glycemic status and age-related macular degeneration: a nationwide population-based cohort study. Diabetes Metab. 2023;49(3):101442. doi: 10.1016/j.diabet.2023.101442.
31. Kersten E, Paun CC, Schellevis RL, et al. Systemic and ocular fluid compounds as potential biomarkers in age-related macular degeneration. Surv Ophthalmol. 2018;63(1):9-39. doi: 10.1016/j.survophthal.2017.05.003.
32. Basyal D, Lee S, Kim HJ. Antioxidants and mechanistic insights for managing dry age-related macular degeneration. Antioxidants (Basel). 2024;13(5):568. doi: 10.3390/antiox13050568.
33. Blasiak J, Pawlowska E, Ciupińska J, Derwich M, Szczepanska J, Kaarniranta K. A new generation of gene therapies as the future of wet AMD treatment. Int J Mol Sci. 2024;25(4):2386. doi: 10.3390/ijms25042386.
34. Xu H, Yi C, Chen M. The complement pathway as a therapeutic target for neovascular age-related macular degeneration-mediated subretinal fibrosis. Curr Opin Pharmacol. 2024;76:102448. doi: 10.1016/j.coph.2024.102448.

https://doi.org/10.52645/MJHS.2025.3.08

UDC: 616.24-002:616.12-008.46-036.12

RESEARCH ARTICLE

Community-acquired pneumonia in chronic heart failure: approach through the oxidative stress and systemic inflammation

Virginia Cascaval[1*], Tatiana Dumitras[1], Diana Fetco-Mereuta[1], Sergiu Matcovschi[1], Livi Grib[2]

[1]Clinical Synthesis Discipline, Department of Internal Medicine, *Nicolae Testemițanu* State University of Medicine and Pharmacy, Chisinau, Republic of Moldova
[2]Cardiology Discipline, Department of Internal Medicine, *Nicolae Testemițanu* State University of Medicine and Pharmacy, Chisinau, Republic of Moldova

ABSTRACT

Introduction. Diagnosing community-acquired pneumonia in patients with chronic heart failure can be challenging. Oxidative stress and inflammatory response play an important role in the development and diagnosis of community-acquired pneumonia and are also involved in many cardiovascular diseases, including chronic heart failure.

Materials and methods. A total of 210 patients were enrolled and divided into two groups: group 1 (n = 105) – patients with community-acquired pneumonia associated with chronic heart failure, and group 2 (n = 105) – patients with community-acquired pneumonia without chronic heart failure. Several biomarkers were measured. For oxidative stress, we assessed prooxidant markers (ischemic modified albumin, advanced glycation end-products, advanced oxidation protein products, malonic dialdehyde) and antioxidant markers (total antioxidant activity with CUPRAC and ABTS methods, superoxide dismutase and catalase). Inflammatory status was assessed by determining leukocyte count, erythrocyte sedimentation rate, lactate dehydrogenase, fibrinogen and C-reactive protein. In all patients, N-terminal pro b-type natriuretic peptide values were determined.

Results. The age of patients in the study group ranged from 50 to 92 years, with an overall mean of 70.6 ± 8.89 years (95% CI [68.8-72.3]), (F = 18.109; p = 0.205). Ischemic modified albumin values were higher in patients in Group 1 compared to Group 2: 236.60 ± 57.23 μM/L and 229.77 ± 64.35 μM/L, respectively (F = 0.660; p = 0.045). Serum lactate dehydrogenase had higher values in Group 1, compared to the control group: 232.65 ± 109.80 units/L and 192.40 ± 44.98 units/L, respectively (p = 0.001). The mean fibrinogen values were also higher in Group 1 (5.24 ± 1.60 g/L), compared to Group 2 (4.51 ± 1.78 g/L), p = 0.002. Total antioxidant activity by CUPRAC method, had higher values in Group 1 (6.70 ± 4.62) versus Group 2 (4.99 ± 2.29), p = 0.006.

Conclusions. The coexistence of community-acquired pneumonia and chronic heart failure resulted in a higher inflammatory response and greater accumulation of pro-oxidative reaction products. This condition was characterized by increased serum lactate dehydrogenase, erythrocyte sedimentation rate and fibrinogen levels. Furthermore, the state of heightened oxidative stress was marked by increased ischemic modified albumin and total antioxidant activity detected with CUPRAC method.

Keywords: community-acquired pneumonia, heart failure, oxidative stress, inflammatory response.

Cite this article: Cascaval V, Dumitras T, Fetco-Mereuta D, Matcovschi S, Grib L. Community-acquired pneumonia in chronic heart failure: approach through the oxidative stress and systemic inflammation. Mold J Health Sci. 2025;12(3):53-59. https://doi.org/10.52645/MJHS.2025.3.08.

Manuscript received: 13.07.2025

Accepted for publication: 11.08.2025

Published: 15.09.2025

[*]**Corresponding author**: **Virginia Cascaval,** MD, assistant professor
Clinical Synthesis Discipline, Department of Internal Medicine,
Nicolae Testemițanu State University of Medicine and Pharmacy
165, Stefan cel Mare si Sfânt blvd., Chisinau, Republic of Moldova, MD2004
e-mail: virginia.cascaval@usmf.md

Key messages

What is not yet known on the issue addressed in the submitted manuscript

The inflammatory status and oxidative stress in patients with community-acquired pneumonia and chronic heart failure are not sufficiently known.

The research hypothesis

Community-acquired pneumonia in patients with chronic heart failure exhibit a greater inflammatory status and more pronounced

Authors' ORCID ID
Virginia Cascaval – https://orcid.org/0009-0008-5899-100X
Tatiana Dumitras – https://orcid.org/0000-0001-5538-189X
Diana Fetco-Mereuta – https://orcid.org/0000-0002-7469-045X
Sergiu Matcovschi – https://orcid.org/0000-0003-1623-930X
Livi Grib – https://orcid.org/0000-0001-6913-0864

oxidative stress that those without chronic heart failure.

The novelty added by the manuscript to the already published scientific literature

Our research results report that community-acquired pneumonia in chronic heart failure is associated with a more pronounced inflammatory response, as evidenced by elevated serum lactate dehydrogenase and fibrinogen levels. Oxidative stress activation was determined by higher levels of ischemic modified albumin levels, which correlated positively with radiological extent of the pulmonary infiltrate. The research data may also contribute to the prognosis prediction in patients with severe pneumonia and chronic heart failure, by assessing the ischemic modified albumin values, with a threshold value of 218.98 μM/L.

Introduction

Community-acquired pneumonia (CAP) represents a significant public health concern due to its steadily rising incidence, estimated at 5-12 cases per 1,000 individuals. It remains the leading cause of mortality among infectious diseases and ranks as the sixth among the primary causes of death globally. The incidence of CAP increases markedly with age, reaching 25-40% in individuals over 65 years [1].

Several risk factors are associated with unfavorable outcomes in CAP, with pre-existing cardiovascular disease being the most significant. Elderly patients (over 65 years) frequently present with comorbidities, the most prevalent being chronic obstructive pulmonary disease, ischemic heart disease, chronic congestive heart failure, diabetes mellitus, and cerebrovascular disease [2].

Chronic heart failure (CHF) is a widespread clinical syndrome, particularly among the elderly. Its prevalence in the general population is estimated at 2-3%, with a sharp increase in individuals aged 70-80 years, reaching 10-20%. Among these patients, the four-year mortality rate approaches 50% [3]. The diagnosis of CHF is complex and requires a combination of clinical evaluation and objective evidence of cardiac dysfunction. Diagnostic confirmation is supported by paraclinical investigations such as electrocardiography, chest radiography, and echocardiography, alongside laboratory testing, including complete blood counts, biochemical markers, and natriuretic peptide levels. A favorable clinical response to appropriate therapy further strengthens the diagnosis [4].

Oxidative stress (OS) and reactive oxygen species (ROS) are central to the mechanisms underlying cellular dysfunction and tissue injury. ROS contribute significantly to the inflammatory cascade triggered by bacterial infections [5]. Furthermore, ROS influence intracellular signaling pathways, leading to the activation of transcription factors and the release of pro-inflammatory mediators. Despite the recognized role of oxidative stress in both CAP and CHF, current literature provides limited insight into its dynamics in patients with co-existing CAP and CHF [6, 7].

The interest in knowing the different patterns of inflammation and their related factors has led to a better understanding of the immunopathogenic process that occurs in CAP. The natural course of the infection and its systemic inflammatory pattern in patients with concomitant CHF remain poorly studied [8]. Our first hypothesis is that patients with CAP and CHF have an expressed inflammatory response. And the second hypothesis of our study is that this group of patients have increased levels of oxidative markers. So far, there is a lack of published data about this aspect, which we considered key for interpreting the inflammatory and oxidative stress pattern in patients with CAP and CHF.

Material and methods

This is a prospective, observational, analytic cohort study, conducted in the Department of Internal Medicine, *Holy Trinity* Municipal Clinical Hospital, Chisinau, Republic of Moldova, during October 2021 – October 2022. The study design included 210 patients hospitalized with CAP, divided into two groups according to the presence of chronic heart failure: Group 1 – 105 patients with CAP and CHF (study group), Group 2 – 105 patients with CAP and without CHF (control group). The study was approved by the Research Ethics Committee of *Nicolae Testemițanu* State University of Medicine and Pharmacy, No.18 from April 12, 2019.

Study inclusion criteria were: patients with and without chronic heart failure with community-acquired pneumonia and mandatory presence of clinical and paraclinical features for pneumonia – acute onset, physical pulmonary consolidation syndrome, pulmonary infiltrate at the chest X-ray; presence of criteria for chronic heart failure (edema, dyspnea, cough, wet rales in the lower lungs, decreased exercise tolerance); previously established chronic heart failure (confirmed by medical records such as outpatient charts or hospital discharge summaries); patient age over 50 years; ability of patients to communicate well with the researcher and the ability to understand and comply with the requirements of the study; signed informed consent for inclusion in the study.

We determined the values of prooxidant markers: ischemic modified albumin (IMA), advanced glycation end-products (AGE), advanced oxidation protein products (AOPP), malonic dialdehyde (MDA), and antioxidant markers: total antioxidant activity (TAA) with CUPRAC and ABTS methods, superoxide dismutase (SOD) and catalase. Inflammatory

status was assessed by determining leukocyte count, erythrocyte sedimentation rate (ESR), lactate dehydrogenase (LDH), fibrinogen, C-reactive protein (CRP). Additionally, N-terminal pro-B-type natriuretic peptide (NT-pro-BNP) values were determined in all patients.

Statistical analysis was performed using IBM SPSS Statistics 26.0 and Microsoft Office Excel 2010. All results are presented as M ± m, where M is the sample mean and m is the error of the mean. The following methods were used for statistical data processing: Fisher test (or Fisher-Irwin test, exact χ^2 test) for non-parametric data and One-Way ANOVA test ("analysis of variance") for parametric data.

Results

The age of patients in the study group ranged from 50 to 92 years, with a mean of 70.6 ± 8.89 years (95% CI [68.8-72.3]; Mn = 70.0; IQRR = 11). In the control group, the mean age was 68.7 ± 7.56 years (95% CI [64.2-68.2]; Mn = 68.0; IQRR = 11) (F = 18.109; p = 0.205). The proportion of women in Group 1 was higher than that of men, at 57 (54.3%; CI 95% [44.8-64.1]) and 48 (45.7%; CI 95% [35.9-55.2]). In Group 2 there were more men than women: 54 (51.4%; CI 95% [42.3-61.0]) and 51 (48.6%; CI 95% [39.0-57.7]), respectively, (χ2 = 0.686; df = 1; p = 0.407) (Fig. 1).

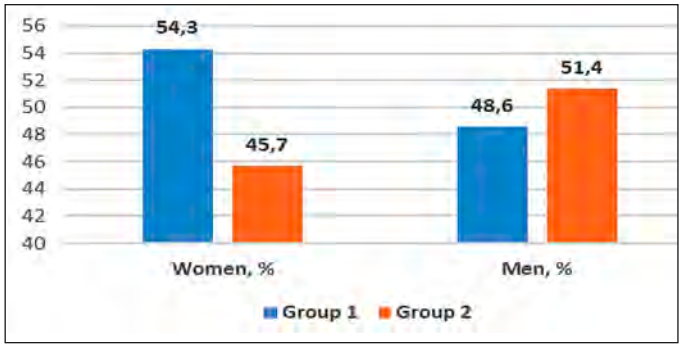

Fig. 1. Distribution of subjects with community-acquired pneumonia and chronic heart failure according to gender.

Note: *The diagram illustrates gender distribution among studied patients. The proportion of women in Group 1 exceeded that of men, while the opposite was true for Group 2. Data are presented in percentages (%).*

Assessing the severity of chronic heart failure according to the New York Heart Association (NYHA) classification in the study group, the following were found: NYHA class II was present in 42 (40.0%; 95% CI [30.5-49.5]) patients, and NYHA class III in 63 (60.0%; 95% CI [50.5-69.5]) patients. According to etiology, CHF had several causes: ischemic – 16 patients (15.2%; 95% CI [8.8-22.2]), valvular – 1 patient (1.0%; 95% CI [0.0-3.2]), and mixed – 88 patients (83.8%; 95% CI [76.6-90.7]).

Patients with community-acquired pneumonia and chronic heart failure had a longer hospital stay, compared to those without CHF: 11.96 ± 0.36 versus 10.82 ± 0.28 days, which was statistically significant (F = 6.020; p = 0.012).

On the objective examination of the respiratory system in Group 1, we determined that 21 (20.0%; 95% CI [12.3-28.4]) patients presented increased vocal fremitus, increased vesicular murmur – 37 (35.2%; 95% CI [26.0-44.4]) patients, dullness – 13 (12.4%; 95% CI [6.5-18.8]) patients, decreased local vesicular murmur – 74 (70.5%; 95% CI [60.6-78.6]) patients. Unilateral crepitant rales were observed in 27 (25.7%; 95% CI [17.9-35.2]) patients, bilateral – 41 (39.0%; 95% CI [30.6-48.6]) patients, sibilant rales were present in 6 (5.7%; 95% CI [1.8-10.5]) patients. No statistical significance was found between the groups.

Arterial hypertension was the most common comorbidity in the study group – 103 (98.0%) patients, compared to 84 (80.1%) patients in the control group. Diabetes mellitus was found in 41 (39.0%; 95% CI [29.9-48.4]) patients in the study group, occurring twice as frequently as in the control group, where it was present in only 25 (23.8%; 95% CI [15.8-32.4]) patients (p = 0.017). Cerebrovascular disease was present in 47 (44.8%; 95% CI [35.5-54.3]) patients in the study group and in 25 (23.8%; 95% CI [16.0-32.3]) patients in the control group (p = 0.001). Simple chronic bronchitis occurred less frequently in patients in Group 1 compared to Group 2: 29 (27.6%; 95% CI [19.6-35.6]) and 39 (37.1%; 95% CI [28.2-46.9]), respectively (p = 0.140). Chronic kidney disease occurred more frequently in Group 1 compared to Group 2: 21 (20.0%; 95% CI [12.6-27.4]) patients and 6 (5.7%; 95% CI [1.9-10.8]) patients, respectively (p = 0.002). Atrial fibrillation was present only in Group 1 – 54 (51.4%; 95% CI [42.2-61.0]) patients, p < 0.0001.

An important aspect explored in the study, was the radiological picture in patients with CAP and CHF, represented by alveolar infiltrate, identified in 38 (36.2%; 95% CI [27.3-45.1]) patients in the study group (p = 0.886), while interstitial infiltrate was found in 67 (63.8%; 95% CI [54.9-72.7]) patients (p = 0.885). Bilateral infiltrate extent was more frequently observed in patients with CAP and CHF – 63 (60.0%; 95% CI [50.5-69.1]) patients – followed by polysegmental involvement in 27 (25.7%; 95% CI [17.7-34.3]) patients, segmental involvement (1-2 segments) in 10 (9.5%; 95% CI [4.3-15.5]) patients, and lobar involvement in 5 (4.8%; 95% CI [1.0-9.3]) patients, also without significant differences between groups. Pleural effusion was significantly higher in patients in the study group compared to those in the control group: 41 (39.0%; 95% CI [30.6-49.5]) patients and 14 (13.3%; 95% CI [7.3-20.0]) patients, respectively (χ^2 = 17.958; df = 1; p < 0.0001).

Significant differences between groups were observed in relation to the mean value of NT-pro-BNP. Thus, in Group 1, NT-pro-BNP had a mean value of 1371.88 ± 498.91 pg/mL, compared to Group 2: 58.19 ± 48.22 pg/mL, (F = 721.542; p < 0.0001), with a threshold value of NT-pro-BNP in patients with CHF and severe course of CAP of 1665.73 pg/mL.

There were no statistical differences between groups in terms of leukocyte counts, with a mean of 10.36 ± 7.13 × 10^9/L and 10.52 ± 5.58 × 10^9/L in both groups, respectively (F = 0.033; p = 0.856). Increased inflammatory status was determined by higher serum LDH values in the CHF group, compared to the control group: 232.65 ± 109.80 units/L and 192.40 ± 44.98 units/L, respectively, (F = 12.076; p = 0.001) (Fig. 2.).

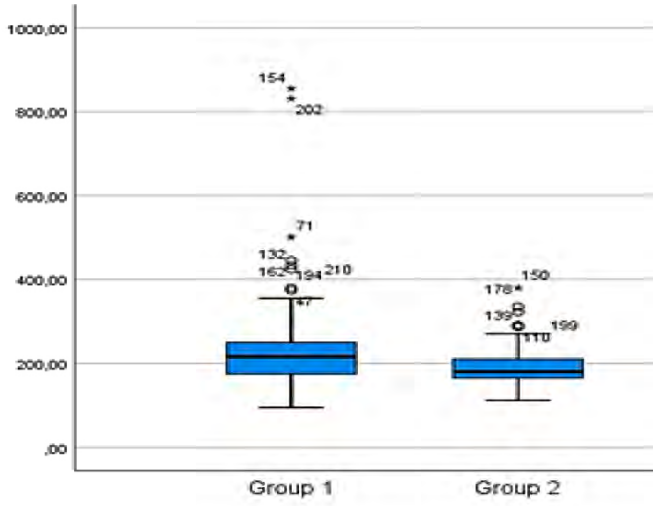

Fig. 2. Lactate dehydrogenase levels in patients with community-acquired pneumonia and chronic heart failure, u/L**.**

Note: *The boxplot illustrates lactate dehydrogenase levels in patients with CAP and CHF. Group 1 shows a higher median LDH level and greater variability. In contrast, Group 2 has a slightly lower median and a narrower interquartile range. The following statistical data were calculated: median, interquartile range, minimum and maximum values.*

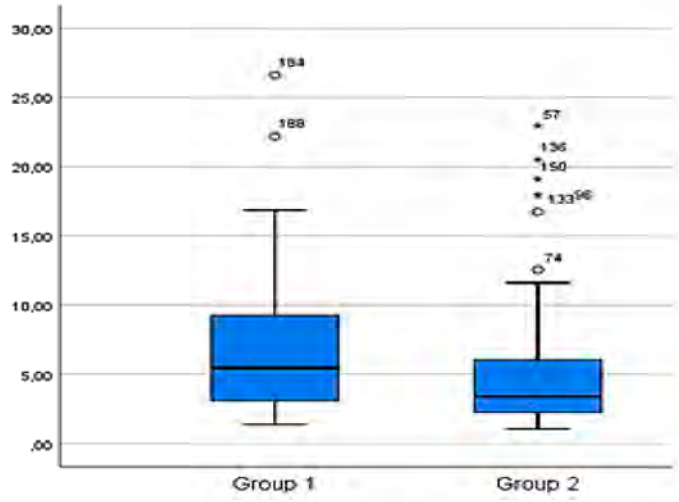

Fig. 3. Total antioxidant activity with CUPRAC method in patients with community-acquired pneumonia and chronic heart failure, compared to the control group.

Note: *The boxplot illustrates total antioxidant activity with CUPRAC method levels in patients with CAP and CHF. Group 1 shows a higher median antioxidant activity and greater variability compared to Group 2. The following statistical data were calculated: median, interquartile range, minimum and maximum values.*

The mean ESR value was significantly higher in Group 1 compared to Group 2: 29.89 ± 15.98 mm/h and 21.17 ± 19.47 mm/h, (F = 12.561; p < 0.0001), and the median values were as follows: Mn = 17.0; IQR = 20.0 compared to Mn = 26.0; IQR = 29.0, respectively. The mean fibrinogen values were also higher in Group 1 (5.24 ± 1.60 g/L), compared to Group 2 (4.51 ± 1.78 g/L), (F = 9.692; p = 0.002).

Analyzing changes in oxidative status, we determined a more pronounced pro-oxidative markers, manifested by higher values of ischemic modified albumin in patients in Group 1 compared to Group 2: 236.60 ± 57.23 µM/L and 229.77 ± 64.35 µM/L, respectively, (F = 0.660; p = 0.045). The threshold value of IMA in patients with CHF and severe course of CAP was 218.98 µM/L.

AGE-pentosidine-like, AGE-vesperlysine-like values, advanced oxidation protein products, malonic dialdehyde values showed no statistically significant differences between the groups (Table 1).

Table 1. Comparison of oxidative stress markers in patients with community-acquired pneumonia and chronic heart failure.

Oxidative stress parameters	Group 1 (n = 105)		Group 2 (n = 105)		F	P
	Mean	SD ±	Mean	SD ±		
IMA, µM/L	236.6077	57.23919	229.7775	64.35578	0.660	0.045
AGE- pentosidin-like, µM/L	598.7908	251.68051	544.5575	197.20439	3.021	0.084
AGE- verperlisin-like, **µM**/L	449.1497	169.38287	455.2475	160.66932	0.072	0.789
AOPP, µM/L	95.2128	63.05108	105.9567	55.21101	1.726	0.190
MDA, µM/L	17.4629	6.94660	16.0739	4.72922	2.869	0.092
Catalase, **µM**/L	21.8819	10.01078	23.1646	11.54527	0.740	0.391
TAA with CUPRAC, µM/L	6.7012	4.62461	4.9987	2.29101	7.647	0.006
TAA with ABTS, µM/L	132.2233	21.48573	128.2355	22.21592	1.748	0.188
SOD, units/g	62.7206	13.37431	62.3362	16.47029	0.034	0.853

Note: *IMA - ischemic modified albumin; AGE - advanced glycation end-products; AOPP - advanced oxidation protein products; TAA - total antioxidant activity; SOD - superoxide dismutase; MDA - malonic dialdehyde. The table presents the oxidative markers changes in patients with CAP and CHF, manifested through increased IMA levels and counterbalanced by antioxidant system – increased TAA with CUPRAC method. For data analysis it was used One-Way ANOVA statistical test.*

Further, we analyzed the values of antioxidant markers. The counterbalancing of antioxidant status was determined through a higher total antioxidant activity with CUPRAC method in patients from Group 1 (6.70 ± 4.62 µM/L) compared to Group 2 (4.99 ± 2.29 µM/L), (F = 7.647; p = 0.006) (Fig. 3.).

Total antioxidant activity using the ABTS method was also higher in patients with CHF (132.22 ± 21.48 µM/L) compared to those without CHF (128.23 ± 22.21 µM/L), (F = 1.748; p = 0.188). Superoxide dismutase values were not significantly different between Group 1 and Group 2: 62.72

± 13.37 units/g and 62.33 ± 16.47 units/g, respectively. At the same time, catalase levels were lower in patients in Group 1 (21.88 ± 10.01 μM/L) compared to Group 2 (23.16 ± 11.54 μM/L), (F = 0.740; p = 0.391)

In patients with CAP and concomitant CHF, total antioxidant activity determined by the CUPRAC method had a significant positive correlation with atrial fibrillation (rs = 0.343; p = 0.038), arterial hypertension (rs = 0.329; p = 0.001), worsening of pre-existing dyspnea (rs = 0.308; p = 0.002), and the presence of pericardial effusion (rs = 0.357; p = 0.023).

At the same time, ischemic modified albumin showed a significant positive correlation with radiological extension of the pulmonary infiltrate (rs = 0.435; p = 0.010) and with fibrinogen levels (rs = 0.387; p = 0.050). Advanced oxidation protein products had a positive correlation with total hospital length of stay (rs = 0.341; p = 0.041). AGE-pentosidine-like compounds showed a significant positive correlation with the presence of pleural effusion on chest X-rays (rs = 0.334; p = 0.001). Lactate dehydrogenase levels had a positive correlation with radiological extent of the pulmonary infiltrate (rs = 0.394; p = 0.025).

Discussions

In our analysis of comorbidities among patients with community-acquired pneumonia and chronic heart failure, hypertension emerged as the most prevalent coexisting condition, identified in 98.0% of cases. This data are similar to the results of a systematic review and meta-analysis, that investigated the impact of comorbidities and risk factors on community-acquired pneumonia in the Indian population. Analyzing 23 observational studies published between 1990 and 2021, the study found that the most common comorbidities among CAP patients were chronic obstructive pulmonary disease (24.2%), hypertension (23.7%), and diabetes mellitus (16%) [9, 10].

In our study, radiologic findings in patients with community-acquired pneumonia and chronic heart failure revealed interstitial-type infiltrates in most of the patients. The most frequent distribution pattern was bilateral involvement, followed by polysegmental extension, segmental involvement and lobar involvement. Bobilev et al. conducted a study to evaluate the clinical features and progression of community-acquired pneumonia in patients with chronic heart failure, reporting alveolar infiltrates in 60% of cases and interstitial infiltrates in 32% [11]. Pleural effusion was determined in 41 patients (39.0%) with community-acquired pneumonia and chronic heart failure. In contrast, a prospective cohort study by Bartoli A. et al., which investigated pleural effusion in hospitalized patients with decompensated chronic heart failure, reported a higher prevalence—67.5%, with bilateral effusion in 53.6% of cases and unilateral effusion in 15.6% [12, 13].

The results of our study demonstrate that NT-proBNP levels were higher in patients with CAP and CHF and correlated positively with radiological extent of the pulmonary infiltrate and with pneumonia severity. This data is supported by Li J et al., who aimed to evaluate, whether plasma B-type natriuretic peptide levels can accurately predict the severity of CAP, and showed that BNP levels strongly correlated with CAP severity and mortality risk. A BNP threshold of ≥125 pg/mL may flag high-risk patients, while ≥299 pg/mL indicates elevated risk of death [14]. Also, NT-proBNP had a strong predictive value for 30-day mortality in hospitalized CAP patients, with an area under the curve (AUC) of 0.735 [95% CI (0.642–0.828)], p < 0.001. The optimal NT-proBNP cut-off for predicting both ICU admission and 30-day mortality was 1,434.5 pg/mL [15].

Laboratory analysis in our study showed that mean fibrinogen levels were higher in patients with concomitant chronic heart failure, suggesting an increased inflammatory response in this population. These results can be explained by an acute-phase response and systemic inflammation in patients with CAP associated with the low-grade systemic inflammation, determined in CHF. Our data is supported by a study that aimed to evaluate the prognostic value of fibrinogen levels in patients with acute exacerbation of chronic heart failure. A total of 554 patients were analyzed and stratified into two groups based on fibrinogen levels: low (≤284 mg/dL) and high (≥284 mg/dL), with the cut-off determined by ROC curve analysis. The area under the curve for predicting 90-day mortality was 0.65 (95% CI; 0.59–0.70). High fibrinogen levels were significantly associated with increased 90-day mortality, with an unadjusted hazard ratio of 3.33 (95% CI; 2.15–5.15). The study concluded that elevated fibrinogen is an independent predictor of 90-day mortality in chronic heart failure population [16].

Our study also demonstrated significantly elevated lactate dehydrogenase levels in patients with community-acquired pneumonia and chronic heart failure compared to the control group. A related study examined the predictive value of LDH, C-reactive protein and neutrophil counts in assessing the severity of community-acquired pneumonia. Reported LDH levels ranged from 266 to 1,424 U/L, with a mean of 598.1 ± 286.79 U/L, while CRP values ranged from 22.75 to 202.25 mg/L, averaging 53.5 ± 23.14 mg/L. The study found a significant positive correlation between neutrophil count, LDH, CRP, and the CURB-65 severity score [17].

Subsequently, we analyzed oxidative damage markers (ischemic-modified albumin, advanced glycation end products, advanced oxidation protein products, malonic dialdehyde) in patients with CAP and CHF. Ischemic modified albumin, which is evaluated as a cardiac ischemia marker, was more pronounced in patients with CAP and CHF compared to the control group and showed a significant positive correlation with radiological extension of the pulmonary infiltrate. Our results are supported by a study, that aimed to evaluate the diagnostic utility of IMA levels in patients with CAP presenting to the Emergency Department and included 162 adult participants: 81 patients diagnosed with CAP and 81 healthy controls. The results showed significantly elevated IMA levels in CAP patients (0.532 ± 0.117 IU/mL) compared to controls (0.345 ± 0.082 IU/mL), p < 0.05. An IMA cutoff value of 0.442 IU/mL yielded a sensitivity of 75.3%

and a specificity of 91.3% for CAP diagnosis. A moderate positive correlation was observed between IMA and CRP levels ($r = 0.506$, $p < 0.05$). These data suggest that IMA may serve as a novel and practical biomarker to aid in the early diagnosis of CAP [18, 19].

In our study, the antioxidant defense system in patients with community-acquired pneumonia and chronic heart failure was evaluated through measurements of total antioxidant activity using the CUPRAC and ABTS methods, both of which showed elevated levels. However, catalase activity was found to be reduced in the CHF group. The increased antioxidant activity observed may reflect a compensatory response to oxidative stress, driven by an imbalance between the heightened production of reactive oxygen species and the limited capacity for their elimination or neutralization – potentially linked to hypoxia, as suggested by elevated LDH levels [20, 21].

In the present study, it is necessary to mention the difficulty of collecting biological material in some cases, , due to the overlap of study collection with the COVID-19 pandemic. Thus, during that period, sputum collection for microscopic and bacteriological examination was restricted. There were also limitations regarding the measurament of serum procalcitonin, as well as performing chest computed tomography.

Conclusions

Community-acquired pneumonia in patients with chronic heart failure is associated with an enhanced inflammatory response, as demonstrated by elevated lactate dehydrogenase, erythrocyte sedimentation rate and fibrinogen levels. Furthermore, increased oxidative stress is indicated by significantly elevated levels of ischemic modified albumin, which positively correlated with the radiological extent of pulmonary infiltrates. Ischemic modified albumin may serve as a novel and practical biomarker to support the early diagnosis of community-acquired pneumonia in patients with chronic heart failure.

Competing interests

None declared.

Authors' contributions

VC conceived the study and participated in study design. TD helped drafting the manuscript and participated in data analysis. DF had a substantial contribution to acquisition of data. SM and LG contributed to final approval of the version to be published. All the authors reviewed the work critically and approved the final version of the manuscript.

Ethics approval

The research project was approved by the Research Ethics Committee of *Nicolae Testemițanu* State University of Medicine and Pharmacy (Minutes no. 18 from 12.04.2019).

Patient consent

Obtained.

Acknowledgements and funding

No external funding.

Provenance and peer review

Not commissioned, externally peer reviewed.

References

1. Divino V, Schranz J, Early M, et al. The annual economic burden among patients hospitalized for community-acquired pneumonia (CAP): a retrospective US cohort study. Curr Med Res Opin. 2020;36(1):151-160. doi: 10.1080/03007995.2019.1675149.
2. Marin-Corral J, Pascual-Guardia S, Amati F, et al. Aspiration risk factors, microbiology, and empiric antibiotics for patients hospitalized with community-acquired pneumonia. Chest. 2021;159(1):58-72. https://doi.org/10.1016/j.chest.2020.06.079.
3. Shen L, Jhund P. S, Anand I. S, et al. Incidence and outcomes of pneumonia in patients with heart failure. Journal of the american college of cardiology. 2021;77(16):1961-1973. https://doi.org/10.1016/j.jacc.2021.03.001.
4. Mancini D, Gibson G. Impact of pneumonia in heart failure patients. J Am Coll Cardiol. 2021;77(16):1974-1976. https://doi.org/10.1016/j.jacc.2021.03.010.
5. Carr AC, Spencer E, Dixon L, et al. Patients with community acquired pneumonia exhibit depleted vitamin C status and elevated oxidative stress. Nutrients. 2020;12(5):1318. https://doi.org/10.3390/nu12051318.
6. Zhang Q, Ju Y, Ma Y, Wang T. N-acetylcysteine improves oxidative stress and inflammatory response in patients with community acquired pneumonia: a randomized controlled trial. Medicine (Baltimore). 2018;97(45):e13087. doi: 10.1097/MD.0000000000013087.
7. Cascaval V, Matcovschi S, Grib L, et al. Oxidative stress in patients with community-acquired pneumonia and pre-existing heart failure. Arch Balk Med Union. 2024;59(4):336-342. https://doi.org/10.31688/ABMU.2024.59.4.02.
8. Méndez R, Menéndez R, Cillóniz C, et al. Initial inflammatory profile in community-acquired pneumonia depends on time since onset of symptoms. Am J Respir Crit Care Med. 2018;198(3):370-378. https://doi.org/10.1164/rccm.201709-1908OC.
9. Ghia CJ, Rambhad GS. Systematic review and meta-analysis of comorbidities and associated risk factors in Indian patients of community-acquired pneumonia. SAGE Open Med. 2022;10. doi: 10.1177/20503121221095485.
10. Cha YS, Lee KH, Lee JW, et al. The usefulness of the delta neutrophil index for predicting superimposed pneumonia in patients with acute decompensated heart failure in the emergency department. PLoS One. 2016;11(9):e0163461. doi: 10.1371/journal.pone.0163461.
11. Bobylev A, Rachina S, Avdeev S, et al. Etiologiia vnebol'nichnoi pnevmonii u lits s khronicheskoi serdechnoi nedostatochnost'iu [Etiology of commu-

nity-acquired pneumonia in patients with chronic heart failure]. Pulmonologiya. 2019;29(3):293-301. https://doi.org/10.18093/0869-0189-2019-29-3-293-301. Russian.
12. Bartoli A, Donadoni M, Ceriani E, et al. Phenotyping pleural effusion in patients hospitalized in Internal Medicine wards with decompensated heart failure. Eur J Intern Med. 2024;120:131-133. doi: 10.1016/j.ejim.2023.11.008.
13. Marinkovic SP, Topuzovska IK, Stevanovic M, et al. Features of parapneumonic effusions. Pril Makedon Akad Nauk Umet Odd Med Nauki. 2018;39(1):131-141. doi: 10.2478/prilozi-2018-0033.
14. Li J, Ye H, Zhao L. B-type natriuretic peptide in predicting the severity of community-acquired pneumonia. World J Emerg Med. 2015;6(2):131-6. doi: 10.5847/wjem.j.1920-8642.2015.02.008.
15. Akpınar EE, Hoşgün D, Akpınar S, et al. Do N-terminal pro-brain natriuretic peptide levels determine the prognosis of community acquired pneumonia? J Bras Pneumol. 2019;45(4):e20180417. https://doi.org/10.1590/1806-3713/e20180417.
16. Meng Z, Zhao Y, He Y. Fibrinogen Level Predicts Outcomes in Critically Ill Patients with Acute Exacerbation of Chronic Heart Failure. Dis Markers. 2021; 2021:6639393. doi: 10.1155/2021/6639393.
17. Hendy RM, Elawady MA, EL Kareem HMA. Role of lactate dehydrogenase and other biomarkers in predicting prognosis of community-acquired pneumonia. Egypt J Bronchol. 2019;13:539-544. https://doi.org/10.4103/ejb.ejb_22_19.
18. Bolatkale M, Duger M, Ülfer G, et al. A novel biochemical marker for community-acquired pneumonia: Ischemia-modified albumin. The American journal of emergency medicine. 2017;35(8):1121-1125. https://doi.org/10.1016/j.ajem.2017.03.018.
19. Cascaval V, Dumitras T, Fetco-Mereuta D, et al. Clinical-radiological features and oxidative stress in patients with community-acquired pneumonia and heart failure. Pneumologia. 2024;73:1-7. https://doi.org/10.2478/pneum-2025-0001.
20. Fetco-Mereuta D, Dumitras T, Grib L, et al. Clinical and paraclinical approach to community-acquired pneumonia in obese individuals. Mold J Health Sci. 2024;11(2):3-7. https://doi.org/10.52645/MJHS.2024.2.01.
21. Reshetar DV. Indices of the oxidant and antioxidant system and endogenous intoxication in the convalescents after community-acquired pneumonia. Galician Med J. 2015;22(1):115-118. https://ifnmujournal.com/gmj/article/view/276.

https://doi.org/10.52645/MJHS.2025.3.09

UDC: 616.24-007.271-036.12

RESEARCH ARTICLES

The impact of comorbidities on chronic obstructive pulmonary disease

Ecaterina Iavrumov*, Alexandru Corlateanu

Pneumology and Allergology Discipline, Department of Internal Medicine, *Nicolae Testemițanu* State University of Medicine and Pharmacy, Chisinau, Republic of Moldova

ABSTRACT

Introduction. Chronic obstructive pulmonary disease is a major cause of morbidity and mortality worldwide, often associated with multiple comorbidities that may complicate its clinical course. These comorbidities can exacerbate respiratory symptoms, impair lung function, alter imaging findings, and significantly affect prognosis.

Material and methods. This analytical, observational, cross-sectional study included 80 patients with confirmed chronic obstructive pulmonary disease, divided into two equal subgroups according to spirometric severity: GOLD 1-2 (n = 40) and GOLD 3-4 (n = 40). Clinical, functional, and radiological parameters were evaluated. Comorbidity burden was assessed using validated composite indices: Charlson Comorbidity Index, COTE, COPDCoRi, CODEX, and COMCOLD. Associations between comorbidity scores, pulmonary function, high-resolution computed tomography findings, and clinical outcomes were analyzed using SPSS v22.0. A p-value < 0.05 was considered statistically significant.

Results. The presence of comorbidities was high across all domains, with only minor differences between spirometric stages. Structural abnormalities (emphysema, bronchiectasis, pulmonary hypertension) were more prevalent in GOLD 3-4 patients. A strong correlation was observed between composite indices and parameters such as forced expiratory volume in 1 second, dyspnea, exacerbation rate, radiological findings, and GOLD stages. Logistic regression models showed that the combination of COPD-specific indices (COTE, CODEX, COPDCoRi) significantly outperformed the Charlson index in predicting severe COPD (AUC 0.86 vs. 0.63). High-resolution computed tomography findings variables also demonstrated strong predictive value (AUC 0.81).

Conclusions. Comorbidities play a central role in shaping chronic obstructive pulmonary disease severity and prognosis. The integration of composite comorbidity indices and imaging biomarkers enhances multidimensional patient stratification, aligning with GOLD 2024 recommendations for personalized care.

Keywords: COPD, comorbidities, HRCT, GOLD, composite indices.

Cite this article: Iavrumov E, Corlateanu A. The impact of comorbidities on chronic obstructive pulmonary disease. Mold J Health Sci. 2025;12(3):60-65. https://doi.org/10.52645/MJHS.2025.3.09.

Manuscript received: 23.07.2025

Accepted for publication: 25.08.2025

Published: 15.09.2025

***Corresponding author: Ecaterina Iavrumov**, MD, assistant professor
Pneumology and Allergology Discipline, Department of Internal Medicine
Nicolae Testemițanu State University of Medicine and Pharmacy
165 Stefan cel Mare și Sfant blvd, Chisinau, Republic of Moldova, MD-2004
e-mail: ecaterina.iavrumov@usmf.md

Authors' ORCID IDs
Ecaterina Iavrumov – https://orcid.org/0000-0001-7332-6587
Alexandru Corlateanu – https://orcid.org/0000-0002-3278-436X

Key messages

What is not known yet about the issue addressed in the submitted manuscript

Despite the growing evidence of the burden of comorbidities in chronic obstructive pulmonary disease (COPD), limited data exist on how validated composite comorbidity indices correlate with functional impairment, radiological severity, and GOLD spirometric stages.

The research hypothesis

The severity of comorbidities, quantified using composite indices (Charlson, COTE, COPDCoRi, CODEx, COMCOLD), is significantly associated with functional decline, HRCT abnormalities, and clinical prognosis in COPD, and may serve as a predictor of disease progression.

The novelty added by the manuscript to the already published scientific literature

This study integrated five validated comorbidity indices and imaging evaluation into the multidimensional assessment of COPD severity, highlighting their practical utility in stratifying patients by GOLD stages and improving prognostic accuracy.

Introduction

Chronic obstructive pulmonary disease (COPD) is a major global health burden, characterized by persistent airflow limitation and progressive decline in lung function. According to the Global Initiative for Chronic Obstructive Lung Disease (GOLD 2024), COPD affects approximately 400 million people worldwide and remains the third leading cause of death globally [1]. In recent years, it has become increasingly evident that COPD extends beyond the respiratory system, acting as a systemic disease, frequently accompanied by a wide range of comorbidities [2].

The presence of comorbidities in COPD patients – such as cardiovascular disease, diabetes mellitus, metabolic syndrome, osteoporosis, anxiety, depression, gastrointestinal disorders, and respiratory comorbidities [3] – not only complicates disease management, but is also associated with increased frequency of exacerbations and hospitalizations, accelerated disease progression, reduced quality of life, and higher morbidity [4-6]. Many of these conditions interact pathophysiologically with COPD, amplifying systemic inflammation, altering therapeutic response, and complicating disease management [7].

Recent clinical guidelines recommend a multidimensional approach to COPD assessment that includes both respiratory and non-respiratory factors. Several composite indices have been developed to quantify the burden of comorbidities and facilitate prognostic evaluation. Among them, the Charlson Comorbidity Index (CCI), the COPD-specific Co-morbidity Test (COTE), the COPD Co-morbidity Risk Index (COPDCoRi), the CODEX Index (which integrates comorbidity, dyspnea, and exacerbation history), and the COMCOLD Index are increasingly used in both clinical practice and research [8-10].

The aim of this study was to assess the impact of comorbidities on COPD severity by analyzing their association with functional parameters (FEV_1), clinical outcomes, and High-Resolution Computed Tomography (HRCT) findings. We further explored the predictive value of composite indices in stratifying disease severity based on the GOLD classification, with the goal of supporting a more personalized and evidence-based approach to patient management.

Material and methods

This was an analytical, observational, cross-sectional study conducted on a representative sample of patients diagnosed with COPD and associated comorbidities. The study was approved by the Research Ethics Committee of *Nicolae Testemițanu* State University of Medicine and Pharmacy (Minutes No. 30 dated 31.03.2022). Patients were stratified into two comparable subgroups based on the severity of airflow limitation, according to the current GOLD spirometric classification: GOLD stages 1-2 versus GOLD stages 3-4.

Study population. A total of 80 patients with confirmed COPD were enrolled from two tertiary medical institutions in the Republic of Moldova: *Chiril Draganiuc* Institute of Pneumology and the *Saint Archangel Michael* Municipal Clinical Hospital. The study was conducted between 2022 and 2025.

Inclusion and exclusion criteria. Eligible participants were aged over 40 years with a confirmed diagnosis of COPD based on spirometry (post-bronchodilator FEV_1/FVC < 0.70) and at least one clinically or paraclinically documented comorbidity. Additional criteria included availability of complete medical documentation (clinical history, spirometry, and imaging), and a recent spirometry (performed within the last 12 months) during a period of respiratory stability. All participants provided written informed consent.

Patients were excluded if they were under 40 years old, had no relevant comorbidities, incomplete medical records, or alternative diagnoses such as asthma (FEV_1/FVC > 0.70), idiopathic pulmonary fibrosis, advanced severe primary bronchiectasis, or active lung cancer. Patients with terminal chronic illnesses (e.g., NYHA IV heart failure), active tuberculosis, and severe post- COVID-19 pulmonary fibrosis were also excluded. Refusal to participate in the study was considered a definitive exclusion criterion.

Statistical data. Data were collected through direct patients' interviews and medical records review, including demographic, anthropometric, clinical, functional and imaging parameters. Five validated composite indices were used to assess comorbidity burden: Charlson Comorbidity Index (CCI), the COPD-specific Co-morbidity Test (COTE), COPD Co-morbidity Risk Index (COPDCoRi), CODEX Index, and COMCOLD Index.

Statistical methods. Statistical analysis was performed using Microsoft Excel 2016, IBM SPSS Statistics (version 22.0), and MedCalc. Data normality was assessed using the Kolmogorov-Smirnov test. Continuous variables with normal distribution were reported as mean±standard deviation (SD), while non-normally distributed variables were presented as medians and interquartile range (IQR). Categorical variables were expressed as absolute and relative frequencies (%). To assess the association between composite indices and clinical, functional, and imaging parameters, Pearson correlation was used for continuous variables with normal distribution, while Spearman's rank correlation was applied for ordinal or non-normally distributed data. Discriminative capacity was assessed via Receiver Operating Characteristic (ROC) curve analysis and area under the curve (AUC) interpretation.

Results

The study included 80 patients diagnosed with COPD, as indicated in Table 1. The majority were male (n = 59; 73.7%), while females constituted a smaller proportion (n = 21; 26.2%). Mean age = 65.6 years, SD = 8.28 years.

Table 1. Demographic and baseline data of participants (*n = 80*)

Variable	Category	N (%)
Gender	Male	59 (73.75%)
	Female	21 (26.25%)
Age (years)	Mean = 65.6, SD = 8.28, Median = 66, IQR = 44-89	
Environment	Urban	41 (51.25%)
	Rural	39 (48.75%)
Smoking status	Non-smoker	10 (12%)
	Smoker	38 (47.5%)
	Ex-smoker	31 (38.75%)
	Passive smoker	1 (1.25%)
Occupational exposure	Non-exposed	52 (65%)
	Exposed	28 (35%)
Socioeconomic status	Satisfactory	65 (81.25%)
	Unsatisfactory	15 (18.75%)

Note: *Values are expressed as mean±SD for continuous variables (independent t-test) and n (%) for categorical variables (Chi-square test/Fisher's exact test); SD – standard deviation; IQR- interquartile range.*

According to spirometric staging, 13.7% (n = 11) of patients were classified as GOLD 1, 36.2% (n = 29) as GOLD 2, 35% (n = 28) as GOLD 3, and 15% (n = 12) as GOLD 4. The mean post-bronchodilator FEV_1 was 52.86% (SD = 19.12), ranging from 16.0% to 86.0%. Based on GOLD ABE classification, 11.2% of patients (n = 9) were in group A, 36.2% (n = 29) in group B, and 52.5% (n = 42) in group E. Details are summarized in Table 2.

Table 2. Functional and clinical parameters

Variable	Category	n (%)
GOLD stage	GOLD 1	11 (13.75%)
	GOLD 2	29 (36.25%)
	GOLD 3	28 (35%)
	GOLD 4	12 (15%)
FEV_1 (%) Mean ±SD	52.86 ± 19.12	
Group	Group A	9 (11.25%)
	Group B	29 (36.25%)
	Group E	42 (52.5%)
Disease duration (years)	<10 years	34 (42.5%)
	10-20 years	37 (46.25%)
	>20 years	9 (11.25%)
mMRC Dyspnea scale	Grade 1	4 (5%)
	Grade 2	15 (18.75%)
	Grade 3	37 (46.25%)
	Grade 4	24 (30%)
Number of exacerbation (in last years)	1 exacerbation	38 (47.5%)
	2 exacerbations	28 (35%)
	3 exacerbations	12 (15%)
	4 exacerbations	2 (2.5%)
SaO_2	<92%	30 (37.5%)
	93%-95%	26 (32.5%)
	>95%	24 (30.0%)

Note*: Values are expressed as mean ± SD for continuous variables (independent t-test) and n (%) for categorical variables (Chi-square test/Fisher's exact test). GOLD – Global Initiative for Obstructive Lung Disease; FEV_1 – forced expiratory volume in 1 second; SD – standard deviation; mMRC – modified Medical Research Council scale; SaO_2 – Oxygen saturation; IQR- interquartile range.*

According to Table 3, a substantial burden of comorbidities was observed. Respiratory comorbidities – including recurrent pneumonia, bronchiectasis, bronchial asthma, lung cancer, and obstructive sleep apnea syndrome (OSAS) – were present in 75% of patients (n = 60). Cardiovascular diseases were highly prevalent (93.7%, n = 75) comprising ischemic heart disease, heart failure, arterial hypertension, arrhythmias, and peripheral arterial disease. Metabolic disorders (diabetes mellitus, dyslipidemia, and metabolic syndrome) affected 56.2% (n = 45). Osteoarticular conditions, such as osteoporosis or a history of vertebral fractures, were observed in 32.5% (n = 26). Cerebrovascular events (stroke) were reported in 2 cases (2.5%). Neuropsychiatric comorbidities – including depression, anxiety, and cognitive impairment – were present in 58.7% (n = 47). Gastrointestinal disorders were identified in 32.5% (n = 26). Other comorbidities, such as anemia, polycythemia, and non-pulmonary malignancies, were found in 47.5% (n = 38).

Table 3. Distribution of comorbidities by GOLD stage

Comorbidities	GOLD 1-2 (n = 40)	GOLD 3-4 (n = 40)
Cardiovascular disease	37	38
Metabolic disorders	23	22
Neuropsychiatric conditions	25	22
Osteoarticular conditions	11	15
Gastrointestinal disorders	12	14
Respiratory comorbidities	30	30
Other (anemia, polycythemia, malignancies)	12	19

Note: *Values represent the number of patients with each comorbidity in GOLD subgroups; GOLD – Global Initiative for Chronic Obstructive Lung Disease.*

HRCT identified a variety of structural abnormalities. Centrilobular emphysema was present in 40.0% of patients, cylindrical bronchiectasis in 35.0%, and radiological signs of pulmonary hypertension (PH) in 42.5%. Coronary artery calcifications were found in 27.5%, and radiological signs of vertebral fractures or osteoporosis in 20.0%. When comparing GOLD subgroups, patients with GOLD 3-4 had a significantly higher prevalence of structural lung damage. Cylindrical bronchiectasis ($p = 0.016$), centrilobular emphysema ($p = 0.004$), signs of PH ($p = 0.001$), coronary artery calcifications ($p = 0.036$), and osteoporosis ($p = 0.044$) were more frequently observed in the GOLD 3-4 group.

Correlation analysis showed a strong positive relationship between the number of exacerbations and hospitalizations ($r = 0.483$). Additionally, the number of exacerbations was positively correlated with the dyspnea score (mMRC) ($r = 0.393$), GOLD stage ($r = 0.273$), and ABE classification ($r = 0.271$). The mMRC score also showed significant positive correlations with disease duration ($r = 0.258$), GOLD stage ($r = 0.301$), ABE group ($r = 0.354$), and the Charlson Index ($r = 0.306$).

HRCT findings were also significantly correlated with clinical and functional variables. Cylindrical bronchiectasis showed a positive correlation with the number of exacerbations ($r = 0.41$, $p < 0.01$), while centrilobular emphysema exhibited a moderate negative correlation with post-bron-

chodilator FEV_1 (r = –0.53, p < 0.001). Signs of PH were moderately associated with lower oxygen saturation (r = –0.48, p <0 .01) and higher dyspnea scores (r = 0.46), both statistically significant (p < 0.001).

As shown in Table 4, the Charlson Comorbidity Index was significantly correlated with several parameters, including frequency of hospitalizations (r = 0.255), number of exacerbations (r = 0.213), GOLD stage (r = 0.301), and mMRC score (r = 0.306). Among all indices, the CODEX score showed the strongest correlations with multiple clinical severity markers. Specifically, it showed a strong positive correlation with post-bronchodilator FEV_1 severity classified by GOLD 2024 (r = 0.59). Additionally, the CODEX index was positively associated with the mMRC dyspnea scale (r = 0.46), number of exacerbations (r = 0.41), and ABE classification (r = 0.47). The COMCOLD score showed strong correlations with other comorbidity indices, including CCI (r = 0.57), CODEX (r = 0.34), and COTE (r = 0.32). It also exhibited weak-to-moderate associations with dyspnea severity (mMRC, r = 0.16) and BMI (r = 0.09). The COTE index was modestly correlated with disease duration (r = 0.26), number of exacerbations (r = 0.15), and gender (r = 0.20). Lastly, the COPDCoRi index showed modest associations with COTE (r = 0.41), COMCOLD (r = 0.33), and CCI (r = 0.32). Notably, it also showed a negative correlation with peripheral oxygen saturation (SaO_2, r = –0.15).

Table 4. Correlation of composite indices and clinical variables

Clinical Variable	Charlson	CODEX	COMCOLD	COTE	COPDCoRi
Hospitalizations	r = 0.255**	r = 0.34**	-	-	-
Exacerbations	r = 0.21*	r = 0.41***	-	r = 0.15*	-
GOLD (FEV_1)	r = 0.30**	r = 0.59***	-	-	r=0.41**
mMRC	r = 0.30**	r = 0.46***	r = 0.16*	-	-
Disease duration	-	-	-	r = 0.26**	-
ABE type	-	r = 0.47***	-	-	-
Smoking status	-	-	-	r = 0.20*	r = 0.33*
BMI	-	-	r = 0.09	-	-
Charlson	-	-	r = 0.57***	-	r = 0.32*
CODEX	-	-	r = 0.34**	-	-
COTE	-	-	r = 0.32*	-	r = 0.41**
COMCOLD	r = 0.57***	r = 0.34**	-	r = 0.32***	r = 0.33*
COPDCoRi	r = 0.32**	-	r = 0.33*	r = 0.41***	-

Note: *Values represent correlation coefficients (r) between composite indices and clinical variables. Pearson or Spearman correlation coefficients were used depending on data distribution; * p < 0.05; ** p < 0.01; *** p < 0.001; - No analysis or non-significant correlation; GOLD – Global Initiative for Chronic Obstructive Lung Disease; FEV_1 – forced expiratory volume in 1 second; mMRC – modified Medical Research Council scale; ABE – GOLD 2024 classification; BMI – body mass index; CCI – Charlson Comorbidity Index; CODEX – Comorbidity, Obstruction, Dyspnea, and Exacerbation risk index; COMCOLD – COPD Comorbidity and Depression index; COTE - COPD –specific Comorbidity test; COPDCoRi – Comorbidity Risk Index.*

To evaluate the predictive performance of selected composite comorbidity indices in distinguishing severe forms of COPD (GOLD 3-4), we performed binary logistic regression analyses followed by ROC curve assessment. Logistic regression analysis revealed that the Charlson Comorbidity Index (CCI) alone had limited predictive ability for advanced COPD (AUC = 0.63), indicating modest discriminatory ability. However, when a combination of composite indices – the COTE index, the CODEX index, and the COPDCoRi index – was included as predictors, the multivariable logistic model

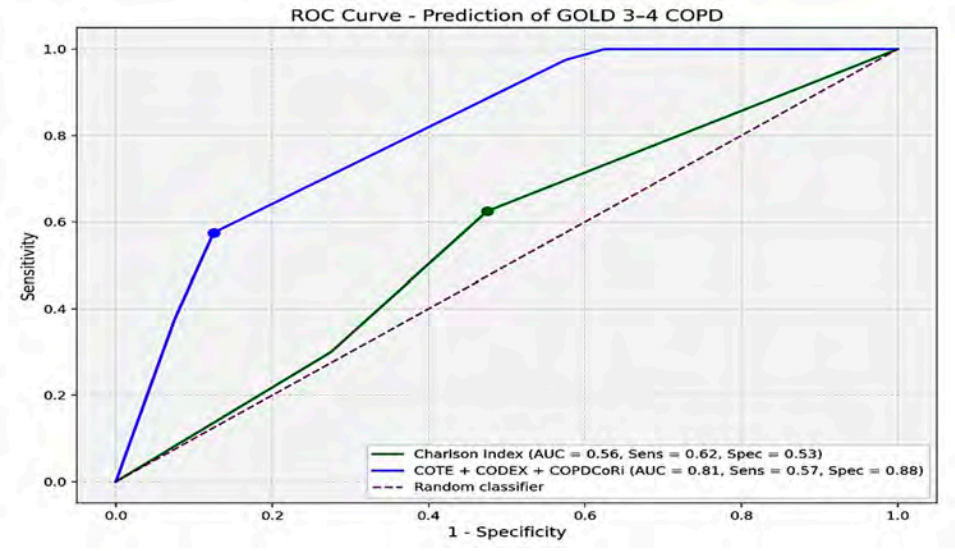

Fig. 1 Receiver Operating Characteristic (ROC) curve for prediction of GOLD 3-4 COPD

Note: *The ROC curve compares the predictive performance of the Charlson Index (green line) and a combined model incorporating COTE, CODEX, and COPDCoRi scores (blue line) in identifying patients with GOLD 3-4 COPD. The Charlson Comorbidity Index showed poor discriminative performance, with an AUC = 0.56 (p = 0.355), Sensitivity = 0.62, Specificity = 0.53. These results were not statistically significant, and further studies with larger cohorts are needed to confirm its predictive value in COPD severity. In contrast, the combined model including COTE, CODEX, and COPDCoRi scores demonstrated a significantly higher discriminative capacity (AUC = 0.81, p < 0.001), Sensitivity = 0.57, Specificity = 0.88. Among predictors, CODEX was statistically significant (p < 0.001), COTE showed a trend (p = 0.099), and COPDCoRi did not reach statistical significance (p = 0.214); however, its potential clinical relevance warrants further investigation in larger cohorts. AUC – Area Under the Curve.*

demonstrated substantially higher discriminative power, with an AUC = 0.86. All three indices showed positive regression coefficients, suggesting that elevated scores are significantly associated with advanced GOLD classification (Fig. 1).

To further assess the predictive value of HRCT findings, logistic regression models were built. In the GOLD 3-4 group, HRCT variables such as centrilobular emphysema and PH signs emerged as significant predictors. ROC curve analysis demonstrated good discrimination for severe COPD (AUC = 0.81), and moderate discrimination for GOLD 1-2 (AUC = 0.71).

Discussion

This study underscores the multidimensional nature of COPD, reaffirming prior findings that comorbidities substantially impact disease burden and prognosis [11-13]. In agreement with earlier observations, our results confirm the high prevalence of cardiovascular and metabolic comorbidities, especially in patients with advanced stages of COPD.

The radiological presence of bronchiectasis and emphysema in more severe GOLD stages is consistent with previous CT-based classifications. Lynch et al. and Martinez et al. have emphasized that structural abnormalities correlate with both functional impairment and exacerbation risk, which aligns with our data showing an inverse relationship between emphysema scores and FEV_1 values [14, 15]. Furthermore, the co-occurrence of bronchiectasis and exacerbations supports findings by Martinez-Garcia et al., reinforcing their clinical significance [16].

Among the composite indices assessed, CODEX exhibited the strongest correlation with clinical severity markers [17, 18], corroborating its multidimensional nature. The COPDCoRi index also demonstrated robust associations, in line with recent efforts to integrate comorbidity burden into COPD phenotyping [19]. While the COTE index was originally designed to predict mortality [20], our findings show that it retains relevance for stratifying patients by disease characteristics.

ROC analysis confirmed that disease-specific indices such as CODEX and COPDCoRi yielded higher AUCs for GOLD stage prediction, outperforming general indices like the Charlson. These results support earlier validations of these indices in stratifying COPD risk and outcomes [21]. Moreover, HRCT features such as emphysema extent and pulmonary hypertension added prognostic value, underscoring the importance of imaging biomarkers. Taken together, these findings support the GOLD 2024 recommendations for multidimensional evaluation of COPD patients. By combining functional, clinical, and imaging variables, more accurate risk stratification becomes feasible.

Limitations of the study include its cross-sectional design and moderate sample size, potentially limiting generalizability. Additionally, some comorbidities may have been underreported due to retrospective data collection.

Future research should investigate the longitudinal predictive value of composite indices and HRCT biomarkers, as suggested by studies on disease progression and mortality prediction in COPD.

Conclusions

This study reinforces the central role of comorbidities and structural lung changes in defining COPD severity. By integrating validated composite indices (Charlson, CODEX, COTE, COPDCoRi, COMCOLD) and HRCT findings, we demonstrate that a multidimensional assessment better reflects disease complexity and prognosis than conventional measures alone. The findings support the use of COPD-specific tools and imaging biomarkers in routine evaluation, promoting a more personalized and evidence-based management approach in line with GOLD 2024 recommendations.

Competing interest

None declared.

Contribution of authors

AC – research coordinator, conceived the research idea, developed the aim and objectives, and supervised data interpretation. EI performed data collection, analysis, and manuscript drafting. Both authors critically reviewed and approved the final manuscript.

Ethics approval

The study was conducted as part of a doctoral research project approved by the Research Ethics Committee of the *Nicolae Testemițanu* State University of Medicine and Pharmacy (Minutes No. 30 dated 31.03.2022).

Patient consent

Obtained.

Acknowledgements and funding

No external funding.

Provenance and peer review

Not commissioned; externally peer-reviewed.

References

1. Venkatesan P. GOLD COPD report: 2024 update. Lancet Respir Med. 2024;(1):15-6. doi: 10.1016/S2213-2600(23)00461-7
2. Agustí A, Celli BR, Criner GJ, Halpin D, Anzueto A, Barnes P, et al. Global Initiative for Chronic Obstructive Lung Disease 2023 Report: GOLD executive summary. Eur Respir J. 2023 Apr 1;61(4). https://doi.org/10.1183/13993003.00239-2023
3. Natali D, Cloatre G, Hovette P, Cochrane B. Screening for comorbidities in COPD. *Breathe (Sheff).* 2020;16(1):190315. https://doi.org/10.1183/20734735.0315-2019
4. Divo M, Cote C, de Torres JP, Casanova C, Marin JM, Pinto-Plata V, et al. Comorbidities and risk of mortality in patients with chronic obstructive pulmonary disease. *Am J Respir Crit Care Med.* 2012 Apr 19;186(2):155-61. doi: 10.1164/rccm.201201-0034OC
5. Mannino DM, Thorn D, Swensen A, Holguin F. Prevalence and outcomes of diabetes, hypertension and cardiovascular disease in COPD. *Eur Re-*

spir J. 2008 Sep 30;32(4):962-9. https://doi.org/10.1183/09031936.00012408
6. Corlateanu A, Covantev S, Scutaru E, Rusu D, Botnaru V, Corlateanu O, Siafakas N. COPD and comorbidities in the Republic of Moldova. *Eurasian J Pulmonol.* 2022 Feb 08;24(1):9-17. doi: 10.14744/ejop_78_21
7. Barnes PJ, Celli BR. Systemic manifestations and comorbidities of COPD. *Eur Respir J.* 2009 Jan 05;33(5):1165-85. https://doi.org/10.1183/09031936.00128008
8. Ly K, Wakefield D, Zu Wallack R. The usefulness of Charlson Comorbidity Index (CCI) scoring in predicting all-cause mortality in Outpatients with Clinical Diagnoses of COPD. *J Multimorb Comorb.* 2025 Jan 25;15:1-7. https://doi.org/10.1177/26335565251315876
9. Divo MJ, Casanova C, Marin JM, Pinto-Plata VM, De-Torres JP, Zulueta JJ, et al. COPD comorbidities network. *Eur Respir J.* 2015 Aug 31;46(3):640-50. https://doi.org/10.1183/09031936.00171614
10. Frei A, Muggensturm P, Putcha N, Siebeling L, Zoller M, Boyd CM, et al. Five comorbidities reflected the health status in patients with chronic obstructive pulmonary disease: the newly developed COMCOLD index. *J Clin Epidemiol.* 2014 Apr 29;67(8):904-11. https://doi.org/10.1016/j.jclinepi.2014.03.005
11. Smith MC, Wrobel JP. Epidemiology and clinical impact of major comorbidities in patients with COPD. *Int J Chron Obstruct Pulmon Dis.* 2014 Aug 27;9:871-88. https://doi.org/10.2147/COPD.S49621
12. dos Santos NC, Miravitlles M, Camelier AA, de Almeida VDC, Tosta Maciel RRB, Rosa Camelier FW. Prevalence and impact of comorbidities in individuals with chronic obstructive pulmonary disease: a systematic review. *Tuberc Respir Dis (Seoul).* 2022 May 27;85(3):205-20. https://doi.org/10.4046/trd.2021.0179
13. Negewo NA, Gibson PG, McDonald VM. COPD and its comorbidities: impact, measurement and mechanisms. *Respirology.* 2015 Sep 16;20(8):1160-71. https://doi.org/10.1111/resp.12642
14. Dou S, Zheng C, Cui L, Xie M, Wang W, Tian H, et al. High prevalence of bronchiectasis in emphysema-predominant COPD patients. *Int J Chron Obstruct Pulmon Dis.* 2018 Jun 27;13:2041-7. https://doi.org/10.2147/COPD.S163243
15. Mets OM, De Jong PA, Van Ginneken B, Gietema HA, Lammers JWJ. Quantitative computed tomography in COPD: possibilities and limitations. *Lung.* 2012 Dec 17;190(2):133-45. https://doi.org/10.1007/s00408-011-9353-9
16. Miravitlles M, Calle M, Soler-Cataluña JJ. Clinical phenotypes of COPD: identification, definition and implications for guidelines. *Arch Bronconeumol.* 2012 Feb 1;48(3):86-98. doi: 10.1016/j.arbr.2012.01.003
17. Deng D, Zhou A, Chen P, Shuang Q. CODEXS: a new multidimensional index to better predict frequent COPD exacerbators with inclusion of depression score. *Int J Chron Obstruct Pulmon Dis.* 2020 Feb 3;15:249-59. https://doi.org/10.2147/COPD.S237545
18. Corlateanu A, Plahotniuc A, Corlateanu O, Botnaru V, Bikov A, Mathioudakis AG, et al. Multidimensional indices in the assessment of chronic obstructive pulmonary disease. *Respir Med.* 2021 Jun 22;185:106519. https://doi.org/10.1016/j.rmed.2021.106519
19. Cazzola M, Calzetta L, Matera MG, Muscoli S, Rogliani P, Romeo F. Chronic obstructive pulmonary disease and coronary disease: COPDCoRi, a simple and effective algorithm for predicting the risk of coronary artery disease in COPD patients. *Respir Med.* 2015 May 25;109(8):1019-25. https://doi.org/10.1016/j.rmed.2015.05.021
20. Chen Q, Wang X, Yao X, Zhang L, Liu X. COTE and pulmonary comorbidities predict moderate-to-severe acute exacerbation and hospitalization in COPD. *Int J Chron Obstruct Pulmon Dis.* 2025 Jun 11;20:1893-913. https://doi.org/10.2147/COPD.S518218
21. Kotlyarov S. The role of multidimensional indices for mortality prediction in chronic obstructive pulmonary disease. *Diagnostics (Basel).* 2023 Apr 4;13(7):1344. https://doi.org/10.3390/diagnostics13071344

https://doi.org/10.52645/MJHS.2025.3.10

UDC: 616.127-002-07

RESEARCH ARTICLE

Natural course of inflammatory cardiomyopathies

Andrei Braniște[1], Vladimir Naumov[2], Valeriu Cobeț[1], Tudor Braniște[3*]

[1] Pathology Department, *Nicolae Testemițanu* State University of Medicine and Pharmacy, Chișinău, Republic of Moldova
[2] Department of Heart Failure and Myocardial Diseases, *A.L.Miasnikov* Institute of Clinical Cardiology of the National Medical Research Center for Cardiology of the Ministry of Health of the Russian Federation
[3] Internal Medicine-Semiology Discipline, Department of Internal Medicine, *Nicolae Testemițanu* State University of Medicine and Pharmacy, Chișinău, Republic of Moldova

ABSTRACT

Introduction. Refractory heart failure with a poor prognosis is a key feature of dilated cardiomyopathy. Inflammatory cardiomyopathy, often diagnosed via *in vivo* subendomyocardial biopsy, is considered a potential precursor to dilated cardiomyopathy. The Dallas criteria, applied to morphometric and electron microscopic studies of biopsy samples, are essential for differentiating the features of various inflammatory stages. Building upon these established diagnostic principles, our study integrates immunohistological analysis with measurements of intramyocardial indices and intracardiac hemodynamics. This comprehensive approach aims to characterize the natural course of inflammatory cardiomyopathy, seeking to improve the understanding of the clinical trajectories and tissue structures that define both inflammatory cardiomyopathy and its progression to dilated cardiomyopathy.

Material and methods. The study included 75 patients with inflammatory cardiomyopathies and 75 patients with dilated cardiomyopathies. The following procedures were performed: coronary angioventriculography, repeated subendomyocardial biopsy, immunohistologic analysis, and assessment of intracardiac and intramyocardial hemodynamics.

Results. Morphohistologic analysis of inflammatory cardiomyopathies at different stages revealed a maximum of 10-12 lymphocytes, which decreased to only isolated lymphocytes in late stages. In biopsies from early-stage inflammatory dilated cardiomyopathies, the morphologic appearance showed lymphocytic infiltration of the myocardial stroma, vasculitis of intramural arteries and arterioles. The biopsies performed after 36 months showed dystrophic structures, microfocal and diffuse replacement fibrosis, predominantly perivascular, which are indistinguishable from the features of dilated cardiomyopathy. Intracardiac hemodynamic indices in patients with dilated and inflammatory cardiomyopathies did not differ. Similarly, left ventricular regional contractility, as verified by radiopaque ventriculography, was not significantly different. The degree of radiotracer detection on thallium-201 scintigraphy was statistically insignificant between the two conditions. Immune complexes and immunoglobulins G, M, and A in the blood were elevated in both groups, likely as a consequence of heart failure.

Conclusions. Morphostructural analysis of biopsies taken from patients with inflammatory dilated cardiomyopathies, at different stages of its natural course reveals the progressive development of dilated cardiomyopathies. These structural changes correlate closely with findings from intracavitary and hemodynamic assessments and measures of regional contractility, supporting a direct link between dilated and inflammatory cardiomyopathies.

Keywords: cardiomyopathy, cardiomyocyte, scintigraphy, heart failure.

Cite this article: Braniște A, Naumov V, Cobeț V, Braniște T. Natural course of inflammatory cardiomyopathies. Mold J Health Sci. 2025;12(3):66-69. https://doi.org/10.52645/MJHS.2025.3.10.

Manuscript received: 7.07.2025

Accepted for publication: 6.08.2025

Published: 15.09.2025

***Corresponding author. Tudor Braniște**, MD, PhD, associate professor Internal Medicine-Semiology Discipline, Department of Internal Medicine *Nicolae Testemițanu* State University of Medicine and Pharmacy,

Key messages

What is not yet known on the issue addressed in the submitted manuscript

The specific markers and progression patterns that would allow clinicians to predict when inflammatory cardiomyopathy will transition into dilated cardiomyopathy are still unknown.

37 Gheorghe Caşu str., Chişinău, Republic of Moldova, MD-2025
e-mail: tudor.braniste@usmf.md

Authors' ORCID IDs
Andrei Braniște – https://orcid.org/0000-0002-5190-1357
Vladimir Naumov – https://orcid.org/0009-0004-4632-4104
Valeriu Cobeț – https://orcid.org/0000-0002-6141-1108
Tudor Braniște – https://orcid.org/0009-0004-9164-7172

The research hypothesis

The study utilized a complex morphohistological analysis of submyocardial biopsies and intracardiac hemodynamic indices for assessment of traits regarding inflammatory cardiomyopathy evolution during 36 months in a comparison with hallmarks of dilated cardiomyopathy.

The novelty added by the manuscript to the already published scientific literature

Myocardial morphostructural analysis at 36 months revealed that inflammatory cardiomyopathy evolution exhibit features, such as dystrophic changes, microfocal and diffuse fibrosis, that are indistinguishable from those in dilated cardiomyopathy. Likewise, functional assessments showed no significant differences in either intracardiac hemodynamic indices or left ventricular regional contractility, as verified by radiopaque ventriculography. These findings provide strong evidence suggesting inflammatory cardiomyopathy progresses to dilated cardiomyopathy.

Introduction

In primary diseases of the heart, particularly dilated cardiomyopathy (DCM), the heart is subjected to significant hemodynamic volume overload, leading to heart failure that is often refractory to conventional treatment [1-4]. The complexity of DCM lies in a wide array of causative factors that serve both as a basis in the initiation and development of acquired and familial dilated cardiomyopathy [5-8]. Among these, inflammatory cardiomyopathy (ICM) is recognized as an important potential precursor to DCM, a diagnosis confirmed by morphological analysis of the myocardium [9, 10]. The identification of myocardial inflammatory processes, particularly those with an insidious evolution such as inflammatory dilated cardiomyopathy (IDCM), is a difficult endeavor due to the heterogeneous nature of the clinical and diagnostic findings. Currently, the most sensitive and definitive method for confirming the existence of an inflammatory process and viral infection in the heart muscle is the subendomyocardial biopsy, which is considered the "gold standard". The use of the 1986 Dallas morphological classification of inflammatory cardiomyopathy or the 1997 Marburg Agreement on the Diagnosis of Inflammatory Cardiomyopathy increases the order of differentiation of acute and chronic inflammatory processes [10, 11]. These classifications, combined with the ability to type different immunocompetent cell populations, expand the understanding of viruses with cardiotropic potential in patients with IDCM and DCM [11, 12]. By applying these methods, it becomes feasible to track the natural history of ICM from its early, asymptomatic phases, where risk stratification is critical, to the late stages of cardiomyopathic syndromes. This approach facilitates a better understanding of the clinical course and shared morphofunctional features of these pathologies, aiming to open new avenues for therapeutic development.

Materials and methods

This retrospective study analyzed morphofunctional data from 75 patients with inflammatory cardiomyopathy (IDCM) and 75 patients with dilated cardiomyopathy (DCM). The investigations performed included coronaroventriculography, scintigraphy of myocardium, intracardiac and intramyocardial hemodynamics, repeated subendomyocardial biopsy, immunohistology study, using the WHO expert group classification with mandatory use of the Dallas morphological criteria. Morphologically confirmation of the diagnosis was confirmed in 58 (77.3%) patients with IDCM and in 40 (53.3%) with DCM. At autopsy, the diagnosis was established in 17 (22.7%) IDCM patients and in 35 (46.7%) DCM patients. In 8 patients with IDCM, verified by intravital subendomyocardial biopsy, the diagnosis was established postmortem on histological analysis of the myocardium.

The distribution of patients according to age, sex and severity of heart failure (NYHA) are shown in Table 1.

Table 1. Patient distribution by gender, age and degree of heart failure

Index	ICM	DCM	P
Number of patients	75	75	Non-significant (NS)
Men	64 (85,3%)	66 (88%)	NS
Women	11 (14,7%)	9 (12%)	NS
Age (years) (M ± m)	38,5 + 1,4 (15-58)	35,6 + 1,3 (16-67)	NS
FC I	19 (25,3%)	2 (2,7%)	
FC II	30 (40%)	30 (40,0%)	
FC III	23 (30,7%)	41 (54,7%)	
FC IV	3 (4%)	2 (2,6%)	
Average FC (M ± m)	2,0 ± 0,1	2,6 ± 0,08	P < 0,05

Note: *FC – Functional class, M ± m – Mean value, ICM – Inflammatory cardiomyopathy, DCM – Dilated cardiomyopathy, P – Student's-test, NS – Non-significant.*

The groups of patients with IDCM and DCM did not differ in terms of age and sex, and both groups showed a clear predominance of male patients. The degree of heart failure in patients with IDCM was significantly lower compared to those with DCM ($p < 0.0005$).

Scintigraphy of myocardium with Thallium-201 (TL 201) was performed using a gamma camera equipped with a conversion collimator, in three positions: (1) anterior, (2) 45° left anterior oblique (LAO) and (3) left lateral. Image acquisition began 5-10 minutes after intravenous administration of 1.5-2.0 micrograms of TL-201 chloride, containing 2 mg of thallium substance, with an action of 55-74 MBq. The data were digitally stored as a 64x64 pixel matrix and the resulting scintigrams were processed using the RDR 11/34 computer program.

The following parameters were determined from coronaroventriculographic: end-diastolic volume (EDV), end-systolic volume (STV), stroke index (BI), ejection fraction (EF), cytosolic index (CI), left ventricular myocardial mass (LVMM), mean velocity of circumferential fiber shortening (LVFSV), left ventricular end-diastolic volume (LVEDV), right ventricular pressure (RVP) and heart rate (HR). Regional contractility of the LV and RV was assessed after percentage shortening of 90 radii and percentage area restriction across 5 sectors of each ventricle.

Subendomyocardial biopsy (SEM) was performed at the end of the angiographic investigation. Multiple tissue samples (3–5 biopsies) were obtained from the septum, RV wall, LV apex and, less rarely, the inferior wall of the left ventricle. Morphological analysis was performed using both light and electron microscopy.

Results and discussion

Coronary angiography in patients with IDCM and DCM revealed wide, sinuous coronary arteries of typological significance. The passage of contrast medium and its subsequent washout, both in the large trunks and in the 3rd and 4th order arteries, were slowed. While coronary blood flow at rest was normal in both groups, the administration of coronary vasodilators resulted in increased vascular resistance and impaired arterial dilation, indicating increased vascular tone and reduced coronary reserve. Furthermore, there were no significant differences between the IDCM and DCM groups in the systolic and diastolic diameters of the coronary arteries or in the calculated extensibility index. ***Ventriculography*** reveled in both patient groups, significant changes in hemodynamics and left ventricular (LV) volumes: the end-diastolic (EDV) and systolic (STV) volumes were significantly increased and the ejection fraction (EF) and the mean velocity of circumferential fiber shortening (FSV) were reduced. The stroke index (BI) and systolic index (SI) were normal, likely due to the compensatory effect of the LV cavity.

Despite normal left ventricular (LV) systolic and aortic diastolic pressures, LV myocardial mass was markedly increased in both patient groups. This was attributed to eccentric hypertrophy, characterized by LV cavity dilation with normal free wall thickness. Also, in IDCM, a significant difference in end-diastolic volume index (EDVI), ($P < 0.01$), end-systolic volume (ESV) ($P < 0.01$), and end-systolic volume index (ESVI) ($P < 0.005$) were revealed. Thus, in IDCM-ST RV was 32.1 ± 1.9 versus 43.4 ± 3.6 ($P < 005$); differences were found in all pulmonary artery pressure indices: in IDCM-ST in PA (pulmonary artery) was equal to 32.3 ± 2.0 versus 44.8 ± 3.7 in DCM group ($P < 0.005$); DP AP was 14.3 ± 1.5 in IDCM and 20.6 ± 2.0 in DCM ($P < 0.05$); and mean PAP (mean pulmonary artery pressure) in AP in the group of patients with IDCM was equal to 22.0 ± 1.9 and in DCM – 32.6 ± 3.3 ($P < 0.005$). A comparison of right- and left-heart function revealed that in the IDCM group, hemodynamic parameters were similarly affected on both sides. In contrast, the DCM group exhibited predominantly left-sided hemodynamic compromise, which accounts for the more significantly elevated pulmonary pressures observed in these patients.

Compared to healthy individuals, patients in both the inflammatory cardiomyopathy (IDCM) and dilated cardiomyopathy (DCM) groups showed significantly elevated serum levels of circulating immune complexes (CICs) and immunoglobulins (IgG, IgM, and IgA). There was no significant difference in these levels between the two patient groups, suggesting that their elevation is likely a secondary phenomenon related to the severity of heart failure rather than a primary disease marker. Lymphocyte subpopulations in patients with DCM showed a significant decrease in T-lymphocytes as well as T helper inducer T-lymphocytes, with preservation of T-cytokine suppressors in normal parameters, respectively reduction of immunoregulatory index. The number of T-suppressors in patients with IDCM is obviously lower, with a higher immunoregulatory index than in those with DCM. The presented data show an appreciably greater increase in T-suppressors in patients with DCM than in those with a morphologically confirmed diagnosis of IDCM. The observed difference in T-cell profiles between the two conditions may be attributed to variations in the functional class of heart failure and the duration of disease at the time of assessment. It should be noted that these deviations from normal values were noted only in 5-25% of patients with DCM.

Myocardial scintigraphy revealed disturbances of local myocardial contractility. Areas of hypokinesia were recorded in the following regions of LV: in septum area – 2 (18.2%) patients with IDCM, in anterior wall area – in 1 patient with DCM, in antero-septal area – in 4 patients with IDCM (36.4%), in apex area – in 1 patient with ICM, in the antero-lateral area – in 2 patients with DCM (22.2%), in the lower apical area – in 1 patient with ICM and in 1 patient with DCM, in the diaphragmatic area – in 1 patient with IDCM and in 1 patient with DCM. Areas of akinesia: in the septal area – in 1 patient with DCM; in some patients there were areas of pathological asynchrony in the LV septal area – in 2 (27.3%) patients with IDCM, in the septal-apical area – in 1 patient with IDCM, in the inferior apical area in 1 patient with IDCM. In 3 patients with DCM and in 1 patient with IDCM, the areas of pathological asynchrony were combined with areas of akinesia and hypokinesia. Despite these individual findings, there were no statistically significant differences in the overall prevalence or distribution of wall motion abnormalities between the IDCM and DCM groups.

Morphological changes in inflammatory cardiomyopathies

Morphological and morphometric analysis of patients from different groups on subendomyocardial biopsy specimens detected similar features but also some differences between them. Patients in the first group with IDCM showed cardiomyocyte injury with pronounced cellular reaction in the interstitium. The lymphocyte count was 10-12. Electron microscopy revealed vacuolization of the sarcoplasmic reticulum, destruction of mitochondrial cristae and partial death of mitochondrial cristae were observed. In the 2nd group, the acuteness of the inflammatory process was moderate, the number of lymphocytes did not exceed 5, eosinophils and neutrophils were rarely detected. Electron microscopy revealed in the vicinity of the thinned capillaries with osmiophilic wall, flococytic masses and diapedesis hemorrhages. In group 3 the number of lymphocytes in the visual field was up to 5. In the interstitium, neutrophils were rare and macrophage elements were frequently present. Necrotized cardiomyocytes were uncommon. In the 4th group the structural changes were characterized by a chronic process or residual traces, reminiscent of the inflammatory process.

Conclusions

The double immunohistological analysis performed at different stages of the natural course in patients with inflammatory cardiomyopathy highlights morphological and morphometric elements in common with dilated cardiomyopathy. There is also a similarity of intracardiac hemodynamic indices, coronary and intramyocardial blood circulation and regional kinetic disturbances; the indistinct features found in both nosological entities point to direct links between dilated cardiomyopathy and inflammatory cardiomyopathy.

Competing interests

None declared.

Authors' contributions

AB launched the working hypothesis, elaborated the design of study, and analyzed the data. VN interfered with support in the statistical processing of results. VC structured and drafted the article, as well as selected the bibliographical references. TB participated in the results commenting and concluding. All authors critically reviewed the work and approved the final version of the manuscript.

Ethics approval

The research project was approved by the Research Ethics Committee of *Nicolae Testemițanu* State University of Medicine and Pharmacy (Minutes no. 1 from 04.12. 2020/ no. 90 from 31.10.2020).

Patient consent

Obtained.

Acknowledgements and funding

No external funding.

Provenance and peer review

Not commissioned, externally peer reviewed.

References

1. Gigli M, Stolfo D, Merlo M, Sinagra G, Taylor MRG, Mestroni L. Pathophysiology of dilated cardiomyopathy: from mechanisms to precision medicine. Nat Rev Cardiol. 2024 Oct 11;22(3):183-198. doi: 10.1038/s41569-024-01074-2.
2. Ichimura S, Misaka T, Ogawara R, Tomita Y, Anzai F, Sato Y, et al. Neutrophil extracellular traps in myocardial tissue drive cardiac dysfunction and adverse outcomes in patients with heart failure with dilated cardiomyopathy. Circ Heart Fail. 2024 Jun;17(6):011057. doi: 10.1161/CIRCHEARTFAILURE.123.011057.
3. Wang Z, Chen Y, Li W, et al. Identification and validation of diagnostic biomarkers and immune infiltration in dilated cardiomyopathies with heart failure and construction of diagnostic model. Gene. 2025;934:149007. doi: 10.1016/j.gene.2024.149007.
4. Kan A, Fang Q, Li S, Liu W, et al. The potential predictive value of cardiac mechanics for left ventricular reverse remodelling in dilated cardiomyopathy. ESC Heart Fail. 2023;10(6):3340-3351. doi: 10.1002/ehf2.14529.
5. Hershberger RE, Hedges DJ, Morales A. Dilated cardiomyopathy: the complexity of a diverse genetic architecture. Nat Rev Cardiol. 2013;10(9):531-547. doi: 10.1038/nrcardio.2013.105.
6. Arbelo E, Protonotarios A, Gimeno JR, et al. 2023 ESC Guidelines for the management of cardiomyopathies: developed by the task force on the management of cardiomyopathies of the European Society of Cardiology (ESC). Eur Heart J. 2023;44(37):3503-3626. doi: 10.1093/eurheartj/ehad194.
7. Reichart D, Magnussen C, Zeller T, Blankenberg S. Dilated cardiomyopathy: from epidemiologic to genetic phenotypes: a translational review of current literature. J Intern Med. 2019;286(4):362-372. doi: 10.1111/joim.12944.
8. Cobet V, Jeru I, Rotaru V, et al. Pathogenic mechanisms of SARS-Cov-2 infection. Mold J Health Sci. 2020;(1):17-28.
9. Bozkurt B, Colvin M, Cook J, et al. Current diagnostic and treatment strategies for specific dilated cardiomyopathies: a scientific statement from the American Heart Association. Circulation. 2016;134(23):e579-e646. doi: 10.1161/CIR.0000000000000455.
10. Japp AG, Gulati A, Cook SA, et al. The diagnosis and evaluation of dilated cardiomyopathy. J Am Coll Cardiol. 2016;67(25):2996-3010. doi: 10.1016/j.jacc.2016.03.590.
11. Baughman KL. Diagnosis of myocarditis: death of Dallas criteria. Circulation. 2006. Jan 31;113(4):593-595. doi: 10.1161/CIRCULATIONAHA.105.589663.
12. Howlett JG, McKelvie RS, Arnold JM, et al. Canadian Cardiovascular Society Consensus Conference guidelines on heart failure, diagnosis and management of right-sided heart failure, myocarditis, device therapy and recent important clinical trials. Can J Cardiol. 2009 Feb;25(2):85-105. doi: 10.1016/s0828-282x(09)70477-5.

https://doi.org/10.52645/MJHS.2025.3.11

UDC: 616-008.9:577.115

RESEARCH ARTICLE

Lipid profile in young people

Diana Chiosa[1*], Rodica Ignat[1], Alexei Levițchi[2], Ghenadie Curocichin[1,2]

[1]Department of Family Medicine, *Nicolae Testemițanu* State University of Medicine and Pharmacy, Chișinău, Republic of Moldova
[2]Personalized Medicine Laboratory, *Nicolae Testemițanu* State University of Medicine and Pharmacy, Chișinău, Republic of Moldova

ABSTRACT

Introduction. Metabolic risk factors for non-communicable chronic diseases develop from an early age, while the clinical manifestations of cardiovascular diseases associated with these risk factors appear later in life. Dyslipidemia is a modifiable risk factor for cardiovascular diseases. The purpose of the study was to evaluate the lipid profile in young people as an early risk factor for cardiovascular disease.

Material and methods. The study was conducted on 693 healthy young individuals: 71.4% (495) women and 28.6% (198) men, aged between 17 and 30 years. The measured parameters included total cholesterol, HDL-cholesterol, LDL-cholesterol, and triglycerides, measured using the spectrophotometric method. Non-HDL cholesterol was calculated with the formula: non-HDL-C = TC – HDL-C (mmol/l).

Results. A total of 8.2% of young people had total cholesterol levels above the normal threshold (5.0 mmol/l). HDL-cholesterol below the gender-specific threshold values was recorded in 52.5%. Among women, 58.8% had HDL-cholesterol levels ≤ 1.29 mmol/l, and among men, 36.9% had levels below 1.03 mmol/l. Non-HDL cholesterol exceeded the threshold value (3.8 mmol/l) in 5.9% of young people. For 21.4% of participants, LDL-cholesterol was above the threshold (2.59 mmol/l), and 8.2% had triglyceride levels above the normal threshold (1.7 mmol/l).

Conclusions. The study demonstrated that over half of the young people (52.5%) had HDL-cholesterol below the gender-specific thresholds. Deviations in the lipid profile increase the atherogenic potential of plasma, highlighting the need for early preventive interventions in this age group.

Keywords: lipids, young people, risk factors, cardiovascular risk, chronic non-communicable diseases, early prevention.

Cite this article: Chiosa D, Ignat R, Levițchi A, Curocichin G. Lipid profile in young people. Mold J Health Sci. 2025;12(3):70-74. https://doi.org/10.52645/MJHS.2025.3.11.

Manuscript received: 15.07.2025

Accepted for publication: 19.08.2025

Published: 15.09.2025

[*]**Corresponding author:** Diana Chiosa, MD, assistant professor Department of Family Medicine,
Nicolae Testemițanu State University of Medicine and Pharmacy,
137A 31 August 1989 Str, Chișinău, Republic of Moldova, MD2004
e-mail: diana.chiosa@usmf.md

Authors's ORCID IDs
Diana Chiosa – https://orcid.org/0000-0002-3652-8021
Rodica Ignat – https://orcid.org/0000-0002-4934-8820
Alexei Levițchi – https://orcid.org/0000-0003-1784-654X
Ghenadie Curocichin – https://orcid.org/0000-0003-0613-4360

Key messages

What is not yet known about the issue addressed in the submitted manuscript

The lipid profile in the young population is not sufficiently documented. The behavior of metabolic risk factors in young people remains poorly understood, particularly since this group is not typically included in screening programs.

The research hypothesis

Young individuals experience changes in their lipid profile from childhood, which later evolve into specific disease entities as life progresses.

The novelty added by manuscript to the already published scientific literature

The reported study presents the characteristics of the lipid profile among young people in the Republic of Moldova.

Introduction

Alterations in the lipid spectrum are a major cause of atherosclerosis [1]. Numerous epidemiological studies have confirmed a direct link between dyslipidemia and the incidence of cardiovascular events, which are recorded both in apparently healthy individuals and in those with a history of cardiovascular disease. There is also evidence that dyslipidemia can be an independent predictor of cardiovascular events, as well as act in conjunction with other risk factors. Longitudinal studies have demonstrated the persistence of dyslipidemia throughout life, favoring the continuous progression of subclinical atherosclerosis. Scientific evidence supports the relationship between hyperlipidemia and changes in the arterial intimal layer at an early age, further strengthening the hypothesis that atherosclerosis begins early and is a chronic, progressive process [2-5]. Alterations in the lipid spectrum begin early, from childhood and adolescence, persist into youth, and clinical manifestations become apparent in adulthood [6, 7]. Dyslipidemia, particularly characterized by low levels of HDL-cholesterol (HDL-C) and elevated triglycerides (TG), is frequently observed among young people, with a prevalence ranging between 13% and 30% [8-10]. The increase in LDL-C, total cholesterol, and non-HDL-C levels observed during adolescence and youth is associated with a higher long-term cardiovascular risk [8]. Some studies conducted among young populations have shown that cumulative exposure to hyperlipidemia during youth increases the risk of developing coronary heart disease later in life, even in cases where there are only moderate increases in LDL cholesterol [9, 10]. Dyslipidemia is a modifiable cardiovascular risk factor, and early identification, along with prompt intervention, can significantly reduce overall cardiovascular risk, as well as the incidence of fatal and non-fatal events. The aim of the study was to evaluate the lipid profile in young people as an early cardiovascular risk factor.

Material and methods

The cross-sectional study was conducted on a sample of 693 apparently healthy young individuals (495 women and 198 men) aged between 17 and 30 years, who were first-year students at *Nicolae Testemițanu* State University of Medicine and Pharmacy (SUMF), from all integrated study programs: Medicine, Public Health, Pharmacy, and Dentistry. The study received approval from the Research Ethics Committee of *Nicolae Testemițanu* State University of Medicine and Pharmacy (Minutes no. 9 from November 20, 2012) and was carried out between September and November 2011. To analyze the lipid profile, the following parameters were assessed: total cholesterol (TC), HDL-cholesterol (HDL-C), non-HDL cholesterol (non-HDL-C), LDL-cholesterol (LDL-C), and triglycerides (TG). Venous blood was collected in the morning after at least 8 hours of fasting; the serum was separated, aliquoted, and stored at –70°C. The period before freezing did not exceed 6 hours. Serum lipids were determined in the INVITRO Diagnostics Laboratory. Tests were performed using ABBOTT Architect ci8200 equipment. Triglyceride concentration was determined using the enzymatic-colorimetric method (Triglycerides Mono SL NEW, ELITech Clinical Systems, France, and ARCHITECT Triglyceride, 7D74-21, Abbott). Total cholesterol was assessed by the enzymatic method (Cholesterol SL ELITech Clinical Systems, France, and ARCHITECT Cholesterol, 7D62-21, Abbott). HDL-cholesterol concentration was estimated by the enzymatic-spectrophotometric method with precipitation (HDL-Cholesterol ELITech Clinical Systems, France, and ARCHITECT ULTRA HDL, 3K33-21, Abbott). LDL-cholesterol content was measured directly (ARCHITECT Direct LDL, 1E31-20, Abbott). Non-HDL cholesterol was calculated using the formula: non-HDL-C = TC – HDL-C (mmol/l) [11]. The evaluation of changes in the lipid spectrum was carried out according to the recommendations of the European Society of Cardiology and the National Clinical Protocol for Dyslipidemias [12, 13] (Table 1).

Table 1. Threshold values for interpretation of lipid parameters (mmol/l)

	TC	LDL-C	HDL-C	non-HDL-C	TG
Normal level	< 5.0	< 2.6	≥ 1.0* ≥ 1.3**	< 3.8	< 1.7
Modified level	≥ 5.0	≥ 2.6	< 1.0* < 1.3**	≥ 3.8	≥ 1.7

Note: ** – men; ** – women;. TC – total cholesterol; LDL-C – LDL-cholesterol; HDL-C – HDL-cholesterol; non-HDL-C – non-HDL cholesterol; TG – triglycerides.*

The R programming environment was used to calculate the statistical parameters, employing the EpiTool applications [14-16]. The differences between the statistically significant mean values ($p < 0.05$) and their 95% confidence intervals were calculated.

Results

The stratified analysis of the lipid profile of the evaluated young people showed that total cholesterol (TC) values ranged from 1.71 to 6.89 mmol/l, with a mean value of 3.89 ± 0.845 mmol/l. In men, TC ranged from 1.88 to 6.89 mmol/l, and in women from 1.71 to 6.52 mmol/l ($p = 0.5239$). The mean value of TC was higher in women (3.90 ± 0.855 mmol/l) than in men (3.85 ± 0.845 mmol/l) ($p = 0.4354$). Mean HDL cholesterol (HDL-C) was 1.22 ± 0.328 mmol/l, with a range between 0.53 and 2.80 mmol/l. HDL-C values ranged from 0.57 to 2.01 mmol/l in men and from 0.53 to 2.80 mmol/l in women ($p = 0.0068$). In women, the mean HDL-C value was higher (1.26 ± 0.337 mmol/l) compared to men (1.14 ± 0.328 mmol/l), the difference being statistically significant ($p = 3.56 \times 10^{-6}$). Non-HDL cholesterol (non-HDL-C) in the study group had a mean value of 2.66 ± 0.718 mmol/l, with limits ranging from 0.62 to 5.76 mmol/l. In men, non-HDL-C values ranged from 1.18 mmol/l to 5.76 mmol/l, while in women from 0.62 mmol/l to 4.92 mmol/l ($p = 0.2885$). Mean non-HDL-C was higher in men (2.70 ± 0.685 mmol/l) than in women (2.65 ± 0.731 mmol/l) ($p = 0.334$). The LDL-cholesterol (LDL-C) content ranged from 0.30 to 5.04 mmol/l, with a mean value of 1.94 ± 0.787 mmol/l. LDL-C values ranged from 0.47 mmol/l to

5.04 mmol/l in men and from 0.62 mmol/l to 4.92 mmol/l in women (p = 0.1304). The mean LDL-C was higher in men (2.00 ± 0.787 mmol/l) compared to women (1.92 ± 0.807 mmol/l) (p = 0.2079). Triglyceride (TG) concentration ranged from 0.18 mmol/l to 7.16 mmol/l, with a mean value of 1.16 ± 0.572 mmol/l. In women, TG values ranged from 0.24 mmol/l to 7.16 mmol/l and from 0.18 mmol/l to 5.24 mmol/l in men (p = 0.130). Mean TG content was significantly higher (p = 0.0042) in men (1.26 ± 0.572 mmol/l) than in women (1.13 ± 0.586 mmol/l) (Table 2).

Table 2. Comparative characteristics of lipid parameters (n = 693).

Statistical parameter	Sex	TC mmol/l	HDL-C mmol/l	non-HDL-C mmol/l	LDL-C mmol/l	TG mmol/l
Range of variation	Total	1.71–6.89	0.53–2.80	0.62–5.76	0.30–5.04	0.18–7.16
	M	1.88–6.89	0.57–2.01	1.18-5.76	0.47–5.04	0.18–5.24
	F	1.71–6.52	0.53–2.80	0.62–4.92	0.30-3.97	0.24–7.16
Median	Total	3.96	1.19	2.69	2.03	1.27
	M	3.99	1.11	2.75	2.06	1.32
	F	3.95	1.21	2.64	2.00	1.24
Mean ± SD	Total	3.89 ± 0.845	1.22 ± 0.328	2.66 ± 0.718	1.94 ± 0.787	1.16 ± 0.572
	M	3.85 ± 0.845	1.14 ± 0.328	2.70 ± 0.685	2.00 ± 0.787	1.26 ± 0.572
	F	3.90 ± 0.855	1.26 ± 0.337	2.65 ± 0.731	1.92 ± 0.807	1.13 ± 0.586
	t-test	-0.7808	-4.698	0.9666	1.2615	2.8779
	p value	0.4354	3.56×10^{-6}	0.3344	0.2079	0.0042
	F-test	0.9244	0.7162	0.8782	0.8309	0.7964
	p value	0.5239	0.0068	0.2885	0.1304	0.0633

Note: *n(M) = 198 –number of men. n(F) = 495 –number of women. TC – total cholesterol; LDL-C – LDL-cholesterol; HDL-C – HDL-cholesterol; non-HDL-C – non-HDL cholesterol; TG – triglycerides. Statistical significance was set at p < 0.05. The t-test was applied to assess differences between mean values; F-test was applied to assess differences in variance between datasets.*

The majority of the evaluated young people (91.8%) had TC values within normal limits (less than 5.0 mmol/l), while 8.2% had levels above the threshold considered normal. Among women, the proportion of those with TC above the threshold value was 9.3%, and among men, 5.6% (p = 0.106). It is important to note that more than half of the participants (52.5%) had HDL-C values below the gender-specific thresholds. Thus, 58.8% of the women had HDL-C levels ≤ 1.29 mmol/l, and 36.9% of the men had levels ≤ 1.03 mmol/l. The association between HDL-C and gender was statistically significant ((χ^2 = 27.249, p=5 × 10-4). Non-HDL-C concentrations were within normal limits (≤ 3.8 mmol/l) in 94.1% of participants, and 5.9% were above the reference threshold. Analysis by gender revealed elevated non-HDL-C levels in 6.7% of women and 4.0% of men (p = 0.218). Also, LDL-C remained within normal limits (≤ 2.59 mmol/l) in 78.6% of participants, while 21.4% had values above the recommended threshold. According to gender, 22.2% of men and 21.0% of women had elevated LDL-C values, with no statistically significant difference between the two groups (p = 0.779). Regarding TG, 91.8% of participants had levels within normal limits (< 1.7 mmol/l), while 8.2% had values above the threshold. Elevated TG levels were observed in 8.7% of women and 7.1% of men (p = 0.528) (Fig. 1). Therefore, the comparative analysis of the lipid profile according to sex revealed a statistically significant difference only for HDL-C (χ^2 = 27.249, p = 5×10^{-4}). The proportion of women with pathological HDL-C levels (≤ 1.29 mmol/l) was significantly higher (58.8%) compared to men (36.9%). For the other parameters (TC, LDL-C, non-HDL-C, and TG), sex differences were not statistically significant (Fig. 1).

Discussions

The results of our study, using threshold values for lipid parameters [12, 13], revealed a relatively high prevalence, with more than half (52.5%) of the young assessed individuals having HDL-C levels below gender-specific thresholds. Low HDL-C levels among youth have also been documented in international research on this age group, with a prevalence ranging from 13% to 30% [9, 17, 18]. Our study recorded HDL-C levels below gender-specific threshold values in 58.8% of women and 36.9% of men, with a statistically significant difference (p = 5×10^{-4}). Other research conducted in the same age group demonstrated the presence of this risk factor in 18.2% of men and 8.1% of women [17]. More comprehensive data are provided by a large-scale study from China involving 22,379 young students, which reported a high proportion (74%) of individuals with low HDL-C levels, particularly among men (23% vs. 7.2% in women). Elevated triglycerides (14.5%) were also noted, but as in our research, other risk factors such as diet, physical activity level, and age-specific hormonal characteristics were not analyzed [10]. A study conducted among medical students in Sri Lanka highlighted numerous deviations in the lipid profile among young people, including a prevalence of hypercholesterolemia of 25.4% and hypertriglyceridemia of 5.3%. The authors reported that these abnormalities were significantly more frequent among men (12.3%) compared to women (1.6%), with the difference being statistically significant (p = 0.006). Additionally, low HDL-C levels were observed in approximately 31.6% of participants, while 12.2% had elevated LDL-C values [19]. Several local studies among young medical students have likewise demonstrated changes in lipid profile parameters. Thus, a cross-sectional study conducted on a sample of 456

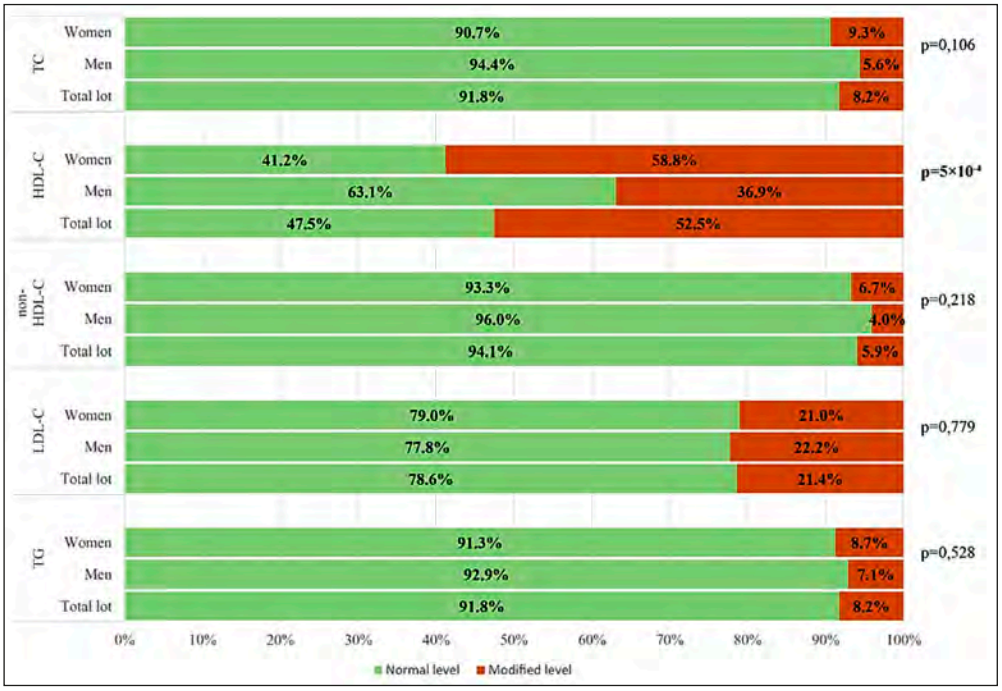

Fig. 1 Frequency of lipid parameter levels in relation to threshold values (mmol/l)

Note: *TC – total cholesterol; LDL-C – LDL-cholesterol; HDL-C – HDL-cholesterol; non-HDL-C – non-HDL cholesterol; TG – triglycerides. Normal level – the percentage of subjects with the parameter within normal limits; Modified level – the percentage of subjects with values above the threshold (TC; LDL-C; non-HDL-C; TG) and below the sex-specific threshold (HDL-C). $p < 0.05$ was considered statistically significant.*

students from the *Nicolae Testemițanu* State University of Medicine and Pharmacy revealed alterations in the lipid profile in 52.0% of participants, of whom 40.9% had HDL-C values below gender-specific reference thresholds, 11.8% had hypertriglyceridemia, and 7.3% had hypercholesterolemia [20]. Another study conducted among students at the same institution reported a prevalence of 53.0% for at least one altered lipid parameter among 302 women. Within this sample, 34.1% of participants had low HDL-C levels, 13.6% had hypertriglyceridemia, and 14.2% had hypercholesterolemia, while 7.0% exhibited elevated non-HDL-C values [21]. At the same time, among men, at least one altered lipid parameter was identified in 34.0% of 138 medical students, with low HDL-C being the most frequently observed abnormality [22]. These data confirm the trend observed in our own analysis, suggesting a significant frequency of dyslipidemia among the young population.

In comparison, data from the STEPS studies conducted in the Republic of Moldova indicate that, among the general population aged 18 to 29, 17.8% of young people had mean total cholesterol (TC) values above 5.0 mmol/l. The differences between sexes were statistically significant, with a higher prevalence in women (20.0%) compared to men (15.5%) [23, 24]. The changes observed in the lipid profile may potentially be influenced by genetic factors, considering the concept that genetic factors shape individuals' health status in youth, while behavioral and environmental factors become more significant with age – a point that should be taken into account when developing personalized preventive strategies.

Conclusions

The study demonstrated that more than half of the young individuals (52.5%) had HDL-C levels below gender-specific thresholds. These changes in the lipid profile increase the atherogenic potential of plasma, highlighting the importance of implementing early preventive measures in this age group. In this context, it is essential to expand the use of cardiovascular risk assessment tools among the young population.

Competing interests

None declared.

Authors' contributions

All authors contributed equally to the conduct of the study and the drafting of the manuscript. All authors reviewed the work critically and approved the final version of the manuscript.

Informed consent for publication

Obtained.

Acknowledgements and funding

The current study is an integral part of the institutional projects no. 11.817.09.21A, 2011-2014 "Molecular Genetic Polymorphism of Metabolic Cardiovascular Risk Factors in Young People", and no. 15.817.04.42A, 2015-2018 "Identification and Validation of Genetic and Epigenetic Biomarkers in Chronic Non-Communicable Diseases with Major Impact on Public Health".

The group of authors expresses deep gratitude to the University Primary Health Care Clinic of *Nicolae Testemițanu* State University of Medicine and Pharmacy and INVITRO Diagnostics Laboratory for their support in generating the lipid profile data.

Ethics approval

The study protocol was approved by the Research Ethics Committee of the *Nicolae Testemițanu* State University of Medicine and Pharmacy (Minutes no. 9, dated November 20, 2012).

Provenance and peer review

Not commissioned, externally peer-reviewed.

References

1. Visseren FLJ, Mach F, Smulders YM, Carballo D, Koskinas KC, Bäck M, et al. 2021 ESC Guidelines on cardiovascular disease prevention in clinical practice: developed by the Task Force for cardiovascular disease prevention in clinical practice with representatives of the European Society of Cardiology and 12 medical societies with the special contribution of the European Association of Preventive Cardiology (EAPC). Eur Heart J. 2021;42(34):3227-3337. doi: 10.1093/eurheartj/ehab484.
2. Palacio-Portilla EJ, Roquer J, Amaro S, Arenillas JF, Ayo-Martín O, Castellanos M, et al. Dyslipidemias and stroke prevention: recommendations of the Study Group of Cerebrovascular Diseases of the Spanish Society of Neurology. Neurología (English Ed.). 2022;37(1):61-72. doi: 10.1016/j.nrleng.2020.07.021.
3. Zokaei A, Ziapour A, Khanghahi ME, Lebni JY, Irandoost SF, Toghroli R, et al. Investigating high blood pressure, type-2 diabetes, dislipidemia, and body mass index to determine the health status of people over 30 years. J Educ Health Promot. 2020;9(1):333. doi: 10.4103/jehp.jehp_514_20.
4. Orozco-Beltran D, Gil-Guillen VF, Redon J, Martin-Moreno JM, Pallares-Carratala V, Navarro-Perez J, et al. Lipid profile, cardiovascular disease and mortality in a Mediterranean high-risk population: the ESCARVAL-RISK study. PloS One. 2017;12(10):e0186196. doi: 10.1371/journal.pone.0186196.
5. Sadeghi M, Golshahi J, Talaei M, Sheikhbahaei E, Ghodjani E, Mansouri M, et al. 15-year lipid profile effects on cardiovascular events adjusted for cardiovascular risk factors: a cohort study from Middle-East. Acta Cardiol. 2021;76(2):194-199. doi: 10.1080/00015385.2020.1717096.
6. Teo KK, Rafiq T. Cardiovascular risk factors and prevention: a perspective from developing countries. Can J Cardiol. 2021;37(5):733-743. doi: 10.1016/j.cjca.2021.02.009.
7. Truthmann J, Schienkiewitz A, Kneuer A, Du Y, Scheidt-Nave C. Tracking of serum lipids from prepuberty to young adulthood: results from the KiGGS cohort study. Lipids Health Dis. 2024;23(1):421. doi: 10.1186/s12944-024-02409-1.
8. Kiechl SJ, Staudt A, Stock K, Gande N, Bernar B, Hochmayr C, et al. Predictors of carotid intima-media thickness progression in adolescents - the EVA-Tyrol study. J Am Heart Assoc. 2021;10(18):e020233. doi: 10.1161/JAHA.120.020233.
9. Navar-Boggan AM, Peterson ED, D'Agostino RB Sr, Neely B, Sniderman AD, Pencina MJ. Hyperlipidemia in early adulthood increases long-term risk of coronary heart disease. Circulation. 2015;131(5):451-458. doi: 10.1161/CIRCULATIONAHA.114.012477.
10. Liu LY, Aimaiti X, Zheng YY, Zhi XY, Wang ZL, Yin X, et al. Epidemic trends of dyslipidemia in young adults: a real-world study including more than 20,000 samples. Lipids Health Dis. 2023;22(1):108. doi: 10.1186/s12944-023-01876-2.
11. Catapano AL, Graham I, De Backer G, Wiklund O, Chapman MJ, Drexel H, et al. 2016 ESC/EAS guidelines for the management of dyslipidaemias. Rev Esp Cardiol (English ed.). 2017;70(2):115. doi: 10.1016/j.rec.2017.01.002.
12. Ministry of Health of the Republic of Moldova; Ivanov V, Dumanschi C. Dislipidemiile: protocol clinic național (PCN-78) [Dyslipidemias: national clinical protocol]. Chisinau: The Ministry; 2017. Romanian.
13. Mach F, Baigent C, Catapano AL, Koskinas KC, Casula M, Badimon L, et al. 2019 ESC/EAS Guidelines for the management of dyslipidaemias: lipid modification to reduce cardiovascular risk: the Task Force for the management of dyslipidaemias of the European Society of Cardiology (ESC) and European Atherosclerosis Society (EAS). Eur Heart J. 2020;41(1):111-188. doi: 10.1093/eurheartj/ehz455.
14. Wickham H. Reshaping data with the reshape package. J Stat Softw. 2007;21:1-20. doi: 10.18637/jss.v021.i12.
15. Wickham H. Ggplot2: elegant graphics for data analysis. 2nd ed. Dordrecht: Springer; 2009. 277 p. doi: 10.1007/978-0-387-98141-3.
16. Begum GS, Adari P, Manjunatha G, Kore SE, Eshwaret MD. A study of diagnostic parameters in assessment of metabolic syndrome (MetS) among medical students. Biomedicine. 2022;42(6):1361-1367. doi: 10.51248/.v42i6.1822.
17. Abuzhalihan J, Wang YT, Adi D, Ma YT, Fu ZY, Yang YN, et al. Prevalence of dyslipidemia in students from Han, Uygur, and Kazakh ethnic groups in a medical university in Xinjiang, China. Sci Rep. 2019;9(1):19475. doi: 10.1038/s41598-019-55480-5.
18. Senevirathne T, Samaranayake D, Ojithmali M, Wickramarachchi P, Weerasinghe A, Muthuthamby MM, et al. Cardio-metabolic risk among undergraduate medical students of a selected Faculty of Medicine in Colombo. Res Square. 2020 March 26. doi: 10.21203/rs.3.rs-19253/v1.
19. Gavriliuc S, Ignat R, Levitchi A, Lupu L, Chiosa D, Buza A, et al. Prevalence of lipid abnormalities among young Moldovans. In: MedEspera: 6th International Medical Congress for Students and Young Doctors; 2018 Mai 12-14; Chișinău, Republic of Moldova: abstract book. Chișinău: [s. n.]; 2016. p. 53-54.
20. Gavriliuc S. The rate of obesity and dyslipidaemia among young moldovan women. In: MedEspera: 7th International Medical Congress for Students and Young Doctors, 2018 Mai 3-5; Chișinău, Republic of Moldova. Chisinau; 2018. p. 92.
21. Gavriliuc S, Buza A, Butovscaia C, Istrati V. Silent cardiovascular risk factors among medical students. Mold Med J. 2021;64(1): 41-44. doi: 10.5281/zenodo.4527088.
22. World Health Organization (WHO). Prevalence of noncommunicable disease risk factors in the Republic of Moldova: STEPS 2013. Copenhagen: WHO Regional Office for Europe; 2014. 220 p.
23. World Health Organization (WHO). Noncommunicable diseases: progress monitor 2022 Geneva: WHO regional Office for Europe; 2022. 225 p.

https://doi.org/10.52645/MJHS.2025.3.12

UDC: 616.61-036.11-02:[616.98:578.834.1]-06

RESEARCH ARTICLE

Acute kidney injury – a severe complication secondary to COVID-19

Marinela Murea*, Andrei Bradu, Andrei Oprea, Andrei Galescu, Emil Ceban

Department of Urology and Surgical Nephrology, *Nicolae Testemițanu* State University of Medicine and Pharmacy, Chișinău, Republic of Moldova

ABSTRACT

Introduction. The COVID-19 pandemic has posed the biggest challenge to the global health system. Kidney damage is common in COVID-19 and ranges from mild proteinuria to severe acute kidney injury.

Objective. The aim of the study was to establish the dynamics of COVID-19 in patients who develop acute kidney injury and to identify risk factors for developing acute kidney injury associated with COVID-19.

Materials and methods. A retrospective descriptive study was conducted, including 40 patients of both sexes, aged between 37 and 88 years, who were admitted to the intensive care unit of the *Timofei Moșneaga* Republican Clinical Hospital during the period 2020-2022. Statistical analysis was performed using the Student's t-test.

Results. The most common factors identified as determinants were advanced age, comorbidities, mechanical ventilation, and nephrotoxic drugs. The presence of proteinuria, hematuria, and leukocyturia was identified. Urea and creatinine levels were elevated on admission and continued to rise; 10% of patients required renal replacement therapy. It was observed that the greater the degree of lung damage, the earlier mechanical ventilation was instituted, which could lead to the development of early acute kidney injury. All patients were mechanically ventilated and developed acute kidney injury, contributing to a severe course of COVID-19.

Conclusions. Acute kidney injury is one of the most frequent and severe complications encountered among mechanically ventilated patients with severe forms COVID-19 and is often associated with a fulminant course and a high mortality rate.

Keywords: COVID-19, acute kidney injury, complications, mechanically ventilated patients.

Cite this article: Murea M, Bradu A, Oprea A, Galescu A, Ceban E. Acute kidney injury – a severe complication secondary to COVID-19. Mold J Health Sci. 2025;12(3):75-79. https://doi.org/10.52645/MJHS.2025.3.12.

Manuscript received: 16.07.2025

Accepted for publication: 22.08.2025

Published: 15.09.2025

***Corresponding author: Marinela Murea**, MD, resident
Department of Urology and Surgical Nephrology
Nicolae Testemițanu State University of Medicine and Pharmacy
29 Nicolae Testemițanu str, Chisinau, Republic of Moldova, MD-2025
e-mail: murea.marinela@gmail.com

Authors' ORCID IDs
Marinela Murea – https://orcid.org/0009-0007-7350-4495
Andrei Bradu – https://orcid.org/0000-0001-7285-8717
Andrei Oprea – https://orcid.org/0000-0001-9269-5468
Andrei Galescu – https://orcid.org/0000-0002-7953-2450
Emil Ceban – https://orcid.org/0000-0002-1583-2884

Key messages

What is not yet known about the issue addressed in the submitted manuscript

Acute kidney injury is one of the most common and severe complications encountered among mechanically ventilated patients with severe forms of COVID-19 and is often associated with a fulminant course and a high mortality rate. There is limited data available on how to prevent the development of this medical condition.

The research hypothesis

The risk of developing acute kidney disorders in patients with COVID-19 is influenced by several clinical and paraclinical factors.

The novelty added by manuscript to the already published scientific literature

The manuscript explores, for the first time in the Republic of Moldova, the impact of various risk factors involved in the development of acute kidney injury in patients with severe forms of COVID-19.

Introduction

The Coronavirus disease 19 (COVID-19) pandemic remains the biggest challenge facing healthcare systems around the world. Although the respiratory system is the primary target of SARS-CoV-2 (Severe Acute Respiratory Syndrome Coronavirus 2), other systems and organs can also be affected by the virus via the circulatory system, including the renal system. Reports indicate that kidney involvement is common and ranges from mild proteinuria to severe acute kidney injury (AKI) [1, 2]. The pathogenetic mechanisms by which SARS-CoV-2 induces the development of AKI remain unclear; however, studies suggest that AKI appears to be closely related to the direct action of the virus on the kidneys [3].

Even though early in the pandemic, reports from China suggested low rates of kidney damage (0.5%), studies from the USA and Europe have reported increasing rates of AKI, particularly in intensive care settings, where approximately 45% of patients require renal replacement therapy [4, 5]. A 2020 meta-analysis reported that the combined incidence of AKI among hospitalized COVID-19 patients was 28.6% in the USA and Europe and 5.5% in China. Worldwide, among patients admitted to intensive care units, it is estimated that 29% develop AKI, and this proportion rises to 78% in those requiring intubation [6]. According to a 2022 study, AKI is a frequent complication of SARS-CoV-2 infection, with a cumulative incidence of 19.76% and a mortality rate exceeding 54.24% [7]. Differences in results may be due to the population studied and the definitions of AKI used.

Since the beginning of the pandemic, 607,450 cases of COVID-19 have been registered in the Republic of Moldova. From the total number of registered cases, 5,145 patients were admitted to the *Timofei Moşneaga* Republican Clinical Hospital, of which 10% (514) developed acute kidney injury. Of the total number, 80.68% (4,151) of patients had a favorable evolution, but 19.32% (994) died.

Therefore, the aim of the study was to establish the dynamics of COVID-19 in patients who develop AKI and to identify risk factors for developing AKI associated with COVID-19.

Material and methods

This retrospective descriptive study was carried out based on the clinical observation sheets of a group of 40 patients, of both sexes, aged between 37 and 88 years (mean age 64.08 ± 10.04 years). The inclusion criterion was the development of AKI secondary to COVID-19, and the exclusion criterion was the absence of signs of kidney damage. The analysis of the clinical observation sheets of these patients was carried out using a questionnaire that included the following criteria: age, sex, day of illness at admission, vaccination status, symptoms at admission, comorbidities, laboratory investigations (general urinalysis, complete blood count, biochemical blood analysis, inflammatory markers, coagulation tests), instrumental investigations (pulmonary radiography), treatment, need for mechanical ventilation, discharge status, and death. For each patient, data were collected on three different days: the day of admission (first investigation), during hospitalization (second investigation), and the last day of hospitalization (third investigation), which allowed us to identify the development of AKI and its dynamic evolution. Statistical analysis of the data was performed using the Student's t-test.

Results

The clinical observation sheets were studied as a whole to observe the evolution of the patients' condition over time and to determine the existence of a correlation between COVID-19 infection and kidney damage. The patients included in the study were admitted to the COVID-19 Intensive Care Unit on the 8.66 ± 3.76 day of illness in a serious condition. According to the epidemiological history, 5% (n = 2) of the patients were vaccinated: one had received two doses of the Pfizer/BioNTech vaccine, and one had received a single dose of the Jonhson&Jonhson (Janssen) vaccine; 15% (n = 6) were not vaccinated, and for 80% (n = 32), vaccination status was not documented. Initially, the patients' symptoms at admission were studied. It was determined that all 40 patients presented with typical symptoms of SARS-CoV-2 infection: low-grade fever - 27.50% (n = 11), fever - 62.50% (n = 25), wet cough - 15% (n = 6), dry cough - 62.50% (n = 25), general weakness - 97.50% (n = 39), headache - 52.50% (n = 21), dyspnea - 95% (n = 38), myalgia - 37.50% (n = 15), chills - 7.50% (n = 3), hypogeusia - 7.50% (n = 3), hyposmia - 7.50% (n = 3). Additionally, 80% (n = 32) did not present with any symptoms of kidney damage at admission.

The comorbidities identified in the studied patients were consistent with those described in the specialized literature and had the following frequencies: chronic cardiovascular diseases - 95% (n = 38), diabetes - 50% (n = 20), obesity - 52.50% (n = 21), chronic kidney disease (CKD) - 35% (n = 14), chronic kidney disease on dialysis - 5% (n = 2), and other conditions - 57.5% (n = 23). These comorbidities can be considered decisive factors in the development of AKI.

Analyzing the laboratory investigations, it was found that from the first day of hospitalization, patients already presented changes suggestive of kidney damage. In the general urinalysis, hematuria, leukocyturia, and proteinuria were observed, with values worsening over the course of the disease. As shown in Figure 1, on the day of hospitalization (urinalysis I), the following results were recorded: erythrocytes – mean 19.75/HPF, 95% CI: 7.27-32.26, $p < 0.001$; leukocytes – 10.47/HPF, 95% CI: 2.25-23.19, $p = 0.10$; proteins – 0.73 g/L, 95% CI: 0.49-0.97, $p < 0.001$. During hospitalization (urinalysis II): erythrocytes – 23.96/HPF, 95% CI: 12.26-35.69, $p < 0.001$; leukocytes – 6.21/HPF, 95% CI: 3.62-8.79, $p < 0.001$; proteins – 0.68 g/L, 95% CI: 0.49-0.87, $p < 0.001$. On the last day of hospitalization (urinalysis III): erythrocytes – 32.15/HPF, 95% CI: 13.75-50.56, $p < 0.001$; leukocytes – 9.83/HPF, 95% CI: 4.42-15.24, $p < 0.001$; proteins – 0.75 g/L, 95% CI: 0.53-0.97, $p < 0.001$. The difference between the values on the first and last day of hospitalization was statistically significant ($p < 0.001$).

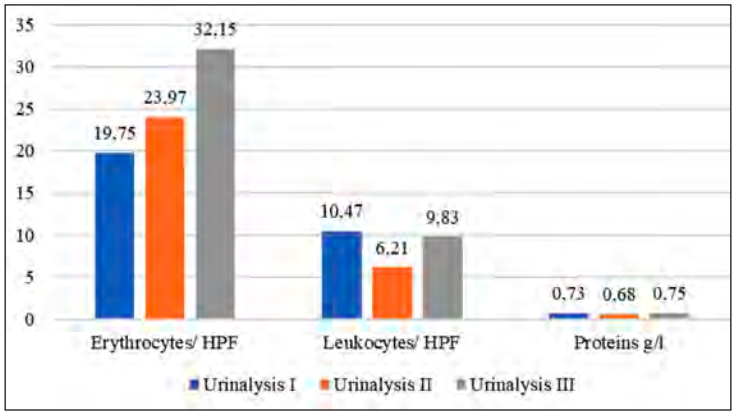

Fig. 1 Urinalysis values in dynamics

Note: *Urinalysis I – day of admission, Urinalysis II – during hospitalization, Urinalysis III – last day, HPF – High-Power Field.*

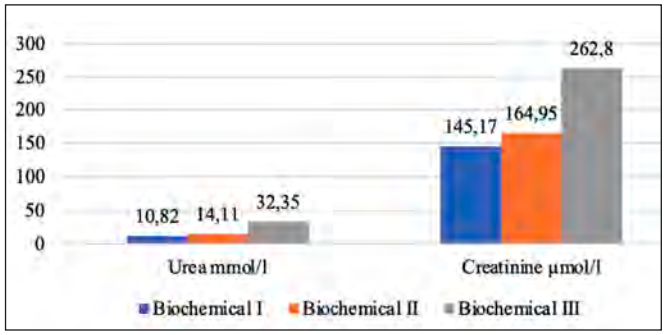

Fig. 2 Markers of renal function in dynamics

Note: *Biochemical I – the day of admission, Biochemical II – during hospitalization, Biochemical III – last day.*

The presence of a severe inflammatory syndrome was also observed, being associated with an increased severity of COVID-19. This was demonstrated by the dynamic analysis of inflammatory markers. On the day of admission (urinalysis I), the following values were recorded: ESR – 36.57 mm/h, 95% CI: 31.17-41.97, p < 0.001: CRP – 624.18 mg/dl, 95% CI: 435.71-1684.08, p = 0.24; LDH – 447.74 U/l, 95% CI: 378.3-517.13, p < 0.001. During hospitalization (urinalysis II): ESR – 39.30 mm/h, 95% CI: 34.54-44.05, p < 0.001; CRP – 119.31 mg/dl, 95% CI: 90.06-148.55, p < 0.001; LDH – 606.91 U/l, 95% CI: 342.99-871.84, p < 0.001. On the last day (urinalysis III): ESR – 40.72 mm/h, 95% CI: 34.62-46.82, p < 0.001; CRP – 208.89 mg/dl, 95% CI: 66.19-531.59, p = 0.003; LDH – 550.98 U/l, 95% CI: 369.27-733.70, p < 0.001. According to these results, the difference in ESR, CRP, and LDH values between the first, second, and third measurements were statistically significant (p < 0.001), except for CRP on admission (p = 0.24), which was not statistically significant.

Studies report that in severe forms of COVID-19, where there is a considerable increase in cytokine levels, there is also a marked increase in ferritin, which is much higher in patients showing signs of kidney damage. Thus, ferritin can serve as a marker of severity and prognosis in SARS-CoV-2 infection [8].

The presence of elevated ferritin levels was also attested in our study from the day of admission and continued to increase dynamically along with the progression of COVID-19, a fact that confirms the data from the literature. On the first day (ferritin I) – 787.21 ng/ml, 95% CI: 601.50-972.93, p < 0.001; during hospitalization (ferritin II) – 943.59 ng/ml, 95% CI: 749.78-1137.39, p < 0.001; and on the last day (ferritin III) – 1029.00 ng/ml, 95% CI: 833.87-1224.12, p < 0.001. The values were statistically significant for p < 0.001.

To establish the presence of AKI, markers of renal function – urea and creatinine – were studied. Following Figure 2, we notice that on the day of admission (biochemical I), the average value of urea was 10.82 mmol/l, 95% CI: 8.29-13.34, p < 0.001, and of creatinine 145.17 µmol/l, 95% CI: 73.73-216.62, p < 0.001. These data demonstrate that signs of renal function impairment were present even before the patients were admitted and showed a negative dynamic over time, especially after the initiation of mechanical ventilation through orotracheal intubation. During hospitalization (biochemical II), the average value of urea was 14.11 mmol/l, 95% CI: 11.83-16.40, p < 0.001, and of creatinine 164.95 µmol/l, 95% CI: 110.34-219.62, p < 0.001. On the last day (biochemical III), the average value of urea was 32.35 mmol/l, 95% CI: 27.3-37.3, p < 0.001, and of creatinine 262.80 µmol/l, 95% CI: 207.49-318.11, p < 0.001. Of the total number of 40 patients, 10% (n = 4) required renal replacement therapy. The values were statistically significant for p < 0.001.

Analyzing the dynamic coagulation tests of the patients, a deviation in their values was observed, indicating a state of hypocoagulation, in contrast to data reported in the literature, where it is stated that patients with severe forms of COVID-19 typically develop a hypercoagulable state. This discrepancy may be attributed to the high doses of anticoagulants used in the treatment of COVID-19. On the day of hospitalization (coagulation tests I), the mean value of PT was 74.64%, 95% CI: 68.56-80.72, p < 0.001; INR – 1.44, 95% CI: 1.39-1.49, p < 0.001; fibrinogen – 4.30 g/l, 95% CI: 3.85-4.75, p < 0.001; aPTTT – 36.69 sec, 95% CI: 32.01-41.37, p < 0.001. During hospitalization (coagulation tests II), PT – 70.93%, 95% CI: 67.60-74.27, p < 0.001; INR – 1.68, 95% CI: 1.08-2.27, p < 0.001; fibrinogen – 5.20 g/l, 95% CI: 2.84-7.55, p < 0.001; aPTT – 44.14 sec, 95% CI: 39.49-48.78, p < 0.001. On the last day (coagulation tests III), PT – 67.62%, 95% CI: 63.19-72.05, p < 0.001; INR – 1.51, 95% CI: 1.30-1.60, p < 0.001; fibrinogen – 4.12 g/l, 95% CI: 3.70-4.53, p < 0.001, aPTT – 43.87 sec, 95% CI: 38.65-49.09, p < 0.001. All values were statistically significant (p < 0.001).

Analyzing the treatment regimens of the patients included in the study, the use of several drugs with nephrotoxic effects was identified, which could be considered additional potential factors in the development of AKI in patients with COVID-19. The identified drugs were as follows: vancomy-

cin – 22.5% (n = 9), colistin – 40% (n = 16), gentamicin – 20% (n = 8), amikacin – 10% (n = 4), lopinavir/ritonavir (Aluvia) – 10% (n = 4), ascorbic acid – 90% (n = 36), hydroxychloroquine – 10% (n = 4), and others – 92.5% (n = 37), including ciprofloxacin, meropenem, pospenem, imipenem with cilastatin, ampicillin, amoxicillin with clavulanic acid, piperacillin with tazobactam, cefoperazone with sulbactam, and cefazolin. All patients (100%, n = 40) received combinations of two or more of the above-mentioned drugs as part of their treatment regimens. The development of AKI in patients with COVID-19 may also be explained by the lung-kidney interaction. Respiratory failure can trigger AKI through systemic hypoxia, which develops in patients with severe forms of COVID-19, as well as through hypercapnia and even mechanical ventilation [9]. Therefore, we can conclude that the degree of lung damage is correlated with kidney injury and the development of AKI. The greater the degree of pulmonary damage, the earlier mechanical ventilation is instituted, which may lead to the development of early AKI. Evaluating the results of chest radiographs, it was determined that on the day of admission (radiograph I), the degree of lung damage had an average of 66.90% ± 13.82, 95% CI: 62.48-71.32, $p < 0.001$. During hospitalization (radiograph II), the degree of lung damage was 68.38% ± 11.78, 95% CI: 64.60-72.15, $p < 0.001$. On the last day (radiograph III), it reached 69.00% ± 10.20, 95% CI: 65.74-71.26, $p < 0.001$. The differences between the radiographic values were statistically significant ($p < 0.001$).

All patients (100%, n = 40) were mechanically ventilated via orotracheal intubation for a mean duration of 7.73 ± 5.09 days. The average length of hospitalization was 15.43 ± 7.63 days. The clinical course in all patients (100%, n = 40) was fulminant and ended in death.

Discussions

Being a pathology with predominant damage to the respiratory system, COVID-19 can also affect other systems and organs, including the kidneys, which are particularly susceptible to infection with the SARS-CoV-2 virus, with AKI being the most common manifestation of kidney damage.

The consequences of the COVID-19 pandemic are drastic. Evidence shows that patients with CKD or those with risk factors for developing kidney disease are significantly affected. Patients with CKD undergoing renal replacement therapy and those with a kidney transplant are at higher risk of complications from COVID-19, while patients with severe forms of SARS-CoV-2 infection are at increased risk of developing AKI, with devastating consequences both in the short and long term [10].

It is well known that in severe forms of infection with the SARS-CoV-2 virus, a cytokine storm occurs, causing a considerable elevation of inflammatory markers and the release of a large number of cytokines into the circulation. Subsequently, a state of shock, hypoxia, and rhabdomyolysis can develop, which may eventually lead to the onset of AKI [11]. In kidney damage, an important role is played by the drug treatment administered to patients with COVID-19. The administration of drugs with nephrotoxic potential, such as aminoglycosides, vancomycin, and colistin, has been reported as a major risk factor in the development of AKI in patients infected with SARS-CoV-2. Even though beneficial effects of antiviral treatment with Remdesivir have been reported, it can also exert nephrotoxic effects through mitochondrial damage in renal tubular cells, especially when used in high doses. Cases of AKI associated with Lopinavir and low-dose Ritonavir therapy have also been reported during the management of COVID-19 [12]. Another drug commonly used in the treatment of COVID-19 is ascorbic acid. In addition to its antioxidant properties, it can lead to hyperoxaluria with severe and irreversible AKI, especially in patients with pre-existing CKD. Therefore, it is necessary to take renal function into account before using high doses of vitamin C [13]. During the first phase of the pandemic, hydroxychloroquine was used in the standard treatment protocols for COVID-19 patients. In addition to its antimalarial activity, it also possesses anti-inflammatory properties. As the pandemic evolved, it was found that hydroxychloroquine could contribute to AKI by increasing lysosomal pH and inhibiting autophagy. However, the results remain controversial, as other studies show that hydroxychloroquine does not have direct nephrotoxic activity, with toxicity likely potentiated by the drug combinations [11, 14].

Studies show that mechanical ventilation alters systemic hemodynamics and neurohormonal status. It can lead to changes in renal perfusion due to increased intrathoracic pressure, elevated pulmonary vascular resistance, and increased central venous pressure, which together reduce venous return and contribute to right ventricular dysfunction [15, 16].

In this study, the most common factors identified as decisive in the development of AKI in COVID-19 patients were advanced age, the presence of multiple comorbidities such as chronic cardiovascular diseases, diabetes mellitus, obesity, chronic kidney disease, mechanical ventilation via orotracheal intubation, and the use of drugs with nephrotoxic potential. Hospitalized at 8.66 ± 3.76 days after symptom onset, the patients were in serious condition, with evident signs of kidney damage that continued to worsen over time. Urinalysis revealed proteinuria, hematuria, and leukocyturia from the day of admission. Urea and creatinine levels were elevated on admission and continued to rise, with urea increasing from 10.82 mmol/l to 32.35 mmol/l and creatinine from 145.17 μmol/l to 262.80 μmol/l; 10% of patients required renal replacement therapy. These changes were associated with considerable increases in inflammatory markers: ESR rose from 36.57 mm/h to 40.72 mm/h, CRP from 624.18 mg/dl to 208.89 mg/dl, LDH from 447.74 U/l to 550.98 U/l, and ferritin from 787.21 ng/ml to 1029.00 ng/ml–values that were directly proportional to the severity of the patients' condition. Based on these results, we cannot accurately specify the etiology and mechanisms underlying AKI in COVID-19 patients, but it is clear that once AKI develops, the disease progression is fulminant.

Conclusions

1. Acute kidney injury is a frequent and severe complication among mechanically ventilated intensive care unit patients with COVID-19, often associated with rapid deterioration and high mortality.
2. This study highlights the significant contribution of comorbidities and nephrotoxic drugs to AKI development in this population.
3. Our findings underscore the need for increased vigilance and early monitoring of the renal status to improve outcomes in critically ill COVID-19 patients.

Competing interests

None declared.

Authors' contributions

All authors participated in the design of the study and had significant contributions to the drafting of the manuscript. All authors reviewed the work critically and approved the final version of the manuscript.

Informed consent for publication

Obtained.

Acknowledgements and funding

No external funding.

Ethics approval

The study was approved by the Ethics Committee of the *Timofei Moșneaga* Republican Clinical Hospital (Minutes No. 11, from 29.07.2025)

Provenance and peer review

Not commissioned, externally peer-reviewed.

References

1. Ahmadian E, Hosseiniyan Khatibi SM, Razi Soofiyani S, Abediazar S, Shoja MM, Ardalan M, et al. COVID-19 and kidney injury: pathophysiology and molecular mechanisms. Rev Med Virol. 2021;31(3):e2176. doi: 10.1002/rmv.2176.
2. Cheng Y, Luo R, Wang K, Zhang M, Wang Z, Dong L, et al. Kidney disease is associated with in-hospital death of patients with COVID-19. Kidney Int. 2020;97(5):829-38. https://doi.org/10.1016/j.kint.2020.03.005.
3. Sabaghian T, Kharazmi AB, Ansari A, Omidi F, Kazemi SN, Hajikhani B, et al. COVID-19 and acute kidney injury: a systematic review. Front Med (Lausanne). 2022;9:705908. doi: 10.3389/fmed.2022.705908.
4. Izzedine H, Jhaveri KD. Acute kidney injury in patients with COVID-19: an update on the pathophysiology. Nephrol Dial Transplant. 2021;36(2):224-6. doi: 10.1093/ndt/gfaa184.
5. Legrand M, Bell S, Forni L, Joannidis M, Koyner JL, Liu K, et al. Pathophysiology of COVID-19-associated acute kidney injury. Nat Rev Nephrol. 2021;17(11):751-764. doi: 10.1038/s41581-021-00452-0.
6. Fu EL, Janse RJ, De Jong Y, Van Der Endt VHW, Milders J, Van Der Willik EM, et al. Acute kidney injury and kidney replacement therapy in COVID-19: a systematic review and meta-analysis. Clin Kidney J. 2020 Sep 2;13(4):550-563. doi: 10.1093/ckj/sfaa160.
7. Raina R, Mahajan ZA, Vasistha P, Chakraborty R, Mukunda K, Tibrewal A, et al. Incidence and outcomes of acute idney injury in COVID-19: a systematic review. Blood Purif. 2022;51(3):199-212. doi: 10.1159/000514940.
8. Kaushal K, Kaur H, Sarma P, Bhattacharyya A, Sharma DJ, Prajapat M, et al. Serum ferritin as a predictive biomarker in COVID-19. A systematic review, meta-analysis and meta-regression analysis. J Crit Care. 2022;67:172-81. doi: 10.1016/j.jcrc.2021.09.023.
9. Hu B, Guo H, Zhou P, Shi ZL. Characteristics of SARS-CoV-2 and COVID-19. Nat Rev Microbiol. 2021;19(3):141-154. doi: 10.1038/s41579-020-00459-7.
10. Jager KJ, Kramer A, Chesnaye NC, Couchoud C, Sánchez-Álvarez JE, Garneata L, et al. Results from the ERA-EDTA Registry indicate a high mortality due to COVID-19 in dialysis patients and kidney transplant recipients across Europe. Kidney Int. 2020;98(6):1540-8 doi: 10.1016/j.kint.2020.09.006.
11. Mauthe M, Orhon I, Rocchi C, Zhou X, Luhr M, Hijlkema KJ, et al. Chloroquine inhibits autophagic flux by decreasing autophagosome-lysosome fusion. Autophagy. 2018;14(8):1435-55. doi: 10.1080/15548627.2018.1474314.
12. Gérard AO, Laurain A, Fresse A, Parassol N, Muzzone M, Rocher F, et al. Remdesivir and acute renal failure: a potential safety signal from disproportionality analysis of the WHO safety database. Clin Pharmacol Ther. 2021;109(4):1021-1024. doi: 10.1002/cpt.2145.
13. Lemee N, Chamley P, Francois A, Guincestre T, Duval M, Promerat A, et al. MO116: Vitamin C nephrotoxicity in a COVID-19 patient: a case report. Nephrol Dial Transplant. 2022;37(Suppl 3):i168. https://doi.org/10.1093/ndt/gfac066.019.
14. Liao ZM, Zhang ZM, Liu Q. Hydroxychloroquine/chloroquine and the risk of acute kidney injury in COVID-19 patients: a systematic review and meta-analysis. Ren Fail. 2022;44(1):415-25. doi: 10.1080/0886022X.2022.2046609.
15. Chong WH, Saha BK. Relationship between severe acute respiratory syndrome coronavirus 2 (SARS-CoV-2) and the etiology of acute idney injury (AKI). Am J Med Sci. 2021;361(3):287-96. doi: 10.1016/j.amjms.2020.10.025.
16. Li Z, Wu M, Yao J, Guo J, Liao X, Song S, et al. Caution on kidney dysfunctions of COVID-19 patients. medRxiv. 2020;2020.02.08.20021212. doi: 10.1101/2020.02.08.20021212.

https://doi.org/10.52645/MJHS.2025.3.13

UDC: 616.74-007.23+ 616.12-008.46

RESEARCH ARTICLE

Sarcopenia and frailty: risk profiles in patients with chronic heart failure

Anastasia Ivanes[1*], Lucia Mazur-Nicorici[1], Virginia Şalaru[2], Livi Grib[1], Snejana Vetrilă[1]

[1]Discipline of Cardiology, Department of Internal Medicine, *Nicolae Testemițanu* State University of Medicine and Pharmacy, Chisinau, Republic of Moldova
[2]Department of Family Medicine, *Nicolae Testemițanu* State University of Medicine and Pharmacy, Chisinau, Republic of Moldova

ABSTRACT

Introduction. Patients with heart failure frequently present with varying degrees of skeletal muscle dysfunction, from early fatigue to sarcopenia and cachexia. Sarcopenia, defined as the loss of muscle mass and/or function, contributes to the physical dimension of frailty. Both conditions are associated with adverse outcomes in heart failure. Although sarcopenia and frailty often coexist, they are distinct syndromes with a bidirectional relationship with heart failure. According to European data, the prevalence of sarcopenia ranges from 20-50% in heart failure with reduced ejection fraction and approximately 18% in heart failure with preserved ejection fraction. This study aimed to evaluate sarcopenia among frail patients with chronic heart failure and to identify associated risk and protective factors.

Material and methods. A cross-sectional observational study was conducted on 44 frail patients with chronic heart failure. Data collection included clinical, functional, and anthropometric parameters, using the SARC-Calf questionnaire, gait speed and the Timed Up and Go test. Patients were stratified into three study groups according to frailty severity assessed by the Edmonton Frail Scale: Study Group 1 – mild frailty, Study Group 2 – moderate frailty, and Study Group 3 – severe frailty. Statistical analysis included Chi-square and Fisher's exact tests. Odds Ratios with 95% Confidence Intervals were calculated. A $p < 0.05$ was considered statistically significant.

Results. Of the 44 patients included, 32 (72.7%) were women and 12 (27.3%) men, with a mean age of 67.3 ± 8.9 years. Sarcopenia risk (SARC-Calf ≥4) was identified in 56.8%, and severe sarcopenia in 15.9%, exclusively among women. Functional impairment was present in 88.9% of Study Group 1, 91.7% of Group 2, and 100% of Group 3. Arterial hypertension (71.4%), diabetes mellitus (57.1%), and obesity (42.8%) were more prevalent among sarcopenic patients. C-reactive protein levels >6 mg/L and elevated NT-proBNP were associated with sarcopenia risk ($p = 0.039$). Metformin use was linked to absence of sarcopenia ($p = 0.008$), while low physical activity, statin use, and inflammation were more frequent in sarcopenic patients.

Conclusions. Sarcopenia was highly prevalent in frail heart failure patients, particularly among women. Cardiac dysfunction, inflammation, and metabolic comorbidities are key contributors, highlighting the need for early screening and tailored interventions.

Keywords: heart failure, frailty, sarcopenia, SARC-Calf questionnaire.

Cite this article: Ivanes A, Mazur-Nicorici L, Şalaru V, Grib L, Vetrilă S. Sarcopenia and frailty: risk profiles in patients with chronic heart failure. Mold J Health Sci. 2025;12(3):80-85. https://doi.org/10.52645/MJHS.2025.3.13.

Manuscript received: 23.07.2025

Accepted for publication: 26.08.2025

Published: 15.09.2025

[*]**Corresponding author**: **Anastasia Ivanes**, PhD student
Discipline of Cardiology, Department of Internal Medicine
Nicolae Testemițanu State University of Medicine and Pharmacy, Chisinau, Republic of Moldova
165, Ștefan cel Mare și Sfânt blvd., Chisinau, Republic of Moldova, MD 2004
e-mail: anastasiabogaciova@gmail.com

Key messages

What is not yet known on the issue addressed in the submitted manuscript

Although the interaction between frailty and sarcopenia in heart failure is recognized, there is a lack of data about their interaction in Eastern European populations and on the influence of sociodemographic and therapeutic variables on both the risk and severity of sarcopenia.

Authors' ORCID IDs
Anastasia Ivanes – https://orcid.org/0009-0008-5964-9003
Lucia Mazur-Nicorici – https://orcid.org/0000-0003-3983-8292
Virginia Șalaru – https://orcid.org/0000-0003-2683-6917
Livi Grib – https://orcid.org/0000-0001-6913-0864
Snejana Vetrilă – https://orcid.org/0000-0003-0834-8901

The research hypothesis

In chronic heart failure, sarcopenia risk and severity are influenced by frailty burden, inflammatory markers and specific therapeutic strategies.

The novelty added by manuscript to the already published scientific literature

The present research enhances understanding of the sarcopenia burden in frail heart failure patients from Moldova, underlining clinical and demographic factors that may facilitate or mitigate its progression.

Introduction

The coexistence of frailty and cardiovascular diseases is recognized, yet remains an emerging concept in cardiology, with reported prevalence ranging from 19% to 76%. In the context of chronic heart failure (CHF), the prevalence of sarcopenia ranges from 11-12% in stable conditions to up to 65% among inpatients. In frail patients with heart failure, the presence of sarcopenia significantly influences clinical decision-making, especially regarding the selection and timing of diagnostic and therapeutic approaches. On the other hand, frailty and sarcopenia are major syndromes with a significant impact on the course of CHF, due to the reduction of physiological reserves and a diminished ability to adapt to both endogenous and exogenous stressors. In CHF, these conditions frequently coexist, amplifying the risk of decompensation, hospitalization and mortality [1, 2].

Although introduced by Rosenberg in 1989 to define age-related muscle mass and strength decline, sarcopenia was only officially classified as a disease by the World Health Organization in 2016. It is defined as the age-related loss of muscle mass and function and is associated with frequent falls, osteoporosis and increased mortality. The prevalence of sarcopenia among individuals over 65 years old ranges between 6% and 22%, escalating with age [3].

Several international expert groups such as the International Working Group on Sarcopenia, the Asian Working Group for Sarcopenia (AWGS), and the European Working Group on Sarcopenia in Older People (EWGSOP2) have attempted to create a standardized definition and diagnostic system. A stepwise assessment approach *F-A-C-S (Find, Assess, Confirm, Severity)* is commonly recommended, beginning with screening questionnaires, followed by evaluation of muscle strength and concluding with severity evaluation based on physical performance and muscle mass. Despite these efforts, a universally accepted definition and diagnostic tool remain lacking [4].

Various tools are available for sarcopenia assessment, including the SARC-F questionnaire, its extended SARC-Calf version (incorporating calf circumference), handgrip strength, chair stand test, gait speed, the Short Physical Performance Battery (SPPB), the Timed Up and Go (TUG) test, and the 6-minute walk test. Recommended imaging modalities include dual-energy X-ray absorptiometry (DXA), bioelectrical impedance analysis (BIA), computed tomography (CT), and magnetic resonance imaging (MRI). Where advanced technologies are unavailable, anthropometric assessments serve as a validated and practical alternative. International guidelines endorse these methods, while highlighting the importance of adapting them to specific population contexts [5-7].

Considering that sarcopenia is a recognized component of physical frailty that impairs functionality and often remains underdiagnosed, we conducted a study focused on assessing sarcopenia in frail patients with chronic heart failure.

This study aimed to assess sarcopenia in patients with chronic heart failure (CHF) and frailty syndrome, focusing on the identification of both risk and protective factors to support early diagnosis and inform personalized clinical management.

Material and methods

An observational, cross-sectional study was conducted on 44 frail patients hospitalized for decompensated chronic heart failure between January and June 2025 at the Institute of Cardiology. Inclusion criteria comprised a confirmed diagnosis of CHF, frailty identified using the 11-item Edmonton Frail Scale and signed informed consent (approval № 48, issued on 23 May 2024). Exclusion criteria included acute exacerbations of comorbidities, conditions interfering with anthropometric evaluation (e.g., pressure ulcers, significant edema, recent thrombosis, or lower limb deformities) and cognitive impairment precluding reliable assessment.

Data were collected using a structured questionnaire encompassing demographic characteristics (including marital status: single, married, divorced, widowed), anthropometric measurements, cardiovascular risk factors, comorbidities, laboratory parameters (serum glucose, lipid profile, NT-proBNP, creatine kinase – CK, and C-reactive protein – CRP), as well as instrumental findings such as a resting electrocardiogram (ECG).

Comorbidities were evaluated using the Charlson Comorbidity Index, which stratifies patients as follows: 0 points (no comorbidities), 1-2 points (low), 3-4 points (moderate), and ≥5 points (high comorbidity burden). Sarcopenia assessment was conducted in accordance with EWGSOP2 recommendations, applying the F-A-C-S algo-

rithm (Find-Assess-Confirm-Severity). Initial screening involved the SARC-Calf questionnaire, and patients scoring ≥4 underwent further evaluation, including muscle strength via the chair stand test, muscle mass by calf circumference (CC), and physical performance through the Timed Up and Go (TUG) test and gait speed. Calf circumference was the primary indicator of muscle mass, with thresholds of <34 cm for men and <33 cm for women indicating low muscle mass. Measurements were taken with the patient seated, knee flexed at 90°, and the muscle relaxed at the widest point of the calf. Each measurement was performed twice, with the highest value recorded.

Patients were categorized into three groups: Study Group 1 (G1) – mild frailty, Study Group 2 (G2) – moderate frailty, and Study Group 3 (G3) – severe frailty. Comparative and correlational analyses were conducted across groups, evaluating sociodemographic, clinical, biological, and instrumental variables, alongside risk factors, comorbidities, and treatment regimens. Logistic regression models were used to analyse the associations between clinical data, functional and laboratory parameters, and the presence of sarcopenia in frail CHF patients. Odds Ratios (OR) and 95% Confidence Intervals (CI) were reported, and a $p < 0.05$ was considered statistically significant. Data analysis was performed using SPSS software.

Results

The study included 44 patients with a mean age of 67.3 ± 8.9 years (range: 43-82 years), of whom 32 (72.7%) were female and 12 (27.3%) were male. Marital status distribution included 25 (56.8%) married individuals, 14 (31.8%) widowed, 3 (6.8%) divorced, and 2 (4.5%) single. Regarding social status, most participants were retired (61.4%), followed by those with varying degrees of disability (20.5%), employed individuals (15.9%), and a single unemployed patient (2.3%). Regarding heart failure etiology, ischemic heart disease was identified in 70.5% of patients, while 29.5% had a non-ischemic origin, primarily of valvular etiology (accounting for 69.2% of non-ischemic cases). Heart failure phenotypes were predominantly represented by patients with reduced ejection fraction (HFrEF, 45.5%), followed by those with preserved ejection fraction (HFpEF, 40.9%) and mildly reduced ejection fraction (HFmrEF, 13.6%). Using the SARC-Calf questionnaire, 25 (56.8%) patients were identified as being at increased risk of sarcopenia (OR = 4.11; 95% CI: 0.62-27.10; $p = 0.048$), and 7 (15.9%) were diagnosed with severe sarcopenia based on the EWGSOP2 algorithm. Comorbidities were assessed using the Charlson Comorbidity Index, which showed a mean score of 4.8 (range 1-9), indicating a high burden of associated chronic conditions.

Patients were stratified into three groups based on frailty severity, assessed by the Edmonton Frail Scale: Study Group 1 (G1) – mild frailty (8-9 points), included 27 (61.4%) patients; Study Group 2 (G2) – moderate frailty (10-11 points), included 12 (27.3%) patients; and Study Group 3 (G3) - severe frailty (12-17 points), included 5 (11.7%) patients.

A progressive increase in age was noted across frailty categories, with mean ages of 66.2 ± 8.7 years in G1, 68.0 ± 10.4 years in G2, and 71.6 ± 6.7 years in G3, indicating a positive correlation between advancing age and frailty severity. Female patients predominated in all groups, accounting for 40.9% in G1, 22.7% in G2, and 9.1% in G3, while male representation declined with increasing frailty. Social dependency also showed a proportional rise with frailty. In G1, 13.6% of patients were employed, 2.3% unemployed, 31.8% retired, and 13.6% reported disability. In G2, only 2.3% remained employed, while 20.5% were retired and 4.5% disabled. All G3 patients were either retired (9.1%) or disabled (2.3%). Marital status distribution revealed a predominance of married individuals in the mild frailty group (38.6%), whereas widowed individuals were more common in the moderate (15.9%) and severe (4.5%) frailty groups, suggesting a possible association between living alone and increased frailty.

The baseline patient characteristics are summarized in Table 1.

Cardiovascular risk factors were analyzed across the study groups. Physical activity of at least 30 minutes per day was reported by 62.9% of patients in G1, 25.0% in G2, and 20.0% in G3, suggesting a significant association between hypodynamia and frailty (adjusted OR = 2.52; 95% CI: 1.07-5.95; $p = 0.016$). Dyslipidemia was diagnosed in 44.4% of G1 patients, 16.7% of G2, and none in G3, supporting a potential inverse association between dyslipidemia and advanced frailty stages (adjusted OR = 0.34; 95% CI: 0.09-1.28; $p = 0.019$). Diabetes mellitus was most prevalent in G3 (40.0%), followed by G2 (33.3%) and G1 (18.5%). Obesity was distributed across all groups, with the highest frequency in G3 (80.0%), then G2 (66.7%) and G1 (55.5%). Sleep deprivation (≤5 hours/night) was reported in 40.7% of G1, 66.7% of G2, and 80.0% of G3 patients ($p = 0.022$). High comorbidity burden (Charlson Index ≥5) was noted in 63.0% of G1, 83.3% of G2, and 60.0% of G3 patients. Hospitalization frequency increased with frailty severity: ≥1 hospitalization/year was recorded in 41.1% of G1, 66.7% of G2, and 80.0% of G3.

NT-proBNP elevation was found in 85.1% of G1, 83.3% of G2, and 80.0% of G3. Low creatine kinase (CK) levels were noted in 85.2% of G1, 91.6% of G2, and 80.0% of G3. Elevated CRP was observed in G3 (60.0%), G2 (50.0%), and G1 (18.5%) ($p = 0.039$).

Atrial fibrillation was more common in G3 (80.0%), followed by G1 (55.5%) and G2 (50.0%). HFrEF was more frequent in G1 (48.1%), while HFpEF predominated in G2 (50.0%) and G3 (60.0%).

Metformin was used by 6.8% of G1, 9.1% of G2, and 6.8% of G3 patients ($p = 0.008$). Statin use was more common in G1 (69.0%) than in G2 (24.1%) or G3 (6.9%).

Sarcopenia risk (SARC-Calf ≥4) was identified in 48.1% of G1, 66.7% of G2, and 80.0% of G3. Severe sarcopenia occurred in 18.5% of G1 and 16.7% of G2 (OR = 4.11; $p = 0.048$), all in women. Mean age of sarcopenic patients was lower in G1 (65.4 ± 8.6 years) than in G2 (76.5 ± 2.1 years).

Table 1. Association of clinical parameters with sarcopenia risk and severe sarcopenia according to frailty severity.

Parameter	*OR* L1	Risc L2	*OR* L2	Risc L3	*OR* L3	Sarc L1	*OR* L1	Sarc L2	*OR* L2	Sarc L3	*OR* L3	***p***	Risc L1
QUALITATIVE													
1.Hypertension	13	0.39	8	1,7	4	3,4	5		2	0	0		
2. Obesity	8	1.6	6	3.0	3	2,6	4	8.0	2	0	0	0	0.44
3.Dislipidemia	5	0.6	2	0	0	0,4	3	0.75	0	0	0	0	
4. Diabetes mellitus	2	0.66	2	1.8	0	0.4	2	0	2	0	0	0	0.21
5. Smoking	12		8	0	4	3,8	0	0	0	0	0	0	0.71
6. Preserved physical activity	8	0.88	6	1.0	3		2	0.7	2	0	0	0	
7. Reduced muscle strength	14	0.3	9	1.0	4	2,8	-	-	-	-	-	-	0.12
8. Impaired physical performance	11	0.4	11	0	5	1,14	-	-	-	-	-	-	0.79
9. Sleep duration < 5 hours	3	0,22	4	0.33			4	0	2	0	0	0	
10. Charlson Index ≥5	10	0.8	5	0.33	4	6,4		0		0		0	0.17
11. Metformin use	0		3	1.8	3		5	0	2	0	0	0	0.008
12. Statine use	11	0.33	4	0	2		4	0	0	0	0	0	0.07
QUANTITATIVE													
1. Mean age ± SD (years)	65,2 ± 8,7		70,0 ± 10,4		72,75 ± 6,7		65,4 ± 8,6		76,5 ± 2,1		-		
2. CRP (> 6 mg/L)	2	0.45	4	1.0	2	3,67	2	0.5	2	0	0	0	0.03
3. NT-proBNP (≥300 pq/ml)	4	0.91	2	2.33	0		4	2.0	2	0	0	0	0.77
4.Reduced muscle mass	5	2,29	2	0	0		-		-		-		0.12

Note: ** L1 – mild frailty; L2 – moderate frailty; L3 – severe frailty; OR – odds ratio; p – statistical significance value (p < 0.05 considered significant); "Sarc" – severe sarcopenia according to EWGSOP2 criteria. Chi-square test was used and the Odds Ratio (OR) with 95% Confidence Intervals (CI) was calculated to evaluate risk factors*

Hypertension was present in 48.1% (G1), 66.7% (G2), and 80.0% (G3) of sarcopenic patients. Obesity and diabetes were also more common in advanced frailty. Dyslipidemia was found in G1 and G2, but was absent in G3. All sarcopenic patients were non-smokers.

Reduced muscle strength was recorded in 51.8% (G1), 75.0% (G2), and 80.0% (G3). Physical performance impairment was present in 88.9% (G1), 91.7% (G2), and 100% (G3). Reduced calf circumference was seen in G1 (29.6%) and G2 (16.7%).

Elevated CRP (>6 mg/L) was more frequent in G2 (33.3%) and G3 (40.0%) than in G1 (7.4%) (adjusted OR = 3.67; 95% CI: 0.5–26.81; p = 0.039). Increased NT-proBNP levels associated with sarcopenia risk were noted in G1 (14.8%) and G2 (16.7%).

Metformin appeared protective in G1 (no sarcopenia cases) versus G2 (25.0%) and G3 (60.0%) (adjusted OR = 102.0; 95% CI: 3.7-2810; p = 0.008). Statin therapy was associated with a higher risk of sarcopenia in G1 (40.7%), G2 (33.3%) and G3 (40.0%).

The comparative analysis of OR values for risk factors by frailty severity is presented in Fig. 1.

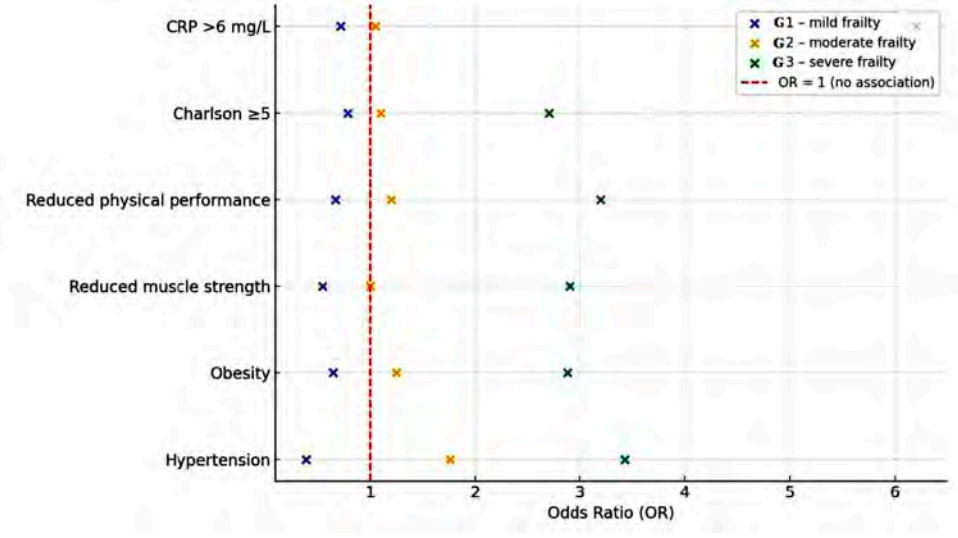

Fig. 1 Comparative analysis of Odds Ratio (OR) values for sarcopenia risk according to frailty severity: mild (G1), moderate (G2), severe (G3).

(Each point represents the effect value estimated for a specific parameter. The vertical red line marks the reference threshold (OR = 1), indicating no association. Parameters with OR values >1 suggest a positive association with sarcopenia risk, while subunitary ORs may indicate a protective role or inverse association).

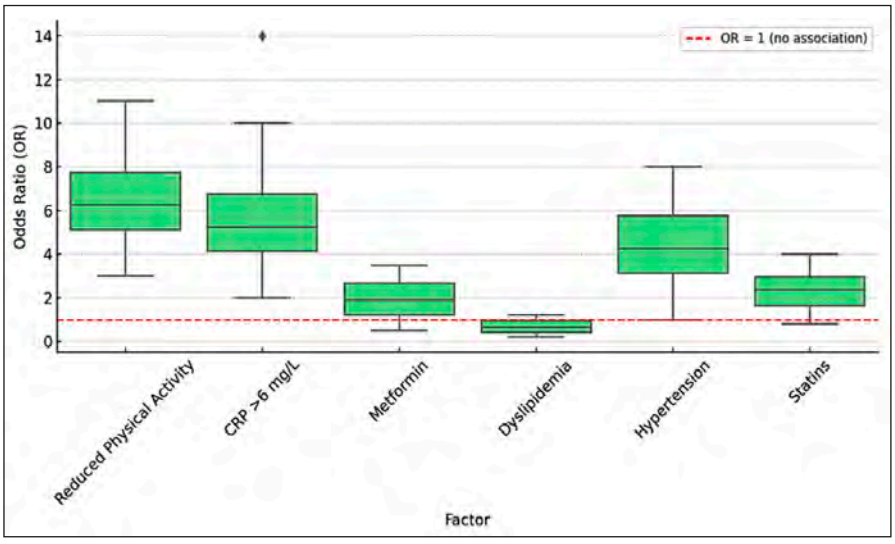

Fig. 2 Distribution of effect estimates for factors associated with severe sarcopenia

(Reduced physical activity and elevated CRP levels (>6 mg/L) exhibited median OR values above the reference threshold, supporting a positive association with sarcopenia. In contrast, dyslipidemia showed subunitary values, suggesting a potential inverse relationship).

Subsequently, the analysis focused on clinically confirmed sarcopenia, based on the three clinical and instrumental criteria recommended by EWGSOP2.

An association between arterial hypertension and confirmed sarcopenia was observed in G1 - 5 (18.5%) cases (OR = 1.70; 95% CI: 0.29-9.97), G2 - 2 (16.7%) (OR = 1.08; 95% CI: 0.18-6.49), and no cases in G3 (0%), which may indicate a potential role of hypertension in the development of sarcopenia among frail patients. Dyslipidemia was associated with sarcopenia exclusively in G1 – 1 (3.7%) case, representing an atypical finding, possibly influenced by underlying metabolic factors or lipid-lowering therapy. Diabetes mellitus was identified in four sarcopenic patients, with higher prevalence in G2 – 2 (16.7%) cases, compared to G1 – 2 (7.4%) cases. Physical activity analysis among sarcopenic patients revealed reduced activity in G1 – 2 (7.4%) and G2 – 2 (16.7%) cases, suggesting that functional decline may be an early clinical marker of sarcopenia (adjusted OR = 3.75; 95% CI: 0.45-30.91; p = 0.016).

Elevated C-reactive protein (CRP) levels were observed in G1 – 2 (7.4%) and G2 – 2 (16.7%) sarcopenic patients, with no cases recorded in G3, supporting the hypothesis of early systemic inflammation involvement in sarcopenia pathogenesis (adjusted OR = 2.75; 95% CI: 0.33-22.92; p = 0.039). Increased NT-proBNP levels were reported in G1 – 4 (14.8%) and G2 – 2 (16.7%) sarcopenic patients, but were absent in G3, reinforcing the link between cardiac dysfunction and muscle mass decline.

Metformin use was reported in 5 (18.5%) patients in G1 and 2 (16.7%) patients in G2, supporting a potential protective effect of this drug on skeletal muscle (adjusted OR = 1.35; 95% CI: 0.22-8.33; p = 0.008). Statin use among sarcopenic patients was documented in G1 – 4 (14.8%) cases, with no such cases in G2 or G3, suggesting a possible link between statin therapy and early muscular impairment.

The estimated distribution of effect sizes associated with severe sarcopenia, based on the conducted analysis, is illustrated in Fig. 2.

Discussion

The frailty syndrome represents an emerging paradigm in cardiology, increasingly recognized for its major clinical impact. Defined as a state of high vulnerability and diminished homeostatic reserves, frailty reflects not only biological aging but also multisystem dysfunction that affects patient autonomy. As opposed to chronological age, frailty has proven to be a more accurate predictor of severe complications, increased morbidity and mortality in chronic diseases. In patients with CHF, frailty plays a crucial role, influencing both prognosis and therapeutic decision-making. Literature data highlight the association between frailty and higher hospitalization rates, more frequent decompensations and increased mortality risk among CHF patients [8].

Sarcopenia, characterized by the loss of muscle mass and strength, is closely linked to frailty and contributes to the worsening functional status of patients with CHF. In our study, severe sarcopenia was identified in 15.9% of frail CHF patients, aligning with existing literature data where reported prevalence ranges between 10% and 34%, depending on the population, diagnostic criteria and assessment methods used. The exclusive presence of sarcopenia among women, predominantly in mild and moderate frailty stages, supports current data about a higher vulnerability of elderly women in the context of cardiovascular disease [9].

A significant association between sarcopenia and systemic inflammation markers, particularly C-reactive protein (CRP > 6 mg/L in 100% of cases, p = 0.039) was observed. This finding is consistent with multiple studies in which chronic inflammation was identified as a central mechanism in the pathogenesis of both sarcopenia and frailty in CHF patients, through impairment of muscle metabolism and mitochondrial dysfunction. Moreover, elevated NT-proBNP levels (≥300 pg/mL in 85.7% of sarcopenic cases) confirm the link between cardiac dysfunction severity and muscle wasting, as previously demonstrated in cohorts such as FRAGILE-HF [10-12].

The high prevalence of hypertension (71.4%), diabetes mellitus (57.1%) and obesity (42.8%) among patients with sarcopenia reflects current research findings on the interplay between metabolic syndrome components and muscle deterioration in CHF. A notable result of this study is the complete absence of sarcopenia among patients treated with metformin (p = 0.008), suggesting a potential protective effect. Similar findings have been reported in NHANES observational studies, in which metformin use was associated with increased muscle strength and reduced sarcopenia risk in diabetic patients, possibly due to indirect anti-inflammatory mechanisms [13]. Statin use was more frequent

among patients with sarcopenia (57.1%). Although this association did not reach statistical significance (p = 0.075), recent data suggest a possible link between lipid-lowering therapy and early muscle decline in frail individuals [14].

These results support the importance of early functional screening for sarcopenia in frail CHF patients. Simple tools such as the SARC-Calf questionnaire, the Timed Up and Go test (TUG), and calf circumference measurement may be effectively used in clinical practice to identify at-risk patients and enable early, targeted interventions, both pharmacological and functional, to reduce the risks of decompensation, disability, and mortality in this population.

Conclusions

More than half of frail patients with chronic heart failure are at risk of developing sarcopenia (56.8%), while severe sarcopenia was confirmed in 15.9%, predominantly among women with frailty syndrome. Elevated NT-proBNP and CRP levels in sarcopenic patients highlight the central role of cardiac dysfunction and systemic inflammation in the pathogenesis of sarcopenia. Early screening for sarcopenia, along with optimal management of hypertension, diabetes and obesity is essential for the prevention and clinical management of sarcopenia in frail women with chronic heart failure.

Competing interests

None declared.

Authors' contributions

AI conceived the study, performed data collection and analysis. LMN contributed to critical manuscript revision. VS provided methodological support and assisted in interpretation of parameters. LG supervised data analysis and contributed to the clinical interpretation of findings. SV coordinated study design and data interpretation, drafted the manuscript and critically reviewed it for intellectual content. All authors read and approved the final version of the manuscript.

Ethics approval

The study protocol was approved by the Research Ethics Committee of the *Nicolae Testemițanu* State University of Medicine and Pharmacy (minutes no. 48, issued on 23 May 2024).

Patient consent

Obtained.

Acknowledgements and funding

No external funding.

Provenance and peer review

Not commissioned, externally peer reviewed.

References

1. Vetrilă S, Grib L, Ivanes A. The pattern of the frailty syndrome in chronic heart failure. Ro J Med Pract. 2023;18(2):59-65. doi: 10.37897/RJMP.2023.2.2.
2. Kitamura A, Seino S, Abe T, Nofuji Y, Yokoyama Y, Amano H, Nishi M, Taniguchi Y, Narita M, Fujiwara Y, Shinkai S. Sarcopenia: prevalence, associated factors, and the risk of mortality and disability in Japanese older adults. J Cachexia Sarcopenia Muscle. 2021 Feb;12(1):30-38. doi: 10.1002/jcsm.12651.
3. Liu Y, Su M, Lei Y, Tian J, Zhang L, Xu D. Sarcopenia predicts adverse prognosis in patients with heart failure: a systematic review and meta-analysis. Rev Cardiovasc Med. 2023;24(9):273. doi: 10.31083/j.rcm2409273.
4. Boshnjaku A, Krasniqi E. Diagnosing sarcopenia in clinical practice: international guidelines vs. population-specific cutoff criteria. Front Med (Lausanne). 2024;11:1405438. doi: 10.3389/fmed.2024.1405438.
5. Kim HJ, Kim JY, Kim SH. Performance of calf circumference in identifying sarcopenia in older patients with chronic low back pain: a retrospective cross-sectional study. BMC Geriatr. 2024;24(1):674. doi: 10.1186/s12877-024-05263-z.
6. Voulgaridou G, Tyrovolas S, Detopoulou P, Tsoumana D, Drakaki M, Apostolou T, et al. Diagnostic criteria and measurement techniques of sarcopenia: a critical evaluation of the up-to-date evidence. Nutrients. 2024;16(3):436. doi: 10.3390/nu16030436.
7. Kiss CM, Bertschi D, Beerli N, Berres M, Kressig RW, Fischer AM. Calf circumference as a surrogate indicator for detecting low muscle mass in hospitalized geriatric patients. Aging Clin Exp Res. 2024;36(1):25. doi: 10.1007/s40520-024-02694-x.
8. Denfeld QE, Winters-Stone K, Mudd JO, Gelow JM, Kurdi S, Lee CS. The prevalence of frailty in heart failure: A systematic review and meta-analysis. Int J Cardiol. 2017 Jun 1;236:283-289. doi: 10.1016/j.ijcard.2017.01.153.
9. Marzetti E, Calvani R, Tosato M, Cesari M, Di Bari M, Cherubini A, Collamati A, D'Angelo E, Pahor M, Bernabei R, Landi F; SPRINTT Consortium. Sarcopenia: an overview. Aging Clin Exp Res. 2017 Feb;29(1):11-17. doi: 10.1007/s40520-016-0704-5.
10. Pothier K, Gana W, Bailly N, Fougère B. Associations between frailty and inflammation, physical, and psycho-social health in older adults: a systematic review. Front Psychol. 2022;13:805501. doi: 10.3389/fpsyg.2022.805501.
11. Sato R, Vatic M, da Fonseca GWP, von Haehling S. Sarcopenia and frailty in heart failure: is there a biomarker signature? Curr Heart Fail Rep. 2022 Dec;19(6):400-411. doi: 10.1007/s11897-022-00575-w.
12. Matsue Y, Kamiya K, Saito H, Saito K, Ogasahara Y, Maekawa E, et al. Prevalence and prognostic impact of the coexistence of multiple frailty domains in elderly patients with heart failure: the FRAGILE-HF cohort study. Eur J Heart Fail. 2020;22(11):2112-2119. doi: 10.1002/ejhf.1926.
13. Hu Y, Lu S, Xue C Hu Z, Wang Y, Zhang W, et al. Exploring the protective effect of metformin against sarcopenia: insights from cohort studies and genetics. J Transl Med. 2025;23(1):356. https://doi.org/10.1186/s12967-025-06357-x.
14. Huang ST, Otsuka R, Nishita Y, Meng LC, Hsiao FY, Shimokata H, et al. Risk of sarcopenia following long-term statin use in community-dwelling middle-aged and older adults in Japan. J Cachexia Sarcopenia Muscle. 2025;16(1):e13660. doi: 10.1002/jcsm.13660.

https://doi.org/10.52645/MJHS.2025.3.14

UDC: 616-056.52-008.9-055.2

RESEARCH ARTICLE

Osteocalcin and metabolic dysfunction in young women with obesity

Carolina Piterschi[1,2]*, Lorina Vudu[1,2]

[1]Department of Endocrinology, *Nicolae Testemițanu* State University of Medicine and Pharmacy, Republic of Moldova
[2]Laboratory of Endocrinology, *Nicolae Testemițanu* State University of Medicine and Pharmacy, Republic of Moldova

ABSTRACT

Introduction. Osteocalcin, a bone-derived hormone, has emerged as a potential regulator of energy metabolism, with roles in insulin sensitivity, glucose homeostasis, and lipid metabolism. Although an inverse association between osteocalcin and body mass index has been previously reported, data on its link with metabolic parameters in young, otherwise healthy women with obesity remain limited. The objective of this study was to investigate the relationship between circulating osteocalcin levels and key metabolic parameters in this specific population.

Material and methods. A cross-sectional observational study was conducted among 85 Caucasian women aged 18-45 years, without chronic disease or medication use. Participants were classified into two groups: normal weight (BMI 18.5-24.9 kg/m^2, n = 47) and with obesity (BMI ≥ 30 kg/m^2, n = 38). Anthropometric, hemodynamic, and biochemical parameters, including glucose, insulin, lipid profile, osteocalcin, and adiponectin, were assessed. Insulin resistance was evaluated using HOMA-IR and QUICKI. Group comparisons and Pearson correlation analyses were performed.

Results. Osteocalcin levels were significantly lower in the group of women with obesity compared to the normal weight group (12.99 ± 4.7 vs. 19.75 ± 4.09 ng/mL, $p < 0.001$). It was inversely correlated with BMI ($r = -0.56$), waist-to-hip ratio, waist-to-height ratio, insulin, HOMA-IR, total and LDL cholesterol, and positively associated with QUICKI ($r = 0.39$) and adiponectin ($r = 0.31$) (all $p < 0.001$). A progressive decline in osteocalcin levels was observed across obesity grades.

Conclusions. Circulating osteocalcin is inversely associated with adiposity and metabolic dysfunction, suggesting its potential as an early biomarker of cardiometabolic risk in young women with obesity.

Keywords: osteocalcin, obesity, insulin resistance, cardiometabolic risk in young women.

Cite this article: Piterschi C, Vudu L. Osteocalcin and metabolic dysfunction in young women with obesity. Mold J Health Sci. 2025;12(3):86-91. https://doi.org/10.52645/MJHS.2025.3.14.

Manuscript received: 24.07.2025

Accepted for publication: 26.08.2025

Published: 15.09.2025

***Corresponding author**: **Carolina Piterschi**, MD, PhD fellow, Department of Endocrinology
Nicolae Testemițanu State University of Medicine and Pharmacy
29 Nicolae Testemițanu str., Chisinau, Republic of Moldova MD2025
e-mail: carolina.piterschi@usmf.md

Authors's ORCID IDs
Carolina Piterschi – https://orcid.org/0009-0002-5459-1013
Lorina Vudu – https://orcid.org/0000-0002-7481-3843

Key messages

What is not yet known on the issue addressed in the submitted manuscript

Although osteocalcin has been implicated in metabolic regulation, its relationship with adiposity and cardiometabolic markers remains poorly characterized in young, metabolically active individuals without comorbidities. Most existing studies focus on older adults or patients with established metabolic disease, leaving a gap in understanding the early role of osteocalcin in obesity-related dysfunction during the reproductive years.

The research hypothesis

Osteocalcin, a bone-derived hormone traditionally associated with skeletal functions, is increasingly recognized for its role in systemic metabolic regulation. This study explores its potential as an early biomarker of cardiometabolic risk in young, otherwise healthy women.

The novelty added by manuscript to the already published scientific literature

This study offers novel insights into the interaction between bone metabolism and metabolic function in healthy young women, underscoring osteocalcin's potential as a biomarker for early cardiometabolic risk stratification in obesity.

Introduction

Obesity is a growing global health challenge, affecting millions of individuals worldwide [1, 2]. It results from a chronic imbalance between energy intake and expenditure, leading to excessive accumulation of adipose tissue [3]. Adipose tissue is now recognized as a metabolically active endocrine organ due to its ability to secrete a wide array of bioactive molecules with cytokine-like properties, collectively known as adipokines [4, 5]. Beyond their role in inflammation, these adipokines are involved in the regulation of appetite, body weight, insulin sensitivity, immune function, and the reproductive axis. Moreover, they play a pivotal role in the intricate control of bone function [6, 7]. Recent research has highlighted a bidirectional crosstalk between bone and energy homeostasis, pointing to osteocalcin, a bone-specific hormone, as a key player in this process. Produced by osteoblasts, osteocalcin is secreted into the peripheral circulation and promotes glucose uptake, participates in insulin signal transduction, and thus regulates energy metabolism in the whole body [8-10].

Several studies have examined the interplay between serum osteocalcin and body mass index (BMI), consistently reporting an inverse association [9, 11-14]. However, there is limited evidence regarding how circulating osteocalcin correlates with metabolic dysfunction and adiposity-related factors, particularly in young individuals with obesity. Given osteocalcin's role in regulating glucose homeostasis, lipid metabolism, and insulin sensitivity, further investigation in this population may offer valuable insights into the early identification of biomarkers for cardiometabolic risk. Therefore, the aim of this study was to investigate the relationship between circulating osteocalcin levels and key metabolic parameters in young women living with obesity.

Material and methods

A cross-sectional observational study was conducted to explore the relationship between circulating osteocalcin levels and metabolic parameters in a sample of young women living with obesity. This study was carried out at the Department and Laboratory of Endocrinology, *Nicolae Testemițanu* State University of Medicine and Pharmacy, in the Republic of Moldova. Written informed consent was secured from all participants before enrolling in the study. Ethical approval was obtained from the Research Ethics Committee of *Nicolae Testemițanu* State University of Medicine and Pharmacy (minutes No.4, dated November 4, 2016).

A total of 85 young women, aged 18-45 years, with no history of illness or use of medication, were included in the study. The exclusion criteria were as follows: age under 18 or over 45 years, underweight women (BMI ≤ 18,5 kg/m^2), overweight women (BMI 25-29.9 kg/m^2), obesity secondary to other diseases, presence of comorbidities, menopause (natural, induced, or primary ovarian insufficiency), pregnancy or breastfeeding, individuals who refused to participate in the clinical study.

Anthropometric measurements, blood pressure and metabolic parameters were assessed for each participant using standardized procedures and calibrated equipment. BMI was calculated as weight in kilograms divided by the square of height in meters (kg/m^2) [2]. Waist circumference (WC) was measured at the umbilicus using a measuring tape [2]. Hip circumference (HC) was measured around the most prominent area of the buttocks [15]. The waist-to-hip ratio (WHR) and waist-to-height ratio (WHtR) were calculated, based on standard measurement protocols.

Blood pressure was measured with participants seated comfortably after a 5-minute rest, using a calibrated sphygmomanometer.

For laboratory evaluations, venous blood samples were collected in the morning following a 10-hour overnight fast. Serum concentrations of osteocalcin, adiponectin, glucose, insulin, total cholesterol, low-density lipoprotein cholesterol (LDL-cholesterol), and high-density lipoprotein cholesterol (HDL-cholesterol) were measured using standard automated techniques. Insulin resistance was assessed using the Homeostasis Model Assessment of Insulin Resistance (HOMA-IR) and the Quantitative Insulin Sensitivity Check Index (QUICKI) [16, 17].

All statistical analyses were performed using the GNU PSPP (Version 2.0.1) software package. Continuous variables were presented as mean (standard deviation (SD)). Comparisons between the obesity group (BMI ≥ 30 kg/m^2) and the normal weight group (BMI 18.5-24.9 kg/m^2) were analyzed using ANOVA. Pearson correlation analysis was used to evaluate the linear relationship between osteocalcin levels and anthropometric, hemodynamic, and metabolic parameters. Statistical significance was set at $p < 0.05$ for all analyses.

Results

According to the eligibility criteria, 85 young Caucasian women (mean age 31.92 (6.72) years) were included in the study. Based on their BMI, participants were categorized into two study groups: L0 – 47 women with normal weight (BMI 18.5–24.9 kg/m^2), and L1 – 38 women with obesity (BMI ≥ 30 kg/m^2).

Table 1 summarizes the anthropometric, hemodynamic, and metabolic characteristics of the study population by BMI category. No significant difference was observed in age between the two groups ($p = 0.338$), indicating appropriate age matching.

Table 1. Clinical characteristics of the study population by BMI category (mean (SD)).

Variables	Total n = 85	BMI 18.5-24.9 kg/m^2, n = 47 (L0)	BMI ≥ 30 kg/m^2, n = 38 (L1)	*p*-value
Age	31.92 (6.72)	31.2 (6.22)	32.68 (7.24)	0,338
Weight, kg	80.04 (22.32)	61.63 (6.49)	99.43 (15.89)	< 0.001
BMI, kg/m^2	28.6 (7.5)	22.01 (1.85)	35.55 (4.30)	< 0.001
WHR, cm	0.86 (0.07)	0.82 (0.06)	0.92 (0.05)	< 0.001
WHtR, cm	0.56 (0.12)	0.46 (0.04)	0.67 (0.06)	< 0.001
SBP, mmHg	116.28 (10.27)	112.5 (10.31)	120.26 (8.85)	< 0.001
DBP, mmHg	72.5 (6.59)	69.88 (6.75)	75.26 (5.32)	< 0.001
Osteocalcin, ng/mL	16.46 (5.51)	19.75 (4.09)	12.99 (4.7)	< 0.001
Adiponectin, µg/mL	20.15 (15.5)	28.98 (15.28)	10.86 (9.48)	< 0.001
Fasting glucose, mmol/L	4.82 (0.63)	4.66 (0.54)	4.98 (0.69)	= 0.022
Insulin, µU/mL	10.18 (6.56)	6.47 (2.59)	14.07 (7.29)	< 0.001
HOMA-IR	2.23 (1.63)	1.33 (0.56)	3.17 (1.86)	< 0.001
QUICKI	0.35 (0.03)	0.37 (0.03)	0.33 (0.02)	< 0.001
Total cholesterol, mmol/L	5.28 (0.72)	5.01 (0.61)	5.56 (0.75)	< 0.001
LDL-cholesterol, mmol/L	2.55 (0.81)	1.95 (0.45)	3.18 (0.61)	< 0.001
HDL-cholesterol, mmol/L	1.74 (0.37)	1.89 (0.25)	1.57 (0.41)	< 0.001

Note: *Data are presented as mean (standard deviation, SD). BMI – body mass index; WHR – waist-to-hip ratio; WHtR – waist-to-height ratio; SBP – systolic blood pressure; DBP – diastolic blood pressure; HOMA-IR – homeostasis model assessment of insulin resistance; QUICKI – quantitative insulin sensitivity check index; LDL – low-density lipoprotein; HDL – high-density lipoprotein. The study population was divided into two groups according to BMI: normal weight (L0, 18.5–24.9 kg/m^2) and obesity (L1, ≥30 kg/m^2). Groups were compared using ANOVA procedure. A p-value <0.05 was considered statistically significant.*

As expected, women with obesity (L1, BMI ≥ 30 kg/m^2) had significantly higher mean body weight and BMI compared to the normal-weight group (L0, BMI 18.5-24.9 kg/m^2). Central adiposity markers, including waist-to-hip ratio (WHR) and waist-to-height ratio (WHtR), were also significantly elevated in the L1 group ($p < 0.001$), reflecting increased visceral fat accumulation.

Hemodynamic parameters differed significantly between groups. Both SBP and DBP were higher in the L1 group ($p < 0.001$), indicating a trend toward elevated cardiovascular risk in women with obesity.

Regarding biochemical parameters, serum levels of osteocalcin and adiponectin were significantly lower in the L1 group compared to L0 ($p < 0.001$ for both), suggesting hormonal dysregulation associated with increased adiposity.

Markers of glucose metabolism showed significant group differences. Women with obesity exhibited higher fasting glucose ($p = 0.022$), insulin ($p < 0.001$), and HOMA-IR values ($p < 0.001$), while QUICKI was significantly lower ($p < 0.001$), indicating decreased insulin sensitivity.

Lipid profile analysis revealed a more atherogenic pattern in the L1 group, with significantly higher total cholesterol and LDL cholesterol, and lower HDL cholesterol levels ($p < 0.001$ for all).

Table 2. Pearson correlation between serum osteocalcin, adiponectin and anthropometric, metabolic, and cardiovascular parameters in the total study population (n = 85)

Variables	Osteocalcin		Adiponectin	
	r	*p*-value	*r*	*p*-value
BMI, kg/m^2	-0.56	< 0.001	-0.48	< 0.001
WHR, cm	-0.54	< 0.001	-0.50	< 0.001
WHtR, cm	-0.57	< 0.001	-0.48	< 0.001
SBP, mmHg	-0.22	= 0.040	-0.24	= 0.007
DBP, mmHg	-0.29	= 0.007	-0.29	= 0.001
Osteocalcin, ng/mL	-	-	0.31	= 0.005
Adiponectin, µg/mL	0.31	= 0.005	-	-
Fasting glucose, mmol/L	-0.13	= 0.237	0.47	0.590
Insulin, µU/mL	-0.37	< 0.001	-0.45	< 0.001
HOMA-IR	-0.35	< 0.001	-0.41	< 0.001
QUICKI	0.39	< 0.001	0.48	< 0.001
Total cholesterol, mmol/L	-0.40	< 0.001	-0.30	< 0.001
LDL-cholesterol, mmol/L	-0.54	< 0.001	-0.48	< 0.001
HDL-cholesterol, mmol/L	0.21	0.054	0.31	< 0.001

Note: *Data are presented as Pearson correlation coefficients (r) with corresponding p-values. BMI – body mass index; WHR – waist-to-hip ratio; WHtR – waist-to-height ratio; SBP – systolic blood pressure; DBP – diastolic blood pressure; HOMA-IR – homeostasis model assessment of insulin resistance; QUICKI – quantitative insulin sensitivity check index; LDL – low-density lipoprotein; HDL – high-density lipoprotein. Correlations were assessed using the Pearson correlation test. A p-value <0.05 was considered statistically significant.*

These findings highlight the presence of significant metabolic, hormonal, and cardiovascular alterations in young women with obesity, supporting the hypothesis that increased adiposity is associated with dysregulation of both classic cardiometabolic markers and bone-derived hormones such as osteocalcin.

Table 2 presents Pearson correlation coefficients between serum osteocalcin and adiponectin levels and anthropometric, hemodynamic, and metabolic parameters.

Both osteocalcin and adiponectin showed strong negative correlations with indicators of adiposity, including BMI, WHR, and WHtR (all $p < 0.001$), indicating that lower concentrations of these hormones are associated with increased fat accumulation.

In terms of hemodynamic measures, both markers were inversely associated with SBP and DBP. The correlation was stronger for DBP (osteocalcin: $r = –0.29$, $p = 0.007$; adiponectin: $r = –0.29$, $p = 0.001$).

Regarding insulin resistance, both osteocalcin and adiponectin were negatively correlated with insulin and HOMA-IR ($p < 0.001$), and positively correlated with QUICKI ($p < 0.001$), suggesting their involvement in glucose homeostasis and insulin sensitivity.

For the lipid profile, both markers were negatively correlated with total cholesterol and LDL cholesterol, and positively associated with HDL cholesterol. The association with HDL cholesterol was statistically significant for adiponectin ($p < 0.001$) and borderline for osteocalcin ($p = 0.054$).

Additionally, a positive correlation was observed between osteocalcin and adiponectin themselves ($p = 0.005$), suggesting potential synergistic or complementary roles in metabolic regulation.

Further subgroup analysis of osteocalcin levels by obesity grade revealed a stepwise decline in concentrations with increasing adiposity (Fig. 1). The highest mean value was observed in the normal-weight group (20.10 ± 4.47 ng/mL). The lowest level occurred in women with grade I obesity (12.14 ± 4.84 ng/mL), while slightly higher values were recorded in those with grade II (14.24 ± 5.19 ng/mL) and grade III obesity (13.32 ± 2.97 ng/mL). These results further emphasize the inverse association between osteocalcin levels and the degree of adiposity.

Fig. 1 Mean osteocalcin levels by weight category

Note: *Mean osteocalcin concentrations (ng/mL) are presented for normal-weight women and for those with obesity grades I–III. Data are shown as mean values. Group comparisons were performed using one-way ANOVA procedure. A p-value <0.05 was considered statistically significant.*

Discussion

This study examined the association between circulating osteocalcin levels and key metabolic markers in young women with obesity. Findings revealed that osteocalcin concentrations were significantly lower in women with obesity compared to those with normal weight. Furthermore, osteocalcin showed strong inverse correlations with measures of adiposity (BMI, WHR, WHtR), insulin resistance (insulin, HOMA-IR), and lipid disturbances (total and LDL cholesterol), while being positively correlated with insulin sensitivity as measured by QUICKI. A moderate positive correlation between osteocalcin and adiponectin was also observed, indicating possible complementary or synergistic functions in metabolic regulation.

These findings align with previous studies reporting an inverse association between osteocalcin and BMI, and expand current knowledge by revealing robust associations with metabolic and cardiovascular risk markers. In a meta-analysis of 28 studies comprising 18,630 participants aged 36 to 75.3 years, Kord-Varkaneh et al. (2017) confirmed a significant inverse relationship between serum osteocalcin and BMI in adult populations [11]. Similarly, Riquelme-Gallego et al. (2020) conducted a recent population-based study that investigated the association between total osteocalcin levels and obesity, hypertension, and type 2 diabetes. Their findings demonstrated that osteocalcin was significantly and negatively associated with BMI, waist circumference, and HbA1c, and positively associated with HDL cholesterol and systolic blood pressure [18].

Notably, most prior research on osteocalcin has focused on older adults, postmenopausal women, or individuals with established comorbidities such as type 2 diabetes, cardiovascular disease, or osteoporosis [18-23]. In contrast, the present study addresses an important gap by evaluating these associations in a metabolically active population of young women without overt chronic illness, thereby providing early insights into the role of bone-derived hormones in cardiometabolic health.

A key observation was the progressive decline in osteocalcin concentrations across obesity grades, reinforcing the concept of a reciprocal interaction between bone and energy metabolism and suggesting that osteocalcin may serve as a valuable early biomarker of metabolic dysregulation.

The biological plausibility of these findings is supported by experimental evidence showing that osteocalcin enhances insulin secretion and sensitivity, promotes glucose uptake, and regulates lipid metabolism [8, 10]. The observed positive correlation with adiponectin, a key insulin-sensitizing adipokine, further supports the role of osteocalcin in modulating endocrine and metabolic pathways.

This study has several strengths, including its focus on a relatively homogeneous and young cohort without co-

morbid conditions, and the comprehensive assessment of metabolic and hormonal parameters. However, some limitations should be noted. The cross-sectional design limits the ability to draw causal inferences, and the sample size, while sufficient for correlation analysis, may limit broader generalizability.

Future research should explore longitudinal associations to better understand osteocalcin's dynamic role in metabolic regulation. Studies in larger, more diverse cohorts and interventional trials may help clarify the potential of osteocalcin as a predictive marker or therapeutic target in obesity-related metabolic dysfunction.

Conclusions

This study demonstrates that circulating osteocalcin levels are significantly reduced in young women with obesity and are strongly associated with key metabolic parameters, including indicators of adiposity, insulin resistance, and lipid abnormalities. The progressive decline in osteocalcin concentrations across obesity grades highlights its potential involvement in the early pathophysiology of metabolic dysfunction.

The observed inverse correlations with BMI, insulin, HOMA-IR, and LDL cholesterol, along with positive associations with insulin sensitivity (QUICKI) and adiponectin, suggest that osteocalcin may serve as a sensitive early biomarker of cardiometabolic risk in this population. These findings underscore the importance of a comprehensive and multifactorial approach to the assessment of individuals living with obesity to support earlier identification of at-risk individuals and more effective prevention of obesity-related complications.

Competing interests

None declared.

Authors' contributions

LV conceived the study and participated in study design and helped drafting the manuscript. CP participated in the study design, performed the statistical analysis, and drafted the manuscript. Both authors reviewed the work critically and approved the final version of the manuscript.

Patient consent

Obtained.

Ethics approval

The study was approved by the Research Ethics Committee of *Nicolae Testemiţanu* State University of Medicine and Pharmacy (minutes No. 4, dated 04.11.2016).

Acknowledgements and funding

No external funding.

Provenance and peer review

Not commissioned, externally peer-reviewed.

References

1. Abad-Jiménez Z, Vezza T. Obesity: a global health challenge demanding urgent action. Biomedicines 2025;13(2):502. https://doi.org/10.3390/biomedicines13020502.
2. World Health Organization. Obesity and overweight 2024 [Internet]. Geneva: WHO; c2025- [cited 2025 May 13]. Available from: https://www.who.int/news-room/fact-sheets/detail/obesity-and-overweight
3. Jin X, Qiu T, Li L, Yu R, Chen X, Li C, et al. Pathophysiology of obesity and its associated diseases. Acta Pharm Sin B. 2023;13(6):2403-24. https://doi.org/10.1016/j.apsb.2023.01.012.
4. Kershaw EE, Flier JS. Adipose tissue as an endocrine organ. J Clin Endocrinol Metab. 2004;89(6):2548-56. https://doi.org/10.1210/jc.2004-0395.
5. Romacho T, Elsen M, Röhrborn D, Eckel J. Adipose tissue and its role in organ crosstalk. Acta Physiol. 2014;210(4):733-53. https://doi.org/10.1111/apha.12246.
6. Clemente-Suárez VJ, Redondo-Flórez L, Beltrán-Velasco AI, Martín-Rodríguez A, Martínez-Guardado I, Navarro-Jiménez E, et al. The role of adipokines in health and disease. Biomedicines. 2023;11(5):1290. https://doi.org/10.3390/biomedicines11051290.
7. Hemat Jouy S, Mohan S, Scichilone G, Mostafa A, Mahmoud AM. Adipokines in the crosstalk between adipose tissues and other organs: implications in cardiometabolic diseases. Biomedicines. 2024;12(9):2129. https://doi.org/10.3390/biomedicines12092129.
8. Moser SC, van der Eerden BCJ. Osteocalcin – a versatile bone-derived hormone. Front Endocrinol (Lausanne). 2019;10:794. https://doi.org/10.3389/fendo.2018.00794.
9. Smith C, Lin X, Parker L, Yeap BB, Hayes A, Levinger I. The role of bone in energy metabolism: a focus on osteocalcin. Bone. 2024;188:117238. https://doi.org/10.1016/J.BONE.2024.117238.
10. Zhou R, Guo Q, Xiao Y, Guo Q, Huang Y, Li C, et al. Endocrine role of bone in the regulation of energy metabolism. Bone Res. 2021;9(1):25. https://doi.org/10.1038/s41413-021-00142-4.
11. Kord-Varkaneh H, Djafarian K, khorshidi M, Shab-Bidar S. Association between serum osteocalcin and body mass index: a systematic review and meta-analysis. Endocrine. 2017;58(1):24-32. https://doi.org/10.1007/s12020-017-1384-4.
12. Nowicki JK, Jakubowska-Pietkiewicz E. Osteocalcin: beyond bones. Endocrinol Metabol. 2024;39(3):399-406. https://doi.org/10.3803/EnM.2023.1895.
13. Kanazawa I. Osteocalcin as a hormone regulating glucose metabolism. World J Diabetes. 2015;6(18):1345-54. https://doi.org/10.4239/wjd.v6.i18.1345.
14. Guedes JAC, Esteves J V, Morais MR, Zorn TM, Furuya DT. Osteocalcin improves insulin resistance and inflammation in obese mice: Participation of white adipose tissue and bone. Bone. 2018;115:68-82. doi: 10.1016/j.bone.2017.11.020.
15. Physical status: the use and interpretation of anthropometry. Report of a WHO Expert Committee. World

Health Organ Tech Rep Ser. 1995;854:1-452.
16. Katz A, Nambi SS, Mather K, Baron AD, Follmann DA, Sullivan G, et al. Quantitative insulin sensitivity check index: a simple, accurate method for assessing insulin sensitivity in humans. J Clin Endocrinol Metab. 2000;85(7):2402-10. https://doi.org/10.1210/jcem.85.7.6661.
17. Matthews DR, Hosker JP, Rudenski AS, Naylor BA, Treacher DF, Turner RC. Homeostasis model assessment: insulin resistance and beta-cell function from fasting plasma glucose and insulin concentrations in man. Diabetologia. 1985;28(7):412-9. https://doi.org/10.1007/BF00280883.
18. Riquelme-Gallego B, García-Molina L, Cano-Ibáñez N, Sánchez-Delgado G, Andújar-Vera F, García-Fontana C, et al. Circulating undercarboxylated osteocalcin as estimator of cardiovascular and type 2 diabetes risk in metabolic syndrome patients. Sci Rep. 2020;10(1):1840. https://doi.org/10.1038/s41598-020-58760-7.
19. Pergola G, Triggiani V, Bartolomeo N, Nardecchia A, Giagulli V, Bruno I, et al. Independent relationship of osteocalcin circulating levels with obesity, type 2 diabetes, hypertension, and HDL cholesterol. Endocr Metab Immune Disord Drug Targets. 2017;16(4):270-5. https://doi.org/10.2174/1871530317666170106150756.
20. Sanchez-Enriquez S, Ballesteros-Gonzalez IT, Villafán-Bernal JR, Pascoe-Gonzalez S, Rivera-Leon EA, Bastidas-Ramirez BE, et al. Serum levels of undercarboxylated osteocalcin are related to cardiovascular risk factors in patients with type 2 diabetes mellitus and healthy subjects. World J Diabetes. 2017;8(1):11. https://doi.org/10.4239/wjd.v8.i1.11.
21. Viswanath A, Vidyasagar S, Amrutha Sukumar C. Osteocalcin and metabolic syndrome. Clin Med Insights Endocrinol Diabetes. 2023;16. https://doi.org/10.1177/11795514231206729.
22. Moon JS, Jin MH, Koh HM. Association between serum osteocalcin levels and metabolic syndrome according to the menopausal status of Korean women. J Korean Med Sci. 2021;36(8):e56. https://doi.org/10.3346/jkms.2021.36.e56.
23. Pattanayak N, Mishra A, Mohanty S, Mishra PK, Bara P. Association of osteocalcin with metabolic syndrome and its correlation with insulin resistance. J Clin Diagn Res. 2021;15(2):15-19. https://doi.org/10.7860/JCDR/2021/47063.14587.

https://doi.org/10.52645/MJHS.2025.3.15

UDC: 616.12-07:616.72-002.77-053.6

RESEARCH ARTICLE

Evaluation of cardiovascular risk factors in juvenile idiopathic arthritis

Livia Bogonovschi*, Angela Cracea, Ninel Revenco

Department of Pediatrics, *Nicolae Testemițanu* State University of Medicine and Pharmacy, Chisinau, Republic of Moldova

ABSTRACT

Introduction. Juvenile idiopathic arthritis is a persistent type of arthritis with no defined cause that develops before the age of 16 years and lasts for at least 6 weeks. The aim of the study was to evaluate cardiovascular risk factors (homocysteine, total cholesterol, and triglycerides) in juvenile idiopathic arthritis.

Material and methods. The study was carried out in the Rheumatology Department of the Mother and Child Institute, Chisinau, Republic of Moldova. The patients' parents signed the written consent to participate in the study. The study was approved by the Ethics Committee of the *Nicolae Testemițanu* State University of Medicine and Pharmacy. The study included 90 children with JIA. The number of painful and swollen joints, the global evaluation of the disease by both the physician and patient, as well as the Childhood Health Assessment Questionnaire, were determined. Paraclinical tests included a complete blood count, acute-phase markers of inflammation (erythrocyte sedimentation rate, C-reactive protein) and the cardiovascular risk factors of interest (homocysteine, total cholesterol, and triglycerides).

Results. Patients with JIA exhibit a relatively higher risk of hyperhomocysteinemia compared to controls. Additionally, individuals with JIA display a relatively moderate risk of hypercholesterolemia and a relatively lower risk of hypertriglyceridemia. Thus, a correlation was noted between JIA and hypercholesterolemia, with a slight inclination towards increased triglyceride levels in these children.

Conclusions. Patients with juvenile idiopathic arthritis are at risk for hyperhomocysteinemia, hypercholesterolemia, and hypertriglyceridemia.

Keywords: juvenile idiopathic arthritis, relative risk, homocysteine, total cholesterol, triglycerides.

Cite this article: Bogonovschi L, Cracea A, Revenco N. Evaluation of cardiovascular risk factors in juvenile idiopathic arthritis. Mold J Health Sci. 2025;12(3):92-100. https://doi.org/10.52645/MJHS.2025.3.15.

Manuscript received: 18.07.2025

Accepted for publication: 31.08.2025

Published: 15.09.2025

***Corresponding author**: **Livia Bogonovschi,** PhD
Nicolae Testemițanu State University of Medicine and Pharmacy,
Department of Pediatrics
93 Burebista Street, Chișinău, Republic of Moldova
E-mail: livia.bogonovschi@usmf.md

Authors' ORCID IDs
Livia Bogonovschi – https://orcid.org/0000-0001-9713-5566
Angela Cracea – https://orcid.org/0000-0002-5283-1178
Ninel Revenco – https://orcid.org/0000-0002-5229-7841

Key messages

What is not yet known on the issue addressed in the submitted manuscript

Although juvenile idiopathic arthritis is a chronic inflammatory disease, the associated cardiovascular risk – particularly related to factors such as homocysteine, total cholesterol, and triglycerides – is not yet fully understood in children with this condition.

The research hypothesis

Children with JIA have an increased risk of developing abnormalities in cardiovascular risk factors, such as hyperhomocysteinemia, hypercholesterolemia, and hypertriglyceridemia.

The novelty added by the manuscript to the already published scientific literature

The study highlights a clear association between JIA and increased risks of hyperhomocysteinemia and hypercholesterolemia in children, providing local and detailed data that contribute to a better understanding of cardiovascular risks in this pediatric population.

Introduction

Juvenile idiopathic arthritis (JIA), as defined by the International League of Associations for Rheumatology (ILAR) refers to a persistent type of arthritis with no defined cause, beginning before the age of 16 years and lasting for at least 6 weeks [1]. JIA is the most common rheumatic disease in children, and can significantly impair joint function, leading to joint deformities, growth failure and persistent active disease into adulthood. The disease is characterized by chronic synovial inflammation, cartilage damage, and bone erosion.

Chronic inflammatory diseases such as JIA pose a major risk of premature coronary heart disease. Dyslipidemia plays a crucial role in atherosclerosis, a condition that might be associated with autoimmune diseases. The risk of developing atherosclerosis increases gradually with rising levels of total cholesterol and triglycerides [2].

Cardiovascular risk factors undergo changes during periods of growth and development. Body mass index, systolic and diastolic blood pressure, and serum concentrations of total cholesterol and triglycerides were strongly associated with the extent of lesions in the aorta and coronary arteries [3].

Disturbances in the traditional lipid profile are considered to be associated with subclinical atherosclerosis [4]. Top of Form

Dyslipidemia, which is defined by an increase in total cholesterol and/or triglycerides, is one of the most well-known risk factors in children with JIA. Consequently, increased disease activity is associated with dyslipidemia in children with JIA [5, 6]. The impact of cholesterol on atherogenesis is well-documented, playing a central role in triggering the process [7].

Patients with JIA have an increased risk of developing changes in their lipid profile in comparison to those without arthritis. As a result, adults with a history of JIA during childhood have a 6-fold increased risk of developing subclinical atherosclerosis, ultimately leading to an increased risk of cardiovascular disease over time [2]. Hence, continuous monitoring of the lipid profile could potentially reduce morbidity and mortality among adult patients [8]. In patients with rheumatoid arthritis (RA), the prevalence of dyslipidemia varies between 55% and 65% [6, 9-12].

The pathogenesis of dyslipidemia and cardiovascular risk in patients with JIA has not been fully elucidated. Cholesterol plays a crucial role in triggering endothelial dysfunction by activating endothelial and muscle cells, as well as secreting inflammatory mediators such as proinflammatory cytokines [13-14].

Although hypercholesterolemia is significant in approximately 50% of patients with cardiovascular disease, it is crucial to consider other contributing factors as well [15]. Atherosclerosis is undoubtedly an inflammatory disease and does not solely result from lipid accumulation.

Homocysteine (Hcy) is a sulfur-containing amino acid derived from the essential amino acid methionine during its conversion to cysteine [16-18]. Its plasma concentration depends on various factors such as age, sex, lifestyle (including coffee consumption, smoking, physical activity, and alcohol consumption), genetic mutations that result in significantly reduced activity of the enzymes involved in homocysteine catabolism, medications, and diseases that interfere with its metabolism. The most significant factor influencing homocysteine levels is the intake of B vitamins [16-19]. For instance, decreased folate concentrations can lead to hyperhomocysteinemia, which is defined by plasma homocysteine concentrations ≥ 15 μM [20].

Hyperhomocysteinemia (HHcy) is a well-known cardiovascular risk factor both in the general population and in patients with inflammatory conditions [18, 21-23]. Considering the cardiovascular risk associated with RA and chronic systemic inflammation, it is essential to implement anti-inflammatory strategies, as well as interventions aimed at lowering homocysteine levels, in this patient population.

Throughout life, serum homocysteine levels gradually increase until puberty. Normal values of serum homocysteine in children and adolescents range from 5 to 15 μmol/L. During puberty, the serum level of homocysteine typically falls within the range of 6 to7 μmol/L; while in adulthood, it varies between 10 and 11 μmol/L. Hyperhomocysteinemia is defined as serum homocysteine levels exceeding 12-15 μmol/L, with the following grades distinguished: mild (15-30 μmol/L), moderate (30-100 μmol/L), and severe (> 100 μmol/L) [16, 24-25].

Mild hyperhomocysteinemia is often detected in healthy, asymptomatic individuals as well [21, 26].

Elevated serum homocysteine levels contribute to endothelial dysfunction and promote platelet aggregation. This initiates an inflammatory response that directly contributes to the development of atherosclerosis, establishing homocysteine as an independent risk factor in the initiation of atherosclerotic processes. Therefore, circulating homocysteine is considered a sensitive marker associated with inflammation and endothelial dysfunction[7, 21, 27-30].

Currently, there is a lack of data on the effectiveness of homocysteine-lowering strategies for cardiovascular disease (CVD) prevention in this population. However, almost all prospective studies have clearly demonstrated a reduction in morbidity and mortality attributed to methotrexate treatment, partially due to folic acid supplementation reducing methotrexate-induced HHcy [31].

It is worth mentioning that patients with RA have a 60% increased risk of death from myocardial infarction and stroke compared to the general population, along with a 48% increased risk of incident myocardial infarction [32]. Therefore, homocysteine-lowering strategies might be suitable for reducing CVD risk in RA populations.

Homocysteine (Hcy) plays a primary role in the onset of early endothelial dysfunction. It participates in the oxidation process of low-density lipoproteins, the proliferation of smooth muscle cells, and the activation of platelets. Elevated Hcy concentrations in both children and adults have direct and indirect toxic effects on the vascular endothelium, posing an additional risk factor for cardiovascular damage and early cerebrovascular accidents, especially when associated with other risk factors such as hypercholesterolemia [4].

Children with chronic rheumatic diseases exhibit an increased prevalence of accelerated atherosclerosis in adulthood. Therefore, it is crucial to identify childhood risk factors to prevent cardiovascular manifestations in adulthood [33].

The aim of the study was to evaluate certain cardiovascular risk factors (homocysteine, total cholesterol, and triglycerides) in juvenile idiopathic arthritis.

Material and methods

A prospective clinical study was conducted at the Rheumatology Department of the Mother and Child Institute, Chisinau, Republic of Moldova, between 2014 and 2019. The study aimed to evaluate cardiovascular risk factors in children diagnosed with juvenile idiopathic arthritis (JIA). The project was approved by the Research Ethics Committee of *Nicolae Testemițanu* State University of Medicine and Pharmacy (Minutes №49, dated June 8, 2015), and written informed consent was provided by parents or guardians of all participants.

Study population. The study enrolled a total of 215 children, including 90 children diagnosed with JIA (Group 1 – study group) and 125 healthy controls (Group 2 – control group). Diagnosis of JIA was established according to the classification criteria adopted by the International League of Associations for Rheumatology (ILAR, 1997).

Inclusion criteria for the JIA group were as follows:

- Age between 2 and 18 years,
- Clinical diagnosis of JIA,
- Informed consent from parents or legal guardians.

Exclusion criteria included:

- Presence of other chronic rheumatic diseases such as systemic lupus erythematosus (SLE), systemic scleroderma, juvenile dermatomyositis, or systemic vasculitis,
- Refusal of participation by parents or patients.

Children in the control group were healthy individuals matched for age and sex, randomly selected from the general population, with similarly obtained consent .

Data collection and clinical assessment

Clinical evaluation included:

- Number of painful joints (NPJ),
- Number of swollen joints (NSJ),
- Physician Global Assessment (PhGA) and Patient Global Assessment (PGA),
- Physical function assessed using the Childhood Health Assessment Questionnaire (CHAQ), a validated tool comprising 13 items recommended by the American College of Rheumatology.

Disease activity was further quantified using the Disease Activity Score in 28 joints (DAS28).

Laboratory assessments

Paraclinical investigations included:

- Complete blood count,
- Acute-phase inflammatory markers: erythrocyte sedimentation rate (ESR) and C-reactive protein (CRP),
- Biochemical analysis of homocysteine, total cholesterol (TC), triglycerides (TG), and total lipids.

Blood samples were collected in the morning following an overnight fast. Homocysteine was measured using enzymatic ELISA techniques from plasma obtained after centrifugation within 30 minutes of collection (EDTA tubes used). Total lipids, cholesterol, and triglycerides were quantified enzymatically by spectrophotometry (cholesterol oxidase/peroxidase method) using the Cobas C 311 biochemical analyzer.

Reference pathological values were defined as:

- Total cholesterol ≥ 5.2 mmol/L,
- Triglycerides > 1.7 mmol/L,
- Homocysteine > 12 μmol/L.

Statistical analysis. Data were processed and analyzed using IBM SPSS Statistics version 20 and Microsoft Excel 2010. Qualitative variables were summarized in contingency tables, and associations were tested by the Chi-square (χ^2) test. The Student's t-test was applied for comparison of means between two groups, while analysis of variance (ANOVA) was used for comparisons involving three or more groups. Correlations between quantitative variables (e.g., anthropometric, hemodynamic, biochemical, and ultrasound parameters) were evaluated using Pearson's correlation coefficient (r), interpreted according to Hopkins' scale:

- $r < 0.1$: negligible correlation,
- $0.1 \leq r < 0.7$: moderate correlation,
- $0.7 \leq r < 0.9$: strong correlation,
- $r \geq 0.9$: very strong/almost perfect correlation.

Statistical significance was set at $p < 0.05$, with further gradations for high significance ($p < 0.01$ and $p < 0.001$).

Risk assessment. Relative risk (RR) and odds ratio (OR) were calculated to estimate the association between JIA and cardiovascular risk factors, specifically hyperhomocysteinemia, hypercholesterolemia, and hypertriglyceridemia.

The RR was computed based on the 2x2 contingency table:

	Outcome+	Outcome-	Total
Exposed (JIA)	a	b	a+b
Unexposed	c	d	c+d

Risk in exposed (JIA) group: $P_1 = a/a+b$

Risk in unexposed (control) group: $P_0 = c/c+d$

Relative Risk (RR): $RR=P_1/P1_0=a/a+b/c/c+d= a(c+d)/c(a+b)$

Confidence intervals (CI) for the relative risk (RR) were calculated using the formula:

$$CI=RR\times(1\pm z\cdot SE)$$

where:

- RR= relative risk,
- z=1.96 for 95% confidence,
- SE = standard error of the RR, which was derived from the chi-square distribution or 2×2 table counts.

Interpretation criteria were:

- RR > 1 with CI excluding 1 indicates a positive association (risk factor),
- RR = 1 suggests no effect,
- RR < 1 with CI excluding 1 indicates a protective factor,
- If CI includes 1, the factor is considered indifferent.

Odds ratios were interpreted as follows:

- OR ≈ 1 indicates no association,
- OR > 1 indicates a positive correlation, suggesting causality,
- OR < 1 indicates a protective effect.

The required sample size was calculated using the formula incorporating expected prevalence rates (Po = 45% from literature, P1 = 80% anticipated in study), power (90%), significance level (95%), and an estimated 10% attrition rate.

Results

Participant demographics. The study population of children with juvenile idiopathic arthritis (JIA) was stratified by age and gender to better characterize the sample distribution. Among the 90 children with JIA, the following distribution was observed:

- **Ages 6-8 years:** 2 girls (4.4%) and 3 boys (6.6%),
- **Ages 9-11 years:** 4 girls (9%) and 4 boys (9%),
- **Ages 12-17 years:** 24 girls (53.3%) and 8 boys (17.7%).

This indicates a higher prevalence of older girls (12-17 years) in the JIA cohort, consistent with known gender and age patterns in autoimmune diseases, where adolescent females are often more affected.

Dyslipidemia as a cardiovascular risk factor in JIA. Dyslipidemia, characterized by abnormalities in lipid metabolism, is a well-recognized cardiovascular risk factor and was assessed through comprehensive lipid profiling (lipidogram) in all participants. The lipidogram included measurements of total cholesterol (TC) and triglycerides (TG), performed on both the JIA group (n = 90) and the control group (n = 125).

Total cholesterol levels. Children diagnosed with JIA exhibited significantly elevated total cholesterol levels compared to control group:

- The mean total cholesterol concentration in the JIA group was 5.3 ± 0.11 mmol/L, with values ranging from 3.2 mmol/L to 7.9 mmol/L.
- In contrast, the control group had a mean total cholesterol level of 4.7 ± 0.05 mmol/L, with a range of 3.47 mmol/L to 6.10 mmol/L.

The difference between these groups was statistically significant (F = 28.286, p < 0.001), indicating that children with JIA have a higher burden of hypercholesterolemia. The threshold for elevated cholesterol was set at >5.2 mmol/L, consistent with clinical guidelines for cardiovascular risk.

Triglyceride levels. In contrast to total cholesterol, no statistically significant difference was observed in triglyceride levels between children with JIA and the control group:

- The mean triglyceride level in the JIA group was 1.38 ± 0.05 mmol/L, with individual values ranging from 0.57 mmol/L to 3.97 mmol/L.
- The control group had a mean triglyceride level of 1.41 ± 0.02 mmol/L, ranging from 0.75 mmol/L to 2.15 mmol/L (Tab.1).

Statistical analysis yielded a non-significant p-value (p > 0.05), indicating comparable triglyceride levels between the two groups.

Table 1. Mean lipidogram values in children with JIA (group 1), compared to the control group (group 2)

Indices	Group 1 (90 children)		Group 2 (125 children)		F	p
	Mean value ± SD	Variation intervals	Mean value ± SD	Variation intervals		
Total cholesterol, mmol/l	5.34 ± 0.11	3.20-7.90	4.70 ± 0.05	3.47-6.10	28.286	<0.001**
Triglycerides, mmol/l	1.38 ± 0.05	0.57-3.97	1.41 ± 0.02	0.75 – 2.15	0.169	> 0.05

Note: *JIA – Juvenile Idiopathic Arthritis, Values are presented as mean ± standard deviation for numerical data; SD – standard deviation; **- p<0.001 – considered significant; p>0.05 – considered insignificant*

These findings suggest that total cholesterol, but not triglycerides, is significantly elevated in children with JIA compared to healthy peers, highlighting hypercholesterolemia as an important cardiovascular risk factor in this population. This elevation may contribute to the increased cardiovascular morbidity associated with chronic inflammation in JIA, necessitating regular lipid monitoring and early interventions targeting cholesterol management.

The prevalence of hypercholesterolemia was significantly higher in in children with JIA than in the control group: 58 children (64.4%) vs. 36 children (28.8%), $\chi 2 = 27.019$, gl = 1, p<0.001 (Fig.1).

Increased TG values (TG > 1.9 mmol/l) were observed in 13 children (14.4%) from the JIA group and in 9 children (7.2%) from the control group (p > 0.05).

Approximately 50% of patients with cardiovascular disease exhibit hyperhomocysteinemia [37]. Therefore, the study aimed to analyze homocysteine as a non-traditional

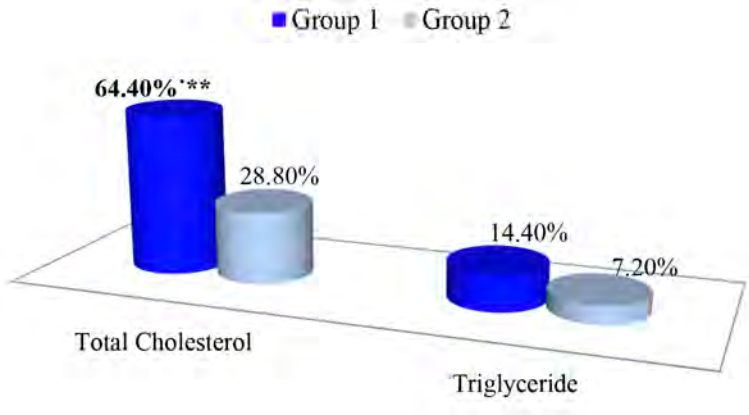

Fig. 1 Lipidogram results in children with JIA compared to the control group

*Note: JIA – Juvenile Idiopathic Arthritis Group 1 – children with juvenile idiopathic arthritis; Group 2 – children from the control group; **- p<0.01, statistically significant value*

cardiovascular risk factor. Hcy levels were assessed in 90 children with JIA and in 95 children from the control group. The mean value of hyperhomocysteinemia in children with JIA was 14.69 ± 0.61 mmol/l (minimum value – 2.50 mmol/l, maximum value – 29.50 mmol/l) and 9.43 ± 0.29 mmol/l (minimum value – 2.50 mmol/l, maximum value – 16.20 mmol/l) in control group (Tab. 2).

Table 2. Mean values of homocysteine in children with JIA compared to the control group

Parameter	Group 1 (90 children)		Group 2 (95 children)		F	p
	Mean value ± SD	Variation intervals	Mean value ± SD	Variation intervals		
Homocysteine, mmol/l	14.69 ± 0.61	2.50-29.50	9.43 ± 0.29	2.50-16.20	61.889	< 0.001**

***Note**: JIA – Juvenile Idiopathic Arthritis, values are presented as mean ± standard deviation for numerical data; ** - p<0.01, considered statistically significant; SD – standard deviation; Group 1 – children with juvenile idiopathic arthritis; Group 2 – children from the control group*

In children with JIA, significantly increased values of homocysteine (Hcy > 12 mmol/l) were found in 61 children (67.7%), compared to only in 15 children (15.78%) from the control group (where $\chi 2 = 51.328$, gl = 1, p< 0.001).

Among the children included in the study, hyperhomocysteinemia was observed in 67.8% of cases (61 children), with 40 (65.6%) being girls and 21 (34.4%) being boys, compared to 32.2% of cases (29 children) with normal homocysteine values (Fig. 2).

Following this analysis, it can be concluded that patients with JIA exhibit an increased risk of hyperhomocysteinemia compared to the control group.

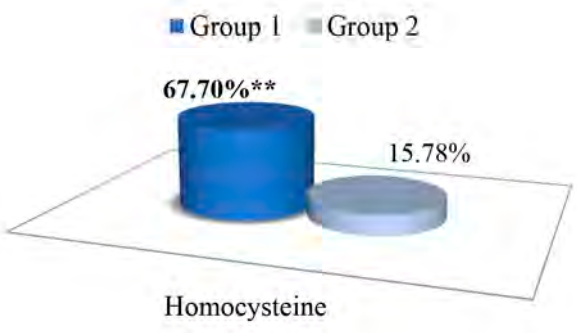

Fig. 2 Comparative analysis of homocysteine in children with JIA and the control group

***Note**: JIA – Juvenile Idiopathic Arthritis, Group 1 – children with juvenile idiopathic arthritis; Group 2 – children from the control group; ** - p<0.001, statistically significant value*

The relative risk (RR) was calculated for the following parameters: homocysteine, total cholesterol, and triglycerides, using the "2x2 Table" and calculating the required indicators with the interpretation of the obtained results.

According to the study results, a relative risk (RR) of 3.0 was obtained. When the relative risk has values greater than 1, it indicates a correlation between the risk factor and the occurrence of the disease. This suggests that the risk factor could be a cause of the disease onset in those exposed rather than in unexposed individuals. Therefore, it can be concluded that patients with juvenile idiopathic arthritis have a threefold increased risk of hyperhomocysteinemia compared to subjects in the control group (Tab. 3).

It was also essential to calculate the Odds Ratio (OR) between the rate of disease in those exposed (children with JIA) and the rate of disease in unexposed ones (healthy children). In this case, OR was 11.2, indicating that children's exposure to JIA influences hyperhomocysteinemia. An OR value significantly greater than 1 suggests a strong association between the exposure and the outcome.

Table 3. Assessment of the risk of hyperhomocysteinemia in children with JIA compared to unexposed children

	Children with JIA	Children from the control group	Total
Exposed	61	15	76
Unexposed	29	80	109
Total	90	95	185

***Note**: JIA – Juvenile Idiopathic Arthritis, exposed, unexposed, increased risk identified*

The relative risk (RR) was also calculated for hypercholesterolemia. Based on the obtained results, patients with JIA, have a 2.3-fold increased risk of developing hypercholesterolemia compared to the unexposed ones (RR = 2.3).

The Odds Ratio (OR) between the odds of disease in exposed children (JIA patients) and the odds of disease in unexposed individuals was found to be 4.5. Thus, it can be concluded that children's exposure to JIA influences the increase in total cholesterol (hypercholesterolemia), showing a moderate correlation trend between them (Tab. 4).

Table 4. Assessment of the relative risk of hypercholesterolemia in children with JIA vs. unexposed children.

	Children with JIA	Children from the control group	Total
Exposed	58	36	94
Unexposed	32	89	121
Total	90	125	215

***Note:** JIA – Juvenile Idiopathic Arthritis, exposed, unexposed, increased risk identified*

The relative risk (RR) was also calculated for hypertriglyceridemia for the exposed subjects (children with JIA) and unexposed subjects (control group). The calculations yielded a relative risk of 1.5, indicating that patients with JIA have a relatively low risk of developing hypertriglyceridemia compared to unexposed subjects. However, there is

a slight trend of correlation between JIA and increased triglyceride values.Top of Form

Furthermore, similar results were also obtained after calculating the Odds Ratio between the rate of disease in exposed children (JIA patients) and the rate of disease in unexposed individuals, where the Odds Ratio was found to be 4.5. Thus, it can be concluded that children's exposure to JIA slightly influences the increase in triglycerides (hypertriglyceridemia), showing a slight correlation tendency between them (Tab. 5).

Table 5. The relative risk of hypertriglyceridemia in children with JIA versus unexposed children

	Children with JIA	Children from the control group	Total
Exposed	13	9	22
Unexposed	77	115	192
Total	90	124	214

Note: *JIA – JIA – Juvenile Idiopathic Arthritis, exposed, unexposed, slight correlation*

Discussion

The present study contributes to the growing body of evidence indicating that children with juvenile idiopathic arthritis (JIA) may present with dysregulation of lipid metabolism. Our results demonstrated elevated levels of total cholesterol (TC) and a trend toward increased triglycerides (TG) in JIA patients compared to healthy controls. These findings are consistent with previous studies, such as those by Urban et al. [34] and Goncalves et al. [27], which also reported increased concentrations of TC and TG in children with JIA at disease onset. These alterations in lipid profile occurred despite the absence of clinical signs of obesity, suggesting that systemic inflammation may independently influence lipid metabolism in pediatric rheumatic diseases.

Conversely, not all studies have reported consistent findings. Bakkaloglu et al. [35] identified elevated TC levels without a corresponding increase in TG, while Maher et al. [11] did not observe significant lipid abnormalities in JIA patients. These discrepancies could be attributed to heterogeneity in study populations, disease duration, treatment regimens, or methodological differences. Moreover, Semb et al. and Skare et al. [36, 37] reported that lipid profile changes may be modulated by disease activity, highlighting the importance of considering inflammatory status when interpreting metabolic parameters.

The study also assessed plasma homocysteine (Hcy) levels, given the well-documented role of hyperhomocysteinemia as an independent cardiovascular risk factor. Our findings revealed elevated Hcy levels in children with JIA compared to controls, supporting earlier observations by Huemer et al. [31]. Elevated plasma Hcy concentrations have been associated with endothelial dysfunction, smooth muscle cell proliferation, oxidative stress, and thrombogenesis – all of which contribute to the pathogenesis of atherosclerosis [25, 38]. Meta-analyses have shown that a 5 μmol/L increase in plasma Hcy may result in a 60-80% increased risk of coronary heart disease [39, 40].

Despite the clear association between Hcy and cardiovascular risk in adults, its relevance in pediatric autoimmune diseases remains under investigation. In our study, no significant correlations were found between Hcy and inflammatory markers, disease activity, or lipid parameters – findings that align with those of Goncalves et al. [27] and Friso et al. [41]. However, other studies have reported differing associations; for instance, Chiang et al. [42] found a positive correlation between erythrocyte sedimentation rate (ESR) and Hcy, while Annan et al. [43] reported an association between Hcy and TG, but not TC. These inconsistencies underscore the multifactorial etiology of hyperhomocysteinemia, which is influenced by genetic predisposition (e.g., MTHFR polymorphisms), drug therapy (notably methotrexate), diet, and systemic inflammation [18, 32].

Treatment with methotrexate (MTX), a cornerstone in JIA management, has been implicated in elevated Hcy levels. Van Ede et al. [44] demonstrated that MTX therapy may increase plasma Hcy concentrations, and Goncalves et al. [27] observed elevated Hcy in four out of five children undergoing MTX treatment. These findings raise important considerations regarding the balance between therapeutic efficacy and cardiovascular risk, especially in long-term treatment regimens.

While some studies suggest that hyperhomocysteinemia may be a consequence of chronic inflammation, others propose that it may actively contribute to the inflammatory process [45, 46]. This bidirectional relationship could account for the complex and often contradictory findings in the literature. Furthermore, the role of exogenous factors such as reduced mobility, nutritional deficiencies, and prolonged disease course cannot be overlooked.

Importantly, several interventional studies have demonstrated that folic acid supplementation can effectively reduce plasma Hcy levels and improve endothelial function in patients with hyperhomocysteinemia [47, 48]. This positions folic acid as a potential preventive strategy in JIA patients at elevated cardiovascular risk, although large-scale, longitudinal trials are required to establish definitive clinical guidelines.

This study has several limitations that should be acknowledged. First, its cross-sectional design precludes conclusions regarding causality or temporal relationships between inflammation, lipid metabolism, and homocysteine levels. Second, genetic factors such as MTHFR polymorphisms were not assessed, which may influence individual susceptibility to hyperhomocysteinemia. Third, dietary intake, physical activity, and nutritional status were not controlled, potentially introducing confounding variables. Furthermore, the sample size may have limited the statistical power to detect subtle associations or stratify findings by disease subtype or treatment exposure.

Future research should aim to address these limitations through well-designed, multicenter, longitudinal studies that include genetic profiling, dietary assessments, and standardized disease activity scores. Investigations into the

impact of folic acid and vitamin B supplementation on cardiovascular markers in JIA are also warranted. Additionally, advanced imaging techniques, such as carotid intima-media thickness and endothelial function testing, may offer further insight into the subclinical cardiovascular changes associated with hyperhomocysteinemia and dyslipidemia in this population.

The present study adds to the growing evidence that children with JIA are at increased risk for metabolic alterations, including dyslipidemia and hyperhomocysteinemia, which may contribute to long-term cardiovascular morbidity. Although some inconsistencies exist in the literature, the findings support the need for early cardiovascular risk assessment and consideration of nutritional interventions. Further research is needed to clarify the mechanisms linking chronic inflammation, homocysteine metabolism, and lipid abnormalities, and to develop evidence-based strategies for cardiovascular risk reduction in pediatric rheumatology.

Conclusions

This study reinforces the association between juvenile idiopathic arthritis (JIA) and alterations in lipid metabolism and homocysteine levels, underscoring the potential cardiovascular risk in affected children. While variability exists across published findings, our results support the hypothesis that systemic inflammation and treatment-related factors may contribute to metabolic disturbances in JIA. The added value of this research lies in its integrated evaluation of both lipid profile and homocysteine levels in a pediatric inflammatory context, highlighting the importance of early cardiovascular risk assessment and the need for tailored preventive strategies in clinical practice.

Competing interests

None declared.

Authors' contributions

LB was responsible for data collection, questionnaire administration, and statistical analysis. AC contributed to data collection and manuscript drafting. NR served as the project coordinator and supervised the overall research. All authors read and approved the final manuscript.

Ethics approval

The research project was approved by the Research Ethics Committee of *Nicolae Testemițanu* State University of Medicine and Pharmacy (Minutes no. 49 from 08.06.2015).

Patient consent

Obtained.

Acknowledgements and funding

No external funding.

Provenance and peer review

Not commissioned, externally peer reviewed.

References

1. Thomson W, Barrett JH, Donn R, et al. Juvenile idiopathic arthritis classified by the ILAR criteria: HLA associations in UK patients. Rheumatology (Oxford). 2002;41(10):1183-1189. doi: 10.1093/rheumatology/41.10.1183.
2. Sule S, Fontaine K. Metabolic syndrome in adults with a history of juvenile arthritis. Open Access Rheumatol. 2018;10:67-72. doi: 10.2147/OARRR.S157229.
3. Aranda-Valera IC, De la Rosa IA, Roldán-Molina R, et al. Subclinical cardiovascular risk signs in adults with juvenile idiopathic arthritis in sustained remission. Paediatr Rheumatol. 2020;18:1-12. doi: 10.1186/s12969-020-00448-3.
4. Momin M, Jia J, Fan F, et al. Relationship between plasma homocysteine level and lipid profiles in a community-based Chinese population. Lipids Health Dis. 2017;16:54. doi: 10.1186/s12944-017-0441-6.
5. Del Giudice E, Dilillo A, Tromba L, et al. Aortic, carotid intima-media thickness and flow- mediated dilation as markers of early atherosclerosis in a cohort of paediatric patients with rheumatic diseases. Clin Rheumatol. 2018;37(6):1675-1682. doi: 10.1007/s10067-017-3705-7.
6. Boyer JF, Bongard V, Cantagrel A, et al. Link between traditional cardiovascular risk factors and inflammation in patients with early arthritis: results from a French multicentre cohort. Arthritis Care Res (Hoboken). 2012;64(6):872-880. doi: 10.1002/acr.21623.
7. Panfile E, Ivanov V, Ştirbul A. Ateroscleroza şi procesul inflamator imun [Atherosclerosis and the immune inflammatory process]. Bull Acad Sci Mold. Med Sci. 2010;(2):132-136. Romanian.
8. Toms TE, Panoulas VF, Douglas KMJ, et al. Are lipid ratios less susceptible to change with systemic inflammation than individual lipid components in patients with rheumatoid arthritis? Angiology. 2011;62(2):167-175. doi: 10.1177/0003319710373749.
9. Ahmed S, Jacob B, Carsons SE, et al. Treatment of cardiovascular disease in rheumatoid arthritis: a complex challenge with increased atherosclerotic risk. Pharmaceuticals (Basel). 2021;15(1):11. doi: 10.3390/ph15010011.
10. Liao KP, Solomon DH. Inflammation, disease-modifying antirheumatic drugs, lipids, and cardiovascular risk in rheumatoid arthritis. Arthritis Rheumatol. 2015;67(2):327-329. doi: 10.1002/art.38925.
11. Maher SE, Abdel Raheem M, Moness HM. Subclinical atherosclerosis in children with rheumatologic diseases in Minia Children University Hospital, Egypt. Int J Pediatr. 2019;7(3):9159-9167. https://doi.org/10.22038/ijp.2018.36402.3174.
12. Liao KP, Cai T, Gainer VS, et al. Lipid and lipoprotein levels and trend in rheumatoid arthritis compared to the general population. Arthritis Care Res (Hoboken). 2013;65(12):2046-2050. doi: 10.1002/acr.22091.
13. Liao KP, Liu J, Lu B, et al. Association between lipid levels and major adverse cardiovascular events in rheumatoid arthritis compared to non-rheumatoid arthritis patients. Arthritis Rheumatol. 2015;67(8):2004-2010. doi: 10.1002/art.39165.

14. Marangoni RG, Hayata AL, Borba EF, et al. Decreased high-density lipoprotein cholesterol levels in polyarticular juvenile idiopathic arthritis. Clinics. 2011;66(9):1549-52. doi: 10.1590/s1807-59322011000900007.
15. Zota I, Lîsîi L, Munteanu A. Corelaţia patogenetică între sindromul metabolic şi ateroscleroza [Pathogenetic correlation between metabolic syndrome and atherosclerosis]. In: Scientific Annals of *Nicolae Testemiţanu* SUMPh. Chisinau; 2009. Vol. 1. p. 41-48. Romanian.
16. Alam MF, Islam MM, Haque M, et al. Serum homocysteine level in children with Juvenile Idiopathic Arthritis. Bangladesh Med Res Counc Bull. 2020;46:12-16. doi: 10.3329/bmrcb.v46i1.47463
17. Anestiadi V, Zota E, Groppa S, et al. Unele aspecte în patogenia aterosclerozei [Some aspects in the pathogenesis of atherosclerosis]. Bull Acad Sci Mold. Med Sci. 2005;(2):37-43. Romanian.
18. Ganguly P, Alam SF. Role of homocysteine in the development of cardiovascular disease. Nutr J. 2015;14:6. doi: 10.1186/1475-2891-14-6.
19. McCully KS. Homocysteine, vitamins, and vascular disease prevention. Am J Clin Nutr. 2007;86(5):1563-1568. doi: 10.1093/ajcn/86.5.1563S.
20. Bivol D. Afectarea sistemului cardiovascular la pacienţii cu artrită reumatoidă = Cardiovascular disease in rheumatoid arthritis pacients. In: Scientific abstracts of students, residents and young researchers of *Nicolae Testemiţanu* SUMPh. Chisinau: Medicina; 2018. p. 126.
21. Holven KB, Aukrust P, Retterstol K, et al. Increased levels of C-reactive protein and interleukin-6 in hyperhomocysteinemic subjects. Scand J Clin Lab Invest. 2006;66(1):45-54. doi: 10.1080/00335510500429821.
22. Du Plessis JP, Nienaber-Rousseau C, Lammertyn L, et al. The relationship of circulating homocysteine with fibrinogen, blood pressure, and other cardiovascular measures in African adolescents. J Pediatr. 2021;234:158-163. doi: 10.1016/j.jpeds.2021.03.034.
23. Chori BS, Danladi B, Inyang BA, et al. Hyperhomocysteinemia and its relations to conventional risk factors for cardiovascular diseases in adult Nigerians: the REMAH study. BMC Cardiovasc Disord. 2021;21(1):102. doi: 10.1186/s12872-021-01913-x.
24. Dutca G, Groppa S. Homocisteina – factor de risc în apariţia accidentului vascular cerebral acut şi corecţia ei medicamentoasă [Homocysteine - the risk factors in the apperance of acute cerebral vascular stroke]. In: Scientific Annals of *Nicolae Testemiţanu* SUMPh. Chisinau; 2008. Vol. 3. p. 354-356. Romanian.
25. Lazzerini PE, Capecchi PL, Selvi E, et al. Hyperhomocysteinemia, inflammation and autoimmunity. Autoimmun Rev. 2007;6(7):503-509. doi: 10.1016/j.autrev.2007.03.008.
26. Wu H, Wang B, Ban Q, et al. Association of total homocysteine with blood pressure in a general population of Chinese adults: a cross-sectional study in Jiangsu province, China. BMJ Open. 2018;8(6):e021103. doi: 10.1136/bmjopen-2017-021103.
27. Gonçalves M, D'Almeida V, Guerra-Shinohara EM, et al. Homocysteine and lipid profile in children with Juvenile Idiopathic Arthritis. Pediatr Rheumatol. 2007;5:2. doi: 10.1186/1546-0096-5-2.
28. Drînga E. Factorii de risc minori pentru ateroscleroză = Minor risk factors for atherosclerosis. In: Scientific abstracts of students, residents and young researchers of *Nicolae Testemiţanu* SUMPh. Chisinau: Medicina; 2019. p. 22.
29. Bichir-Thoreac L. Homocisteina factor de risc independent în hipertensiunea arterială la copii [Homocysteine as an independent risk factor in arterial hypertension at children]. Bull Acad Sci Mold. Med Sci. 2016;(2):169-171. Romanian.
30. Lai WKC, Kan MY. Homocysteine-induced endothelial dysfunction. Ann Nutr Metab. 2015;67(1):1-12. doi: 10.1159/000437098.
31. Huemer M, Fodinger M, Huemer C, et al. Hyperhomocysteinemia in children with juvenile idiopathic arthritis is not influenced by methotrexate treatment and folic acid supplementation: a pilot study. Clin Exp Rheumatol. 2003;21(2):249-55.
32. de Oliveira Leite L, Costa Dias Pitangueira J, Ferreira Damascena N, et al. Homocysteine levels and cardiovascular risk factors in children and adolescents: systematic review and meta-analysis. Nutr Rev. 2021;79(9):1067-1078. doi: 10.1093/nutrit/nuaa116.
33. Aronov A, Kim YJ, Sweiss NJ, et al. Cardiovascular disease risk evaluation impact in patients with rheumatoid arthritis. Am J Prev Cardiol. 2022;12:100380. doi: 10.1016/j.ajpc.2022.100380.
34. Urban M, Pietrewicz E, Górska A, Głowińska B. [Lipids and homocysteine level in juvenile idiopathic arthritis]. Pol Merkur Lekarski. 2004;17(99)235-238. Polish.
35. Bakkaloglu A, Kirel B, Ozen S, et al. Plasma lipids and lipoproteins in juvenile chronic arthritis. Clin Rheumatol. 1996;15(4):341-345. doi: 10.1007/BF02230355.
36. Semb AG, Holme I, Kvien TK, et al. Intensive lipid lowering in patients with rheumatoid arthritis and previous myocardial infarction: An explorative analysis from the incremental decrease in endpoints through aggressive lipid lowering (IDEAL) trial. Rheumatology (Oxford). 2011;50(2):324-329. doi: 10.1093/rheumatology/keq295.
37. Skare TL, Silva MB, Negreiros P. Lipid profile in adult patients with idiopathic juvenile arthritis. Rev Bras Rheumatol. 2013;53(4):371-374.
38. McCully KS. Vascular pathology of homocysteinemia: implications for the pathogenesis of arteriosclerosis. Am J Pathol. 1969;56(1):111-28.

39. Dinavahi R, Falkner B. Relationship of homocysteine with cardiovascular disease and blood pressure. J Clinical Hypertension. 2004;6(9):494-8. doi: 10.1111/j.1524-6175.2004.03643.x.
40. Fan R, Zhang A, Zhong F. Association between homocysteine levels and all-cause mortality: a dose-response meta-analysis of prospective studies. Sci Rep. 2017;7(1):4769. doi: 10.1038/s41598-017-05205-3.
41. Friso S, Jacques PF, Wilson PW, et al. Low circulating vitamin B6 is associated with elevation of the inflammation marker C-reactive protein independently of plasma homocysteine levels. Circulation. 2001;103(23):2788-2791. doi: 10.1161/01.cir.103.23.2788.
42. Chiang PK, Gordon RK, Tal J, et al. S-Adenosylmethionine and methylation. FASEB J. 1996;10(4):471-480.
43. Anan F, Masaki T, Umeno Y, et al. Correlations between homocysteine levels and atherosclerosis in Japanese type 2 diabetic patients. Metabolism. 2007;56(10):1390-1395. doi: 10.1016/j.metabol.2007.05.010.
44. Van Ede AE, Laan RFJM, Blom HJ, et al. Methotrexate in rheumatoid arthritis: An update with focus on mechanisms involved in toxicity. Semin Arthritis Rheum. 1998;27(5):277-292. doi: 10.1016/s0049-0172(98)80049-8.
45. Mansoor MA, Seljeflot I, Arnesen H, et al. Endothelial cell adhesion molecules in healthy adults during acute hyperhomocysteinemia and mild hypertriglyceridemia. Clin Biochem. 2004;37(5):408-414. doi: 10.1016/j.clinbiochem.2004.01.003.
46. Li M, Chen J, Li YS, et al. Folic acid reduces adhesion molecules VCAM-1 expression in aortic of rats with hyperhomocysteinemia. Int J Cardiol. 2006;106(2):285-288. doi: 10.1016/j.ijcard.2005.07.006.
47. Yi X, Zhou Y, Jiang D, et al. Efficacy of folic acid supplementation on endothelial function and plasma homocysteine concentration in coronary artery disease: a meta- analysis of randomized controlled trials. Exp Ther Med. 2014;7(5):1100-10. doi: 10.3892/etm.2014.1553.
48. Balkarli A, Tekintürk S, Kaptanoğlu B, et al. Relationship between plasma levels of homocysteine and pro-inflammatory cytokines in patients with rheumatoid arthritis. J Clin Exp Invest. 2016;7(2):163-167. doi: 10.5799/ahinjs.01.2016.02.0590.

https://doi.org/10.52645/MJHS.2025.3.16

UDC: 612.015.11:[546.56+577.121.7]

RESEARCH ARTICLE

Targeting redox balance: antioxidant effects of thiosemicarbazones on human peripheral blood

Valeriana Pantea[1], Ecaterina Pavlovschi[1,2*], Silvia Stratulat[2], Aurelian Gulea[3], Olga Tagadiuc[2], Valentin Gudumac[1]

[1]Laboratory of Biochemistry, *Nicolae Testemițanu* State University of Medicine and Pharmacy, Chisinau, Republic of Moldova
[2]Department of Biochemistry and Clinical Biochemistry, *Nicolae Testemițanu* State University of Medicine and Pharmacy, Chisinau, Republic of Moldova
[3]Laboratory of Advanced Materials in Biopharmaceutics and Technics, Moldova State University, Republic of Moldova

ABSTRACT

Introduction. Thiosemicarbazones represent a class of organic compounds with well-documented pharmacological properties, including antitumor, antimicrobial, and antiviral activities. Contemporary research highlights their role in modulating cellular redox equilibrium through antioxidant pathway regulation. The growing interest in copper-based coordination complexes with thiosemicarbazones is driven by the unique redox flexibility and high biocompatibility of copper ions, properties that underlie their potential in therapeutic and diagnostic applications. This investigation assessed the capacity of specific local bioactive thiosemicarbazones to impact the antioxidant system using *in vitro* methodologies.

Material and methods. Peripheral blood samples from ten healthy volunteers were used to evaluate *in vitro* the influence of 10 copper-based coordination complexes with thiosemicarbazones at concentrations of 10.0 μM/L and 1.0 μM/L on antioxidant markers – total antioxidant activity (via ABTS assay), total antioxidant capacity, antioxidant substance mass, and antioxidants total activity.

Results. Data indicated that targeted copper-based coordination complexes with thiosemicarbazones affect general antioxidant markers. The study demonstrates that thiosemicarbazones exhibit concentration- and structure-dependent redox modulation, disclosing distinct mechanisms of action across three structural classes – benzothiazole, phenyl, and allyl thiosemicarbazone derivatives. Structural optimization (e.g., benzothiazole with methoxy groups) yields compounds like MG-22 that maintain redox equilibrium, while pro-oxidant variants (CMA-18) offer therapeutic potential through selective oxidative cytotoxicity.

Conclusions. Copper-based coordination complexes with thiosemicarbazones represent a promising class of redox modulators with tunable biological effects. Their bidirectional activity, manifested by stimulation or inhibition of antioxidant mechanisms, confirms the potential of these derivatives as selective therapeutic agents. When these results are integrated in the context of personalized medicine, thiosemicarbazones become valuable candidates in the development of therapeutic strategies aimed at maintaining cellular homeostasis, especially in pathologies characterized by increased oxidative stress, such as cancer and neurodegenerative diseases.

Keywords: copper-based coordination complexes with thiosemicarbazones, blood, antioxidant system.

Cite this article: Pantea V, Pavlovschi E, Stratulat S, Gulea A, Tagadiuc O, Gudumac V. Targeting redox balance: antioxidant effects of thiosemicarbazones on human peripheral blood. Mold J Health Sci. 2025;12(3):101-109. https://doi.org/10.52645/MJHS.2025.3.16.

Manuscript received: 30.06.2025

Accepted for publication: 31.07.2025

Published: 15.09.2025

***Corresponding author: Ecaterina Pavlovschi**, MD, PhD, associate professor, senior researcher
Laboratory of Biochemistry
Nicolae Testemițanu State University of Medicine and Pharmacy.
27 Nicolae Testemițanu str, Chisinau, Republic of Moldova, MD-2025
e-mail: ecaterina.pavlovschi@usmf.md

Key messages

What is not yet known on the issue addressed in the submitted manuscript

The selective redox effects of new, local copper-based coordination complexes with different thiosemicarbazones in healthy cells are unknown.

The research hypothesis

The study hypothesizes that copper-based coordination complexes with thiosemicarbazones exhibit structure-dependent redox

Authors' ORCID IDs
Valeriana Pantea – https://orcid.org/0000-0002-8835-6612
Ecaterina Pavlovschi – https://orcid.org/0000-0003-0385-4805
Stratulat Silvia – https://orcid.org/0000-0003-0985-307X
Aurelian Gulea – https://orcid.org/0000-0003-2010-7959
Olga Tagadiuc – https://orcid.org/0000-0002-5503-8052
Valentin Gudumac – https://orcid.org/0000-0001-9773-1878

modulation, where specific ligand modifications optimize antioxidant profiles while others induce pro-oxidant effects.

The novelty added by manuscript to the already published scientific literature

This work contributes novel insights into the redox behaviour of copper coordination complexes with thiosemicarbazones by employing a comparative *in vitro* analysis using human blood-derived samples. The findings reveal structure- and concentration-dependent redox modulation and distinguish between redox-active and redox-inert compounds, supporting their potential for targeted therapeutic development in oxidative stress-related conditions.

Introduction

Disclosing the complexities of biological regulatory mechanisms and metabolic pathways at the molecular, cellular, tissue, and systemic levels continues to be a central challenge in contemporary biomedical research, particularly in efforts to elucidate the origins and development of cancer. Alongside these scientific efforts, there is an increasing focus on designing alternative *in vitro* approaches for toxicological assessment of chemical compounds, motivated by both ethical considerations and the need for more efficient research models. A significant barrier in this area is the conception of robust non-animal testing strategies that can reliably anticipate the potential adverse effects of substances following repeated systemic exposure. For such substitutive methods to be effective, it is essential to account for the physicochemical characteristics of the tested compounds, including their aggregation state and pharmaceutical formulation [1, 2].

Among the most intensively studied classes of compounds are copper-based coordination complexes (CCCs), which have attracted substantial attention due to the versatile redox behavior and biological compatibility of copper ions. The pharmacological profile of these metal complexes can be precisely modulated by altering the nature of the coordinating ligands and donor atoms. Particularly, copper complexes have shown considerable promise as antitumor agents, providing a potentially less toxic and more accessible alternative to traditional chemotherapeutics. In addition, their therapeutic applications extend to the management of inflammatory conditions and infectious diseases, including tuberculosis, malaria, and fungal infections [3, 4].

The antitumor efficacy of copper complexes is largely explained by their ability to induce intracellular accumulation of reactive oxygen species (ROS), a process facilitated by their oxidation-reduction potential. The resultant enhancement in ROS levels stimulates cellular antioxidant defense systems in response to oxidative stress (OS). These results highlight the therapeutic potential of ROS-generating copper complexes as antiproliferative agents in cancer treatment strategies [5, 6].

Cellular homeostasis depends critically on balanced redox signaling, where ROS function as physiological mediators. Disruption of this equilibrium contributes to multifactorial pathologies, with malignancies exhibiting particularly pronounced dysregulation. Cancer cells generate elevated ROS through accelerated metabolic activity – a double-edged phenomenon that both triggers tumor progression and gives rise to targetable vulnerabilities for therapeutic exploitation. Selective cytotoxicity can be achieved by further OS elevation in these compromised cells. OS emerges from imbalance between ROS production and antioxidant capacity, causing cumulative damage to proteins, lipids, and DNA. The molecular deterioration accelerates aging processes and initiates carcinogenic pathways. Malignancies exhibit amplified redox discrepancy due to combined endogenous/exogenous reactive species (ROS/RNS), which disrupt signaling networks and promote oncogenic transformation [7].

To counteract such risks, cells rely on a sophisticated network of antioxidant defense mechanisms, encompassing both enzymatic and non-enzymatic components. Key markers of this system include total antioxidant activity (TAA, often measured by ABTS assay), total antioxidant capacity (TAC), and antioxidant substance mass (ASM). The antioxidants, distributed across various cellular compartments, function in unison to ensure reliable protection against oxidative assaults [8, 9].

The complex duality of ROS involved in both tumor initiation and therapeutic targets highlights the central role of oxidative stress modulation in oncology. CCCs represent potential therapeutic agents in the treatment of multifactorial diseases due to their ability to regulate antioxidant systems [10]. This research examines the *in vitro* antioxidant properties of biologically active thiosemicarbazones using human-derived biological specimens.

The aim of this study was to evaluate the biological potential of copper-based coordination compounds with different thiosemicarbazones by examining their influence on antioxidant markers *in vitro* in the supernatant obtained from the peripheral blood of clinically healthy donors.

Material and methods

Study design and biological sample preparation. The research was conducted *in vitro* using biological samples collected in accordance with current principles of biological standardization for experimental procedures. The study

protocol was approved by the Research Ethics Committee of the *Nicolae Testemițanu* State University of Medicine and Pharmacy of the Republic of Moldova (approval no. 5, ref. no. 38, dated June 20, 2024). The study was conducted in compliance with the Declaration of Helsinki and its subsequent amendments (Somerset West Amendment, 1996), regarding the use of human subjects in research [11]. Enrollment in the study was contingent upon participants providing written informed consent.

The research focused on copper-based coordination compounds featuring thiosemicarbazone ligands, which were synthesized at the Advanced Materials Research Laboratory in Biopharmaceutics, Moldova State University [12].

Substances used in the in vitro experiment. The test compounds were classified into the following distinct categories:

- Benzothiazole derivatives of thiosemicarbazone – CMA-18, CMD-8, MG-22;
- Phenyl thiosemicarbazone derivatives – CMC-34, CMJ-33, CMT-67;
- Allyl thiosemicarbazone derivatives – CMG-41, TIA -123, TIA-160.

Table 1. Copper-based coordination compounds with thiosemicarbazones included in the research [13].

No.	Code	Chemical name of the substance
1	Control	0.1 ml of 0.9% saline solution + Dulbecco's modified eagle medium (DMEM)
2	DOXO	Doxorubicin
Benzothiazole derivatives of thiosemicarbazone		
3	CMA-18	Chloro-{1-(1,2-benzothiazol-3-yl)-2-[1-(pyridin-2-yl) ethylidene]diazanido}copper
4	CMD-8	Chloro-{4-ethyl-2-[phenyl(pyridin-2-yl)methylidene] hydrazine-1-carbothioamido} copper
5	MG-22	Chloro-{N'-(4-methoxyphenyl)-N,N-dimethylcarbamimidothioato} copper
Phenyl thiosemicarbazone derivatives		
6	CMC-34	Chloro-{N'-[phenyl(pyridin-2-yl)methylidene]-N-pyridin-2-ylcarbamohydrazonothioato} copper
7	CMJ-33	Chloro-{4-(3-methoxyphenyl)-2-[1-(pyridin-2-yl) ethylidene]hydrazine-1-carbothioamido} copper
8	CMT-67	Nitrato-{N-phenyl-N'-(pyridin-2-ylmethylidene)carbamohydrazonothioato} copper
Allyl thiosemicarbazone derivatives		
9	CMG-41	Nitrato-{N'-[phenyl(pyridin-2-yl)methylidene]-N-prop-2-en-1-ylcarbamohydrazonothioato} copper
10	TIA-123	Chloro-{N'-[phenyl(pyridin-2-yl)methylidene]-N-prop-2-en-1-ylcarbamohydrazonothioato} copper
11	TIA-160	Acetato-{2-({[(methylsulfanhyl)(prop-2-en-1-lamino) ethylidene]hydrazinylidene} methyl) enolato}copper

Note: *Code – identifier assigned to each compound by the synthesizing researcher; DOXO – Doxorubicin (positive control); Compounds are categorized based on the structure of their thiosemicarbazone ligand: benzothiazole, phenyl, or allyl derivatives. All chemical names refer to copper-based coordination compounds used in the in vitro assays.*

Experimental design. Peripheral blood specimens were obtained from 10 healthy volunteers to assess the bioactivity of local copper-based coordination compounds (CCCs). Samples were collected via cubital venipuncture (5 mL/subject) in the morning under fasting conditions using adapted vacutainers.

Sample preparation. Blood was immediately transferred to sterile culture flasks containing 20 mL Dulbecco's modified eagle medium (DMEM) supplemented with:

- Heparin (2.5 IU/mL)
- Gentamicin (100 μg/mL)
- L-Glutamine (0.6 mg/mL)

Aliquots (0.9 mL) of this suspension were distributed into 24-well plates for antioxidant response assessment.

Treatment protocol. Control wells (n = 4) received 0.1 mL 0.9% NaCl. The other wells were supplemented with the studied CCCs (CMA-18, CMD-8, MG-22, CMC-34, CMJ-33, CMT-67, CMG-41, TIA-123, TIA-160) at final concentrations of 10.0 μM/L and 1.0 μM/L. The compounds were diluted in physiological saline (0.1 mL/well). All experimental treatments were performed twice to ensure data reproducibility.

Incubation and processing. Plates underwent 48-hour incubation at 37°C/3.5% CO_2. Post-incubation, well contents were:

1. transferred to 2.0 mL Eppendorf tubes;
2. centrifuged (3000 rpm, 5 min);
3. supernatants aliquoted into 1.5 mL cryovials;
4. stored at −40°C until analysis.

Blinded coding ensured sample anonymity and traceability throughout the study.

Evaluation of antioxidant system markers. All biochemical assays used to evaluate the antioxidant system parameters were carried out in the Biochemistry Laboratory of *Nicolae Testemițanu* State University of Medicine and Pharmacy of the Republic of Moldova. The methods originally described by Re R. et al. and Zhang M. et al., were adapted and optimized for application with the Synergy H1 Hybrid Microplate Reader (BioTek Instruments, USA) [14, 15].

In the collected supernatant, the following antioxidant system markers were assessed using spectrophotometric micromethods: total antioxidant activity (TAA using ABTS), total antioxidant capacity (TAC), antioxidant substance mass (ASM), antioxidant total activity (ATA). All parameters were expressed in conventional units (c.u.).

The determination of total antioxidant activity using ABTS (TAA-ABTS) was performed according to the method described by Re R. [14], with modifications introduced by Gudumac V. et al. [16]. This assay is based on the neutralization of the 2,2'-azino-bis-3-ethylbenzothiazoline-6-sulfonic acid radicals (ABTS*) upon interaction with antioxidant compounds present in the biological sample. The neutralization of the radical was measured spectrophotometrically at 734 nm.

The TAC, ASM, and ATA were evaluated based on the method originally described by Zhang M. [15], with adaptations by Tagadiuc O. [17]. This redox-based assay utilizes potassium permanganate ($KMnO_4$) in the assessment of all the mentioned parameters in biological samples. The antioxidants in the sample, inhibit color development in

proportion to their concentration. To determine TAC, ASM, and ATA, absorbance was measured initially (A_0) and after 30 minutes of incubation (A_{30}) under continuous agitation (700 rpm) at 570 nm, using serial dilutions of the biological sample in 0.9% saline (1:10; 1:20; 1:40; 1:80; 1:160), followed by the addition of $KMnO_4$ solution. Dilution factors were logarithmically transformed into the following values: 1.0, 1.3, 1.6, 1.9, and 2.2. Specific formulas were applied to calculate TAC, ASM, and ATA.

The evaluation of the *in vitro* effects of the CCCs was performed according to the standard methodology described by Ryzhikova S. L. et al. [18].

Statistical data processing. Data analysis was performed using SPSS v23 (IBM Corp., Armonk, NY). After verifying data distribution and homogeneity of variances, intergroup differences in biochemical parameters were assessed via one-way ANOVA with Games-Howell post-hoc testing for multiple comparisons. Statistical significance was established at $p < 0.05$. Results are reported as medians with interquartile ranges (IQR).

Results

The present study aimed to investigate the antioxidant activity of copper coordination compounds with thiosemicarbazones (CCCTs), bearing various substituents (benzothiazole, phenyl, and allyl groups), tested at two distinct concentrations (10.0 μM/L and 1.0 μM/L). The effects were evaluated in comparison to both the control group and the pharmacological reference standard – doxorubicin. The results of the biochemical analyses are summarized in Figure 1.

The analysis of the results of TAA evaluation confirms that the compounds CMA-18 and CMD-8 produced a statistically significant decrease at both concentrations, ranging from 10% to 24%, $p < 0.001$, exhibiting moderate pro-oxidant effects, with inhibition of antioxidant activity at both tested concentrations. Simultaneously, in the *in vitro* testing of the coordination compound MG-22, a non-significant decrease was recorded at both concentrations, ranging from 1% to 6%, $p > 0.05$, compared to the control group, maintaining almost the entire antioxidant activity. These findings suggest effective oxidative protection and enhanced cellular tolerance.

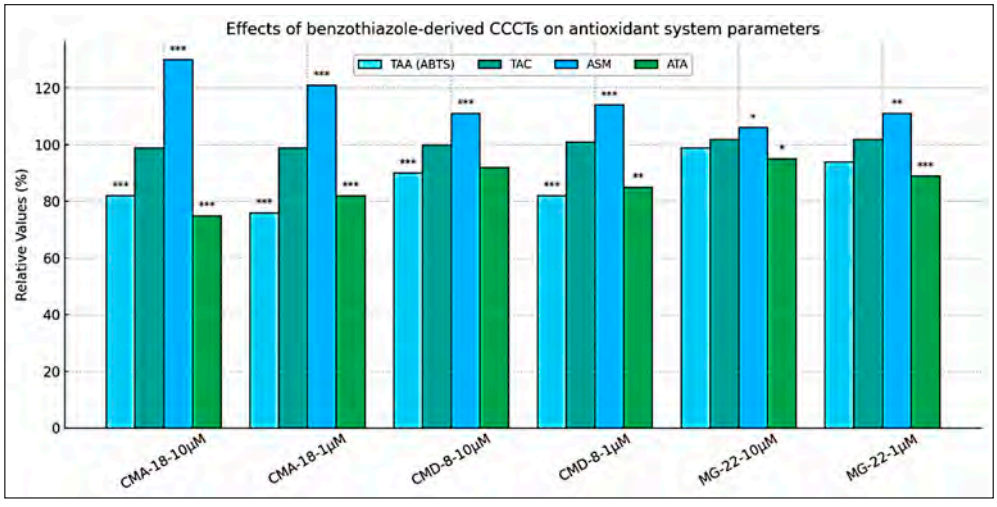

Fig. 1 *In vitro* effects of benzothiazole-derived copper coordination compounds with thiosemicarbazones at concentrations of 10.0 μM/L and 1.0 μM/L on antioxidant system parameters

Note: *The values for the control group were taken as the reference (100%). Statistical significance comparative to the control group: * – p < 0,05; ** – p < 0,01; *** – p < 0,001; TAA (ABTS): total antioxidant activity measured with ABTS; TAC: total antioxidant capacity; ASM: antioxidant substance mass; ATA: antioxidants total activity.*

The total antioxidant capacity (TAC) of human serum results from the combined contribution of enzymatic and non-enzymatic branches of the system. Oxidative stress arises when the balance between the production of ROS and the body's natural antioxidant mechanisms is disrupted, impairing the efficient neutralization of these reactive species [19].

In conditions where the antioxidant system is functioning suboptimally, the harmful effects of the free radicals become more pronounced. Previous research has predominantly concentrated on evaluating tissue antioxidant capacity, either through the analysis of key antioxidant enzyme activities or by determining levels of low-molecular-weight non-enzymatic antioxidants [20-23]. Therefore, assessing the overall antioxidant capacity of the body has lately become a major area of interest in biomedical research.

The *in vitro* evaluation of the influence of *benzothiazolic copper coordination compounds with thiosemicarbazones* on total antioxidant capacity at concentrations of 10.0 μM/L and 1.0 μM/L revealed that all tested compounds maintained or slightly enhanced TAC in a non-significant manner. Notably, MG-22 emerged as the most promising candidate, showing a consistent increase in TAC by 2% at both concentrations ($p > 0.05$ vs. control group).

In parallel, ASM was significantly elevated under the action of the local compound CMA-18, suggesting a substantial increase in antioxidant load. This may reflect an adaptive response to OS and potential activation of endogenous defense mechanisms. Meanwhile, CMD-8 induced a moderate increase in antioxidant content ($p > 0.001$), likely associated with mild OS and compensatory activation of antioxidant responses. By contrast, MG-22 induced the lowest increase in antioxidant mass, implying a diminished oxidative risk and a more sensitive cellular activation, with moderate effects on the antioxidant system.

The results of the evaluation of TAA under the influence of CMA-18 revealed a significant decrease at both concen-

trations, ranging from 18% to 25% ($p < 0.001$), indicating a pronounced pro-oxidant effect. This reduction in total antioxidant capacity suggests a redox imbalance. At the same time, the compound CMD-8 exhibited a milder effect, although it still led to a slight decrease in TAA, particularly at the lower concentration, with a reduction of 15% ($p < 0.01$). Conversely, MG-22 proved to be the most promising compound, showing only a minimal decrease in TAA with statistically significant values at both doses. This outcome suggests a favorable antioxidant profile, especially at the higher concentration.

All three compounds studied (CMA-18, CMD-8, and MG-22) demonstrated concentration- and structure-dependent modulation of *in vitro* antioxidant system parameters (Table 2).

1. CMA-18 exhibits a distinctly pro-oxidant profile, potentially associated with oxidative cytotoxic effects, as it significantly reduced both TAA and TAC to 75–82% of control values. Although it induced a substantial increase in ASM up to 130%, this appears to represent a compensatory cellular response rather than a protective effect.
2. CMD-8 demonstrates a moderate oxidative impact, accompanied by mild activation of compensatory antioxidant mechanisms. It is more balanced than CMA-18, causing a slight reduction in TAA and TAC, while inducing a moderate increase in ASM (111–114%). TAC levels remained near control values (100–101%), suggesting preserved systemic antioxidant function.
3. MG-22 presents the most favorable antioxidant profile, displaying well-regulated redox effects and potential for biomedical applications with low oxidative risk. It maintained TAC and TAA at values close to the control (95–102%) and induced only a minimal increase in ASM, indicating a limited oxidative stimulus and reduced impact on antioxidant defenses.

The evaluation of the TAA of the *phenyl group compounds* showed that CMC-34 demonstrated a significant decrease in antioxidant activity compared to the control at both tested concentrations (25% –26% reduction, $p < 0.001$), suggesting a strong inhibitory effect on antioxidant defense mechanisms. In contrast, CMJ-33, at both 10.0 μM/L and 1.0 μM/L, exhibited a slightly more favorable profile, with values of 77.05 μM/L; IQR 3.34; and 78.68 μM/L; IQR 3.28, corresponding to 92% and 94% of the control, respectively. These findings indicate an antioxidant activity nearly comparable to the control group (see Figure 2). CMT-67, at both concentrations (10.0 μM/L and 1.0 μM/L), did not show statistically significant deviations from the control, with values of 82.10 μM/L; IQR 5.12; and 83.28 μM/L; IQR 1.83; representing 98% and 99%, respectively. This outcome reflects a stable antioxidant effect, almost identical to that of the untreated samples.

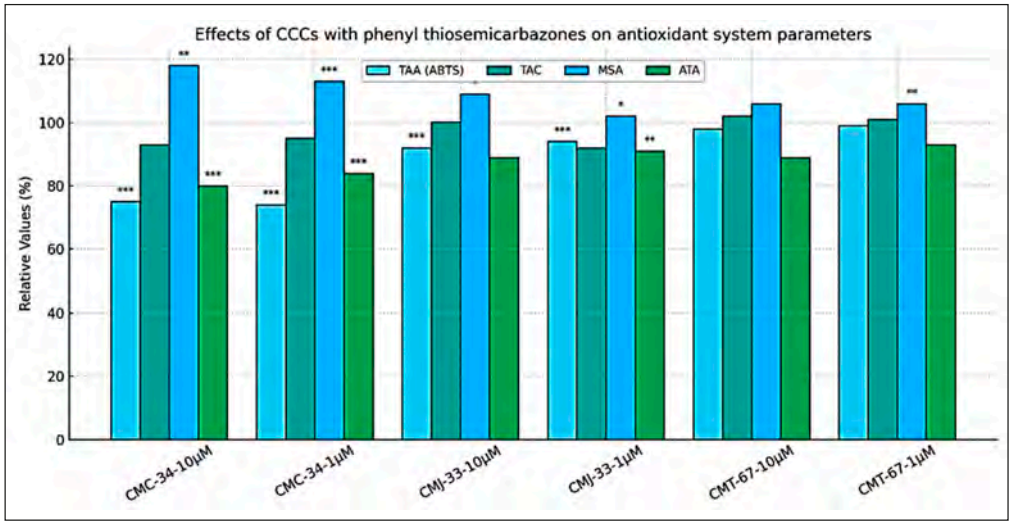

Fig. 2 In vitro effects of copper coordination compounds with phenyl thiosemicarbazones at 10.0 μm/l and 1.0 μm/l on antioxidant system parameters

***Note**: The values for the control group were taken as the reference (100%). Statistical significance relative to the control group: * – p< 0,05; ** – p< 0,01; *** – p< 0,001; TAA (ABTS): total antioxidant activity measured with ABTS; TAC: total antioxidant capacity; ASM: antioxidant substance mass; ATA: antioxidants total activity.*

Statistical analysis of TAC for the compound CMC-34 at both concentrations (10.0 μM/L and 1.0 μM/L) showed slightly reduced, non-significant values (5% and 7%). Similarly, CMJ-33 at the concentration of 1.0 μM/L also showed an inconclusive 8% decrease in TAC, while at the concentration of 10.0 μM/L TAC did not change compared to the control (by 0.2%). The compound CMT-67 demonstrated the best results among all tested compounds. At both concentrations of 10.0 μM/L and 1.0 μM/L, TAC values at the control level (+ 1% and 2%), indicating a a neutral and protective effect on the marker values. Therefore, among the phenyl group derivatives, the compound CMT-67 stands out as the most efficient in terms of total antioxidant capacity, with a clear stimulation of cellular defense against free radicals.

Evaluation results of ASM following the action of the phenyl compound CMC-34 showed the most significant increases: 18%, $p < 0.01$ (at 10.0 μM/L) and 13%, $p < 0.001$ (at 1.0 μM/L), compared to the control group. This suggests a clear activation of the antioxidant system as a compensatory response to oxidative stress. CMJ-33 induced a modest increase at both concentrations (2–9%), with statistically significant activation at 10.0 μM/L, $p < 0.05$. Meanwhile, for CMT-67, val-

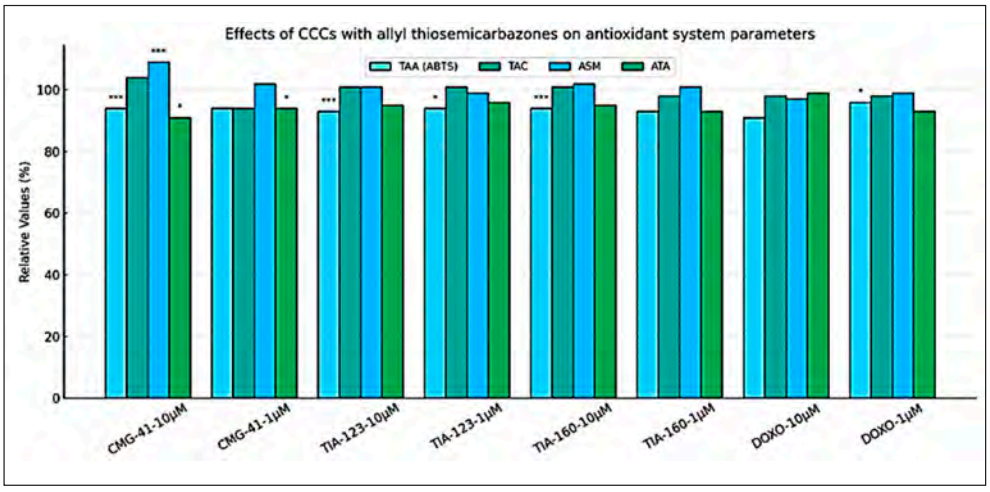

Fig. 3 The action of copper coordination compounds with allyl-thiosemicarbazone *in vitro* at concentrations of 10.0 μm/l and 1.0 μm/l on antioxidant system parameters

***Note**: The values for the control group were taken as the reference (100%). Statistical significance relative to the control group: * – p< 0,05; ** – p< 0,01; *** – p< 0,001; TAA (ABTS): total antioxidant activity measured with ABTS; TAC: total antioxidant capacity; ASM: antioxidant substance mass; ATA: antioxidants total activity.*

ues remained constant at both concentrations (6% increase), with significance only at 1.0 μM/L, $p < 0.01$ (Figure 3).

Statistical analysis of TAA under the influence of the local compound CMC-34 showed the lowest values at both concentrations (a 16-20% reduction), $p < 0.001$. These reductions indicate a clear pro-oxidant effect, reflecting redox imbalance. Following CMJ-33 administration, a moderate reduction of total antioxidant activity was observed at both concentrations (a 9–11% reduction), statistically significant only at 1.0 μM/L, $p < 0.01$. In the case of CMT-67, values remained relatively close to the control: 2.57 and 2.68 c.u. (a 7%–11% reduction). The effect was minimal and without notable statistical significance, indicating good antioxidant stability and maintenance of values close to control at both concentrations.

The three compounds studied (CMC-34, CMJ-33, CMT-67) demonstrated concentration- and structure-dependent modulation of antioxidant system parameters *in vitro* (Table 2).

1. CMC-34 exhibited a clear pro-oxidant profile, characterized by a significant decrease in TAA of 16–20% and a slight, non-significant reduction in TAC of 5–7%. Despite this redox imbalance, it triggered a notable enhancement in ASM - up to 18% at 10.0 μM/L - indicating compensatory activation of endogenous antioxidant defenses in response to OS.
2. CMJ-33 demonstrated a moderate oxidative effect, with a small reduction in TAA (9–11%) and marginal changes in TAC (0–8% decrease), suggesting partial impairment of antioxidant defenses. ASM increased slightly (2–9%), reflecting a modest cellular response to oxidative stimuli, particularly at the higher concentration. Overall, CMJ-33 maintained intermediate redox behavior with limited antioxidant disruption.
3. CMT-67 displayed the most stable redox profile within the phenyl group derivatives. TAA and TAC remained close to control levels (–7% to –11% and +1% to +2%, respectively), while ASM showed minimal increase (~6%), indicating preservation of redox balance. These findings suggest that CMT-67 exerts a neutral or slightly protective antioxidant effect, making it the most promising candidate among phenyl thiosemicarbazones.

The statistical results of total antioxidant activity (TAA) influenced by *CCCs with allyl-thiosemicarbazone*, tested *in vitro* at both concentrations, showed a reduction ranging from 6% to 7%. This decrease was statistically significant at 10.0 μM/L ($p < 0.001$), while at 1.0 μM/L, significance was observed for TIA-123 ($p < 0.05$), but not for CMG-41 and TIA-160 ($p > 0.05$). Additionally, the reference compound doxorubicin, tested *in vitro* as a positive control, showed the most pronounced reduction in antioxidant activity - by 9% at 10.0 μM/L ($p > 0.05$) and by 4% at 1.0 μM/L ($p < 0.05$) compared to the control group, as shown in Figure 3.

TAC values remained generally stable across all compounds, with only minor deviations from the control. Notably, CMG-41 at 10.0 μM/L slightly exceeded the control value by 4%, however at 1.0 μM/L, TAC decreased by 6% ($p > 0.05$). Other compounds (TIA-123, TIA-160, and DOXO) showed minimal variation, remaining within the 98–101% range relative to the control.

Regarding the antioxidant substance mass (ASM), a statistically significant increase was observed for CMG-41 at 10.0 μM/L (9%, $p < 0.001$), indicating a potential strong stimulation of antioxidant defense. For TIA-123, ASM remained close to control values with no relevant variation. TIA-160 also maintained nearly identical ASM values at both concentrations (2.71 and 2.70 c.u., ~101–102%), suggesting a consistent antioxidant effect. In contrast, doxorubicin produced a 1% to 3% decrease in ASM at both concentrations ($p > 0.05$), compared to the control group.

In the assessment of total antioxidant activity (TAA), CMG-41 demonstrated a statistically significant reduction of 6%–9% at both concentrations ($p < 0.05$). The other tested compounds produced insignificant reductions in TAA, ranging from 4% to 7% ($p > 0.05$). Similarly, statistical evaluation of doxorubicin revealed a modest decline in TAA of 1%–7% ($p > 0.05$), indicating a minimal influence on overall antioxidant activity.

The three compounds studied (CMG-41, TIA-123, TIA-160) demonstrated moderate and structure-sensitive antioxidant modulation *in vitro*.

1. CMG-41 exhibited a dual behavior, with a statistically significant reduction in TAA (6–9%) and a minor in-

crease in ASM (up to 9%), particularly at 10.0 μM/L, suggesting an adaptive antioxidant response to mild oxidative pressure. TAC showed a slight elevation (+4%) at the higher concentration, indicating possible activation of antioxidant reserves. This profile reflects a mild pro-oxidant potential with compensatory stimulation of defenses.

2. TIA-123 demonstrated a stable antioxidant effect, with only marginal reductions in TAA (4–5%) and minimal deviations in TAC (98–100%). ASM remained within normal range, reflecting limited oxidative impact. The results indicate a balanced redox profile, with low cellular stress induction and good tolerability across concentrations.
3. TIA-160 displayed the most favorable antioxidant behavior among allyl derivatives. Both TAA and TAC were well maintained, showing negligible variation from control values (1–2% difference). ASM also remained stable (~101–102%), suggesting excellent redox stability and minimal oxidative burden. This profile highlights TIA-160 as a potentially safe and biocompatible candidate for biomedical use.

Discussion

The present study demonstrates that copper coordination compounds with thiosemicarbazone (CCCTs) exhibit concentration- and structure-dependent redox modulation, disclosing distinct mechanisms of action across three structural classes. Our findings align with emerging research on metal-based therapeutics, particularly regarding their dual capacity to induce OS in malignant cells while preserving redox homeostasis in healthy systems.

Regarding redox profiling and structural correlations, the benzothiazole derivative MG-22 emerged as a lead compound, maintaining TAA and TAC near physiological levels (94–102% of control) while minimally elevating ASM (106–111%). This balanced profile suggests regulated ROS modulation without overwhelming antioxidant defenses, in clear opposition to the pronounced pro-oxidant effects of CMA-18 (TAA reduction to 76–82%). Such divergence underscores how ligand modifications (e.g., methoxy substitution in MG-22) critically determine biological outcomes. These observations resonate with studies showing that N4-methoxyphenyl thiosemicarbazones enhance copper complex stability and redox selectivity [2, 24].

The phenyl derivative CMT-67 displayed TAC conservation (101–102% of control), indicating sustained antioxidant stimulation. This aligns with evidence that CCCTs can activate endogenous antioxidant enzymes like superoxide dismutase (SOD) through copper ion delivery [25, 26]. Conversely, allyl derivatives (e.g., CMG-41) induced ASM spikes (109% increase) alongside a decrease in TAA, making evident adaptive cellular responses to moderate oxidative challenge.

Table 2. Comparative analysis of copper-based coordination compounds with different thiosemicarbazones.

Compound	TAA (% of Control)	TAC (% of Control)	ATA (% of Control)	ASM (% of Control)	Redox Interpretation
CMA-18	↓ 18–24% (76–82%)	≈ 99%	↓ 18–25% (75–82%)	↑ up to 130%	Strong pro-oxidant effect; cytotoxic potential; compensatory antioxidant response
CMD-8	↓ 10–18% (82–90%)	≈ 100–101%	↓ 8–15% (85–92%)	↑ 111–114%	Moderate oxidative effect; partial antioxidant compensation; balanced redox behavior
MG-22	≈ 94–99%	↑ up to 102%	≈ 95–98%	↑ 106–111%	Favorable redox profile; low oxidative burden; minimal stress response
CMC-34	↓ 16–20% (80–84%)	↓ 5–7%	↓ 18–20% (80–82%)	↑ 13–18%	Pro-oxidant behavior; significant oxidative burden; compensatory antioxidant activation
CMJ-33	↓ 9–11% (89–91%)	↓ 0–8%	↓ 9–11% (89–91%)	↑ 2–9%	Mild oxidative effect; limited stress induction; partial compensatory response
CMT-67	↓ 7–11% (89–93%)	≈ 101–102%	↓ 7–11% (89–93%)	↑ 6%	Stable redox behavior; preserved antioxidant function; minimal oxidative effect
CMG-41	↓ 6–9% (91–94%)	↑ 4% (at 10 μM/L)	↓ 6–9%	↑ 9%	Mild oxidative modulation; adaptive antioxidant stimulation
TIA-123	↓ 4–5% (95–96%)	≈ 98–100%	↓ 4–5%	≈ 100%	Balanced redox profile; negligible oxidative stress; good tolerability
TIA-160	↓ 4–7% (93–96%)	≈ 101–102%	↓ 4–7%	≈ 101–102%	Redox stability maintained; minimal stress response; potentially safe profile

Note: *Data are presented as percentage variation relative to the control group (set as 100%). TAA: Total Antioxidant Activity (assessed via ABTS assay); TAC: Total Antioxidant Capacity; ATA: Antioxidants Total Activity; ASM: Antioxidant Substance Mass. ↑ indicates increase vs. control; ↓ indicates decrease vs. control; ≈ indicates no significant change*

As for therapeutic implications for oncology, the pro-oxidant effects observed in CMA-18 and CMC-34 (TAA reduction to 75–85%) may exploit the "redox vulnerability" of cancer cells, which operate at higher basal ROS levels than healthy cells [24, 26]. This supports the therapeutic strategy of further elevating OS in malignancies to trigger selective cytotoxicity, a concept that was validated by the copper-thiosemicarbazones' ability to induce cuproptosis, a copper-dependent cell death pathway [25, 28]. Notably, MG-22's redox-neutral profile suggests potential as a cytoprotective addition to conventional chemotherapeutics, mitigating treatment-induced oxidative damage.

In order to summarize the mechanistic considerations of our study, the compounds' divergent effects on antioxidant parameters (TAA, TAC, ASM) likely reflect a copper redox cycling, as thiosemicarbazone ligands facilitate Cu(II)/

Cu(I) transitions, generating ROS *via* Fenton-like reactions [27, 29]; an enzyme interaction, as CCCTs may directly modulate SOD/catalase activity or expression, as evidenced by TAC stabilization in CMT-67-treated samples and cellular adaptation, as ASM elevations (e.g., 130% with CMA-18) represent compensatory antioxidant synthesis, consistent with Nrf2 pathway activation observed in other thiosemicarbazone-treated models [26, 30].

This study provides a solid foundation for future research directions but also has several limitations. Although the *in vitro* model used here provides valuable insights into redox modulation, a key limitation is the lack of testing of the compounds in standardized and pathological cell lines, including tumor-derived cells, limiting the translational significance of the results. Further studies are needed to evaluate the effects of the tested compounds on specific oxidative stress biomarkers and to conduct correlation analyses to establish a comprehensive understanding of their pro- or antioxidant potential. Future studies should also confirm these results in disease-related models, particularly those assessing tumor growth inhibition. Additionally, evaluation of CCCTs in combination with ROS-enhancing therapies such as radiotherapy and in-depth investigation of copper chelation dynamics using advanced techniques such as X-ray absorption spectroscopy are needed to fully elucidate the therapeutic potential of these novel native compounds.

CCCTs represent a promising class of redox modulators with tunable biological effects. Structural optimization (e.g., benzothiazole with methoxy groups) yields compounds like MG-22 that maintain redox equilibrium, while pro-oxidant variants (CMA-18) offer therapeutic potential through selective oxidative cytotoxicity. These findings underscore copper-thiosemicarbazones' versatility in targeting oxidative stress pathways for oncological applications.

Conclusions

Copper coordination compounds with thiosemicarbazone demonstrate significant biomedical potential owing to their redox-active properties and multifunctional bioactivities, including antitumor, antimicrobial, and antioxidant effects. These compounds exhibit complex modulation of antioxidant pathways, dynamically influencing the equilibrium between reactive oxygen species (ROS) generation and cellular antioxidant defenses.

In vitro investigations reveal specific thiosemicarbazones alter antioxidative defense markers: total antioxidant activity; total antioxidant capacity; mass of antioxidant substances; antioxidant total activity, impairing cellular ROS-neutralizing capacity. Such modulation suggests therapeutic utility in pathologies driven by oxidative stress, including degenerative disorders, inflammatory conditions, and multifactorial diseases.

Competing interests

None declared.

Authors' contributions

VP conceived the study, designed the study, analyzed the data, drafted the manuscript. EP participated in study design, statistical analysis and helped drafting the manuscript. SS critically revised the manuscript and analyzed the data. OT, VG obtained project funding, critically evaluated the results and assessed their applicability. AG offer the analyzed compounds and critically revised the manuscript. All authors reviewed the work critically and approved the final version of the manuscript.

Informed consent for publication

Obtained.

Acknowledgements and funding

The research was funded by the Government of the Republic of Moldova, Ministry of Education and Research, under the institutional subprogram Non-communicable diseases – prevention, diagnosis and personalized treatment (Code 080101, implementation period 2024-2027).

Ethics approval

The study protocol was approved by the Research Ethics Committee of the *Nicolae Testemițanu* State University of Medicine and Pharmacy, under approval no. 5, ref. no. 38, dated June 20, 2024. The study was conducted in compliance with the Declaration of Helsinki and its subsequent amendments, regarding the use of human subjects in research.

Provenance and peer review

Not commissioned, externally peer review.

References

1. Pantea V, Cobzac V, Tagadiuc O, Palarie V, Gudumac V. *In vitro* evaluation of the cytotoxic potential of thiosemicarbazide coordinating compounds in hepatocyte cell culture. Biomedicines. 2023;11(2):366. https://doi.org/10.3390/biomedicines11020366.
2. Shakya B, Yadav PN. Thiosemicarbazones as potent anticancer agents and their modes of action. Mini Rev Med Chem. 2020;20(8):638-661. doi: 10.2174/1389557519666191029130310.
3. Krasnovskaya O, Naumov A, Guk D, Gorelkin P, Erofeev A, et. al. Copper coordination compounds as biologically active agents. Int J Mol Sci. 2020;21(11):3965. doi: 10.3390/ijms21113965.
4. Neguta E, Balan G, Gulea A, et al. Antimicrobial and antifungal activity of Cu(II) and Bi(III) complexes based on amino-polycarboxylate ions and 2-formyl and 2-acetylpyridine thiosemicarbazones. One Health Risk Manag [Internet]. 2021;2(4S):52 [cited 2025 Apr 12]. Available from: https://journal.ohrm.bba.md/index.php/journal-ohrm-bba-md/article/view/220.
5. Pantea V, Andronache L, Globa P, Pavlovschi E, Gulea A, Tagadiuc O, Gudumac V. Copper coordination compounds with thiosemicarbazones: *In vitro* assessment of their potential in inhibiting glioma viability and proliferation. Arch Balk Med Union. 2023;58(3):234-244. https://doi.org/10.31688/ABMU.2023.58.3.02.
6. Kim SJ, Kim HS, Seo YR. Understanding of ROS-inducing strategy in anticancer therapy. Oxid Med Cell Longev. 2019;2019:5381692. doi: 10.1155/2019/5381692.

7. Trapali M, Pavlidis V, Karkalousos P. Molecular insights into oxidative stress and its clinical implications. Open Med Chem J. 2025;19:e18741045373435. http://dx.doi.org/10.2174/0118741045373435250415115811.
8. Zalewska-Ziob M, Adamek B, Kasperczyk J, Romuk E, Hudziec E, et. al. Activity of antioxidant enzymes in the tumor and adjacent noncancerous tissues of non-small-cell lung cancer. Oxid Med Cell Longev. 2019;2019:2901840. doi: 10.1155/2019/2901840.
9. Rusu ME, Fizeşan I, Vlase L, Popa DS. Antioxidants in age-related diseases and anti-aging strategies. Antioxidants (Basel). 2022;11(10):1868. doi: 10.3390/antiox11101868.
10. Gorrini C, Harris IS, Mak TW. Modulation of oxidative stress as an anticancer strategy. Nat Rev Drug Discov. 2013;12(12):931-47. doi: 0.1038/nrd4002.
11. Puri KS, Suresh KR, Gogtay NJ, Thatte UM. Declaration of Helsinki, 2008: implications for stakeholders in research. J Postgrad Med. 2009;55(2):131-4. doi: 10.4103/0022-3859.52846.
12. Gulea A, Poirier D, Roy J, Stavila V, Bulimestru I, et. al. *In vitro* antileukemia, antibacterial and antifungal activities of some 3d metal complexes: chemical synthesis and structure - activity relationships. J Enzyme Inhib Med Chem. 2008;23(6):806-18. https://doi:10.1080/14756360701743002.
13. Pantea V. Efectele metabolice ale compuşilor biologic activi autohtoni cu acţiune antitumorală [The metabolic effects of native bioactive compounds with antitumor activity] [dissertation]. Chisinau: Nicolae Testemiţanu State University of Medicine and Pharmacy; 2023. 128 p. Romanian.
14. Re R, Pellegrini N, Proteggente A, Pannala A, Yang M, Rice-Evans C. Antioxidant activity applying an improved ABTS radical cation decolorization assay. Free Radic Biol Med. 1999;26 (9-10):1231-7. doi: 10.1016/s0891-5849(98)00315-3.
15. Zhang M, Liu N, Liu H. Determination of the total mass of antioxidant substances and antioxidant capacity per unit mass in serum using redox titration. Bioinorg Chem Appl. 2014;2014:928595. doi: 10.1155/2014/928595.
16. Gudumac V, Rîvneac V. Tagadiuc O, et al. Metode de cercetare a metabolismului hepatic: Elaborare metodică [Methods of investigating liver metabolism: Methodological guidelines] Chişinău; 2012. 162 p. Romanian.
17. Tagadiuc O, Andronache L, Pantea V, Gudumac V, Şveţ I, Sardari V. Metodă pentru determinarea capacităţii antioxidante totale, masei substanţelor antioxidante şi a activităţii mediia antioxidanţilor în probele biologice [Method for determining total antioxidant capacity, mass of antioxidant substances and average antioxidant activity in biological samples]. Republic of Moldova Certificate of Innovation no. 5641. 2018 March 26.
18. Ryzhikova SL, Druzhinina IuG, Riabicheva TG, Varaksin NA. Standartizatsiia metodiki opredeleniia produktsii tsitokinov kletkami krovi ex vivo [The standardization of technique of detection of blood cells cytokine production ex vivo. Klin Lab Diagn. 2011;(11):49-53. Russian.
19. Hood E, Simone E, Wattamwar P, Dziubla T, Muzykantov V. Nanocarriers for vascular delivery of antioxidants. Nanomedicine (Lond). 2011;6(7):1257-72. doi: 10.2217/nnm.11.92.
20. Zhang M, Liu N, Liu H. Determination of the total mass of antioxidant substances and antioxidant capacity per unit mass in serum using redox titration. Bioinorg Chem Appl. 2014;2014:928595. doi: 10.1155/2014/928595.
21. Kattamis C, Lazaropoulou C, Delaporta P, Apostolakou F, Kattamis A, et al. Disturbances of biomarkers of iron and oxidant-antioxidant homeostasis in patients with beta-thalassemia intermedia. Pediatr Endocrinol Rev. 2011;8 Suppl 2:256-62.
22. Zujko ME, Witkowska AM. Dietary antioxidants and chronic diseases. Antioxidants (Basel). 2023;12(2):362. doi: 10.3390/antiox12020362.
23. Munteanu IG, Apetrei C. Analytical methods used in determining antioxidant activity: a review. Int J Mol Sci. 2021;22(7):3380. doi: 10.3390/ijms22073380.
24. Rusnac R, Garbuz O, Kravtsov V, Melnic E, Istrati D, Tsapkov V, Poirier D, Gulea A. Novel copper(II) coordination compounds containing pyridine derivatives of N4-methoxyphenyl-thiosemicarbazones with selective anticancer activity. Molecules. 2024;29(24):6002. doi: 10.3390/molecules29246002.
25. Vo TTT, Peng TY, Nguyen TH, Bui TNH, Wang CS, Lee WJ, Chen YL, Wu YC, Lee IT. The crosstalk between copper-induced oxidative stress and cuproptosis: a novel potential anticancer paradigm. Cell Commun Signal. 2024;22(1):353. doi: 10.1186/s12964-024-01726-3.
26. Zilka O, Poon JF, Pratt DA. Radical-trapping antioxidant activity of copper and nickel bis(thiosemicarbazone) complexes underlies their potency as inhibitors of ferroptotic cell death. J Am Chem Soc. 2021;143(45):19043-19057. doi: 10.1021/jacs.1c08254.
27. Singh NK, Yadav PN, Kumbhar AA, Pokhrel YR. Anticancer potency of copper(II) complexes of thiosemicarbazones. J Inorg Biochem. 2020:111134. doi: 10.1016/j.jinorgbio.2020.111134.
28. Luo M, Zhou L, Huang Z, Li B, Nice EC, Xu J, Huang C. Antioxidant therapy in cancer: rationale and progress. Antioxidants (Basel). 2022;11(6):1128. doi: 10.3390/antiox11061128.
29. Kowol CR, Heffeter P, Miklos W, Gille L, Trondl R, Cappellacci L, Berger W, Keppler BK. Mechanisms underlying reductant-induced reactive oxygen species formation by anticancer copper(II) compounds. J Biol Inorg Chem. 2012;17(3):409-23. doi: 10.1007/s00775-011-0864-x.
30. Leal M, Silva M, Marques D, Mendes R, Ximenes R, Machado D, Silva Jj, Rodrigues C, Cruz F, Lima M. Preliminary evaluation of the toxicological, antioxidant and antitumor activities promoted by the compounds 2,4-dihydroxybenzylidene-thiosemicarbazones an in silico, in vitro and in vivo study. An Acad Bras Cienc. 2024;96(2):e20231247. doi: 10.1590/0001-3765202420231247.

https://doi.org/10.52645/MJHS.2025.3.17

UDC: 616.831-005-07-08(478)

RESEARCH ARTICLE

The effectiveness of using a checklist in prehospital stroke interventions in the Republic of Moldova

Natalia Catanoi[1,2], Mihail Peștereanu[1*], Larisa Rezneac[1,2], Natalia Mocanu[1]

[1]*Gheorghe Ciobanu* Department of Emergency Medicine, *Nicolae Testemițanu* State University of Medicine and Pharmacy, Chișinău, Republic of Moldova
[2]Institute of Emergency Medicine, Chisinau, Republic of Moldova

ABSTRACT

Introduction. Stroke remains a major cause of mortality and disability in Moldova and globally. Rapid prehospital intervention is critical for improving outcomes. The adoption of standardized protocols and checklists has enhanced the efficiency of emergency medical services (EMS), especially in stroke recognition and initial management.

Materials and methods. A systematic review of the literature and analysis of statistical data from the National Prehospital Emergency Medical Service were conducted. The study focused on evaluating the use and impact of checklists during prehospital stroke interventions.

Results. Between 2022 and 2023, over 12,000 stroke cases were recorded annually. The implementation of national checklists, in conjunction with the Face, Arm, Speech, Time scale, significantly improved early identification, triage, and transport to specialized centers. Notable outcomes included a higher rate of thrombolysis and thrombectomy, improved coordination, and a modest reduction in overall response time. However, delays due to inter-hospital transfers remain a challenge.

Conclusions. The systematic use of checklists in prehospital stroke management in Moldova proved effective in standardizing care, accelerating intervention, and improving patient outcomes. Continued training and system reorganization are crucial to fully capitalize on these tools and to reduce stroke-related morbidity and mortality.

Keywords: stroke, prehospital, checklist, emergency medical services, thrombolysis, thrombectomy, Moldova, EMS protocols.

Cite this article: Catanoi N, Peștereanu M, Rezneac L, Mocanu N. The effectiveness of using a checklist in prehospital stroke interventions in the Republic of Moldova. Mold J Health Sci. 2025;12(3):110-116. https://doi.org/10.52645/MJHS.2025.3.17.

Manuscript received: 16.07.2025

Accepted for publication: 22.08.2025

Published: 15.09.2025

***Corresponding author: Mihail Peștereanu**, MD, assistant professor
Gheorghe Ciobanu Department of Emergency Medicine
Nicolae Testemițanu State University of Medicine and Pharmacy
1 Toma Ciorbă str., Chisinau, Republic of Moldova, MD2004
e-mail: mihail.pestereanu@usmf.md

Authors' ORCID IDs
Natalia Catanoi – https://orcid.org/0000-0002-5838-0363
Mihail Pestereanu – https://orcid.org/0000-0002-9797-2919
Larisa Rezneac – https://orcid.org/0000-0001-7545-1728
Natalia Mocanu – https://orcid.org/0000-0001-5989-4553

Key messages

What is not yet known about the issue addressed in the submitted manuscript

The quality and limitations of prehospital stroke care in the Republic of Moldova are not well understood. There is a lack of research on the use of checklists and on the impact of logistical barriers in this context.

The research hypothesis

The implementation of a standardized checklist during prehospital stroke interventions is associated with a significant improvement in the quality, consistency, and coordination of care delivered by emergency medical services teams in the Republic of Moldova.

The novelty added by the manuscript to the already published scientific literature

This study is the first to evaluate prehospital stroke care in Moldova and to assess the effectiveness of a checklist adapted to the national context. It identifies key barriers and proposes practical improvements for timely and standardized care.

Introduction

Stroke is one of the most critical medical emergencies and a major cause of mortality and disability both in the Republic of Moldova and globally. Early recognition and rapid intervention are key factors that can mean the difference between life and death, or between full recovery and permanent disability. In this context, the role of prehospital intervention is of paramount importance.

In a healthcare system undergoing modernization and alignment with international standards, the Republic of Moldova is increasingly prioritizing the initial stages of medical response. The implementation of standardized tools, such as checklists, has become essential in optimizing the performance of emergency response teams. These tools help standardize patient assessment, reduce response times, and ensure effective communication between prehospital services and specialized hospital units [1].

Checklists not only support swift decision-making in the field but also provide a clear and scientifically validated framework for applying diagnostic and treatment protocols tailored to local realities. Their systematic use can significantly improve the quality of prehospital care, reduce medical errors, and increase the chances of survival and recovery for stroke patients.

This article evaluates the effectiveness of using checklists in prehospital stroke interventions in the Republic of Moldova, based on an analysis of national statistical data and a systematic review of the scientific literature, including relevant examples from international experience.

Globally, various preventive strategies have been developed to combat acute neurological conditions, especially cerebrovascular diseases, which pose a significant burden on healthcare systems. These strategies reflect the efforts of countries and international organizations to reduce the incidence and impact of such conditions on public health.

The Republic of Moldova's commitment to reducing the incidence and impact of cerebrovascular diseases is reflected in governmental and intersectoral efforts to implement preventive measures and coordinated interventions. National and international strategies for the prevention of acute neurological pathologies emphasize the importance of a well-coordinated approach, adapted to each country's specific context, focused on risk reduction and improved access to diagnosis and treatment.

Reviews indicate that prehospital protocols and stroke-specific checklists (e.g., Face, Arm, Speech, Time (FAST), Cincinnati-based algorithms) enhance diagnostic accuracy, coordination, and time efficiency. In the Moldovan context, the FAST and Cincinnati scales were systematically adopted by emergency teams between 2017 and 2021, contributing to more rapid stroke recognition in the prehospital stage [2-5].

Through these integrated strategies, countries can reduce the incidence of acute neurological diseases, thus contributing to global public health and alleviating pressure on healthcare systems. These examples provide models of best practices for any state seeking to strengthen public health and reduce the burden of cerebrovascular disease [6, 7].

The prompt response of Emergency Medical Services (EMS) teams in the prehospital setting is crucial, and the use of protocols plays an important role in ensuring a fast and effective response. These tools enable emergency teams to perform a systematic assessment of the patient's condition and make the right decisions for stabilization and transport. Standardized protocols provide clear guidance, helping ambulance crews recognize and manage neurological emergencies, thereby reducing response times and the risk of complications [8].

International standardization: Organizations such as the WHO, the American Heart Association (AHA), and the European Stroke Organization (ESO) promote standardized algorithms and checklists like ABCDE (Airway, Breathing, Circulation, Disability, Exposure) and SCALE (Screening for Acute Stroke). These frameworks offer a unified structure for EMS teams across different countries, facilitating comparability and efficiency in stroke management. International algorithms are supported by research and studies demonstrating their effectiveness in reducing response times and improving patient outcomes [9, 10].

Material and methods

This observational, retrospective, and descriptive study combined a systematic literature review with a quantitative statistical analysis of national data from the National Prehospital Emergency Medical Service (NPHEMS) of the Republic of Moldova. The aim was to assess the effectiveness of using checklists during prehospital stroke interventions and their impact on the quality of intervention and response times.

Data sources and selection. The analysis included all stroke cases recorded in the national prehospital database between January 1, 2022, and December 31, 2023. Data were extracted from standardized emergency medical service records, including checklist use, algorithm compliance (e.g., FAST, ABCDE), dispatch-to-arrival times, initial evaluation, stabilization, and transport intervals.

A systematic review of scientific publications indexed in PubMed, Scopus, and Google Scholar was also conducted to contextualize the findings with international practices and to support methodological consistency.

Participants and inclusion criteria. Patients included in the analysis met the following criteria:

- Suspected stroke according to dispatch notes or prehospital diagnosis;
- Managed by mobile emergency teams during the specified period;
- Checklist or stroke-specific protocol (FAST, SCALE) documented in the patient chart;
- Use of the "Checklist for the assessment of a patient with suspected stroke in the prehospital stage," which is a method of data collection and a tool that facilitates the establishment of a preliminary diagnosis at the prehospital stage in 2023. The checklist was developed by the authors of the study, based on international recommendations, and adapted to the national context in cooperation with the National

Prehospital Emergency Medical Assistance Service. This wording serves to clarify that the checklist is not internationally standardized, but rather derived from best practices and adapted to local requirements.

Exclusion criteria:

- Incomplete documentation;
- Secondary stroke diagnosis not confirmed or unrelated dispatch code.

Data collection and processing. Data collected through the NPHEMS internal reporting system and structured questionnaires were entered into Microsoft Excel (Microsoft Corp., 2021) for preliminary data processing. Statistical analysis was performed using variational methods (mean, standard deviation, frequency distribution); comparative and correlational analysis (χ^2, Pearson's correlation); and discriminant analysis for evaluating intergroup differences in response time and outcomes. For extended statistical evaluation, MedCalc® Statistical Software v.20.218 (2023) was used. A p-value <0.05 was considered statistically significant.

Results and discussion

Neurological emergencies pose a significant challenge for Emergency Medical Services (EMS) in the prehospital stage, being among the conditions with the highest rates of misdiagnosis. This difficulty is amplified by the acute nature of such cases and the necessity for rapid intervention within the therapeutic window to prevent irreversible neurological deterioration. Although it is well understood that every minute counts and that timely and correct prehospital interventions can significantly impact patient prognosis, delays at this stage remain frequent [11, 12].

In the Republic of Moldova, the recognition and management of stroke in the prehospital setting are currently based on the use of the FAST scale, applied both by the medical dispatch center and emergency response teams. This method facilitates the rapid identification of clinical signs of stroke, allowing for prompt and effective intervention.

To improve and standardize prehospital interventions in stroke cases, a specific national checklist has been proposed for the management of this condition. The "Checklist

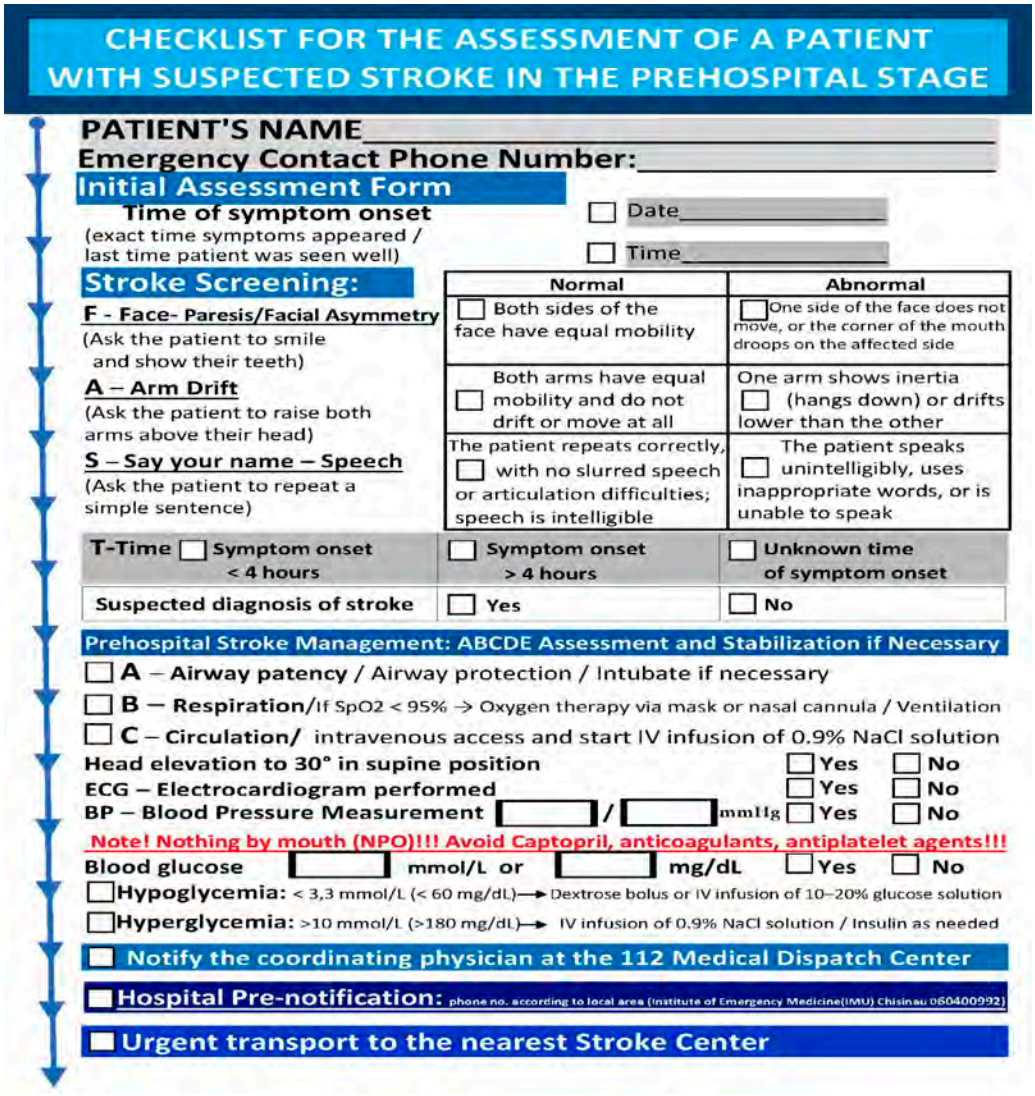

Fig. 1 Checklist for the assessment of a patient with suspected stroke in the prehospital stage

for the assessment of a patient with suspected stroke in the prehospital stage," implemented in 2023, supports medical personnel during the prehospital phase of care (Fig. 1). This tool aims to ensure a unified and comprehensive approach to the evaluation and treatment of stroke patients in the prehospital phase. The uniform adoption and implementation of checklists and specific guidelines, including at the medical dispatch level, are essential for optimizing patient care and reducing stroke-related mortality and morbidity [13] (Fig. 1).

According to data from the National Prehospital Emergency Medical Service, in 2022, 795,884 calls were serviced - 436,820 in urban areas and 359,064 in rural areas. In 2023, the total number of calls decreased to 744,456, with 397,460 recorded in urban areas and 346,996 in rural areas.

Neurological and neurosurgical emergencies represented a significant proportion during both years. In 2022, 106,152 such cases were reported (54,230 urban and 51,922 rural), and in 2023, the figure remained relatively stable at 104,993 cases (53,573 urban and 51,420 rural). Of these, over 25,000 patients required transport to emergency departments (EDs) each year. Special attention is given to stroke, which accounted for approximately 12,400 cases annually. Among them, the majority were reported as unspecified strokes – over 10,000 cases per year. Ischemic, hemorrhagic, and transient strokes made up the remainder, with a decreasing trend observed in ischemic cases (from 1,358 in 2022 to 867 in 2023).

Age group analysis shows that older adults are the most affected. In both years, the majority of stroke cases occurred in patients over the age of 60. In 2023, 4,025 cases were recorded in the 60–70 age group and 6,262 cases among those over 70. The age group under 50 accounted for less than 6% of all stroke cases. The urban-rural distribution remained relatively balanced across all age groups, with a slight predominance of rural cases in the older age categories (Fig. 2) [14, 15].

In 2022, the average response time to stroke (CVA) cases was 13.23 minutes, while in 2023 it slightly increased to 13.4 minutes. Although the difference is minimal, it may reflect factors such as an increased number of calls, longer travel distances, or possible logistical delays (Fig. 3).

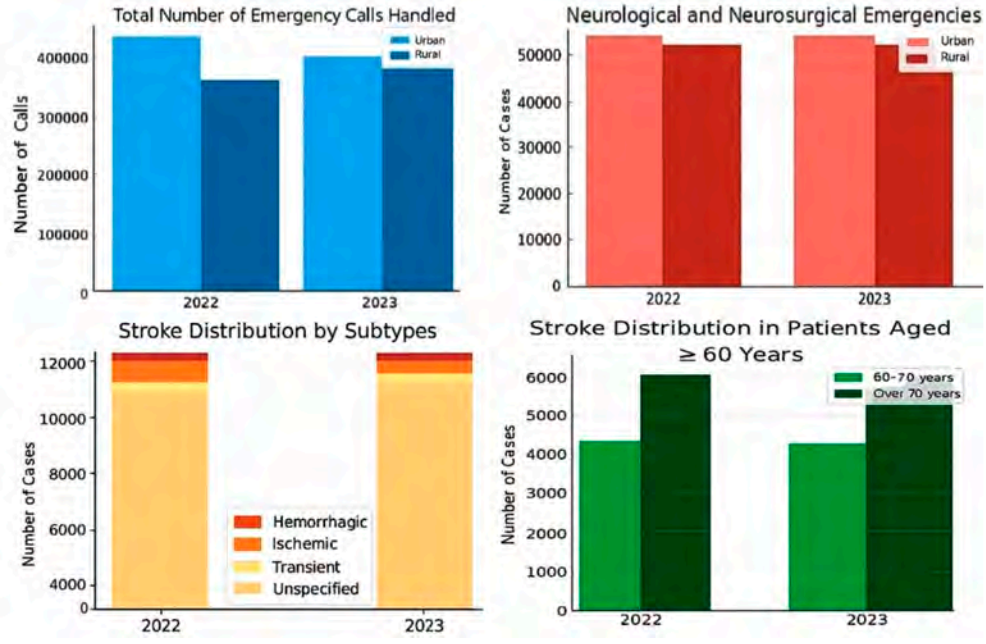

Fig. 2 Evolution of neurological emergency requests in the Republic of Moldova in 2022–2023

***Note**: The upper-left panel illustrates the total number of emergency calls managed, disaggregated by urban and rural areas. The upper-right panel presents neurological and neurosurgical emergency cases by location. The lower-left panel shows stroke cases by subtype (ischemic, hemorrhagic, transient, and unspecified). The lower-right panel indicates stroke distribution among elderly patients aged 60–70 and over 70. The figure highlights a stable volume of neurological emergencies with sustained demand among older age groups.*

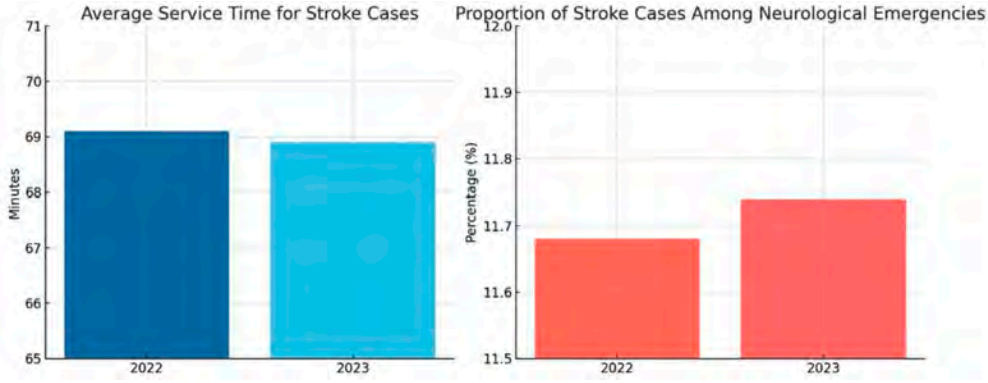

Fig. 3 Trends in Stroke Case Management and Proportion Among Neurological Emergencies in the Prehospital stage, 2022–2023

***Note**: The left panel illustrates a slight reduction in the average service time for stroke cases between 2022 and 2023, indicating a modest improvement in operational efficiency. The right panel shows a marginal increase in the proportion of stroke cases among all neurological emergencies, potentially reflecting enhanced diagnostic accuracy and prehospital identification of stroke.*

The total duration of managing a stroke case – which includes response time, patient evaluation, first aid, and transport to the hospital – has remained relatively stable in recent years. In 2022, the average service time was 69.1 minutes, and in 2023, it slightly decreased to 68.9 minutes. This modest improvement can be attributed to the more efficient application of intervention protocols and the growing experience of emergency teams.

The proportion of stroke cases among all neurological and neurosurgical emergencies has been steadily increasing. In 2022, it was 11.68%, and in 2023, it reached 11.74%. This trend may indicate either a slight increase in the incidence of strokes or an improvement in the identification, diagnosis, and reporting processes.

An essential indicator of prehospital care quality is the percentage of stroke patients transported directly to specialized facilities. As of November 2023, only two tertiary hospitals – the Institute of Emergency Medicine and the *Diomid Gherman* Institute of Neurology and Neurosurgery in Chisinau – met the criteria to function as multidisciplinary stroke centers. In 2022, 92.8% of patients were transported to these centers, with this figure increasing to 94.2% in 2023, reflecting an improvement in triage capacity and patient routing to appropriate structures.

However, due to the absence of a functional regional network, many patients continued to be initially transported to district hospitals before being transferred to specialized centers in Chișinău. This practice caused significant delays, even for patients identified within the therapeutic window, severely limiting access to specific treatments such as intravenous thrombolysis or mechanical thrombectomy.

As a result, inter-hospital transfers of stroke patients increased significantly from 268 cases in 2022 to 403 cases in 2023. This trend reflects a structural imbalance rather than an increase in efficiency, underlining the need for a functional reorganization of the emergency stroke care system, which was initiated in 2023 (Fig. 4).

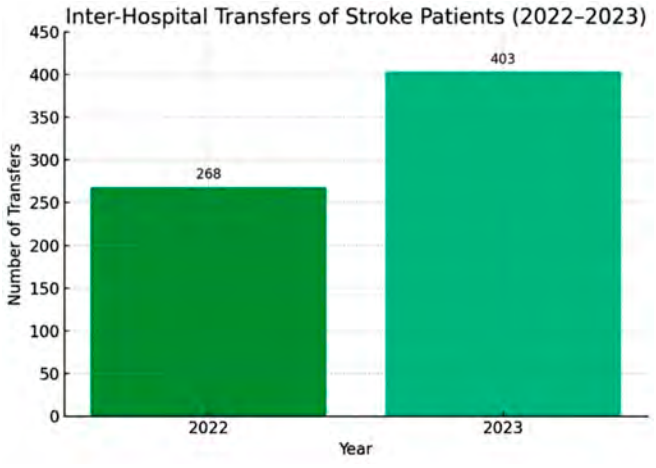

Fig. 4 Interhospital transfers of stroke patients in 2022–2023

Note: *The bar chart shows the number of stroke patients transferred between hospitals in Moldova in 2022 (n = 268) and 2023 (n = 403). The observed increase suggests a growing need for timely access to specialized stroke care. This trend underscores systemic inefficiencies and reinforces the necessity for continued structural reforms in emergency stroke services.*

To address the existing dysfunctions in the management of stroke cases, the Ministry of Health of the Republic of Moldova proposed, during the College meeting on June 29, 2022, the Concept of Functional and Regional Reorganization of the Stroke Reference, Diagnosis, and Treatment System. This concept provides for organizing services on three levels: Primary Stroke Centers, intended for rapid initial interventions; Multidisciplinary Stroke Centers, for managing complex cases; and a Comprehensive Stroke Center, dedicated to severe cases and coordinated by the Institute of Emergency Medicine in Chișinău [16].

Following the opening of 11 primary stroke centers, a significant increase in the number of thrombolysis performed nationwide was recorded. At the Institute of Emergency Medicine, the thrombolysis rate increased by approximately 61% compared to 2022, highlighting the positive impact of the reorganization on treatment time and access. Additionally, the rate of thrombectomies performed at IEM saw a remarkable rise of about 121%, reflecting both an improvement in technical capacity and the flow of eligible patients [17].

A key indicator for evaluating the quality of rapid intervention is the reduction of critical times, such as door-to-CT time and door-to-treatment administration time. In 2023, these indicators showed a monthly decreasing trend, suggesting better coordination between emergency medical teams and hospital staff [18].

Furthermore, approximately 30% of thrombectomies performed at the Institute of Emergency Medicine in Chișinău were carried out on patients transferred from primary stroke centers, reflecting the effective functioning of the new referral network and the strengthening of the clinical pathway for stroke patients.

A notable progress in 2024 was that the primary stroke centers in the district hospitals of Florești, Căușeni, Hîncești, and Soroca performed intravenous thrombolysis procedures for the first time. At the primary center level, the thrombolysis rate stood at 9.3%, a promising indicator for a system in the process of development and consolidation [17, 19].

Equally important was the integration of standardized checklists in the prehospital phase, which significantly contributed to the streamlining of stroke care. These checklists enabled EMS teams to assess neurological symptoms more systematically, reduce diagnostic uncertainty, and ensure the timely relay of essential clinical information to receiving hospitals. Their implementation helped unify the prehospital approach across regions, facilitated earlier identification of eligible candidates for reperfusion therapy, and reduced the risk of delays caused by incomplete or inconsistent initial evaluations.

These advancements reflect the efforts of the Republic of Moldova to build a modern and functional healthcare system that provides rapid, standardized, and high-quality interventions for stroke patients. During the analyzed period, a positive trend in the quality and efficiency of prehospital services

is evident, demonstrated by reduced service times, increased transport rates to specialized centers, and improved early recognition of clinical signs by emergency teams.

To optimize the initial assessment of neurological patients, implementing standardized checklists for all acute neurological conditions is essential. Although the FAST scale remains a valuable tool for rapid stroke identification, recent evidence demonstrates that more comprehensive checklists significantly improve diagnostic accuracy, interprofessional communication, and early initiation of treatment protocols. For example, a 2023 study validating a prehospital nomogram for differentiating hemorrhagic from ischemic stroke showed enhanced triage precision [20]. Moreover, a quality improvement initiative in emergency departments reported that using stroke evaluation checklists increased the odds of delivering thrombolytic therapy within 60 minutes of arrival (OR 6.4; 95% CI 1.1–68.7), underscoring the benefit of structured tools in acute neurological care [3].

The present study is constrained to the prehospital stage in the Republic of Moldova, within the context of the application of the checklist by emergency medical teams.

Conclusions

The implementation of standardized checklists in the prehospital management of stroke has improved the accuracy, timeliness, and coordination of emergency medical interventions in the Republic of Moldova. These tools, alongside system-wide reorganization, have contributed to increased access to reperfusion therapies and better clinical outcomes. Continued integration and training remain essential to sustain these improvements and reduce stroke-related morbidity and mortality.

Competing interests

None declared.

Authors' contributions

NC – substantial contribution to the conception and design of the work, substantial contribution to data acquisition, substantial contribution to data analysis and interpretation, taking responsibility for and being accountable for all aspects of the work. MP – substantial contribution to the conception and design of the work, substantial contribution to data acquisition, substantial contribution to data analysis and interpretation, drafting the article, taking responsibility for and being accountable for all aspects of the work. LR – critical review of the article for important intellectual content, taking responsibility for and being accountable for all aspects of the work. NM – drafting the article. All authors critically reviewed the work and approved the final version of the manuscript.

Informed consent for publication

Informed consent was not required, as only anonymized, retrospective data were used and no direct patient involvement occurred.

Acknowledgements and funding

No external funding was received.

Ethics approval

The study protocol was approved by the Research Ethics Committee of the *Nicolae Testemițanu* State University of Medicine and Pharmacy (no. 38, dated 02.04.2013).

Provenance and peer review

Not commissioned, externally peer-reviewed.

References

1. Manole E, Tiu C, Vilionskis A, Tsiskaridze A, Zota E, Grecu A, et al. Stroke care indicators in the Republic of Moldova – the RES-Q registry. Mold J Health Sci. 2022;(1):32-34. https://doi.org/10.52645/MJHS.2022.1.03
2. Ministerul Sănătății al Republicii Moldova [Ministry of Health of the Republic of Moldova]; Groppa S, Gavriliuc M, Zota E, et al. Accidentul vascular cerebral ischemic: Protocol clinic național [Ischemic stroke: National clinical protocol]. Chisinau: The Ministry; 2017. 112 p. (PCN-13). Romanian.
3. Elam M, Moyal-Smith R, Canfora M, Cohen W, Eum KD, Fischer C, Margo J, McCune M, Moin O, Selim M, Wendell L, Kumar S. A checklist to improve acute stroke evaluation and treatment in the emergency department. Am J Med Qual. 2025 Mar-Apr 01;40(2):53-63. doi: 10.1097/JMQ.0000000000000217.
4. Kessler C, Khaw AV, Nabavi DG, Glahn J, Grond M, Busse O. Standardized prehospital treatment of stroke. Dtsch Arztebl Int. 2011 Sep;108(36):585-91. doi: 10.3238/arztebl.2011.0585.
5. Catanoi N. Managementul accidentului vascular cerebral ischemic la etapa de prespital în Republica Moldova = Management of ischemic stroke at the prehospital stage in the Republic of Moldova. Mold J Health Sci. 2022;(3 Suppl):73. Romanian, English.
6. Luiz T, Moosmann A, Koch C, Behrens S, Daffertshofer M, Ellinger K. Optimized logistics in the prehospital management of acute stroke. Anasthesiol Notfallmed Schmerzther. 2001;36(12):735-41. doi: 10.1055/s-2001-18981. German.
7. Feigin VL, Roth GA, Naghavi M, Parmar P, Krishnamurthi R, Chugh S, et al. Global burden of stroke and risk factors in 188 countries, during 1990-2013: a systematic analysis for the Global Burden of Disease Study 2013. Lancet Neurol. 2016;15(9):913-924. https://doi.org/10.1016/S1474-4422(16)30073-4.
8. Powers WJ, Rabinstein AA, Ackerson T, et al. Guidelines for the Early Management of Patients With Acute Ischemic Stroke: 2019 Update to the 2018 Guidelines for the Early Management of Acute Ischemic Stroke: a guideline for healthcare professionals from the American Heart Association/American Stroke Association. Stroke. 2019;50(12):e344-e418. doi: 10.1161/STR.0000000000000211.
9. Bernic V, Ciobanu N, Ciocanu M, et al. Accidentul vascular cerebral: epidemiologie, factori de risc, prevenție [Stroke: epidemiology, risk factors, prevention]. Groppa S, editor. Chișinău: [s. n.]; 2020. 212 p. Romanian.

10. Zachrison KS, Nielsen VM, Perez de la Ossa N, et al. Prehospital stroke care Part 1: Emergency medical services and the stroke systems of care. Stroke. 2023;54(4):1138-1147. doi: 10.1161/STROKEAHA.122.039586.
11. Guvernul Republicii Moldova [Government of the Republic of Moldova]. Programul național de prevenire și control al bolilor netransmisibile prioritare în Republica Moldova pentru anii 2023-2027 [National Program for the Prevention and Control of Priority Noncommunicable Diseases in the Republic of Moldova for 2023-2027]. Chisinau: The Government; 2023. Romanian.
12. Ministerul Sănătății al Republicii Moldova [Ministry of Health of the Republic of Moldova]. Ordinul nr. 870 din 16.10.2023 cu privire la organizarea Serviciului național de asistență medicală al AVC [Order no. 870 of 16.10.2023 on the organization of the National Stroke Medical Assistance Service] [Internet]. [cited 2025 May 12]. Available from: https://ms.gov.md/wp-content/uploads/2023/10/870-16.10.2023.pdf. Romanian.
13. Catanoi N. Hipertensiunea arterială complicată cu accident vascular cerebral la etapa de prespital [Arterial hypertension complicated with stroke in the prehospital stage] [dissertation]. Chișinău: *Nicolae Testemițanu* State University of Medicine and Pharmacy; 2024. 155 p. Romanian.
14. National Center for Pre-Hospital Emergency Medical Assistance of the Republic of Moldova. Raport de activitate pentru anul 2022 [Annual Activity Report 2022] [Internet]. Chisinau: The Center; 2022 [cited 2025 Apr 14]. Available from: https://ambulanta.md/rapoarte-%C8%99i-statistici. Romanian.
15. National Center for Pre-Hospital Emergency Medical Assistance of the Republic of Moldova. Raport de activitate pentru anul 2023 [Annual Activity Report 2023] [Internet]. Chisinau: The Center; 2023 [cited 2025 Apr 14]. Available from: https://ambulanta.md/storage/uploads/Rapoarte%20%C8%99i%20statistici/09.02.2024%20Raport%20activitate%20pentru%202023.pdf. Romanian.
16. Ministerul Sănătății al Republicii Moldova [Ministry of Health of the Republic of Moldova]. Acces la asistență medicală calificată în 13 centre pentru pacienții care au suferit accident vascular cerebral [Access to specialized medical care in 13 centers for patients who have suffered a stroke] [Internet]. 2023 Oct 16. Chișinău: The Ministry; 2023- [cited 2025 Jun 12]. Available from: https://ms.gov.md/comunicare/comunicate/acces-la-asistenta-medicala-calificata-in-13-centre-pentru-pacientii-care-au-suferit-accident-vascular-cerebral/?utm_source or on: https://emedicina.md/13-centre-pentru-pacientii-cu-avc-vor-fi-infiintate-in-spitalele-din-moldova/?utm_source. Romanian.
17. Institute of Emergency Medicine of the Republic of Moldova. Rapoarte de activitate 2023-2024 [Annual Reports 2023-2024]. Chisinau: The Institute; 2024 [cited 2025 May 12]. Available from: https://www.urgenta.md/rapoarte.html. Romanian.
18. Ministry of Health of the Republic of Moldova. Raportul de activitate pentru anul 2024 [Activity report for 2024] [Internet]. Chisinau: The Ministry; 2024 [cited 2025 May 12]. Avalable from: https://ms.gov.md/wp-content/uploads/2024/12/Raport-de-actvitate-al-MS-pe-parcursul-anului-2024-.pdf?utm_source. Romanian.
19. National Agency for Public Health of the Republic of Moldova. Săptămâna globală de acțiuni pentru prevenirea bolilor netransmisibile [Global Week of Action for the Prevention of Noncommunicable Diseases] [Internet]. Chisinau: The Agency; 2023 [cited 2025 May 12]. Available from: https://ansp.md/apelul-in-saptamana-globala-de-actiuni-pentru-prevenirea-bolilor-netransmisibile-din-acest-an-este-sa-reducem-decalajul-in-ingrijirile-medicale. Romanian.
20. Ye S, Pan H, Li W, Wang J, Zhang H. Development and validation of a clinical nomogram for differentiating hemorrhagic and ischemic stroke prehospital. BMC Neurol. 2023;23(1):95. https://doi.org/10.1186/s12883-023-03138-1.

https://doi.org/10.52645/MJHS.2025.3.18

UDC: 316.647.8:616.89-088.454

RESEARCH ARTICLE

Identifying core stigmatizing beliefs about depression: results from an item-level statistical approach

Jana Chihai[1], Andrei Esanu[1*], Igor Nastas[1,2], Inga Deliv[1], Alina Bologan[1], Cornelia Adeola[1], Radislav Coşulean[2], Madalina Bivol[2], Mihaela Belous[2], Dorin Jelaga[1], Romil Popescu[1]

[1]Department of Mental Health, Medical Psychology and Psychotherapy, *Nicolae Testemițanu* State University of Medicine and Pharmacy, Chisinau, Republic of Moldova
[2]Mental Health Laboratory, Brain Research Center, *Nicolae Testemițanu* State University of Medicine and Pharmacy, Chisinau, Republic of Moldova

ABSTRACT

Introduction. Stigma surrounding depression continues to be a major barrier to treatment, social inclusion, and recovery. While general attitudes toward mental illness have been widely studied, fewer investigations have focused on the specific beliefs that drive stigma toward individuals with depression in a low- and middle-income country (LMIC) in Eastern European settings, particularly in Moldova.

Material and methods. A cross-sectional study was conducted with a sample of 460 participants from Moldova, who completed the Depression Stigma Scale. Each of the nine items reflected a different stigmatizing belief about depression. Descriptive statistics, including mean scores and standard deviations, were calculated for each item. An item-level comparative analysis was performed.

Results. The highest stigma scores were recorded for items such as: "I would not employ someone if I knew they had been depressed", "Depression is not a real medical illness", and "Depression is a sign of personal weakness." The lowest scores were observed for beliefs related to dangerousness and avoidance, including "People with depression are dangerous" and "It is best to avoid people with depression so you don't become depressed yourself." These results suggest that stigma in Moldova is predominantly characterized by doubts about the medical legitimacy of depression and concerns over professional roles, rather than fear-based or exclusionary attitudes.

Conclusions. Anti-stigma interventions in LMICs, such as Moldova should prioritize improving public understanding of depression as a legitimate health condition and addressing discrimination in professional settings.

Keywords: depression, stigma, discrimination, mental health, LMIC.

Cite this article: Chihai J, Esanu A, Nastas I, Deliv I, Bologan A, Adeola C, Coşulean R, Bivol M, Belous M, Jelaga D, Popescu R. Identifying core stigmatizing beliefs about depression: results from an item-level statistical approach. Mold J Health Sci. 2025;12(3):117-121. https://doi.org/10.52645/MJHS.2025.3.18.

Manuscript received: 29.07.2025

Accepted for publication: 30.08.2025

Published: 15.09.2025

[*]**Corresponding author**: **Andrei Eşanu**, PhD, MD, assistant professor
Department of Mental Health, Medical Psychology and Psychotherapy
Nicolae Testemițanu State University of Medicine and Pharmacy
165, Ştefan cel Mare şi Sfânt blvd, Chişinău, Republic of Moldova, MD 2004
e-mail: andrei.esanu@usmf.md

Authors' ORCID IDs
Jana Chihai – https://orcid.org/0000-0002-7720-5544
Andrei Eşanu – https://orcid.org/0000-0003-1289-4622
Igor Nastas – https://orcid.org/0000-0001-8751-9101
Inga Deliv – https://orcid.org/0000-0001-6080-9256
Alina Bologan – https://orcid.org/0000-0002-1771-7476
Cornelia Adeola – https://orcid.org/0009-0002-0728-9196

Key messages

What is not yet known on the issue addressed in the submitted manuscript

While the stigma associated with depression has been widely examined in high-income countries, there is limited evidence from low- and middle-income countries (LMICs), particularly in Eastern Europe. Most existing studies in these settings focus on mental illness stigma in general and report aggregated stigma scores, without exploring the specific beliefs that drive stigma toward depression. As a result, the structure, content, and sociodemographic variation of depression-specific stigma remain poorly understood in LMIC contexts.

The research hypothesis

The hypothesis is that, in a low- and middle-income country (LMIC) such as the Republic of Moldova, public stigma toward de-

Radislav Coşulean – https://orcid.org/0000-0001-8699-6862
Madalina Bivol – https://orcid.org/0009-0005-2827-9992
Mihaela Belous – https://orcid.org/0000-0002-2597-1060
Dorin Jelaga – https://orcid.org/0009-0004-7761-450X
Romil Popescu – https://orcid.org/0009-0007-6414-7377

pression reflects a heterogeneous pattern of beliefs, with certain stigmatizing attitudes more frequently endorsed than others and varying across sociodemographic groups.

The novelty added by manuscript to the already published scientific literature

This study is the first to apply an item-level analysis of the Depression Stigma Scale (DSS) in a low- and middle-income country in Eastern Europe. By identifying the most frequently endorsed stigmatizing beliefs and examining their variation by demographic characteristics, the manuscript provides granular, context-specific evidence. These findings go beyond general stigma assessments and contribute directly to the development of targeted anti-stigma strategies adapted to LMICs.

Introduction

Depression is one of the most prevalent mental health conditions globally, with significant personal, social, and economic consequences. According to the World Health Organization, more than 280 million people are affected by depression worldwide, making it a leading cause of disability and a major contributor to the global burden of disease. Despite advances in mental health care and increased awareness, stigma remains a significant barrier to help-seeking, diagnosis, and treatment adherence among individuals with depression [1-3].

Stigmatization of depression manifests through negative stereotypes, prejudice, and discriminatory behavior directed at those experiencing the condition. Such beliefs may include the perception that people with depression are weak, unreliable, or dangerous, or that depression is not a real illness but rather a matter of personal will [2]. This stigmatization not only impairs the quality of life of those affected but also contributes to social exclusion, workplace discrimination, and internalized shame or self-stigma.

In Eastern European low- and middle-income countries (LMIC) such as the Republic of Moldova, research on mental health stigma remains limited, particularly in relation to depression. Historical neglect of mental health, limited access to services, and culturally embedded misconceptions contribute to the persistence of stigmatizing beliefs in this region [4, 5]. In Moldova, although reforms in mental health care have been initiated, public attitudes continue to reflect fear, misunderstanding, and reluctance to engage with individuals who suffer from depression.

Existing studies tend to focus on general stigma toward mental illness, often without differentiating between disorders. However, depression-specific stigma may take unique forms, especially regarding perceptions of functionality, employability, or moral character. Identifying which specific beliefs are most prevalent is essential for designing targeted anti-stigma interventions. Item-level analysis of validated instruments such as the Depression Stigma Scale (DSS) can provide deeper insights into the patterns of belief within a given population and guide context-sensitive strategies for stigma reduction [2, 6].

This article presents the results of an item-level statistical analysis of the DSS applied to a Moldovan sample, aiming to identify the core stigmatizing beliefs about depression in the general population. The findings may inform national efforts and those in similar LMICs regarding public education, workplace inclusion, and mental health policy.

This study aims to identify the core stigmatizing beliefs about depression in the general population of the Republic of Moldova through an item-level statistical analysis of the Depression Stigma Scale.

Material and methods

This cross-sectional study was conducted on a convenience sample of 476 adult participants from various regions of the Republic of Moldova. Inclusion criteria were: age ≥18 years, informed consent to participate. Individuals with a known diagnosis of psychotic disorders or cognitive impairment were excluded.

The study was approved by the Research Ethics Committee of *Nicolae Testemițanu* State University of Medicine and Pharmacy (minutes No 44, from 29.05.2024), and all participants provided written informed consent.

To assess stigmatizing beliefs about depression, the Depression Stigma Scale (DSS) was used, which contains 9 items measuring the extent of agreement with commonly held stigmatizing beliefs (e.g., "Depression is a sign of personal weakness", "I would not employ someone if I knew they had been depressed", "Depression is not a real medical illness"). Responses were recorded on a 5-point Likert scale from 0 ("strongly disagree") to 4 ("strongly agree").

Sociodemographic data were also collected, including age, gender, education, employment status, income, marital status, and urban/rural residence.

Descriptive statistics (mean, standard deviation, minimum, maximum) were calculated for each of the 9 DSS items. Item-level analysis was conducted to examine the distribution and intensity of stigma-related beliefs. Results were presented in the form of bar plots for visualization.

Although the analysis focused primarily on descriptive patterns, inferential comparisons between items were also explored to identify statistically significant dif-

ferences in the endorsement of specific beliefs. Data were analyzed using SPSS version 24.0, with a significance level set at $p < 0.05$.

Results

A total of 476 individuals participated in this cross-sectional study on stigma toward depression in the Republic of Moldova. The sample included 301 urban residents (63.2%) and 175 rural residents (36.8%), reflecting the geographic distribution of the population and mental health service access. Participants were recruited from 10 administrative units across the country, including both major urban centers (e.g., Chişinău and Bălţi) and smaller districts (e.g., Orhei, Călăraşi, Ialoveni), to ensure diversity in socio-demographic backgrounds.

The sample was composed of 281 women (59%) and 195 men (41%), with ages ranging from 18 to 65 years (mean age = 34.5 years). Educational attainment was distributed as follows: 36.3% (n = 173) had completed 9 years of school, 25.2% (n = 120) had finished 12 years or vocational school, 19.1% (n = 91) had graduated from college, and 10.9% (n = 52) held a university degree. A small proportion, 8.4% (n = 40), reported having completed only primary education.

This stratified sampling approach was designed to ensure representation across key sociodemographic groups relevant to mental health literacy and stigma. It also allowed for later analysis of stigma variation by gender, education, and area of residence.

The Depression Stigma Scale (DSS) was used to assess the level of stigmatizing beliefs toward people with depression. The analysis of item-level responses revealed that the highest agreement rates were observed for the following items: "People with depression could snap out of it if they wanted", "Depression is a sign of personal weakness", and "Depression is not a real medical illness". These beliefs suggest a persistent conceptual stigma, in which depression is perceived as a lack of willpower or not being a genuine illness.

High scores were also recorded for item – "I would not employ someone if I knew they had been depressed", suggesting occupational stigma and the belief that individuals with depression are unfit for professional roles.

Conversely, the items with the lowest levels of agreement were: "People with depression are dangerous", "It is best to avoid people with depression so you don't become depressed yourself", and "People with depression are unpredictable", indicating that fear-based and avoidance-related stigma were less prevalent in this sample.

The average score for the item "People with depression could snap out of it if they wanted" was 3.4 (on a 5-point scale), whereas "People with depression are dangerous" had a mean score of just 1.8. This confirms that the dominant stigma in the Moldovan context tends to be conceptual and occupational rather than fear-based or exclusionary.

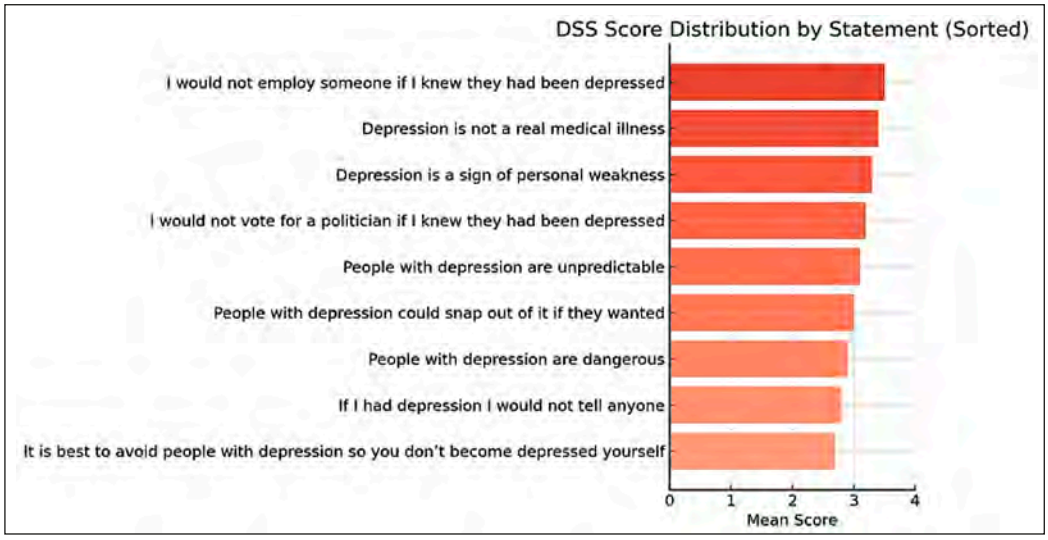

Fig. 1 Mean scores for stigmatizing beliefs about depression

Note: *The chart displays the average agreement level (on a 0–4 Likert scale) with each of the nine DSS items, sorted from highest to lowest mean score. Higher scores indicate stronger endorsement of the respective stigmatizing belief.*

Analysis of stigma variation by gender revealed that men had significantly higher agreement with items suggesting dangerousness and unpredictability. For example, the average score for "People with depression are dangerous" among men was 2.1, compared to 1.6 among women ($p < 0.01$).

Educational level also influenced stigma levels. Respondents with only secondary education were more likely to agree with stigmatizing statements such as "Depression is not a real medical illness" (mean score 3.7 vs. 2.9 among those with higher education; $p < 0.001$).

Urban respondents generally showed lower stigma levels across most items compared to rural respondents, particularly on items relating to avoidance and employment discrimination.

In terms of self-stigma, items "If I had depression I would not tell anyone" and "I would not vote for a politician if I knew they had been depressed" – revealed moderate agreement, suggesting a significant degree of anticipated discrimination and secrecy.

The internal consistency of the scale was high (Cronbach's Alpha = 0.91), confirming the reliability of the instrument in the Moldovan context.

Discussion

This study provides a comprehensive analysis of public attitudes toward depression in a representative sample in the Republic of Moldova, using the Depression Stigma Scale (DSS). The results reveal that stigmatizing beliefs remain prevalent, particularly those that conceptualize depression as a personal weakness or a lack of willpower. The most frequently endorsed items were: "People with depression could snap out of it if they wanted," "Depression is a sign of personal weakness," and "Depression is not a real medical illness." These findings align with prior research highlighting the persistence of conceptual stigma in LMICs, where mental illness is often viewed through a moral or characterological lens rather than a biomedical one [2, 7, 8].

Moreover, the relatively high agreement with occupational stigma – such as "I would not employ someone if I knew they had been depressed" – indicates that discriminatory attitudes may translate into tangible social and economic exclusion. This echoes findings from studies conducted in LMICs, including in Eastern Europe, where mental illness is still associated with reduced trust in competence and productivity [3 ,9, 10].

Conversely, items reflecting fear-based and avoidance stigma (e.g., "People with depression are dangerous" and "It is best to avoid people with depression") were less frequently endorsed. This pattern suggests that although respondents may not view individuals with depression as threatening, they still hold beliefs that contribute to marginalization and discrimination, especially in the workforce and public life [9, 11, 12].

The analysis also demonstrated statistically significant variations in stigma levels across sociodemographic groups. Male respondents exhibited higher endorsement of beliefs related to dangerousness and unpredictability, consistent with gender-based differences observed in international literature. Educational attainment was inversely associated with stigma, with individuals holding only secondary education more likely to deny the medical legitimacy of depression. Similarly, stigma scores were higher among respondents residing in rural areas, supporting evidence that urban environments may provide greater exposure to mental health information and services [13, 14].

Self-stigmatizing attitudes were also evident. Items such as "If I had depression, I would not tell anyone" and "I would not vote for a politician if I knew they had been depressed" revealed moderate levels of internalized stigma and anticipated discrimination. These beliefs are of particular concern, as self-stigma has been shown to negatively impact help-seeking behavior and adherence to treatment [15-17].

The internal consistency of the DSS was high (Cronbach's Alpha = 0.91), confirming its reliability for use in the Moldovan context. The item-level analysis allowed for a nuanced understanding of specific stigma domains – conceptual, occupational, fear-based, and self-stigma – highlighting the complex ways in which public perceptions about depression are structured [18].

Taken together, these findings underscore the need for adapted anti-stigma interventions in in LMICs, such as Republic of Moldova. Efforts should focus on increasing mental health literacy, challenging harmful stereotypes, and promoting recovery-oriented narratives. Special attention should be given to men, individuals with lower educational attainment, and rural communities, where stigma levels are highest. Public health campaigns, inclusion of mental health education in school curricula, and peer-led awareness initiatives may serve as effective tools for reducing stigma [19-21].

Future research should explore causal pathways through longitudinal designs and assess the effectiveness of anti-stigma programs in LMIC settings. Additionally, qualitative studies may offer deeper insights into the lived experiences of individuals affected by depression and stigma.

Conclusions

This study provides the first item-level analysis of depression stigma in the Republic of Moldova, offering a nuanced understanding of the specific beliefs that sustain stigma in a low- and middle-income country context. The findings reveal that the most strongly endorsed beliefs relate to questioning the medical legitimacy of depression, attributing it to personal weakness, and concerns about the employability of individuals with depression. In contrast, fear-based beliefs, such as the idea that people with depression are dangerous or should be avoided, were less commonly held. These insights represent a valuable contribution to the evidence base needed to design targeted and culturally adapted anti-stigma interventions in LMICs.

Competing interests

None declared.

Authors' contribution

JC conceived the study, led the study design, coordinated the data collection process, and drafted the manuscript. AE contributed to the study design, supervised the analysis, and revised the manuscript critically. IN performed statistical analysis and supported interpretation of the findings. ID and AB participated in data collection and contributed to manuscript preparation. CA and RC assisted with participant recruitment and data entry. MB, MBel, and DJ conducted literature review and formatting. RP contributed to data visualization and statistical validation. All authors reviewed the manuscript critically and approved the final version for publication.

Informed consent for publication

Obtained.

Ethics approval

The study was approved by the Research Ethics Committee of *Nicolae Testemițanu* State University of Medicine and Pharmacy (minutes No 44, from 29.05.2024).

Acknowledgements and funding

The authors gratefully acknowledge PhD Associate Professor Evelina Gherghelijiu for her essential support in coordinating the research process and managing participant recruitment and data collection. We thank PhD Associate Professor Oleg Arnaut for his contribution to the statistical analysis and validation of the findings. Special appreciation is extended to

Dr.P.H. Emily Peca, M.A., Adjunct Faculty at the Milken Institute School of Public Health, George Washington University, for her expert guidance throughout the study design and interpretation phases. We also wish to thank Professor Kathleen M. Griffiths, former Director of the National Centre for Mental Health Research, Australian National University, for her foundational role in developing the Depression Stigma Scale (DSS), which served as the core measurement instrument in this study. Finally, we express our deep gratitude to all participants for their openness and contribution to this research.

This study was realized in the framework of the "Implementation Science Study to investigate community-based mental health interventions for high-risk communities in low- and middle-income countries" HEARD, 2024, financed by USAID.

Provenance and peer review

Not commissioned; externally peer-reviewed.

References

1. Esanu A, Morais V, Araújo J, Ramos E. Stigma toward people with mental disorders in adolescents: comparison between Portugal and Moldova. Porto Biomed J. 2020;5(6):e089. doi: 10.1097/j.pbj.0000000000000089.
2. Al-Shannaq Y, Jaradat D, Ta'an WF, Jaradat D. Depression stigma, depression literacy, and psychological help seeking attitudes among school and university students. Arch Psychiatr Nurs. 2023 Oct;46:98-106. doi: 10.1016/j.apnu.2023.08.010.
3. Pybus K, Pickett KE, Lloyd C, Wilkinson R. The socioeconomic context of stigma: examining the relationship between economic conditions and attitudes towards people with mental illness across European countries. Front Epidemiol. 2023;3:1076188. doi: 10.3389/fepid.2023.1076188.
4. Thornicroft G, Brohan E, Rose D, Sartorius N, Leese M. Global pattern of experienced and anticipated discrimination against people with schizophrenia: a cross-sectional survey. Lancet. 2009 Jan 31;373(9661):408-15. doi: 10.1016/S0140-6736(08)61817-6.
5. Rüsch N, Angermeyer MC, Corrigan PW. Mental illness stigma: concepts, consequences, and initiatives to reduce stigma. Eur Psychiatry. 2005 Dec;20(8):529-39. doi: 10.1016/j.eurpsy.2005.04.004.
6. Corrigan PW, Watson AC. Understanding the impact of stigma on people with mental illness. World Psychiatry. 2002 Feb;1(1):16-20.
7. Hansson L, Jormfeldt H, Svedberg P, Svensson B. Mental health professionals' attitudes towards people with mental illness: do they differ from attitudes held by people with mental illness? Int J Soc Psychiatry. 2013 Mar;59(1):48-54. doi: 10.1177/0020764011423176.
8. Griffiths KM, Christensen H, Jorm AF. Predictors of depression stigma. BMC Psychiatry. 2008 Apr 18;8:25. doi: 10.1186/1471-244X-8-25.
9. Mak WWS, Poon CYM, Pun LYK, Cheung SF. Meta-analysis of stigma and mental health. Soc Sci Med. 2007 Jul;65(2):245-61. doi: 10.1016/j.socscimed.2007.03.015.
10. Pescosolido BA, Medina TR, Martin JK, Long JS. The "backbone" of stigma: identifying the global core of public prejudice associated with mental illness. Am J Public Health. 2013 May;103(5):853-60. doi: 10.2105/AJPH.2012.301147.
11. Lasalvia A, Zoppei S, Van Bortel T, Bonetto C, Cristofalo D, Wahlbeck K, et al. Global pattern of experienced and anticipated discrimination reported by people with major depressive disorder: a cross-sectional survey. Lancet. 2013 Nov 9;381(9860):55-62. doi: 10.1016/S0140-6736(12)61379-8.
12. Schomerus G, Schwahn C, Holzinger A, Corrigan PW, Grabe HJ, Carta MG, et al. Evolution of public attitudes about mental illness: a systematic review and meta-analysis. Acta Psychiatr Scand. 2012 Jun;125(6):440-52. doi: 10.1111/j.1600-0447.2012.01826.x.
13. Rüsch N, Müller M, Ajdacic-Gross V, Rodgers S, Corrigan PW, Rössler W. Shame, perceived knowledge and satisfaction associated with mental health as predictors of attitude patterns towards help-seeking. Epidemiol Psychiatr Sci. 2014 Jun;23(2):177-87. doi: 10.1017/S204579601300036X.
14. Evans-Lacko S, Brohan E, Mojtabai R, Thornicroft G. Association between public views of mental illness and self-stigma among individuals with mental illness in 14 European countries. Psychol Med. 2012 Jan;42(8):1741-52. doi: 10.1017/S0033291711002558.
15. Dinos S, Stevens S, Serfaty M, Weich S, King M. Stigma: the feelings and experiences of 46 people with mental illness. Br J Psychiatry. 2004 Dec;184:176-81. doi: 10.1192/bjp.184.2.176.
16. Reavley NJ, Jorm AF. Public recognition of mental disorders and beliefs about treatment: changes in Australia over 16 years. Br J Psychiatry. 2012 Jun;200(5):419-25. doi: 10.1192/bjp.bp.111.104208.
17. Livingston JD, Boyd JE. Correlates and consequences of internalized stigma for people living with mental illness: a systematic review and meta-analysis. Soc Sci Med. 2010 Dec;71(12):2150–61. doi: 10.1016/j.socscimed.2010.09.030.
18. Esanu A, Chihai J. Stigmatizarea persoanelor cu depresie [Stigma towards people with depression]. Stud Univ Mold (Educ Sci Ser). 2018;(9):41-44. Romanian.
19. Wasserman D, Apter G, Baeken C, Bailey S, Balazs J, Bec C, et al. Compulsory admissions of patients with mental disorders: State of the art on ethical and legislative aspects in 40 European countries. Eur Psychiatry. 2020;63(1):e82. doi: 10.1192/j.eurpsy.2020.79.
20. Chihai J, Spinei L, Cerniţanu M, Garaz G, Eşanu A, Bologan A. Probleme psihosociale determinate de pandemia COVID-19 = Psychosocial problems caused by the COVID-19 pandemic. Mold J Health Sci. 2020;(2):161-169. Romanian, English.
21. Harhaji S, Tomori S, Nakov V, Chihai J, Radić I, Mana T, Stoychev K, Esanu A, Pirlog MC. Stigmatising attitudes towards mental health conditions among medical students in five South-Eastern European countries. Zdr Varst. 2024 Sep 23;63(4):188-197. doi: 10.2478/sjph-2024-0025.

https://doi.org/10.52645/MJHS.2025.3.19

UDC: 616.24-002.5+616.98:578.828

RESEARCH ARTICLE

Tuberculosis in new cases: the impact of HIV status on clinical manifestations

Igor Ivanes*, **Aurelia Ustian**, **Constantin Iavorschi**, **Alexandru Corlăteanu**

Department of Pneumology and Allergology, *Nicolae Testemițanu* State University of Medicine and Pharmacy, Chișinău, Republic of Moldova

ABSTRACT

Introduction. Tuberculosis continues to be the primary cause of death among individuals living with human immunodeficiency virus, with co-infection significantly influencing the clinical course, severity, and outcomes of the disease. Although the interaction between the two conditions is well recognized, regional data from Eastern Europe remain insufficient.

Material and methods. A retrospective, cross-sectional comparative study was carried out in the Republic of Moldova in 2021. A total of 320 patients with newly diagnosed pulmonary tuberculosis were included and divided into two matched groups: the study group consisted of 160 patients with confirmed human immunodeficiency virus co-infection, and the control group included 160 patients without human immunodeficiency virus infection. The groups were comparable in terms of age, sex, residence, and resistance profile of *Mycobacterium tuberculosis*. Data were collected from national clinical records and analyzed using descriptive statistical methods.

Results. Among 320 patients, those with HIV co-infection had significantly higher rates of generalized TB (28.8% vs. 2.5%; $p < 0.0001$), subacute onset (71.9% vs. 22.5%; $p < 0.0001$), and severe/very severe condition at diagnosis (27.4% vs. 10.6%; $p = 0.0017$). Anemia (58.8% vs. 23.1%; OR = 4.73, $p < 0.0001$), leukopenia (16.3% vs. 1.3%; OR = 15.33, $p < 0.0001$), and ESR >60 mm/h (25.0% vs. 5.6%; OR = 5.59, $p < 0.0001$) were significantly more common in co-infected patients. Bilateral lung lesions were more frequent (65.6% vs. 59.4%), while cavitary destruction predominated in TB-only patients (59.4% vs. 34.4%; $p < 0.0001$). Smear positivity was lower in the HIV group (38.8% vs. 55.0%; $p = 0.0036$). Complications (48.1% vs. 20.6%; $p < 0.0001$) and opportunistic infections (17.5% vs. 0%) were more prevalent in co-infected patients. Mortality was significantly higher among HIV-positive cases (28.1% vs. 6.9%; OR = 5.20, $p < 0.0001$).

Conclusions. Human immunodeficiency virus infection significantly modifies the clinical presentation of tuberculosis, favoring more severe, atypical, and extrapulmonary forms, along with higher complication rates and mortality. These findings highlight the urgent need for early diagnosis, adapted diagnostic approaches, and integrated treatment strategies in patients with dual infection, particularly in high-burden settings.

Keywords: tuberculosis, human immunodeficiency virus, co-infection, extrapulmonary involvement.

Cite this article: Ivanes I, Ustian A, Iavorschi C, Corlăteanu A. Tuberculosis in new cases: the impact of HIV status on clinical manifestations. Mold J Health Sci. 2025;12(3):122-129. https://doi.org/10.52645/MJHS.2025.3.19.

Manuscript received: 28.07.2025

Accepted for publication: 30.08.2025

Published: 15.09.2025

***Corresponding author: Igor Ivanes,** PhD student
Department of Pneumology and Allergology
Nicolae Testemițanu State University of Medicine and Pharmacy
165, Ștefan cel Mare și Sfânt Blvd., Chișinău, Republic of Moldova, MD-2004
e-mail: ivanesigor@gmail.com

Authors' ORCID IDs
Igor Ivanes – https://orcid.org/0000-0002-7726-3197
Aurelia Ustian – https://orcid.org/0000-0002-2679-5767

Key messages

What is not yet known on the issue addressed in the submitted manuscript

The interplay between tuberculosis and HIV is well established from both clinical and epidemiological perspectives. However, there is a lack of detailed investigation into how HIV-related immunosuppression shapes the clinical manifestations, extent of extrapulmonary involvement, and overall disease severity in newly diagnosed TB patients across Eastern European settings.

The research hypothesis

In newly diagnosed pulmonary TB patients, HIV co-infection sig-

Constantin Iavorschi – https://orcid.org/0000-0002-6371-687X
Alexandru Corlăteanu – https://orcid.org/0000-0002-3278-436X

nificantly alters clinical presentation and increases the frequency and severity of extrapulmonary involvement, with higher rates of complications and mortality.

The novelty added by the manuscript to the already published scientific literature

This study provides novel evidence from the Republic of Moldova, highlighting the distinct clinical patterns of TB in HIV-positive patients compared to HIV-negative individuals. It emphasizes the need for regionally adapted diagnostic and therapeutic approaches in dual-infected patients, offering insights into early diagnosis, disease progression, and prognostic markers within a vulnerable population in Eastern Europe.

Introduction

Tuberculosis (TB) remains one of the leading causes of morbidity and mortality among individuals living with HIV, alongside other opportunistic infections. Co-infection with the human immunodeficiency virus (HIV) substantially increases the risk of developing active TB, with HIV-positive individuals being approximately 15 to 22 times more likely to develop the disease compared to HIV-negative persons. Despite global advances in prevention and care, TB continues to represent the primary cause of death among HIV-infected patients, accounting for an estimated 167,000 deaths in 2023. In low-resource settings, TB often constitutes the initial clinical indicator of underlying HIV infection, further complicating the diagnostic and therapeutic approach. In the World Health Organization (WHO) European Region, approximately 10.8% of TB patients are co-infected with HIV, with the highest burden observed in Eastern Europe [1, 2].

National data reflect similar patterns. In the Republic of Moldova, the rate of TB/HIV co-infection has doubled over the past decade, increasing from 5% in 2011 to over 11.1% of all new and relapsed TB patients by 2022 [3]. This trend underscores an escalating epidemiological challenge and highlights the urgent need for integrated prevention and control strategies. Marked regional disparities are also evident in TB-related mortality. According to WHO data, the estimated TB mortality rate among HIV-infected individuals in the European region is 0.70 per 100,000 population. However, in Eastern Europe, one-year mortality following TB/HIV diagnosis reaches approximately 29%, whereas in Western Europe it remains below 4%, reflecting significant inequalities in access to timely diagnosis, effective anti-TB treatment, and antiretroviral therapy [1, 4]. These findings are consistent with those of a recent meta-analysis on HIV-associated mortality, which reported mortality rates ranging from 5% to 15% across most studies. Furthermore, HIV-infected TB patients exhibit nearly twice the risk of death compared to HIV-negative TB patients (29.1% vs. 15.2%), suggesting a synergistic effect between the two diseases [5]. This highly vulnerable population warrants prioritized clinical attention, with emphasis on early case detection, prompt initiation of combined antiretroviral and anti-tuberculosis therapy, and close follow-up to improve survival outcomes.

The clinical expression of tuberculosis in patients co-infected with HIV diverges considerably from the classical presentation, often manifesting with atypical features that complicate early recognition and diagnosis. This divergence is closely linked to the degree of HIV-associated immunosuppression. In the initial phases of HIV infection, TB may still exhibit typical pulmonary manifestations – such as chronic cough, hemoptysis, cavitary lung lesions on imaging, and systemic signs like persistent fever, weight loss, and night sweats – closely resembling the disease course observed in HIV-negative individuals [6]. However, as immune function declines, the disease presentation becomes progressively atypical, with an increased propensity for extrapulmonary or disseminated forms that lack hallmark radiological signs [7].

In co-infected patients, chest radiographs may still reveal features of pulmonary TB, whereas abdominal ultrasonography often provides valuable clues for detecting extrapulmonary or disseminated involvement. These imaging tools are considered reliable and widely available for clinical use, particularly in low-resource settings [8].

The burden of extrapulmonary TB is disproportionately high among HIV-positive individuals. Multiple studies report that the risk of extrapulmonary tuberculosis may be up to 32-fold higher greater in HIV-infected patients compared to those without HIV [9]. As the level of immunosuppression worsens, the incidence of classic cavitary lesions decreases, while extrapulmonary involvement – including lymphatic, pleural, neurological, pericardial, skeletal, and abdominal localizations – becomes increasingly prevalent [10]. Disseminated TB, frequently involving multiple organ systems, is also more common in advanced stages and is often diagnosed in the absence of bacteriological confirmation [11, 12]. These atypical and smear-negative forms of TB pose significant diagnostic and therapeutic challenges and are associated with poorer outcomes. A meta-analysis confirmed that extrapulmonary TB confers a more than twofold increase in mortality risk compared to pulmonary TB, due to both extensive mycobacterial spread and the more aggressive disease progression associated with HIV co-infection [5].

Given the elevated clinical risk, individuals with TB/HIV co-infection have long been recognized as a “double

priority" group for intervention. When these patients also belong to other vulnerable groups (e.g., people who inject drugs, incarcerated individuals), they are considered a "triple priority" in public health efforts [13]. Beyond TB, these patients often contend with a broad spectrum of comorbidities, including cardiovascular and pulmonary conditions, chronic kidney disease, diabetes mellitus, arterial hypertension, dyslipidemia, obesity, and hepatitis C. Opportunistic infections further complicate the clinical picture, with high prevalence of conditions such as cryptococcal meningitis, HPV-related malignancies, and diseases associated with Kaposi sarcoma herpesvirus (KSHV). Recent cohort data show that over half of TB/HIV co-infected individuals (54.2%) develop opportunistic infections, and among these, mortality reached 61.9%, underscoring the gravity of co-infection and the need for timely, integrated clinical management [14, 15].

Objective of this study was to investigate the clinical manifestations in newly diagnosed patients with pulmonary tuberculosis and human immunodeficiency virus (HIV) co-infection.

Material and methods

A retrospective, cross-sectional comparative study was conducted, including clinical data from 320 patients with newly diagnosed pulmonary tuberculosis (TB) in the Republic of Moldova during the year 2021. Inclusion criteria were: age ≥18 years; newly diagnosed pulmonary TB (classified as "new case" according to WHO definitions); confirmed HIV infection for Group I and documented HIV-negative status for Group II; provision of institutional informed consent. Exclusion criteria included: age <18 years or any TB classification other than "new case".

Group I (study group) comprised all 160 eligible patients with confirmed TB/HIV co-infection, representing almost the entire national cohort of new TB/HIV cases registered that year, including patients from the Transnistrian region. Group II (control group) was selected from the national cohort of new pulmonary TB cases diagnosed in 2021 who tested negative for HIV. From this primary cohort, 160 patients were matched in a 1:1 ratio with Group I based on sex, age (±3 years), place of residence (urban/rural), and *Mycobacterium tuberculosis* drug resistance profile. The latter criterion included four categories: drug-sensitive (susceptible to all first-line drugs), mono-resistant (resistant to a single first-line drug), poly-resistant (resistant to more than one first-line drug, but not to both isoniazid and rifampicin), and multidrug-resistant (MDR-TB, resistant to at least both isoniazid and rifampicin).

Clinical and paraclinical data (including symptoms, physical examination findings, hematological parameters, ESR, and TB-related complications) were obtained directly from inpatient medical histories in the hospitals where they were admitted and from their outpatient medical records (ambulatory cards). Additional epidemiological and laboratory information was retrieved from the National Tuberculosis Monitoring and Evaluation Information System (SIME-TB). All necessary official documents, authorizations, and institutional agreements were obtained to ensure lawful access to medical data from all participating healthcare facilities, including institutions located in the Transnistrian region.

Matching was performed using the IBM SPSS Statistics 28.0 Case-Control Matching procedure. The database was compiled in Microsoft Excel 2010 and exported to SPSS for analysis. Statistical methods included descriptive statistics (frequencies, percentages, means, medians, 95% confidence intervals), Chi-square test or Fisher's exact test for categorical variables, Mann–Whitney U test for non-normally distributed continuous variables, and calculation of odds ratios (OR) with 95% confidence intervals. A p-value <0.05 was considered statistically significant.

The required sample size was calculated using EpiInfo 7.2.2.6 (StatCalc – Sample Size and Power) with a 95% confidence level, based on an estimated TB-HIV association of up to 25%, a design effect of 4, and a 10% non-response adjustment. The adjusted sample size was 160 participants per group, based on defined inclusion and exclusion criteria.

Definitions were applied according to the National Clinical Protocol [3]. General condition was classified as satisfactory, moderate, severe, or extremely severe. Disease onset was defined as acute (<2 weeks), subacute (2-8 weeks), insidious (>8 weeks), or asymptomatic. Clinical 'masks' of tuberculosis referred to atypical presentations initially resembling pneumonia, COPD, lung cancer, or COVID-19. Radiological extent was defined as limited (single lobe, no extensive cavitation) or extensive (≥2 lobes, bilateral or cavitary disease).

The research protocol, patient information sheet, and consent form were approved by the Research Ethics Committee of *Nicolae Testemițanu* State University of Medicine and Pharmacy (minutes No. 66 from 29.09.2023).

Results

A total of 320 patients were enrolled in the study. In both groups, men predominated over women, with a ratio of 121 (75.6% ,95% CI: 68.4-81.6) to 39 (24.4%, 95% CI: 18.4-31.6) women. Most participants were aged between 25 and 54 years. In Group I (TB/HIV), the mean age was 38.9 years, with a median of 38 years (IQR: 32-44), while in Group II (TB-only) the mean age was 38.7 years, with a median of 38 years (IQR: 32-45).

In the TB/HIV group, the median CD4 count at TB diagnosis was 134 cells/mm^3 (interquartile range, IQR: 36-337), with 57.8% of patients having values below 200 cells/mm^3. The median HIV RNA level was 5.40×10^5 copies/mL (IQR: 9.69×10^4 – 1.56×10^6), and 7.1% had undetectable viral load. During TB treatment, antiretroviral therapy was administered regularly in 53.3% of patients, irregularly in 28.9%, and not at all in 17.8%. Passive case finding based on symptomatology was the primary detection method in both groups In group I, it accounted for 108 cases (67.5% (95% CI: 59.9-74.3)), compared to 118 (73.7%) cases in Group II (95% CI: 66.4-79.9). Consequently, active detection through clinical or radiological screening accounted for 32.5% and 26.3%, respectively.

The predominant clinical form in both groups was infiltrative tuberculosis, diagnosed in 98 (61.3%, 95% CI:

53.5-68.5) of cases in Group I and 153 (95.6%, 95% CI: 91.2-97.9) in Group II (p < 0.0001). Generalized TB was significantly more frequent in the co-infected group, in 46 patients (28.8%, 95% CI: 22.3–36.2), compared to only 4 patients in Group II (2.5% ,95% CI: 1.0-6.3) (p < 0.0001). Similarly, disseminated forms was more common in Group 1 (10 cases6.3%, 95% CI: 3.4-11.1) than in Group II (3 cases; 1.9%, 95% CI: 0.6-5.4) (p = 0.045). Lastly, nodular TB was observed only in the Group 1, affecting 6 patients (3.8%, 95% CI: 1.7-7.9). Among the 46 patients with generalized TB in Group I, 26.1% had involvement of a single extrapulmonary organ, 36.9% of two, 21.7% of three, and 15.3% of more than three organs.

Marked differences were noted in disease onset: subacute onset was dominant in Group I -115 (71.9%, 95% CI: 64.5-78.3), p < 0.0001, while insidious onset prevailed in Group II – 114 (71.3%, 95% CI: 63.8-77.7; p < 0.0001). The general condition at the time of diagnosis was more severe in Group I, with 44 (27.4%, 95% CI: 21.2-34.9; p = 0.0215) of patients classified as being in a severe or extremely severe state, compared to 17 in the HIV-negative group (10.6%, 95% CI: 6.7-16.4; p = 0.0071).

Clinical symptomatology differed significantly. Pronounced bronchopulmonary syndrome was observed in 66.2% of Group I versus 47.4% of Group II (OR = 2.17, 95% CI: 1.38-3.41; p = 0.0008). A pronounced intoxication syndrome was also more frequent in the TB/HIV group (66.9% vs. 48.2%; OR = 2.18, 95% CI: 1.38-3.42; p = 0.0008). Hematological findings reflected a more compromised status in HIV-positive patients: anemia occurred in 94 patients (58.8%, 95% CI: 51.0-66.1) vs. 37 patients (23.1%, 95% CI: 17.3-30.2) from Group II (p < 0.0001), leukopenia in 26 patients (16.3%, 95% CI: 11.3-22.7) vs. 2 patients (1.3%, 95% CI: 0.3-4.4) (p < 0.0001), and lymphocytopenia in 19 cases (11.9%, 95% CI: 7.7–17.8) vs. 2 cases (1.3%, 95% CI: 0.3-4.4) (p < 0.0001). The median erythrocyte sedimentation rate (ESR) was also higher in the HIV group (50 mm/h vs. 34 mm/h). ESR distribution differed significantly between groups, as illustrated in Fig. 1.

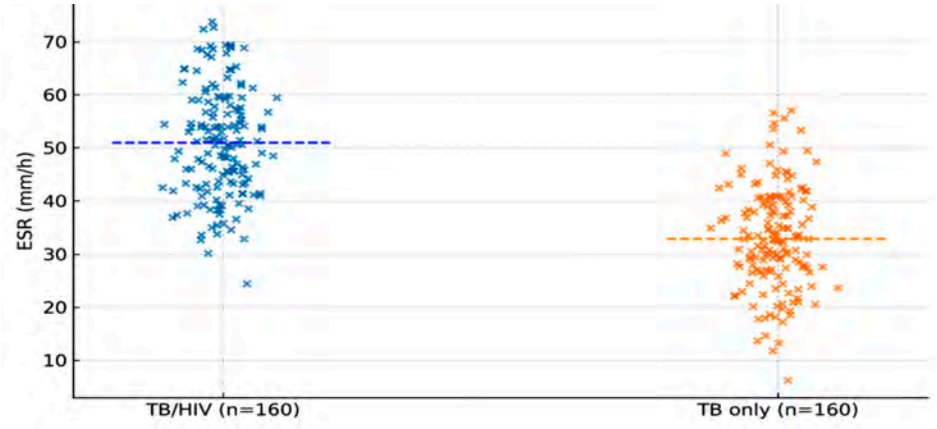

Fig. 1 Distribution of ESR in TB/HIV vs. TB-only patients

***Note**: Median ESR: 50 vs. 34 mm/h (p < 0.0001). Median ESR was significantly higher in the TB/HIV group (50 mm/h) compared to TB-only patients (34 mm/h). Dashed lines indicate group medians. Statistical significance: p < 0.0001 (Mann–Whitney U test).*

Radiologically, bilateral lung involvement was slightly more frequent in Group I – 105 (65.6%, 95% CI: 57.9-72.5) vs. 95 (59.4% ,95% CI: 51.6-66.7), with more extensive lesions 116 (72.5%, 95% CI: 65.1-78.8) vs. 100 (62.5%, 95% CI: 54.8-69.6). However, pulmonary destruction (cavitary lesions) was more frequent in Group II - 95 (59.4%, 95% CI: 51.6-66.7) vs. 55 (34.4%, 95% CI: 27.5-42.0) p < 0.0001, in line with typical immune-competent responses.

From a microbiological standpoint, smear microscopy was positive in 62 cases (38.8%, 95% CI: 31.5-46.5) from Group I compared to 88 cases (55.0%, 95% CI: 47.3-62.5) in Group II (p = 0.0036). GeneXpert testing detected *Mycobacterium tuberculosis* in 93 patients (58.2%, 95% CI: 50.4-65.5) of Group I and 108 (67.5%, 5% CI: 59.9-74.3) of Group II. Analysis of drug-resistance patterns revealed that fully drug-susceptible tuberculosis was more common among TB-only patients, whereas resistance to at least one first-line drug was significantly higher in the TB/HIV co-infected cohort (35% vs. 22%, p = 0.013). Mono- and poly-resistance occurred at comparable frequencies between the two groups (12% vs. 10%, p = 0.61; 9% vs. 6%, p = 0.37, respectively). Multidrug-resistant TB (MDR-TB) was detected more frequently among TB/HIV co-infected patients than in HIV-negative patients (14% vs. 6%), with an odds ratio of 2.55 (95% CI: 1.15–5.66, p = 0.021).

Complications were more frequent in Group I – 77 patients (48.1%, 95% CI: 40.5-55.8) versus 33 patients (20.6%, 95% CI: 15.1-27.5) in Group II (p < 0.0001). In Group I, the most prevalent complications were cachexia (37 cases, 48.1%, 95% CI: 37.3-59.0); p < 0.0001 and pleurisy – 29 cases, (37.6%, 95% CI: 27.7-48.8), followed by hemoptysis (6.5%), pneumothorax (5.2%), and empyema (2.6%). In Group II, cachexia and hemoptysis were recorded in 12 patients (36.4%, 95% CI: 22.2-53.4), pleurisy in 8 (24.2%, 95% CI: 12.8-41.0), and pneumothorax in one case (3.0%). Empyema was not reported in Group II. Clinical complications showed distinct patterns between the two cohorts, as depicted in Fig. 2.

The frequency of comorbidities and coinfections also differed notably. Liver pathology – including hepatitis B and C, toxic hepatitis, and hepatic cirrhosis – was significantly more common in Group I, affecting 66 (41.3%, 95% CI: 33.9-

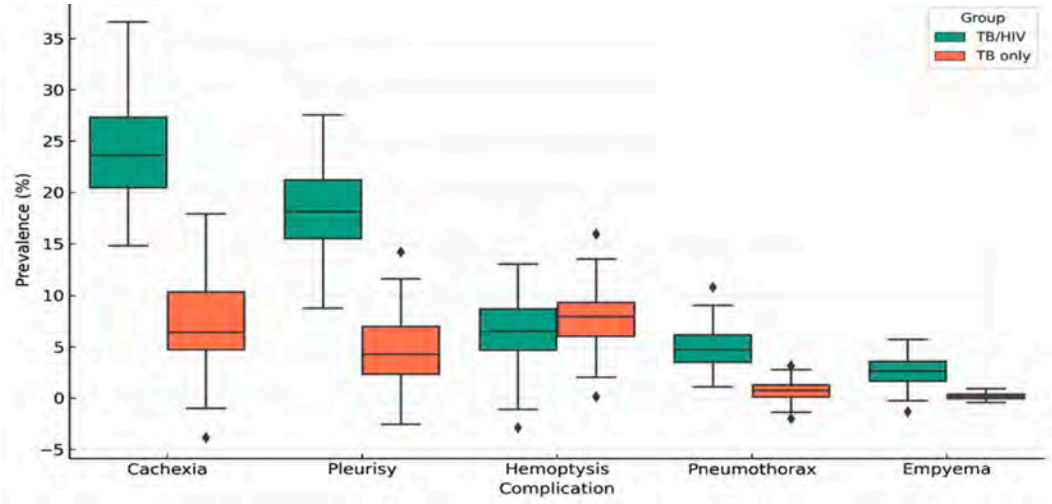

Fig. 2 Distribution of clinical complication prevalence in TB/HIV and TB-only patients.

Note: *Boxplots show higher median and greater variability in cachexia and pleurisy among TB/HIV patients. Hemoptysis shows similar distribution in both groups, while empyema and pneumothorax occurred almost exclusively in TB/HIV group. Boxes indicate interquartile range; whiskers represent 1.5×IQR.*

49.0) compared to 36 in Group II (22.5%, 95% CI: 16.7-30.2; p < 0.0001). Syphilis was diagnosed more frequently in Group I (8.8% vs. 4.3%). Neurological comorbidities such as alcohol-related polyneuropathy and encephalopathy were documented in 9.6% of Group I versus 8.6% of Group II. Epilepsy was identified in 4.1% of Group I and 1.4% of Group II. Conversely, some conditions were more prevalent in the TB-only group. Cerebrovascular accidents occurred more often in Group II (0.8% and 2.9%).Arterial hypertension was more frequent in Group II (5.7% vs. 0.8%). Type 2 diabetes mellitus was present in 1.6% of Group I versus 8.6% of Group II (p = 0.0087), and gastric ulcer was diagnosed in 4.8% versus 14.3% (p = 0.0029), respectively. Isolated cases of laryngeal tuberculosis (1.2% vs. 0.6%), pulmonary cancer, tuberculous peritonitis, and pulmonary abscess (each 0.6%) were also noted across both groups.

Tuberculosis „masks" were identified in both groups: 44 cases (27.5%, 95% CI: 21.2-34.9) in Group I and 36 cases (22.5%, 95% CI: 16.7-29.6) in Group II. Pneumonia was observed more frequently in Group 1, affecting 28 patients (17.5%, 95% CI: 12.4-24.1) compared to 11 (6.8%, 95% CI: 3.9-11.9) cases. Notably, SARS-CoV-2 coinfection was present in 22 patients (13.8%, 95% CI: 9.3-19.9) in Group I compared to 50 patients (31.2%, 95% CI: 24.6–38.8) in Group II. Chronic obstructive pulmonary disease (COPD) was diagnosed in 0.6% of Group I and 1.9% of Group II, while bronchial asthma was reported exclusively in Group II (0.6%).

Opportunistic infections were observed exclusively in Group I – 28 patients (17.5%). The most frequent were oropharyngeal candidiasis 15 (53.6%, 95% CI: 35.8-70.5) and herpes zoster 6 (21.3%, 95% CI: 10.2-39.5), with rare conditions including cryptococcal meningitis, cerebral toxoplasmosis, Kaposi sarcoma, *Pneumocystis jirovecii* pneumonia, non-tuberculous mycobacteriosis, oral leukoplakia, and pulmonary aspergillosis, each identified in a single case.

Mortality was significantly higher in the co-infected group. In Group I, there were 45 deaths (28.1%, 95% CI: 21.7-35.5). Of these, 34 (75.6%, 95% CI: 61.3-85.8) were due to tuberculosis and 11 (24.4%) to tuberculosis associated with other comorbidities. In contrast, Group II recorded 11 deaths (6.9%, 95% CI: 3.9-11.9); p < 0.0001, with 7 (63.6%, 95% CI: 35.4-84.8) attributable to TB and 4 (36.4%) due to TB combined with other underlying conditions.

The clinical and radiological presentations varied significantly between the two groups (Table 1). In the TB/HIV cohort, the clinical picture was often less specific, with a higher proportion of patients presenting with subacute or insidious onset, nonspecific systemic complaints (fatigue, weight loss), and a lower frequency of classical signs such as hemoptysis, compared with the TB-only group.

Table 1. Clinical, paraclinical, and radiological manifestations in patients with tuberculosis and tuberculosis/HIV co-infection.

Parameter	Group I (TB/HIV)	%	Group II (TB only)	%	OR [95% CI]	p-value
Disease onset						
Asymptomatic	12	7.5	10	6.3	1.22 [0.51–2.90]	= 0.83
Insidious	32	20.0	114	71.3	0.10 [0.06–0.17]	<0.0001
Subacute	115	71.9	36	22.5	8.80 [5.30–14.61]	<0.0001
Acute	1	0.6	–	–	NE	1.00
General condition at diagnosis						
Satisfactory	44	27.5	43	26.9	1.03 [0.63–1.70]	= 0.90
Moderate severity	72	45.0	100	62.5	0.49 [0.32–0.75]	= 0.0011
Severe	27	16.8	13	8.1	2.28 [1.13–4.60]	0.0215
Extremely severe	17	10.6	4	2.5	4.60 [1.51–14.01]	0.0071
Bronchopulmonary syndrome						
Absent	13	8.1	6	3.8	1.33 [0.57–3.12]	0.50

Moderate	41	25.7	78	48.8	0.41 [0.25–0.67]	0.0003
Pronounced	106	66.2	76	47.4	2.17 [1.38–3.41]	0.0008
Intoxication syndrome						
Absent	13	8.1	10	6.2	1.33 [0.57–3.12]	0.50
Moderate	40	25.0	73	45.6	0.41 [0.25–0.67]	0.0003
Pronounced	107	66.9	77	48.2	2.18 [1.38–3.42]	0.0008
Hematological changes						
Anemia	94	58.8	37	23.1	4.73 [2.92–7.68]	<0.0001
Leukocytosis	38	23.8	53	33.1	0.63 [0.38–1.03]	0.0828
Leukopenia	26	16.3	2	1.3	15.33 [3.57–65.78]	<0.0001
Lymphocytopenia	19	11.9	2	1.3	10.65 [2.44–46.51]	0.0001
Erythrocyte sedimentation rate (mm/h)						
<20	29	18.2	75	46.9	0.25 [0.15–0.42]	–
21–30	9	5.6	22	13.8	0.37 [0.17–0.84]	0.0140
31–40	18	11.3	18	11.3	1.00 [0.50–2.00]	1.0000
41–50	30	18.7	21	13.1	1.53 [0.83–2.80]	0.1693
51–60	34	21.2	15	9.3	2.61 [1.36–5.01]	0.0032
>60	40	25.0	9	5.6	5.59 [2.61–11.98]	<0.0001
Microscopy						
Smear microscopy (AFB-positive)	62	38.8	88	55.0	0.52 [0.33–0.81]	0.0036
Molecular Genetic test						
GeneXpert positive	93	58.2	108	67.5	0.67 [0.42–1.05]	0.1054
Lesion localization						
Unilateral	55	34.4	65	40.6	0.77 [0.49–1.21]	0.2987
Bilateral	105	65.6	95	59.4	1.31 [0.83–2.06]	0.2987
Lesion extent						
Limited	44	27.5	60	37.5	0.63 [0.39–1.01]	0.0732
Extensive	116	72.5	100	62.5	1.58 [0.99–2.54]	0.0732
Pulmonary destruction	55	34.4	95	59.4	0.36 [0.23–0.56]	0.0000

Note: Odds ratios (OR) with 95% confidence intervals and p*-values were omitted for variables where statistical comparison was not applicable due to low event counts, incomplete data, or non-significant variability between groups. NE- Not estimable.*

The spectrum of disease manifestations, including primary and extrapulmonary involvement, also differed between the two cohorts as described in Table 2.

Table 2. Clinical forms of tuberculosis.

Clinical form	Group I (TB/HIV)	%	Group II (TB only)	%	p-value
Nodular	6	3.6	–	–	
Infiltrative	98	61.3	153	95.6	<0.0001
Disseminated	10	6.3	3	1.9	-
Generalized	46	28.8	4	2.5	<0.0001

Note: *Data are presented as number of patients and percentages. Statistical comparison between groups was performed using Fisher's exact test. A significantly higher proportion of infiltrative forms was observed in Group II (p < 0.0001), while generalized TB was more frequent in Group I (p < 0.0001).*

Associated comorbidities played an important role in shaping the clinical course of patients as shown in Table 3.

Table 3. Associated diseases in patients with tuberculosis and tuberculosis/HIV co-infection.

Associated disease	Group I (TB/HIV)	%	Group II (TB only)	%	p-value
Liver disease (hepatitis B, C, toxic hepatitis, liver cirrhosis)	66	53.3	16	22.8	<0.0001
Type 2 diabetes mellitus	2	1.6	6	8.6	-
Gastric ulcer	6	4.8	10	14.3	-
COVID-19	17	13.7	22	31.4	-
Syphilis	14	11.3	3	4.3	-
Epilepsy	5	4.1	1	1.4	-
Stroke	1	0.8	2	2.9	-
Polyneuropathy and alcohol-related encephalopathy	12	9.6	6	8.6	-
Arterial hypertension	1	0.8	4	5.7	-

Note: *Data are presented as number of patients and percentages. Statistical comparisons were conducted using Fisher's exact test. A significant difference was observed only in the prevalence of liver disease, which was higher in the TB/HIV group (p < 0.0001).*

Discussion

The results of this study highlight the significant impact of HIV infection on the clinical manifestations of newly diagnosed tuberculosis. A comparison of two matched cohorts revealed substantial differences in clinical presentation, disease severity, and associated comorbidities, confirming that HIV-related immunodeficiency alters the clinical spectrum of tuberculosis. These findings are consistent with existing literature indicating that tuberculosis in HIV-positive patients tends to be more severe and atypical [6, 9].

Subacute onset was predominant in the HIV group, whereas insidious onset prevailed in the HIV-negative group, suggesting that immunosuppression accelerates disease progression. Consequently, general condition at diag-

nosis was more severe in co-infected patients, with 27.4% classified as severe or extremely severe, compared to only 10.6% in the control group.

The clinical forms analysis revealed a significantly higher prevalence of generalized tuberculosis in the co-infected group (28.8% vs. 2.5%). Among those with generalized TB in the HIV group, 73.9% had multiple extrapulmonary involvements, indicating more extensive disease. In contrast, the infiltrative form predominated in HIV-negative patients (95.6%), suggesting typical pulmonary localization. These findings align with the study by Stoica Călărașu C. et al., who reported higher incidence of extrapulmonary TB in HIV-positive individuals due to immunosuppression [7].

These findings justify the characterization of TB/HIV cases as "atypical", since the clinical picture deviates from the classical pulmonary TB presentation, with diminished frequency of hallmark respiratory symptoms and predominance of nonspecific systemic manifestations.

Extensive lesions was more frequent in the HIV group, although pulmonary destruction was more common in HIV-negative patients, likely due to cavitary lesions typically formed in immunocompetent hosts.

Bronchopulmonary and intoxication syndromes were more pronounced in co-infected patients. Laboratory results showed higher frequency of anemia, leukopenia, and lymphocytopenia in the HIV group – markers of immunosuppression – while leukocytosis was more common in the HIV-negative group. Median erythrocyte sedimentation rate was also higher in the HIV group (50 mm/h vs. 34 mm/h), with 25% of cases exceeding 60 mm/h, indicating more intense systemic inflammation. Although a blunted inflammatory response would be expected in immunocompromised individuals, in our cohort ESR values were significantly higher in TB/HIV patients. This apparent paradox may be explained by the high prevalence of anemia, hypergammaglobulinemia, and co-existing chronic infections in this group, all of which are known to increase ESR independently of immune competence.

Smear positivity was lower in the HIV group, consistent with Meintjes (2024) who described lower bacillary load in disseminated or extrapulmonary forms in HIV-infected patients. However, GeneXpert detected *Mycobacterium tuberculosis* in a high proportion of both groups, confirming its diagnostic utility. In our study, Xpert MTB/RIF sensitivity in the TB/HIV-negative cohort was lower than expected for immunocompetent patients, despite this test being generally recognized for its high sensitivity in such populations. Possible explanations include a higher proportion of paucibacillary forms, suboptimal specimen quality, or delays in processing, which may have reduced bacterial load and test performance. The impaired immune response in HIV-infected individuals often prevents granuloma formation, facilitating the dissemination of *Mycobacterium tuberculosis* to extrapulmonary sites. This leads to atypical and generalized TB forms, which are frequently smear-negative and require advanced diagnostic tools for detection [16].

Furthermore, integrated screening data from Moldova revealed that in 67.5% of TB/HIV co-infection cases, tuberculosis and HIV were diagnosed simultaneously, underscoring the importance of dual testing among vulnerable populations to ensure early detection and comprehensive management [17].

Radiological findings showed more frequent bilateral and extensive lesions in co-infected patients, though cavitary lesions were less prevalent – typical for anergic forms with deficient cell-mediated immunity, where caseating necrosis and cavity formation are impaired [11].

Complications were more common in the HIV group, especially cachexia and pleurisy. In contrast, hemoptysis was more frequent in the HIV-negative group. Among comorbidities, liver pathology was more prevalent in co-infected patients, linked to viral hepatitis and drug toxicity. SARS-CoV-2 infection was more frequent in HIV-negative patients. Opportunistic diseases (e.g., oropharyngeal candidiasis, herpes zoster) were observed exclusively in the HIV group, emphasizing patient vulnerability.

Mortality was significantly higher in co-infected patients (28.1% vs. 6.9%), with tuberculosis as the primary cause in 75.6% of deaths. These findings are consistent with the 2024 Global Tuberculosis Report, which recognizes tuberculosis as the leading cause of death among HIV-positive individuals, underscoring the urgency of targeted interventions.

This study is not without limitations. Its retrospective design may inherently involve incomplete or inconsistent documentation; however, an exhaustive review of all available medical records was undertaken at the national level, including cases from the Transnistrian region, in order to minimize information bias. Although laboratory and imaging data were unavailable for a small subset of patients who either died shortly after diagnosis or initiated ambulatory treatment, matching procedures ensured comparability between groups with respect to demographic characteristics and drug resistance profiles. The analysis was restricted to a single year (2021), yet this interval was considered representative of the national epidemiological context, as no substantial differences were observed in adjacent years. Finally, the findings, while nationally representative, should be extrapolated to other settings with caution.

Conclusions

This comparative study highlights the considerable influence of HIV on the clinical presentation and progression of tuberculosis. In co-infected patients, TB more often manifests as generalized, extrapulmonary disease with subacute onset and atypical symptoms – marked by anemia, lymphopenia, systemic inflammation, and fewer cavitary lesions, and lower rates of bacteriological confirmation. Higher complication and comorbidity rates in the HIV group underscore the need for early detection, adapted diagnostic strategies, and rapid initiation of both antiretroviral and anti-TB therapy. Clinicians should maintain a high index of suspicion, especially in high-prevalence HIV settings, where TB may mimic other conditions.

Competing interests

None declared.

Authors' contribution

II performed data collection and analysis and prepared the initial manuscript draft. AU provided scientific oversight and contributed significantly to the critical revision of the manuscript. CI supported the methodological framework and participated in the interpretation of clinical parameters. AC supervised the final data interpretation and ensured the comprehensive scientific review of the article.

Ethics approval

The study protocol was approved by the Research Ethics Committee of *Nicolae Testemițanu* State University of Medicine and Pharmacy (minutes No 66 from 29.09.2023).

Informed consent for publication

Obtained.

Acknowledgements and funding

No external funding was received for this study.

Provenance and peer review

Not commissioned, externally peer reviewed.

References

1. World Health Organization. Global tuberculosis report 2024. Geneva: WHO; 2024.
2. Kraef C, Roen A, Podlekareva D, Bakowska E, Nemeth J, Knappik M, et al. Incident tuberculosis in people with HIV across Europe from 2012 to 2022: incidence rates, risk factors and regional differences in a multicentre cohort study. Eur Respir J. 2025;65(6):2401904. doi:10.1183/13993003.01904-2024.
3. Ministry of Health of the Republic of Moldova. [Tuberculosis in adults: National Clinical Protocol]. 6th ed. Chișinău: The Ministry; 2024. Romanian.
4. Kraef C, Bentzon A, Roen A, Bolokadze N, Thompson M, Azina I, et al. Long-term outcomes after tuberculosis for people with HIV in Eastern Europe. AIDS. 2023;37(13):1997-2006. doi: 10.1097/QAD.0000000000003670.
5. Moges S, Lajore BA. Mortality and associated factors among patients with TB-HIV co-infection in Ethiopia: a systematic review and meta-analysis. BMC Infect Dis. 2024;24(1):773. doi: 10.1186/s12879-024-09683-5.
6. Peters JS, Andrews JR, Hatherill M, Hermans S, Martinez L, Schurr E, et al. Advances in the understanding of *Mycobacterium tuberculosis* transmission in HIV-endemic settings. Lancet Infect Dis. 2019;19(3):e65-e76. doi: 10.1016/S1473-3099(18)30477-8.
7. Stoica Călărașu C, Popa Miulescu AM, Turcu AA, Nitu FM. The profile of the patients with double infection HIV and TB in South West of Romania. Curr Health Sci J. 2021;47(1):107-13. doi: 10.12865/CHSJ.47.01.17.
8. Meintjes G, Maartens G. HIV-associated tuberculosis. N Engl J Med. 2024;391(4):343-55. doi: 10.1056/NEJMra2308181..
9. Nzuzi CN, Onyamboko M, Kokolomami J, Tukadila HA, Natuhoyila AN, Longo-Mbenza B. Factors associated with tuberculosis-HIV co-infection in diagnosis in the Nzanza Health Zone. Open Access Libr J. 2021;8(3):1-14. doi: 10.4236/oalib.1107105.
10. Philipose CS, KM S, Haridas H, Ramapuram J, Rai S. Clinico-pathological profile of patients with HIV and tuberculosis co-infection. HIV AIDS Rev. 2024;23(3):204-8. doi: 10.5114/hivar/170270.
11. Patel A, Pundkar A, Agarwal A, Gadkari C, Nagpal AK, Kuttan N. A comprehensive review of HIV-associated tuberculosis: clinical challenges and advances in management. Cureus. 2024;16(9):e68784. doi: 10.7759/cureus.68784.
12. Chan AC, Huang SS, Wong KH, Leung CC, Lee MP, Tsang TY, et al. Changes in the epidemiology and clinical manifestations of human immunodeficiency virus-associated tuberculosis in Hong Kong. Hong Kong Med J. 2024 Aug;30(4):281-290. doi: 10.12809/hkmj2310683.
13. Goncharova O, Abrahamyan A, Nair D, Beglaryan M, Bekbolotov A, Zhdanova E, et al. Triple priority: TB/HIV co-infection and treatment outcomes among key populations in the Kyrgyz Republic: a national cohort study (2018-2022). Trop Med Infect Dis. 2023;8(7):342. doi: 10.3390/tropicalmed8070342.
14. Kerkhoff AD, Havlir DV. CROI 2021: tuberculosis, opportunistic infections, and COVID-19 among people with HIV. Top Antivir Med. 2021;29(2):344-51.
15. Lelisho ME, Wotale TW, Tareke SA, Alemu BD, Hassen SS, Yemane DM, et al. Survival rate and predictors of mortality among TB/HIV co-infected adult patients: retrospective cohort study. Sci Rep. 2022;12(1):18360. doi: 10.1038/s41598-022-23316-4.
16. Ivanes I. TB și HIV: o dublă povară în sănătatea publică [TB and HIV: a double burden in public health]. Bull Acad Sci Mold. Med Sci. 2024;(3):160-165. doi: 10.52692/1857-0011.2024.3-80.29. Romanian.
17. Ivanes I, Ustian A, Iavorschi C, Popa V, Paladi C. Caracteristica cazurilor noi de tuberculoză pulmonară la persoanele care trăiesc cu HIV [Characteristics of new pulmonary tuberculosis cases in people living with HIV]. In: 5th Congress of family doctors of the Republic of Moldova with international participation; 2024 May 17-18; Chișinău, Moldova: Articles and abstracts. Chișinău: Medicina; 2024. p. 158-164. Romanian.

https://doi.org/10.52645/MJHS.2025.3.20

UDC: 582.998.2:581.192(478)

RESEARCH ARTICLE

Comparative assessment of active compounds in *Solidago* species from the flora of the Republic of Moldova

Cornelia Fursenco[1,2*], Violeta Alexandra Ion[3], Tatiana Calalb[1,2], Livia Uncu[2,4]

[1]Department of Pharmacognosy and Pharmaceutical Botany, *Nicolae Testemitanu* State University of Medicine and Pharmacy, Chisinau, Republic of Moldova
[2]Drug Development Center, *Nicolae Testemitanu* State University of Medicine and Pharmacy, Chisinau, Republic of Moldova
[3]Research Center for Studies of Food Quality and Agricultural Products, University of Agronomic Sciences and Veterinary Medicine of Bucharest, Romania
[4]Department of Pharmaceutical and Toxicological Chemistry *Nicolae Testemitanu* State University of Medicine and Pharmacy, Chisinau, Republic of Moldova

ABSTRACT

Introduction. *Solidago virgaurea* (European goldenrod) and *Solidago canadensis* (Canadian goldenrod) are two plant species that have been extensively investigated for their complex phytochemical profiles, particularly represented by flavonoids, phenolic acids, saponins, and essential oils with notable antioxidant and anti-inflammatory properties.

Material and methods. Goldenrod plants were collected during the flowering period (2019–2024), *S. virgaurea* obtained from spontaneous flora and *S. canadensis* from the Scientific-Practical Center in the Domain of Medicinal Plants of *Nicolae Testemitanu* State University of Medicine and Pharmacy. The macroscopic analysis was performed using specific morphological indices of the *Herba* vegetal product, while the microscopic examination was performed on superficial preparations and cross-sections of vegetal material using a *Micros* microscope equipped with a digital imaging system. Dry extracts were prepared using repeated maceration, followed by phytochemical investigations employing qualitative color and sedimentation tests, ultraviolet-visible spectrophotometry (for total polyphenolic compounds, flavonoids, hydroxycinnamic acids, carotenoids, and saponins), and gas chromatography-mass spectrometry for essential oils. The antioxidant potential was assessed *in vitro* using the 2,2'-azino-bis(3-ethylbenzothiazoline-6-sulfonic acid) radical scavenging assay and the metal chelation method. *In vivo* pharmacological studies included antimicrobial activity, assessed via serial dilution in liquid nutrient media, and anti-inflammatory activity, evaluated using the xylene-induced ear edema model in mice and the carrageenan-induced paw edema model in rats.

Results. The biological, macroscopic, and microscopic investigations established reliable diagnostic criteria for the clear differentiation and identification of *Herba*-type vegetal products derived from the two *Solidago* species from the Moldovan flora. Qualitative phytochemical screening using specific color and sedimentation reactions confirmed the presence of flavonoids and triterpenic saponins in the examined vegetal products. Quantitative ultraviolet-visible spectrophotometric analysis revealed that *S. canadensis* contained relatively higher levels of bioactive compounds–flavonoids, hydroxycinnamic acids, saponins, and carotenoids–and exhibited greater antioxidant activity compared to *S. virgaurea*. Gas chromatography-mass spectrometry analysis showed that the essential oils of both species differ more quantitatively than qualitatively. Both *Solidago* species exhibited moderate anti-inflammatory and antibacterial activities.

Conclusions. The results of this complex study support the selection of the vegetal product *Solidaginis canadensis herba* as a promising candidate for the local pharmaceutical industry, serving as a valuable source of new local plant-derived antioxidant, anti-inflammatory, and antibacterial drugs.

Keywords: *S. canadensis* L., *S. virgaurea* L., active compounds, pharmacognostic study.

Cite this article: Fursenco C, Ion VA, Calalb T, Uncu L. Comparative assessment of active principles in *Solidago* species from the Republic of Moldova flora. Mold J Health Sci. 2025;12(3):130-141. https://doi.org/10.52645/MJHS.2025.3.20.

Manuscript received: 17.07.2025

Accepted for publication: 31.08.2025

Published: 15.09.2025

Key messages

What is not yet known on the issue addressed in the submitted manuscript

Biological, macroscopic, microscopic, phytochemical, and pharma-

***Corresponding author: Cornelia Fursenco**, assistant professor
Department of Pharmacognosy and Pharmaceutical Botany
Nicolae Testemitanu State University of Medicine and Pharmacy
66 Malina Mica str., Chișinău, Republic of Moldova, MD-2025
e-mail: cornelia.fursenco@usmf.md

Authors' ORCID IDs
Cornelia Fursenco – https://orcid.org/0000-0003-0692-6819
Violeta Alexandra Ion: https://orcid.org/0000-0002-5158-5454
Tatiana Calalb – https://orcid.org/0000-0002-8303-3670
Livia Uncu – https://orcid.org/0000-0003-3453-2243

ecological studies of *Solidago* species from the flora of the Republic of Moldova.

The research hypothesis

Solidago virgaurea and Solidago canadensis species from the flora of the Republic of Moldova could serve as sources of various active principles (phenolic compounds, saponins, volatile oils) responsible for important therapeutic effects, such as antioxidant, anti-inflammatory, and antibacterial activities.

The novelty added by manuscript to the already published scientific literature

This is the first detailed study on *S. virgaurea* and *S. canadensis* from the Moldovan flora, providing original data on their pharmacognostic features, chemical composition, and biological activities, while highlighting their potential for future therapeutic applications and local pharmaceutical valorization.

Introduction

The genus *Solidago* L. includes approximately 127 species distributed across all continents. Of these, 105 species are native to Canada and the USA, 9 species occur in Mexico, and 11 species are present in South America, the Azores, Europe, and Asia [1]. In the flora of the Republic of Moldova, *S. virgaurea* (European goldenrod) grows spontaneously, while *S. canadensis* (Canadian goldenrod) is an adventive, cultivated species [2, 3]. According to the "Euro+Med PlantBase" database, in addition to *S. virgaurea*, its subspecies *S. virgaurea* subsp. *taurica* (Juz.) is also found in the wild flora of Moldova [4].

Aerial parts collected from both *S. virgaurea* and *S. canadensis* have been used since ancient times in the treatment of urinary tract diseases (nephrolithiasis, prostate disorders), while the leaves and flowers were employed to obtain natural brown and orange dyes [5, 6].

Although the pharmacotherapeutic potential of these plant species was largely overlooked for a long period, they are currently experiencing renewed interest and recognition within modern phytotherapy [5-7].

European goldenrod and Canadian goldenrod are two species widely studied for their rich phytochemical profiles, particularly in relation to phenolic compounds known for their antioxidant and anti-inflammatory properties [7, 8]. Over the years, research has shown that both species contain significant levels of flavonoids, phenolic acids, saponins, and essential oils (EO), which contribute to their therapeutic applications [9-19]. Key phenolic compounds identified in *S. virgaurea* include rutin, quercetin, isoquercitrin, chlorogenic acid, and dicaffeoylquinic acids, whereas *S. canadensis* also contains high concentrations of similar compounds, with chlorogenic acid and rutin being dominant constituents [12-14]. These phenolics have demonstrated strong antioxidant activity through radical scavenging and metal-chelating assays [7, 12, 15]. In particular, isoquercitrin and chlorogenic acid contribute not only to antioxidant potential but also exhibit anti-inflammatory, cardioprotective, and chemopreventive effects [13-15]. It has been shown that the content and composition of phenolic compounds and EO can be influenced by the plant part analyzed and the extraction method used [16, 17]. These findings support the continued pharmacological interest in *Solidago* species and provide a scientific foundation for their use in herbal medicine and phytotherapy.

It should be noted that phytochemical and pharmacological studies on *Solidago* species from the flora of Moldova have not yet been conducted, although their relevance in the prophylaxis and treatment of urinary tract diseases is evident. Thus, the growing interest in *Solidago* species as medicinal plants, along with the limited research on *S. virgaurea* and *S. canadensis* in our country, served as the motivation for conducting this comprehensive pharmacognostic study.

Material and methods

***Plant material for phytochemical and pharmacological studies*.** Plants of *Solidago* species served as biological material: *S. virgaurea* – collected from the spontaneous flora of the *Trebujeni Landscape Reserve* (47°19′36″N, 28°57′24″E), Orhei district, and *S. canadensis* – from the collection of the Scientific-Practical Center in the Domain of Medicinal Plants (SPCDMP) of *Nicolae Testemitanu* State University of Medicine and Pharmacy (46°54′06″N, 28°40′05″E). Aerial parts of the plants (consisting of fragments of stems, leaves, and inflorescences) collected during the flowering period between 2019 and 2024 were used for this study: *Solidaginis virgaureae herba* and *Solidaginis canadensis herba.* The vegetal products were dried under natural conditions in well-ventilated, dry, and dark rooms and stored in paper bags.

Plant material for macro- and microscopic studies. Fresh and dried plant organs were used: rhizomes and roots, stems, leaves, flowers, and fruits were harvested during the flowering period between 2018 and 2020.

***Dry extract preparation*.** The dried aerial parts were

shredded using a grinder, and the powder was sieved through a 0.5 mm pore sieve. The extracts were obtained by the fractional maceration method with 60% ethyl alcohol for 30 minutes of continuous stirring. The extracts were filtered through Whatman No. 2 paper under vacuum using a Büchner funnel. The same procedure was repeated 5 times until maximum exhaustion. The obtained extracts were concentrated at 40 °C using the Laborota 4011 rotary evaporator [20].

Macro- and microscopic assay. The macroscopic study was based on the following indicators: plant height, rhizome morphology (shape, color, surface, and fracture relief), stem morphology (shape, color, surface, and fracture relief), leaf morphology (type, presence or absence of petiole, arrangement on the stem, leaf size, and lamina configuration), inflorescence morphology (type, size, and color), and fruit morphology (type, shape, and size). The microscopic analysis was conducted on clarified (with chloral hydrate or 3% NaOH) superficial preparations of the leaves and flowers, and on cross-sections of the leaf lamina, stem, and rhizome, using the *Micros* binocular optical microscope at 4x, 10x, and 40x objective magnification [20-22].

Extraction of essential oil (EO). EO were extracted by hydro-distillation using a NeoClevenger extractor from fresh aerial parts (stems, leaves, and inflorescences) collected at the full bloom stage [23].

Qualitative identification of active principles. The qualitative chemical study was performed using color and sedimentation reactions for flavonoids and saponins [20, 24], and the individual components of the EO were identified by gas chromatography-mass spectrometry (GC-MS), comparing the unique mass spectral fragmentation patterns of each peak with the mass spectral computer library database (NIST MS Search 2.2) and relevant references [23, 25].

Spectrophotometric assay of phenolic compounds. The ultraviolet-visible (UV-VIS) spectrophotometric analysis of total polyphenolic compounds, flavonoids, and hydroxycinnamic acids in the dry extracts of *Solidago* species was carried out using the Metertech UV/VIS SP 8001 spectrophotometer. The total content of polyphenols was determined by 2 Folin-Ciocalteau methods (FC1 and FC2), expressed in terms of gallic acid at 760 nm [26, 27]. The flavonoid content was determined relative to rutin after a reaction with aluminium chloride at 412 nm [28]. The quantitative determination of hydroxycinnamic acids was performed relative to caffeic acid after a reaction with Arnow's reagent (sodium molybdate and sodium nitrite) at 500 nm [24]. was All experiments were repeated three times for statistical validity.

Spectrophotometric assay of saponins. The total saponin content was determined using the vanillin-sulfuric acid assay in correlation with a standard saponin solution at 540 nm [29].

Spectrophotometric assay of carotenoid pigments. The total carotenoid content was measured at a wavelength of 448 nm [30].

GC-MS of EO. The obtained EO were diluted in hexane (1:100) and analyzed using an Agilent Series GC-MS system, consisting of a GC 7890B gas chromatograph and an MS 5977A mass spectrometer. The capillary column used was HP-5MS Ultra Inert (30 m x 0.25 mm x 0.25 μm). The temperature program was: 50 °C for 8 min, then heated to 280 °C at 4 °C/min. The carrier gas was helium (1 mL/min), and the injection volume was 3 μL with a 50:1 split ratio [23, 25].

Antioxidant activity. To assess antioxidant activity, two complementary *in vitro* chemical methods were used: ABTS (2,2'-azino-bis(3-ethylbenzothiazoline-6-sulfonic acid)) assay and the Ferrozine Test (assay of iron-binding antioxidant capacity) [31].

Anti-inflammatory activity. The anti-inflammatory activity of *Solidago* extracts was evaluated in mice using a xylene-induced ear edema model and in rats using a carrageenan-induced paw edema model. Data were analyzed by one-way ANOVA with Bonferroni post-hoc test [32].

Antibacterial activity. The antibacterial activity was determined using the serial dilution method in liquid nutrient medium (2% peptone meat broth, pH = 7.0). *Staphylococcus aureus* (t. 209, ATCC 25923), *Enterococcus faecalis* (ATCC 19433), *Escherichia coli* (ATCC 25922), *Klebsiella pneumoniae* (ATCC 3534/51), and *Pseudomonas aeruginosa* (ATCC 27853) were used as reference cultures [33].

Statistical analysis. All tests were performed in triplicate, and statistical processing of the obtained data was carried out using MS Excel 2021. Variational statistics were applied to calculate the arithmetic mean **±** standard deviation (SD).

Results

Macro- and microscopic study

Species of the genus *Solidago* share common characteristics: they are rhizomatous perennials that develop simple, alternate, ovate-lanceolate leaves with entire blades. The plants form calathidia clustered in simple or paniculate racemes, with ligulate, yellow, female, marginal flowers, while the central ones are tubular and bisexual. The fruits are cylindrical achenes provided with a pappus formed of seriate bristles [2, 8, 10]. At the same time, there are also distinctive morphological criteria for each species. The main specific macroscopic characters for the differentiated identification of vegetal products of the analysed *Solidago* species were established using dried, shredded aerial parts (fragments of stems, leaves, inflorescences, and separated flowers), according to several criteria, as illustrated in the following table (Table 1) [2, 22].

Microscopic techniques were used to identify the main anatomical features, and specific chemical reagents were applied to highlight the structural composition. Based on these observations, the most relevant microscopic characters were selected to ensure the reliable identification of *Solidaginis virgaureae herba* and *Solidaginis canadensis herba* (Table 2) [21, 22]. This anatomical study revealed distinct structural markers that serve as key diagnostic traits for differentiating *S. virgaurea* and *S. canadensis* within the flora of Moldova.

Table 1. Specific macroscopic characters for vegetal products of *Solidago* species

Specific macroscopic characters *Solidaginis virgaureae herba* *Solidaginis canadensis herba*			Vegetal product	
Stem	Cross-section contour		pentagonal	circular
	Color	External surface	light green	dark green
		Internal surface	whitish-green	light green
	Diameter, cm		0.5-1.0	0.4-0.7
Leaf	Shape		ovate-elliptic, toothed margin	elongated-lanceolate, serrate margin
	Color		light green	dark green
	Size (cm)	Length	0.8-1.2	0.9-2.2
		Width	0.2-0.5	0.2-0.3
Inflorescence	Type		erect raceme + calathidium	pyramidal raceme + calathidium
	Calathidium diameter (cm)		1.0-1.5	0.5-0.6
Flower length	Ligulate		0.8-1.2	0.3-0.5
	Tubular		0.2-0.3	0.2-0.4

Table 2. Specific microscopic characters of vegetal products for *Solidago* species

Specific microscopic characters *Solidaginis virgaureae herba*		Vegetal product *Solidaginis canadensis herba*	
Stem	Cross-section contour	pentagonal	circular
	Secretory tissue	secretory channels	secretory channels
Leaf blade	Anatomical type	dorsoventral mesophyll; amphistomatic leaf	equifacial mesophyll; amphistomatic leaf
	Epidermis	▪ well-defined cells; ▪ anomocytic stomata; ▪ multicellular protective conical trichomes; ▪ flabelliform trichomes; ▪ unicellular secretory trichome	▪ well-defined cells; ▪ anomocytic stomata; ▪ multicellular protective conical trichomes; ▪ flabelliform trichomes; ▪ multicellular secretory trichomes
Ligulate/tubulate flowers	Epidermis	rectangular cells with thin walls	rectangular cells with thin walls
	Pappus	multiseriate, non-branched bristles	multiseriate, branched bristles

Phytochemical studies

Qualitative analysis of active compounds. The qualitative comparative analysis of flavonoids and saponins were carried out using specific color and sedimentation reactions, with the observation of characteristic analytical effects, as summarized in the tables below (Table 3) [18, 19].

Table 3. Qualitative comparative analysis of flavonoids and saponins in *Solidaginis virgaureae herba* and *Solidaginis canadensis herba*

Qualitative analysis of flavonoids					
No	Vegetal product	Shinoda test (Zn + HCl solution)	NaOH solution (10%)	Lead acetate solution (2%)	Vanillin solution (1%) in concentrated HCl
1	*Solidaginis virgaureae herba*	pale-pink strong effervescence	yellow-orange, weak precipitate	yellowish-white precipitate	green color, intensity decreases
2	*Solidaginis canadensis herba*	pale-pink, weak effervescence	yellow-orange, weak precipitate	yellowish-white opalescence	yellow color, intensity decreases

Qualitative analysis of saponins						
No	Vegetal product	Foaming reaction		Lead acetate solution	Liebermann-Burchard test	Lafon test
		HCl solution	NaOH solution			
1	*Solidaginis virgaureae herba*	moderate foam	intense foam	white-pink precipitate	negative reaction	dark greenish-blue color
2	*Solidaginis canadensis herba*	moderate foam	intense foam	yellowish opalescence	negative reaction	dark greenish-blue color

Note: *The table illustrates the specific analytical effects observed in identification reactions for flavonoids and saponins in the vegetal products Solidaginis virgaureae herba and Solidaginis canadensis herba. Abbreviation: No – number.*

Gas chromatography-mass spectrometry analysis of EO extracted from fresh aerial parts of *Solidago* species revealed the presence of 51 chemical constituents in the essential oil of *S. canadensis* and 37 components in that of *S. virgaurea* (Fig. 1). The compounds common to both *Solidago* EO include: α-pinene, camphene, sabinene, β-pinene, β-myrcene, limonene, trans-β-ocimene, terpinolene, borneol, bornyl acetate, γ-elemene, β-elemene, β-caryo-

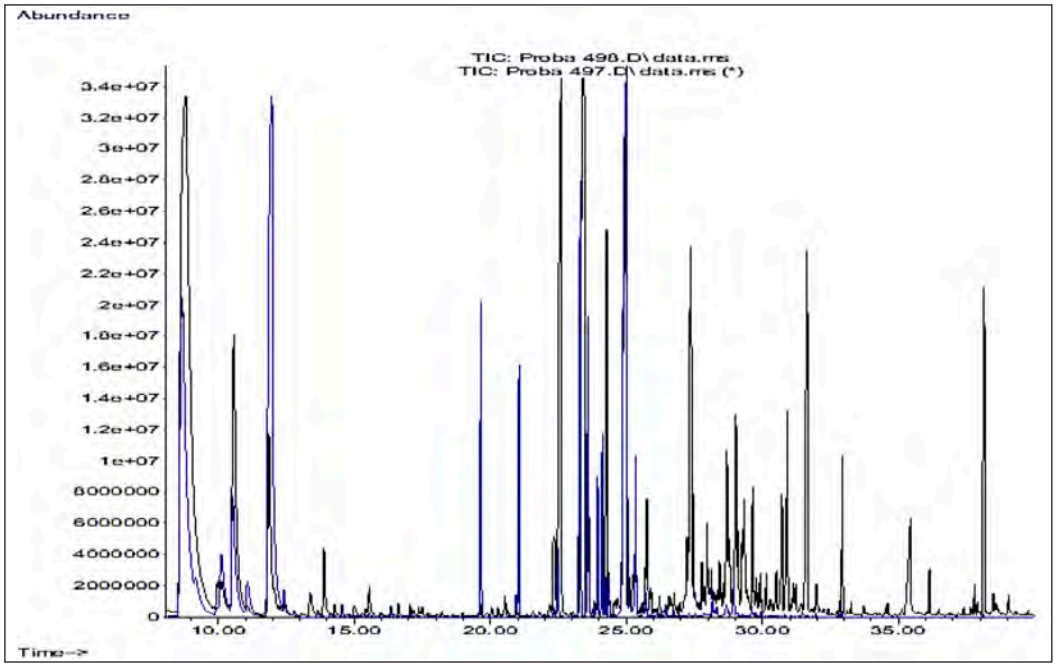

Fig. 1 Chromatogram of *S. canadensis* (sample 497*)* and *S. virgaurea* (sample 498) EO.

Note: *The chromatogram shows the peaks of the separated compounds from the EO of S. canadensis (blue color) and S. virgaurea (black color).*

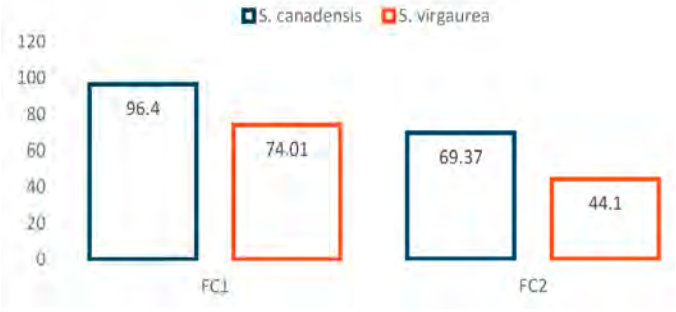

Fig. 2 The total content of polyphenols in *Solidago* extracts by two Folin-Ciocalteu (FC1 and FC2) techniques (mg GAE/g DW).

Note: *The diagram represents the total phenolic content expressed in mg GAE/g DW in Solidago extracts; the blue columns – S. canadensis, the orange ones – S. virgaurea. Variational statistics were applied using MS Excel 2021, and the presented data represent the arithmetic mean of 3 determinations; standard deviations (SD) are as follows: S. canadensis (FC1) – 0.0028; S. virgaurea (FC1) – 0.00047; S. canadensis (FC2) – 0.0010; S. virgaurea (FC2) – 0.00057.*

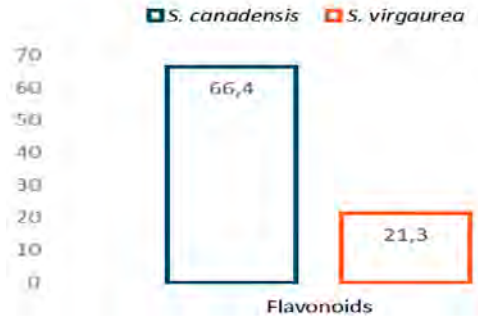

Fig. 3 Total flavonoid content in *Solidago* extracts (mg RE/g DW).

Note: *The diagram represents the total flavonoid content expressed in mg RE/g DW in Solidago extracts.Blue columns – S. canadensis, orange columns – S. virgaurea. Variational statistics were performed using MS Excel 2021. Data represent the arithmetic mean of 3 determinations. Standard deviations (SD) are: S. canadensis – 0.0256; S. virgaurea – 0.0425.*

phyllene, aromadendrene, α -humulene, γ-muurolene, germacrene D, caryophyllene oxide, and phytol. In contrast, some compounds were species-specific, with linalool detected only in *S. canadensis* EO and geraniol identified exclusively in *S. virgaurea* EO (Table 4).

Quantitative analysis of active compounds. The total content of polyphenols in *Solidago* extracts was determined by 2 Folin-Ciocalteau techniques (FC1 and FC2). There are significant differences between the extracts of the analyzed species and between the FC method techniques, in terms of total polyphenol content (FC1: *S. virgaurea* – 74.01, *S. canadensis* – 96.40 mg GAE/g DW; FC2: *S. virgaurea* – 44.10, respectively *S. canadensis* – 69.37 mg GAE/g DW). In the dry extracts of *S. canadensis*, the values of total polyphenol content by both FC techniques are higher than in *S. virgaurea*. The FC1 technique allowed the quantification of a higher concentration of polyphenols for both *Solidago* species (Fig. 2).

The spectrophotometric determination of flavonoids (Fig. 3), in terms of rutin (RE), revealed a higher content of flavonoids in the dry extract of *S. canadensis* (66.4 mg RE/g DW) compared to that of *S. virgaurea* (21.3 mg RE/g DW*)* [34].

The comparative total content of hydroxycinnamic acids (HA), determined by the Arnow spectrophotometric method and expressed as caffeic acid equivalents, showed a concentration of 27 g/100 g DW for the *S. canadensis* extract and 12 g/100 g DW for the *S. virgaurea* extract (Fig. 4) [35].

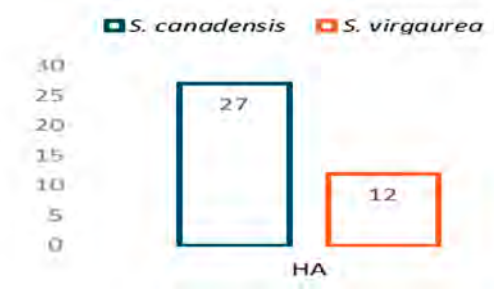

Fig. 4 Total content of HA in *Solidago* extracts (g/100 g DW).

Note: *The diagram represents the total HA content expressed in g/100 g DW in Solidago extracts. Blue columns – S. canadensis, orange columns – S. virgaurea. Variational statistics were performed using MS Excel 2021. Data represent the arithmetic mean of 3 determinations. Standard deviations (SD) are: S. canadensis – 0.0146; S. virgaurea – 0.0049.*

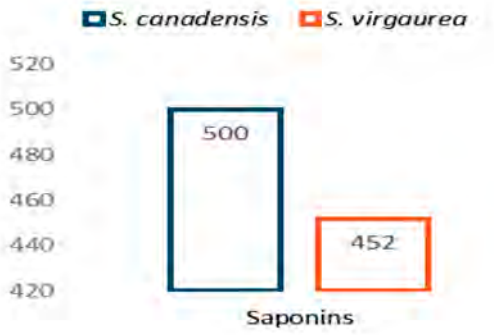

Fig. 5 Total content of saponins in *Solidago* extracts (mg SE/g DW).

Note: *The diagram represents the total saponin content expressed in mg SE/g DW in Solidago extracts. Blue columns – S. canadensis, orange columns – S. virgaurea. Variational statistics were applied using MS Excel 2021, and the presented data represent the arithmetic mean of 3 determinations. Standard deviations (SD) are as follows: S. canadensis – 0.00057; S. virgaurea – 0.00069.*

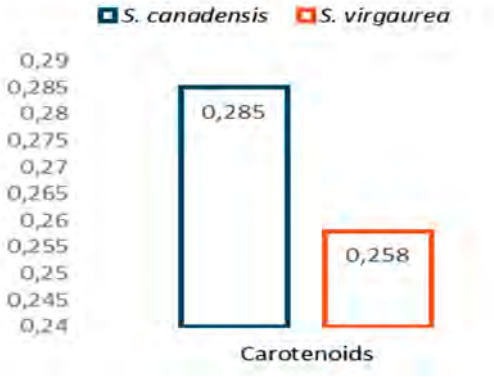

Fig. 6 Total content of carotenoids in *Solidago* extracts (mg βCE/g DW).

Note: *The diagram represents the total carotenoid content in Solidago extracts expressed in mg βCE/g DW. Blue columns – S. canadensis, orange columns – S. virgaurea. Variational statistics were calculated using MS Excel 2021. Data represent the arithmetic mean of 3 determinations. Standard deviations (SD) are: S. canadensis – 0.00054; S. virgaurea – 0.00071.*

Comparative quantitative analysis of saponins (Fig. 5) showed that the dried extract of *S. canadensis* aerial parts contains a higher saponin content (500 mg SE/g DW) compared to the extract of *S. virgaurea* aerial parts (452 mg SE/g DW) [34, 36].

For the spectrophotometric determination of carotenoid pigments (Fig. 6), the following values were obtained: *S. canadensis* – 0.285 mg βCE/g DW, and *S. virgaurea* – 0.258 mg βCE/g DW [34].

Concerning the EO composition of the analyzed *Solidago* species, some compounds were common to both species but different in concentration (Table 4). In *S. virgaurea*, the predominant compound was α-pinene (28.8%), followed by β-caryophyllene (9.96%), β-elemene (8.29%), germacrene D (7.49%), β-myrcene (6.2%), caryophyllene oxide (4.24%), limonene (3.06%), and α-humulene (3.01%). Conversely, the EO of *S. canadensis* was mainly composed of limonene (22.81%), with other major constituents including germacrene D (19.73%), α-pinene (19.03%), β-caryophyllene (6.53%), β-myrcene (4.75%), β-ylangene (4.4%), and bornyl acetate (3.81%) (Table 4).

Table 4. Major chemical constituents in *S. canadensis* and *S. virgaurea* essential oil (EO) analyzed by gas chromatography-mass spectrometry (GC-MS).

No	Compounds	*Solidago canadensis*		*Solidago virgaurea*	
		RT (min)	EO (%)	RT (min)	EO (%)
1	α-Pinene	8.672	19.03	8.672	28.80
2	Camphene	9.163	2.28	na	0.00
3	Sabinene	9.947	0.24	9.947	0.49
4	β-Pinene	10.133	2.66	10.117	0.87
5	β-Myrcene	10.529	4.75	10.529	6.20
6	Limonene	11.972	22.81	11.861	3.06
7	trans-β-Ocimene	12.408	0.67	12.408	0.24
8	Terpinolene	13.645	0.10	13.645	0.07
9	linalool	14.105	0.06	-	0.00
10	Borneol	16.347	0.08	16.347	0.11
11	Geraniol	-	0.00	18.608	0.02
12	Bornyl acetate	19.656	3.81	19.656	0.10
13	γ-Elemene	20.938	0.25	20.938	0.08
14	β-Eiemene	22.485	0.80	22.610	8.29
15	β-Caryophyllene	23.309	6.53	23.447	9.96
16	Aromandendrene	24.117	1.96	24.117	0.73
17	a-Humulene	24.244	0.38	24.244	3.01
18	γ-Muurolene	24.350	0.51	24.350	0.32
19	Germacrene D	24.968	19.73	24.968	7.49
20	Caryophyllene oxide	27.303	0.05	27.357	4.24
21	Phytol	38.084	0.07	38.146	2.66

Note*: The table represents the retention time (RT) expressed in minutes (min) and EO content, expressed in percentage (%), of the main compounds separated by GC-MS from S. canadensis and S. virgaurea EO. The abbreviations used in the table are as follows: No – number, RT – retention time, EO – essential oil, min – minutes.*

Biological activities

The antioxidant activity (Fig. 7) determined by the ABTS assay revealed that leaf extracts from both *Solidago* species exhibited the highest antioxidant activity (44.17 μM TEAC

for *S. canadensis* and 34.31 µM TEAC for *S. virgaurea*), followed by extracts from the aerial parts (39.32 µM TEAC and 33.25 µM TEAC, respectively), and then flower extracts (35.37 µM TEAC for *S. canadensis* and 30.92 µM TEAC for *S. virgaurea*). A comparative analysis using the iron-chelation antioxidant capacity assay showed minimal variation in the results for *S. canadensis* plant materials: the highest chelating ability was observed in the leaves (81.49%), followed by aerial parts (80.19%) and flowers (79.65%). A similar pattern was observed for *S. virgaurea*, with the highest activity in the leaves (80.19%), followed by aerial parts (79.55%) and flowers (79.01%) [34, 37].

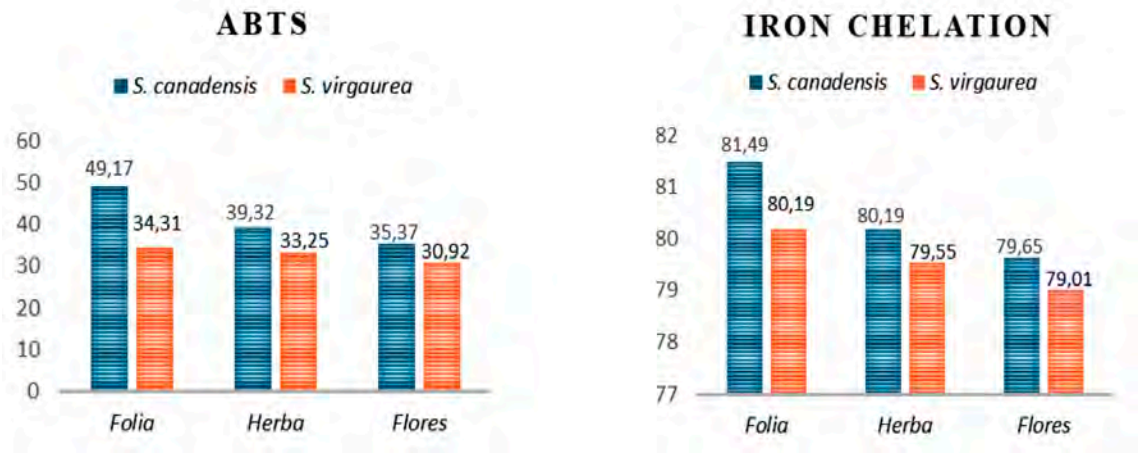

Fig. 7 Comparative antioxidant activity of dried extracts of *S. canadensis* and *S. virgaurea*, determined by ABTS method (µM TEAC) and iron-chelation test (%).

Note: *The diagram represents the comparative antioxidant activity of Solidago extracts (Folia – leaves, Herba – aerial parts, and Flores – flowers) using 2 in vitro methods (ABTS method, expressed in µM TEAC, and iron-chelation test, expressed in %), respectively: the blue columns – S. canadensis, the orange columns – S. virgaurea. Variational statistics were applied using MS Excel 2021, and the presented data represent the arithmetic mean of 3 determinations; standard deviations (SD) 2%.*

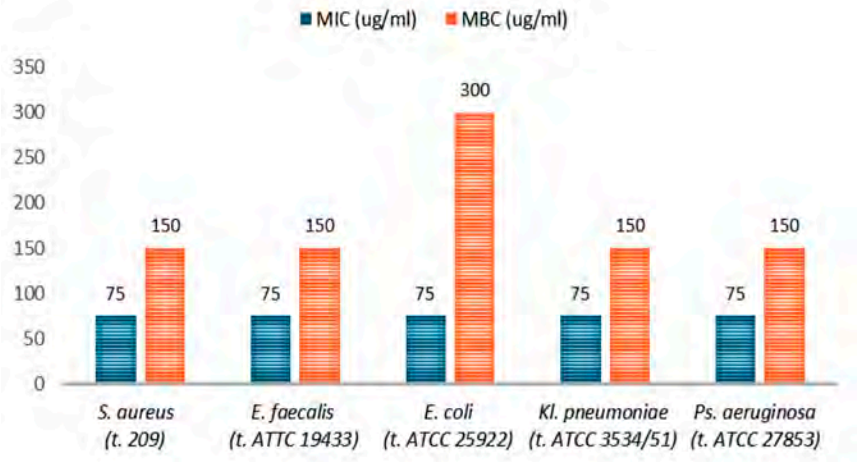

Fig. 8 Antibacterial activity of *S. virgaurea* extract (MIC (µg/ml) – minimum inhibitory concentration, MBC (µg/ml) – minimum bactericidal concentration).

Note: *The diagram represents the antibacterial activity of S. virgaurea extract on different bacterial strains (S. aureus, E. faecalis, E. coli, K. pneumoniae, P. aeruginosa). The blue columns show MIC, expressed in µg/ml, while the orange ones – MBC, expressed in µg/ml.*

The study of the anti-inflammatory activity of *Solidago* aerial parts extracts in the xylene-induced ear edema model in mice showed that, although insignificant compared to the control group, both diclofenac and *Solidago* extracts decreased xylene-induced ear edema. The decrease in edema was more evident with the use of the non-steroidal anti-inflammatory drug and less pronounced with the use of the investigated extracts. The percentage of edema inhibition with diclofenac was 20.38%, and with *Solidago* extracts – 11.99%. When evaluating the anti-inflammatory action of *Solidago* extracts in carrageenan-induced paw edema in rats, a tendency to decrease paw volume compared to the control group was observed, but it was not significant [19, 34].

Determination of the antibacterial activity of *Solidago* extracts was carried out by the serial dilution method in liquid nutrient medium. It was found that the bacteriostatic activity of the *S. virgaurea* aerial parts extract is within the concentration range of 75 µg /ml, and the bactericidal activity varies within the concentration range of 150–300 µg/mL, constituting against *S. aureus* (t. 209), *E. faecalis* (ATCC 19433), *P. aeruginosa* (ATCC 27853), and *K. pneumoniae* (ATCC 3534/51) – 150 µg/ml, and against *E. coli* (ATCC 25922) – 300 µg/mL (Fig. 8).

The bacteriostatic activity of the *S. canadensis* aerial parts extract varies within the concentration range 75 µg/ml – 150 µg/ml and constitutes against *P. aeruginosa* (ATCC 27853) – 75 µg /ml, and against the other investigated bac-

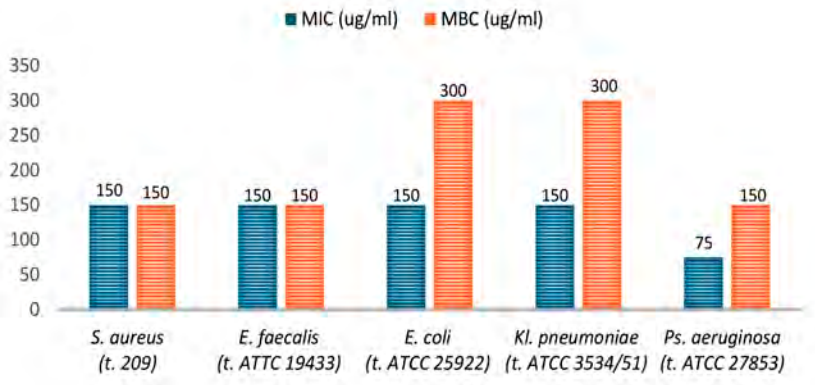

Fig. 9 Antibacterial activity of *S. canadensis* extract (MIC (µg/ml) – minimum inhibitory concentration, MBC (µg/ml) – minimum bactericidal concentration).

Note: *The diagram represents the antibacterial activity of S. canadensis extract on different bacterial strains (S. aureus, E. faecalis, E. coli, K. pneumoniae, P. aeruginosa). The blue columns show MIC, expressed in µg/ml, while the orange ones – MBC, expressed in µg/ml.*

terial cultures – 150 µg /ml. The bactericidal activity varies within the concentration range 150 µg/ml – 300 µg/ml, and constitutes against *S. aureus* (209), *E. faecalis* (ATCC 19433), *P. aeruginosa* (ATCC 27853) – 150 µg/ml, and against *E. coli* (ATCC 25922) and *K. pneumoniae* (ATCC 3534/51) – 300 µg/ml (Fig. 9) [34].

Discussion

This is the first comprehensive comparative study that focused on the biology, macro- and microscopic study, phytochemistry, and main pharmacological activities of *Solidago* species from the flora of Moldova.

Similar studies have been carried out in several European countries, including Romania, Estonia, Bulgaria, Slovenia, Hungary, and Lithuania [9, 10, 12-17, 23, 38, 39]. Our results are in agreement with the majority of the evaluated studies, and we note that there is currently an increasing emphasis on the study of *S. canadensis* for its valorization for both economic and pharmaceutical purposes.

The key distinctive macroscopic features used to differentiate the plant materials of *Solidago* species were identified by examining the dried, shredded aerial parts – including stem, leaf, inflorescence, and individual flower fragments. Also, the distinct structural characteristics with diagnostic significance have been determined: the presence of secretory channels in both the rhizome and stem of both species; the stem's cross-sectional shape (polygonal in *S. virgaurea*, circular in *S. canadensis*); differences in leaf mesophyll (dorsoventral in *S. virgaurea*, equifacial in *S. canadensis*); anomocytic stomata in both species; multicellular protective trichomes of conical and flabelliform types present in both; secretory trichomes differing in structure (with a unicellular base in *S. virgaurea* and a multicellular base in *S. canadensis*); and finally, both species exhibit abundant pappus made of multiseriate bristles and spherical pollen grains [21, 22]. We note that the same mesophyll structure, and specifically multicellular conical and flabelliform trichomes, have also been mentioned by other researchers in *Solidago* species [10, 40].

In most scientific studies, the main researched group of chemical compounds in *Solidago* species are the phenolic ones. This is not by chance, but due to the fact that they are primarily responsible for the antioxidant and anti-inflammatory activities. Our results show a higher content of polyphenols, including the total polyphenols, flavonoids, and hydroxycinnamic acids in the dried extracts of *S. canadensis*, compared to that of *S. virgaurea*, which is also in agreement with other studies [10, 12, 13, 15]. One Romanian research attempts to explain the higher content of phenolic compounds in *S. canadensis* than *S. virgaurea*, based on specific ecological factors and geographical origin that could influence the accumulation of these chemical compounds [10].

Comparative phytochemical studies have demonstrated significant qualitative and quantitative differences in the flavonoid and phenolic acid profiles of these species [13-16, 41, 42]. In *S. virgaurea*, the predominant flavonoids include rutin, quercetin, isoquercitrin, and kaempferol derivatives, which are mainly localized in the aerial parts of the plant [12-13]. In contrast, *S. canadensis* is characterized by a distinct profile, with high concentrations of chlorogenic acid and rutin, along with various glycosylated flavonoids such as hyperoside and quercitrin [15]. Also, a recent Ukrainian study has demonstrated that the high flavonoid content in *S. canadensis*, especially rutin, is closely correlated with the mechanism of invasiveness, being an important element of the strategy for the development and biotransformation of a new habitat [41]. Of particular note is that, for the first time, in Lithuania, analyses of phenolic acids and flavonoids have been conducted on *Solidago × niederederi* Khek, an interspecific hybrid between *S. canadensis* and *S. virgaurea*, in order to assess its phytochemical profile and potential pharmacological relevance [42].

The presence of carotenoid pigments enhances the pharmacological potential of *Solidago* species and supports their use in antioxidant therapies, in particular being investigated as a supporting treatment in cancer [43]. Our results indicate that *S. canadensis* is richer in carotenoid pigments, but we did not identify their individual components. It should be noted that in other studies, individual carotenoid pigments have been isolated, and those characteristic for each *Solidago* species were found: *S. virgaurea* is characterized by a higher content of β-carotene and lutein in its inflorescences, whereas *S. canadensis* tends to accumulate more xanthophylls, particularly zeaxanthin, in both aerial parts and flowers [43, 44].

Saponins are another important class of biologically active compounds specific to *Solidago* species, due to the therapeutic effects they impart, in particular diuretic and antimicrobial properties [5, 7]. Also, it was revealed that triterpenoid saponins extracted from the aerial parts of *S. virgaurea* have shown inhibition of the yeast-to-hyphae transition in *Candida albicans* infection [45].

However, studies on saponins are still limited to date. The present qualitative determination of saponins demonstrated the presence of triterpene saponosides and the absence of steroid ones in the vegetal products of *Solidago* species. Our comparative quantitative saponin analysis shows that *S. canadensis* contains a higher content of saponins (500 mg SE/g DW), in contrast to *S. virgaurea* (452 mg SE/g DW) [34, 36].

Our GC-MS analysis of EO reveals a significant resemblance in the EO composition of both *Solidago* species, especially due to the prominent presence of α-pinene, which appears in greater amounts in *S. virgaurea*. Additionally, monoterpenes and sesquiterpenes were identified as the predominant hydrocarbon classes in the oils of both species, as illustrated in other studies [23, 38]. A notable distinction in our analysis lies in the limonene content – found in high concentrations in *S. canadensis,* but only in minor amounts in *S. virgaurea*. Also, pinene and limonene have been mentioned among the main constituents of *S. canadensis* EO in previous studies [38].

This study confirmed that all tested *Solidago* extracts possess strong antioxidant properties; however, *S. canadensis* extracts showed a more pronounced antioxidant action compared to those of *S. virgaurea*, as reported in other previous studies [12, 15]. Notably, leaf extracts showed significantly higher antioxidant activity in both analytical methods used. These findings are consistent with the results reported in one of the latest scientific papers from Croatia [46].

The antibacterial activity of *Solidago* species has been the subject of several studies, providing insight into their potential as sources of new natural antimicrobial agents. Our study revealed that both *Solidago* extracts showed bactericidal activity between 150–300 μg/mL, while bacteriostatic activity on several bacterial strains was more pronounced at lower concentrations for *S. virgaurea* extract (75 μg/mL). These findings are also consistent with other studies and highlight the moderate variation in antimicrobial potency between these two species [23, 47].

Both *Solidago* species have demonstrated anti-inflammatory effects in various *in vitro* and *in vivo* models, showing efficacy in reducing inflammation associated with chronic conditions such as arthritis, oxidative stress, and tissue damage [39, 47-49]. This study of the anti-inflammatory activity in 2 *in vivo* models demonstrated a mild anti-inflammatory action for both *Solidago* species. According to some authors [39, 46], the anti-inflammatory properties of *S. canadensis* extracts are attributed to both their phenolic compounds and EO. Also, in a rat model using carrageenan-induced edema, *S. virgaurea* extract demonstrated an anti-exudative effect, and both its aqueous and ethanolic extracts have been shown to reduce paw swelling and arthritic inflammation in rats [48]. Additionally, hydroalcoholic extracts of *S. virgaurea* have been found to inhibit dihydrofolate reductase, further supporting their anti-inflammatory potential [49].

Although the current study provides valuable comparative data, further investigations are required to assess the bioavailability, pharmacokinetics, and standardization of active compounds.

Conclusions

The study established clear diagnostic criteria for differentiating *Solidago virgaurea* and *Solidago canadensis* from the Moldovan flora. Comparative phytochemical and pharmacological analyses revealed that these species are rich in biologically active compounds with antioxidant, anti-inflammatory, and antibacterial properties. *S. canadensis* demonstrated a higher content of active principles and greater therapeutic potential, supporting its further investigation for pharmaceutical and nutraceutical applications.

Competing interests

None declared.

Authors' contributions

Conception and design of the work – TC and LU; acquisition of data, experimental part – CF, VI; analysis and interpretation of data – CF, VI, TC, and LU; drafting the article – CF; reviewing the article – LU, TC. All authors revised and approved the final version of the manuscript.

Acknowledgements and funding

The study was carried out with funding from: S/Project code 080301 „Elaboration, analysis, standardization and quality control of pharmaceutical products and monocomponent and combination of synthetic and natural food supplements"; Grant of the Ministry of Research, Innovation and Digitization, CNCS-UEFISCDI, project number PN-IV-P8-8.3-ROMD-2023-0307, within PNCDI IV.

We thank the Department of Pharmacognosy and Pharmaceutical Botany and the Drug Development Center, Scientific Laboratory „Intrahospital Infections", Discipline of Epidemiology, Drug Development Center of *Nicolae Testemitanu* State University of Medicine and Pharmacy, and Research Center for Studies of Food Quality and Agricultural Products, University of Agronomic Sciences and Veterinary Medicine (USAMV) of Bucharest, Romania, for their support in carrying out this study.

Informed consent for publication

Not needed for this study.

Ethics approval

The study protocol was approved by the Research Ethics Committee of the *Nicolae Testemițanu* State University of Medicine and Pharmacy (minutes no. 36, dated 30.05.2019).

Provenance and peer review

Not commissioned, externally peer-reviewed.

References

1. Beck JB, Semple JC, Brull JM, Lance SL, Phillips MM, Hoot SB, Meyer GA. Genus-wide microsatellite primers for the goldenrods (Solidago; Asteraceae). Appl Plant Sci. 2014;2(4):1300093. doi: 10.3732/apps.1300093.

2. Fursenco C, Calalb T. Biologia speciei *Solidago virgaurea* L. din flora Republicii Moldova. [Biology of *Solidago virgaurea* L. species from the flora of the Republic of Moldova]. In: Proceedings of the scientific conference with international participation "Ethical pharmacy: history, realities and prospects", 2018 Apr 19-21, Chisinau, Republic of Moldova. Chişinău; 2018. p.190-196. Romanian.
3. Fursenco C, Calalb T. Species of g. *Solidago* L. in the flora of the Republic of Moldova. Acta Medica Marisiensis. 2018;64(Suppl 3):21. Abstracts of Scientific Aniversary Symposium - 70 years from foundation of University Botanical Garden, Tîrgu-Mureş 1948-2018; 2018 May 30 - June 1; Tîrgu Mureş, Romania.
4. Greuter W. Compositae (pro parte majore). In: Greuter W, von Raab-Straube E, editors. Euro+Med Plantbase – the information resource for Euro-Mediterranean plant diversity; 2006.
5. Melzig MF. [Goldenrod – a classical exponent in urological phytotherapy]. Wien Med Wochenschr. 2004;154(21-22):523-7. doi: 10.1007/s10354-004-0118-4. German.
6. Suleymanova FS, Nesterova OV, Matyushin A. Istoricheskii opyt i perspektivy ispol'zovaniia travy zolotarnika kanadskogo (*Solidago canadensis L.*) v meditsine [The historical background and prospects of Canadian goldenrod (*Solidago canadensis* L.) herb medicinal use]. J Sci Artic Health Educ Millenn. 2017;19(4):142-9. doi: 10.26787/nydha-2226-7425-2017-19-4-142-149. Russian.
7. Apáti P, Szentmihályi K, Kristó ST, Papp I, Vinkler P, Szoke É, Kéry Á. Herbal remedies of *Solidago* – correlation of phytochemical characteristics and antioxidative properties. J Pharm Biomed Anal. 2003;32(4-5):1045-53. doi: 10.1016/s0731-7085(03)00207-3.
8. Fursenco C, Calalb T, Uncu L, Dinu M, Ancuceanu R. *Solidago virgaurea* L.: a review of its ethnomedicinal uses, phytochemistry, and pharmacological activities. Biomolecules. 2020;10(12):1619. doi: 10.3390/biom10121619.
9. Toiu A, Vlase L, Vodnar DC, Gheldiu AM, Oniga I. *Solidago graminifolia* L. Salisb. (Asteraceae) as a valuable source of bioactive polyphenols: HPLC profile, in vitro antioxidant and antimicrobial potential. Molecules. 2019 Jul 23;24(14):2666. doi: 10.3390/molecules24142666.
10. Dobjanschi L, Fritea L, Patay EB, Tamas M. Comparative study of the morphological and phytochemical characterization of Romanian *Solidago* species. Pak J Pharm Sci. 2019;32(4):1571-9.
11. Fursenco C, Balova O, Calalb T. Potenţialul terapeutic al compuşilor fenolici din speciile genului *Solidago.* [Therapeutic potential of phenolic compounds from *Solidago* species]. Mold J Health Sci. 2024;11(3 Suppl 2):734. Abstracts of annual scientific conference "Biomedical and health research: quality, excellence and performance"; 2024 Oct 16-18; Chisinau, Republic of Moldova. Romanian. English.
12. Woźniak D, Ślusarczyk S, Domaradzki K, Dryś A, Matkowski A. Comparison of polyphenol profile and antimutagenic and antioxidant activities in two species used as source of *Solidaginis herba* – goldenrod. Chem Biodivers. 2018 Apr;15(4):e1800023. doi: 10.1002/cbdv.201800023.
13. Thiem B, Wesołowska M, Skrzypczak L, Budzianowski J. Phenolic compounds in two Solidago L. species from in vitro culture. Acta Pol Pharm. 2001 Jul-Aug;58(4):277-81.
14. Rosłoń W, Osińska E, Mazur K, Szprych A. Chemical characteristics of European goldenrod (*Solidago virgaurea* L. subsp. *virgaurea*) from natural sites in central and eastern Poland. Acta Sci Pol Hortorum Cultus. 2014;13(1):55-65.
15. Uzelac Božac M, Poljuha D, Dudaš S, Bilić J, Šola I, Mikulič-Petkovšek M, Sladonja B. Phenolic profile and antioxidant capacity of invasive *Solidago canadensis* L.: potential applications in phytopharmacy. Plants. 2025;14(1):44. doi: 10.3390/plants14010044.
16. Kraujalienė V, Pukalskas A, Venskutonis PR. Biorefining of goldenrod (*Solidago virgaurea* L.) leaves by supercritical fluid and pressurized liquid extraction and evaluation of antioxidant properties and main phytochemicals in the fractions and plant material. J Funct Foods. 2017;37:200-208. doi: 10.1016/j.jff.2017.07.049.
17. Malićanin M, Karabegović I, Đorđević N, Mančić S, Stojanović SS, Brković D, Danilović B. Influence of the extraction method on the biological potential of *Solidago virgaurea* L. essential oil and hydrolates. Plants (Basel). 2024 Aug 7;13(16):2187. doi: 10.3390/plants13162187.
18. Fursenco C, Calalb T, Uncu L. The phytochemical profile of *Solidago* species from the Republic of Moldova flora. In: 20th International Symposium and Summer School on Bioanalysis, 2022 Jun 24-30; Pécs, Hungary: Book of abstracts. Pécs; 2022. p. 38.
19. Fursenco C. Cercetarea compuşilor chimici din produsele vegetale şi extractive ale speciilor genului *Solidago* din flora Republicii Moldova = Research of chemical compounds from vegetal and extractive products of *Solidago* species from the Republic of Moldova flora. In: [Proceedings of the 10th Congress of pharmacists from the Republic of Moldova with international participation "Faculty of Pharmacy – six decades of innovation and progress"; 2024 Nov 22-23; Chisinau: Abstract book]. Chişinău; 2024. p. 310-312. Romanian, English.
20. Nistreanu A, Calalb T. Analiza farmacognostică a produselor vegetale medicinale. [Pharmacognostic analysis of medicinal plant products]. Chişinău: Medicina; 2016. 316 p. Romanian.
21. Calalb T, Fursenco C, Ionita O, Ghendov V. The morpho-anatomical study of *Solidago virgaurea* L. spe-

cies from the flora of the Republic of Moldova. East Eur Sci J. 2018;2(30):4-13.
22. Fursenco C, Calalb T, Uncu L. Comparative microscopic study of *Solidago* species from the Republic of Moldova flora. Mold Med J. 2020;63(3):16-21. doi: 10.5281/zenodo.3958433.
23. Elshafie HS, Gruľová D, Baranová B, Caputo L, De Martino L, Sedlák V, et al. Antimicrobial activity and chemical composition of essential oil extracted from *Solidago canadensis* L. growing wild in Slovakia. Molecules. 2019;24(7):1206. doi:10.3390/molecules24071206.
24. Oniga I, Benedec D, Hanganu D, Toiu A. Metode de analiză farmacognostică a produselor vegetale medicinale. [Methods of pharmacognostic analysis of medicinal plant products]. Vol. 2. Cluj-Napoca: Editura Medicală Universitară "Iuliu Haţieganu"; 2023. 205 p. Romanian.
25. Babushok VI, Linstrom PJ, Zenkevich IG. Retention indices for frequently reported compounds of plant essential oils. J Phys Chem Ref Data. 2011;40(4):043101. doi: 10.1063/1.3653552.
26. Shanaida M, Golembiovska O, Hudz N, Wieczorek PP. Phenolic compounds of herbal infusions obtained from some species of the Lamiaceae family. Curr Issues Pharm Med Sci. 2018;31(4):194-199. doi: 10.1515/cipms-2018-0036.
27. Ion VA, Nicolau F, Petre A, Bujor OC, Badulescu L. Variation of bioactive compounds in organic *Ocimum basilicum* L. during freeze-drying processing. Sci Pap Ser B Hortic. 2020;64(1):397-404.
28. Pravbivtseva OE, Kurkin BA. Issledovaniia po obosnovaniiu novykh podkhodov k standartizatsii syr'ia i preparatov zveroboia prodyriavlennogo [Studies on the justification of new approaches to the standardization of St. John's wort raw materials and preparations]. Khim Rastit Syrya. 2008;(1):81-6. Russian.
29. Du M, Guo S, Zhang J, Hu L, Li M. Quantitative analysis method of the tea saponin. Open J For. 2018;8(1):61-7. doi: 10.4236/ojf.2018.81005.
30. Trineeva OV, Slivkin AI. Validatsiia metodiki opredeleniia karotinoidov v plodakh oblepikhi razlichnykh sposobov konservatsii. [Validation of the methodology for the deter- mination of carotenoids in sea buckthorn fruits of different preservation methods]. Vestnik VGU. Seriia: Khimiia. Biologiia. Farmatsiia. 2016;(2):145-151. Russian.
31. Chedea VS, Pop RM. Total polyphenols content and antioxidant DPPH assays on biological samples. In: Watson RR, editor. Polyphenols in plants. Cambridge (MA): Academic Press; 2019. p. 169-183.
32. Patil KR, Mahajan UB, Unger BS, Goyal SN, Belemkar S, Surana SJ, et al. Animal models of inflammation for screening of anti-inflammatory drugs: implications for the discovery and development of phytopharmaceuticals. Int J Mol Sci. 2019 Sep 5;20(18):4367. doi: 10.3390/ijms20184367.
33. Balouiri M, Sadiki M, Ibnsouda SK. Methods for in vitro evaluating antimicrobial activity: a review. J Pharm Anal. 2016 Apr;6(2):71-79. doi: 10.1016/j.jpha.2015.11.005.
34. Fursenco C, Calalb T, Coretchi I, Ion V, Bujor O, Spînu S, et al. Pharmacognostic and pharmacological evaluation of *Solidago* species from the flora of the Republic of Moldova. In: One Health Student International Conference; 2024 Dec 4-6; Bucharest, Romania: Book of Abstracts. Bucharest; 2024.
35. Rozlovan D, Fursenco C. The total content of hydroxycinnamic acids in *Solidago virgaurea* L. species. In: MedEspera: 9th International Medical Congress for Students and Young Doctors; 2022 May 12-14; Chisinau, Republic of Moldova: Abstract book. Chişinău; 2022. p. 333.
36. Fursenco C. Studiul chimic comparativ al saponozidelor din speciile genului *Solidago*. [Comparative chemical study of saponosides from species of the genus *Solidago*]. In: [Proceedings of the Scientific conference "Perspectives in research of pharmaceutical products of synthetic and natural origin"; 2021 May 14; Chisinau, Republic of Moldova: Abstract book. Chişinău; 2021. p. 64-65. Romanian.
37. Fursenco C. The antioxidant activity of *Solidago* L. species from the Republic of Moldova flora. In: Phytochemical Society of Europe meeting "Natural products in drug discovery and development – advances and perspectives"; 2022 Sep 19-22; Iasi, Romania: Abstract Book. Iasi; 2022. p. 153.
38. Nkuimi Wandjou JG, Quassinti L, Gudžinskas Z, Nagy DU, Cianfaglione K, Mbramucci. Chemical composition and antiproliferative effect of essential oils of four Solidago species (*S. canadensis, S. gigantea, S. virgaurea* and *S.×niederederi*). Chem Biodivers. 2020;17(11):e2000685. doi: 10.1002/cbdv.202000685.
39. Hrytsyk Y, Koshovyi O, Lepiku M, Jakštas V, Žvikas V, Matus T, et al. Phytochemical and Pharmacological Research in Galenic Remedies of *Solidago canadensis* L. Herb. Phyton-Int J Exp Bot. 2024;93(9):2303-2315. doi: 10.32604/phyton.2024.055117.
40. Kiełtyk P, Mirek Z. Taxonomy of the *Solidago virgaurea* group (Asteraceae) in Poland, with special reference to variability along an altitudinal gradient. Folia Geobot. 2014;49:259-282. doi: 10.1007/s12224-013-9180-2.
41. Likhanov A, Oliinyk M, Pashkevych N, Churilov A, Kozyr M. The role of flavonoids in invasion strategy of *Solidago canadensis* L. *Plants*. 2021;10(8):1748. https://doi.org/10.3390/plants10081748.
42. Radušiene J, Marksa M, Karpavičiene B. Assessment of Solidago×niederederi origin based on the accumulation of phenolic compounds in plant raw materials. Weed Sci. 2018;66(3):324-30. doi: 10.1017/wsc.2018.8.
43. Horváth G, Molnár P, Farkas Á, Szabó L, Turcsi E, Deli J.

Separation and identification of carotenoids in flowers of *Chelidonium majus* L. and inflorescences of *Solidago canadensis* L. Chromatographia. 2010;71(Suppl 1):S103-S108. https://doi.org/10.1365/s10337-010-1510-4.

44. Shelepova O, Vinogradova Y, Vergun O, Grygorieva O, Brindza J. Invasive *Solidago canadensis* L. as a resource of valuable biological compounds. Potravinarstvo Slovak J Food Sci. 2019;13(1):280-286. doi: 10.5219/1125.
45. Laurençon L, Sarrazin E, Chevalier M, Prêcheur I, Herbette G, Fernandez X. Triterpenoid saponins from the aerial parts of *Solidago virgaurea* alpestris with inhibiting activity of *Candida albicans* yeast-hyphal conversion. Phytochemistry. 2013 Feb;86:103-11. doi: 10.1016/j.phytochem.2012.10.004.
46. Koshovyi O, Hrytsyk Y, Perekhoda L, Suleiman M, Jakštas V, Žvikas V, Grytsyk L, Yurchyshyn O, Heinämäki J, Raal A*. Solidago canadensis* L. herb extract, its amino acids preparations and 3D-printed dosage forms: phytochemical, technological, molecular docking and pharmacological research. Pharmaceutics. 2025;17(4):407. doi: 10.3390/pharmaceutics17040407.
47. Melzig M, Löser B, Bader G, Papsdorf G. European goldenrod as an anti-inflammatory drug: investigations into the cyto- and molecular pharmacology for a better understanding of the anti-inflammatory activity of preparations from *Solidago virgaurea*. Z Phytother. 2000;21:67-70.
48. Abdel Motaal A, Ezzat SM, Tadros MG, El-Askary HI. In vivo anti-inflammatory activity of caffeoylquinic acid derivatives from *Solidago virgaurea* in rats. Pharm Biol. 2016 Dec;54(12):2864-2870. doi: 10.1080/13880209.2016.1190381.
49. Strehl E, Schneider W, Elstner EF. Inhibition of dihydrofolate reductase activity by alcoholic extracts from *Fraxinus excelsior, Populus tremula* and *Solidago virgaurea.* Arzneimittelforschung. 1995;45(2):172-3.

MJHS Moldovan Journal of Health Sciences
REVISTA DE ȘTIINȚE ALE SĂNĂTĂȚII DIN MOLDOVA

AUTHORS STATEMENT FOR PUBLICATION

Manuscript title:

Corresponding author's full name, e-mail address and tel.:

Please note that all contributing authors are obligated to sign *Authors statement for publication* form otherwise the manuscript will not be published.

Please fill in the table below according to following:

- list the authors in order in which they are stated in manuscript,
- each author should sign this document (on designated place in the table). By signing this form authors take full responsibility for all statements it contains.

No.	Author's full name	Author's signature	Date
1.			
2.			
3.			
4.			
5.			
6.			
7.			

AUTHORSHIP STATEMENT:

According to International Committee of Medical Journal Editors (ICMJE): "An author is considered to be someone who has made substantive intellectual contributions to a published study, takes responsibility and is accountable for what is published. ***All persons listed as authors in the manuscript must meet ALL of the following four criteria for authorship****" (available at: https://www.icmje.org/recommendations/browse/roles-and-responsibilities/defining-the-role-of-authors-and-contributors.html)*

Please fill the table with the initials of each author (e.g., AB for Adrian Belîi) regarding authors contribution to specific component of research. The initials of each author must appear at least once in each of the four criteria below:

Criteria	Component of the research	Author's initials
1.	substantial contribution to conception and design of the work	
	substantial contribution to acquisition of data	
	substantial contribution to analysis and interpretation of data	
2.	drafting the article	
	critically reviewing the article for important intellectual content	
3.	final approval of the version to be published	
4.	taking responsibility and being accountable for all aspects of the work	

All persons who have made substantial contributions to the work (technical editing, writing assistance, general administrative support, financial and material support) **but do not meet all four criteria for authorship** are listed in *Acknowledgments* section and have given us their written permission to be named.

☐ Yes
☐ No
☐ We have not received substantial contributions from non-authors.

ORIGINALITY OF THE WORK STATEMENT:

Editorial board of the Moldovan Journal of Health Sciences strongly promotes research integrity and aims to prevent any type of scientific misconduct according to Committee on Publication Ethics (COPE) flowcharts. (available at: https://publicationethics.org/guidance/Flowcharts)

Please thick the box if the following statements are correct to the best of your knowledge:

☐ the manuscript is not previously published in the same or very similar form in other journal (previous publishing does not apply to abstract or poster presentations at a professional meeting)
☐ the manuscript is not currently under consideration in other journals (that does not apply for manuscripts that have been rejected by other journals)

RESEARCH ETHICS:

According to International Committee of Medical Journal Editors (ICMJE), the research project that involves human subjects must be conducted in accordance with the Helsinki Declaration and approved by the independent local, regional, or national review body or ethics committee.

Ethical approval

Reported research was approved by institutional/national ethics committee:

☐ Yes
☐ No
☐ Not applicable

If yes, please state the name of the approving ethics committee, the protocol number and the date of evaluation: _____

If no, please provide further details: _____

Informed consent

According to International Committee of Medical Journal Editors (ICMJE): „Patients have a right to privacy that should not be violated without informed consent. Identifying information, including names, initials, or hospital numbers, should not be published in written descriptions, photographs, or pedigrees unless the information is essential for scientific purposes and the patient (or parent or guardian) gives written informed consent for publication." (available at: https://www.icmje.org/icmje-recommendations.pdf)

The appropriate informed consent was obtained from all research participants:

☐ Yes
☐ No
☐ Not applicable

If no, please explain: _____

CONFLICT OF INTEREST STATEMENT:

All authors have disclosed all relationships/activities/interests that are related to the content of this manuscript by completing the ICMJE Disclosure Form.

☐ Yes
☐ No

☐ Provide the statement: _____

OR

☐ Nothing to declare.

Date (dd/mm/yyyy) _____

Corresponding author's signature _____

Please, send this filled and scanned form to: editor.mjhs@usmf.md

MJHS Moldovan Journal of Health Sciences
REVISTA DE ȘTIINȚE ALE SĂNĂTĂȚII DIN MOLDOVA

[Revised January, 2025]

GUIDE FOR AUTHORS

Moldovan Journal of Health Sciences is an open access, double blind peer reviewed medical journal, published quarterly. The journal accepts for publication **original research papers**, **review articles**, **case reports**, **letters to the editor**, **In memoriam** and **book reviews**.

The *Moldovan Journal of Health Sciences* follows the ***Recommendations for the conduct, reporting, editing, and publication of scholarly work in medical journals*** set out by the **International Committee of Medical Journal Editors (ICMJE)** and publication ethics practices suggested by the **Committee on Publication Ethics (COPE)**.

GENERAL GUIDELINES

- The manuscripts should be written in **English**;
- Each manuscript must be accompanied by *Authors statement for publication form* signed by all authors;
- The manuscript, including the title page, abstract and keywords, main text, references, figure captions, and tables should be typed in Times New Roman 12-point size font and 1,5 line spacing, with 2 cm margins all around and saved as one file;
- Each figure should be submitted also as separate file in one of the following formats: ".jpeg", ".tiff", ".eps", ".ppt", ".pptx". Scanning resolution should be at least 300 dpi;
- Written permission from the copyright owners must be obtained to reproduce the figure or other material published before, and the original source should be cited in the figure caption or table footnote;
- Use only standard abbreviations and be sure to explain all of them the first time they are used in the text;
- Use System International (SI) measurements;
- Use generic names for drugs, devices and equipment. When brand-names are mentioned in the manuscript, the complete name and location of the manufacturer must be supplied;
- References should be numbered in the order in which they appear in the text. At the end of the article the full list of references should follow the Vancouver style.

MANUSCRIPT SUBMISSION

Manuscripts must be submitted in electronic version to the e-mail: editor.mjhs@usmf.md.

A submitted manuscript should be accompanied by *Authors statement for publication form* signed by all authors (a template is provided by editor).

The corresponding author must ensure that all authors have disclosed all relationships/activities/interests that are related to the content of the manuscript by completing the **ICMJE Disclosure Form**. The summarized statement regarding Conflict of interest must be provided in *Authors statement for publication form* and in the Title page.

The corresponding author holds full responsibility for the submission and correspondence with the editor during the peer-review and publication process. All correspondence, including notification of the Editor's decision and requests for revisions, will be made by e-mail.

MANUSCRIPT ORGANIZATION

Manuscripts should be organized as follows. Instructions for each element appear below the list.

TITLE PAGE	> Article title / Short title > Authors information (full names, academic titles, ORCIDs, affiliations) > Corresponding author's contact details > Authors' contributions > Acknowledgments and funding > Conflict of interest > Article highlights > Word count (for Main text and Abstract)
ABSTRACT AND KEYWORDS	> Structured abstract > Keywords > Clinical trial registration information
MAIN TEXT AND REFERENCES	> Introduction > Materials and methods > Results > Discussion > Conclusions > References
TABLES AND FIGURES	> Tables are inserted immediately after the first paragraph in which they are cited > Figure captions are inserted immediately after the first paragraph in which the figure is cited. Figures should be submitted also as separate files.

TITLE PAGE. *Moldovan Journal of Health Sciences* adheres to a **double-blinded peer-review policy**. The title page must be separated from the main text of the article. **The main text of the article must not include information about the authors**.

> ***Article title*** should be concise, relevant to the content of the manuscript, and reflect the study design (up to 25 words). Abbreviations are not allowed. *Short title* (to be used as a running title) can be a maximum of 8 words.

> ***Author information***. Authors should be listed in order of their contribution to the paper. Members of the research group who do not meet the formal criteria of the authorship, but have had some contribution to the paper, may be mentioned in the "Acknowledgements and funding" section.

Each author's full name, academic titles, the ORCID iD and the affiliation (the full name of department, institution, city and country) should be provided.
Example:
Lilian Șaptefrați, MD, PhD, Professor, **https://orcid.org/0000-0003-2779-718X**, Department of Histology, Cytology And Embryology, *Nicolae Testemitanu* State University of Medicine and Pharmacy, Chisinau, Moldova.
> *Corresponding author's contact details*. Mark the corresponding author with an asterisk and provide in a separate paragraph full contact information, including full name, academic degrees, address (institutional affiliation, city, and country), e-mail address and telephone number.
> *Authors' contributions*. The contributions of all authors must be described, please follow the suggested format: *"HW conceived the study and participated in study design and helped drafting the manuscript. MG performed the processing of specimens and tissue culture methods and drafted the manuscript. TK performed immunofluorescence tests. PN participated in staining and flow-cytometry. AR participated in the study design and performed the statistical analysis. All the authors reviewed the work critically and approved the final version of the manuscript".*
> *Acknowledgements and funding*. People who contributed to the study design, data collection, analysis and interpretation, manuscript preparation and editing, offered general or technical support, contributed with essential materials to the study, but do not meet ICMJE authorship criteria will not be considered as authors, but their contribution will be mentioned in section "Acknowledgements and funding". Also in this section must be specified the sources of work funding. Mention of persons or institutions who have contributed to the work and manuscript can be made only after obtaining permission from each of them.
> A ***Conflict of interest*** statement should summarize all aspects of any conflicts of interest included on the ICMJE form. If there is no conflict of interest, this should also be explicitly stated as „none declared".
> *Article highlights* states the main ideas of the paper: What is not yet known on the issue addressed in the submitted manuscript (described in 1-3 sentences); The research hypothesis (described in 1-2 sentences); The novelty added by manuscript to the already published scientific literature (limited to 1-3 sentences).
> *Word count* for Main body text and Abstract should be provided. The volume of the manuscript text should not exceed 6000 words, and Abstract – 350 words.

ABSTRACT AND KEYWORDS

The *Abstract* should provide the context or background for the study and should state the study's purpose, basic procedures, significant results, main findings, and principal conclusions. The summary text should not exceed 350 words organized according to the following headings: *Introduction, Materials and methods, Results, Conclusions*. These headings may be adapted in the case of theoretical papers and reviews. The abstract should not contain any undefined abbreviations or citations.
Keywords. Immediately after the abstract, provide 4-6 keywords that are representative for the contents of the article. For the selection of keywords, refer to Medical Subject Headings (MeSH) in PubMed (**https://www.ncbi.nlm.nih.gov/mesh/**).
If the article reported the results of a clinical trial, please indicate at the end of the abstract the Name of trial database where registered, unique *clinical trial registration number* and date registered.

MAIN TEXT AND REFERENCES

Original research articles are usually organized according to the IMRAD format: *Introduction, Methods, Results, Discussion,* and *Conclusions.* Other types of articles, such as meta-analyses, case reports, narrative reviews, and editorials may have less structured or unstructured formats.

> Introduction

The Introduction section should: provide a context or background for the study that would allow readers outside the field to understand the purpose and significance of the study; define the problem addressed and explain why it is important; include a brief review of recent literature in the field; mention any relevant controversies or disagreements existing in the field; formulate research hypothesis and present the main and secondary assessed outcomes; conclude with the research' propose and a short comment whether the purpose has been achieved. The Introduction should not contain either results or conclusions.

> Materials and methods

The *Materials and methods* section should present in sufficient details all carried out procedures. Here should be described protocols and supporting information on the used methods. It will include study design, subjects' recruitment procedure, clear description of all interventions and comparisons and applied statistics (*Selection and Description of Participants, Technical Information, Statistics*). The Methods section should be sufficiently detailed such that others with access to the data would be able to reproduce the results. For studies on humans or animals a statement about ethical approval and informed consent of study subjects should be include. Please specify date and number of Ethics Committee (EC) decision, chair of the EC as well as institution within EC is organized.

> Results

Authors must present results logically using text, tables, and figures, giving the main or most important findings first. Results should be explained (not justified or compared in this section) and include fundamental statements related to hypothesis behind the study.

> Discussion

The data should be interpreted concisely without repeating materials already presented in the *Results* section. Describe the impact, relevance and significance of the obtained results for the field. The results are compared with those from previous publications and draw potential future research directions. Discussions should include important interpretations of the findings andresults compared with previous studies. In addition, study limitations and potential bias should be mentioned.

> Conclusions

This section should conclude laconically entire study, and highlight the added-value brought on the studied issue. The conclusions should not provide new information or double (repeat) those presented in the *Results* section.

> References

Moldovan Journal of Health Sciences uses the reference style outlined by the International Committee of Medical Journal Editors (www.icmje.org), also known as "Vancouver style". Example formats are listed below.

In-text reference citations should be numbered consecutively, identified by Arabic numerals in square brackets [ ]. References should be listed at the end of the manuscript and numbered in the order in which they are first mentioned in the text. Every reference cited in the text is also present in the reference list (and vice versa). Journals titles should be abbreviated according to the Index Medicus.

It may be cited only articles orabstracts that have been published and are available through public servers. Personal communications, manuscripts in preparation, and other unpublished data should not be included in the reference list, but may be mentioned in parentheses in the text as "unpublished data" or "unpublished observations", indicating the involved researchers. It is of manuscript authors' responsibility to obtain the permission to refer to unpublished data.

The references in the Cyrillic, Greek, Arabic scripts should be transliterated into Latin script using the ALA-LC Romanization Tables. Non-English titles must be followed by the English translation in square brackets.

All electronic references should include active and available URLs and the access date.

Examples of references

Journal article

Belîi A, Cobâleţchi S, Casian V, Belîi N, Severin G, Chesov I, Bubulici E. Les aspects pharmacoéconomiques dans la gestion de la douleur périopératoire [Pharmaco-economic aspects of perioperative pain management]. Ann Fr Anesth Reanim. 2012;31(1):60-6. French. doi: 10.1016/j.annfar.2011.09.008.

Book

Razin MP, Minaev SV, Turabov IA. Detskaia khirurgiia [Pediatric surgery]. 2nd ed. Moscow: Geotar-Media; 2020. 696 p. Russian.

Chapter in a book

Steiber AL, Chazot C, Kopple JD. Vitamin and trace element needs in chronic kidney disease. In: Burrowes J, Kovesdy C, Byham-Gray L, editors. Nutrition in kidney disease. 3rd ed. Cham: Humana Press; 2020. p. 607-623.

Conference paper

Ojovan V. Medical rehabilitation of children with type 1 diabetes: medical bioethical and psychosocial aspects. In: MedEspera: 9th International Medical Congress for Students and Young Doctors, 12-14 May 2022, Chisinau, Republic of Moldova: Abstract book. Chișinău; 2022. p. 77.

Website reference

World Health Organization (WHO). Therapeutics for Ebola virus disease [Internet]. Geneva: WHO; 2022 [cited 2022 Sep 5]. Available from: https://www.who.int/publications/i/item/9789240055742

TABLES AND FIGURES

Tables should be numbered consecutively with Arabic numerals, and be cited in text. Tables can be placed either next to the relevant text in the article, or on separate page(s) at the end. Tables must be submited as editable text and not as images. Each table should be completely informative in itself, and the data presented in it do not duplicate the results described elsewhere in the article.

The label "Table 1" and a short descriptive title should be provided above the table. Legends, notes, and any abbreviations used in the table should be explained below the table in a footnote. Applied statistical tests and the type of presented data should be also mentioned. Please follow the example:

Table 1. Intra-anesthetic and immediately post-extubation adverse events

	Experimental Cohort (n=100)	Control Cohort (n=100)	p
Dysrhythmia	6.0%	30%	0.49
Hemodynamic instability	7.0%	1.0%	0.034
Prolonged awakening*	11.0%	4.0%	0.19
PONV post-intubation	8.0%	27.0%	0.007
Strong pain on awakening	17.0%	19.0%	1.0

Note: *Unusually slow awaking, after that cerebral concentration of the anesthetic reach the under hypnotic level.
Used statistical analysis: Fisher's exact test.

Figures (photographs or radiographs, drawings, graphs, bar charts, flow charts, and pathways) should be submitted in a suitable format for print publication. Figures should be either professionally drawn and photographed, or submitted as photographic-quality digital prints. Figures' quality should assure the visibility of details. The following file formats are accepted: ".jpeg", ".tiff", ".eps" (preferred format for diagrams), ".ppt", ".pptx" (figures should be of the size of a single slide), with a resolution of at least 300 dpi.
Figures will be included in the main manuscript, and also submitted as separate files. The file title should include the figure number and an identifiable short title.
Figures should be numbered consecutively according to the order in which they have been cited in the text. Write the label **Fig. 1** and a short descriptive title under the figure. Figure's legend should describe briefly the data shown. Figure's description should not repeat the description in the text of the manuscript. When used symbols, arrows, numbers or letters to describe parts of the figure, explain clearly each one of them in the legend. Explain the internal scale and identify the staining method of the photomicrographs.
If a table or figure has been published before, the authors must obtain written permission to reproduce the material in both print and electronic formats from the copyright owner and submit it with the manuscript. The original source should be cited in the figure caption or table footnote. For example, "Reprinted with permission from Calfee DR, Wispelwey B. Brain abscess. Semin Neurol. 2000;20:357." ("Data from . . ." or "Adapted from . . ." may also be used, as appropriate).

ETHICAL ISSUES & RESEARCH REPORTING GUIDELINES

Definition of Authorship

As stated in the guidelines of the International Committee of Medical Journal Editors (ICJME), all persons listed as authors in the manuscript must meet **ALL of the following criteria** for authorship:

1. substantial contributions to the conception or design of the work; or the acquisition, analysis, or interpretation of data for the work; AND
2. drafting the work or reviewing it critically for important intellectual content; AND
3. final approval of the version to be published; AND
4. agreement to be accountable for all aspects of the work in ensuring that questions related to the accuracy or integrity of any part of the work are appropriately investigated and resolved.

Acknowledgements and funding

All contributors, members of the research group who do not meet the criteria for authorship as defined above should be listed in an acknowledgments section. All financial and material support for the conduct of the research and/or preparation of the article from internal or external agencies, including commercial companies, should be clearly and completely identified.

AI in scientific writing

Authors must disclose the use of Artificial Intelligence or (AI)-assisted technologies in the writing process by adding a statement at the end of their manuscript in the core manuscript file, before the References list. The statement should be placed in a new section entitled „*Declaration of Generative AI and AI-assisted technologies in the writing process"*. For example, *„The author(s) used [AI service/ tool name] in order to [reason]. After using this tool/service, the author(s) reviewed and edited the content as needed and take(s) full responsibility for the content of the publication"*. If there is nothing to disclose, there is no need to add a statement. AI and AI-assisted technologies should not be listed as an author or co-author, or be cited as an author.

Conflict of interest disclosure

All authors must disclose any financial, personal or professional relationships with other people or organizations that could inappropriately influence (bias) their work. Examples of potential conflicts of interest are financial support from, or connections to, pharmaceutical companies, political pressure from interest groups, and academically related issues. If there is no conflict of interest, this should also be explicitly stated as none declared.

Copyright, open access, and permission to reuse

Duplicate publication

Material submitted to *Moldovan Journal of Health Sciences* must be original. Submitted manuscript must not have been previously published elsewhere (except as an abstract or a preliminary report), and must not be under consideration by another journal. Related manuscripts under consideration or in press elsewhere must be declared by authors at the time of submission in the cover letter. Dual publication or redundant publication is unethical. For more details please refer to the COPE guidelines on http://www.publicationethics.org.

Plagiarism

Authors should submit only original work that is not plagiarized, and has not been published or being considered elsewhere. Appropriate softwares may be used by the editorial office to check for similarities of submitted manuscripts with existing literature. If the submitted manuscript violates copyright policies; it can be suspended or dismissed, regardless of the stage of the publishing process.

Copyright license

Reproduction of previously published contents

If the submitted manuscript used or reproduced information/material previously published or copyrighted is the responsibility of the corresponding author to obtain a written permission from the copyright owner and properly cite the original source. In order to maintain transparency, it is recommended to submit the permission, as a copy, along with the manuscript.

Self-Archiving

Authors are encouraged to submit the final version of the accepted, peer-reviewed manuscript to their funding body's archive for public release immediately upon publication and to deposit the final version on their institution's repository. Authors should cite the publication reference and DOI number on any deposited version, and provide a link from it to the published article on the journal's website **https://mjhs.md/archive**.

Research reporting guidelines

Moldovan Journal of Health Sciences adheres to the ethical standards described by the Committee on Publication Ethics (COPE) and the International Committee of Medical Journal Editors (ICMJE). Authors are expected to adhere to these standards. Manuscripts submitted to the journal should conform to the **ICMJE Recommendations** and the following guidelines as appropriate:

- STROBE guidelines for observational studies;
- CONSORT guidelines for clinical trials;
- PRISMA guidelines for systematic reviews and meta-analyses;
- STARD guidelines for diagnostic studies;
- CARE statement for clinical cases;
- SAGER guidelines for reporting of sex and gender information in study design, data analyses, results and interpretation of findings.

Ethical approval and Informed consent

If the research project involves human subjects or animals, authors must state in the manuscript that the study was approved by the Ethics Committee of the institution within which the research work was undertaken (the protocol number and the date of evaluation should be provided). Patients' identifying information should not be published in written descriptions and photographs, unless the information is essential for scientific purposes and the patient gave written informed consent for publication. The authors must include a statement confirming that informed consent was obtained from all identifiable study participants (or that no informed consent was required).

Clinical trial registration

The *Moldovan Journal of Health Sciences* follows the trials registration policy of the ICMJE (www.icmje.org) and considers only trials that have been appropriately registered in a public registry prior to submission. Any research that deals with a clinical trial should be registered with a primary national clinical trial registration site, or other primary national registry sites accredited by the World Health Organization (https://www.who.int/ictrp/network/primary/en/). The clinical trial registration number should be provided at the end of the Abstract.

Data access and responsibility

The corresponding author should indicate that he or she had full access to all the data in the study and takes responsibility for the integrity of the data and the accuracy of the data analysis.

FOR MORE DETAILS, PLEASE CONTACT:

Editor-in-chief: **Serghei Popa**, PhD, university professor
tel: +373 60907799
e-mail: editor.mjhs@usmf.md

SPONDI-LIZ

cremă

Medicament combinat pentru tratament local cu acțiune antiinflamatoare, antitrombotică și analgezică.

STOP durerilor

- articulare
- musculare
- de spate
- post-traumatice

Acesta este un medicament. Citiți cu atenție prospectul.
Dacă apar manifestări neplăcute, adresați-vă medicului sau farmacistului.
Numărul de înregistrare 25299 din 07.02.2019

În anul 2005 preparatul Ekvator a fost premiat cu «Grand Prix Innovational» de către Fondul Investiţional Ungar ca fiind cea mai bună invenţie a anului în Ungaria

Un dublu argument

1. Combinație originală fixă
2. Comod pentru administrare - 1 în zi
3. Minimizarea efectelor adverse

COMPENSAT

Ekvator®

10/5 mg N30

lisinopril + amlodipină

DENUMIREA COMERCIALĂ A MEDICAMENTULUI: EKVATOR 10 mg/5 mg comprimate. EKVATOR 20 mg/10 mg comprimate. **COMPOZIŢIA CALITATIVĂ ŞI CANTITATIVĂ:** EKVATOR 10mg/5mg fiecare comprimat conţine lisinopril 10 mg (sub formă de dihidrat) şi amlodipină 5 mg (sub formă de besilat). EKVATOR 20mg/10mg fiecare comprimat conţine lisinopril 20 mg (sub formă de dihidrat) şi amlodipină 10 mg (sub formă de besilat). **Indicaţii terapeutice:** Tratamentul hipertensiunii arteriale esenţiale la adulţi.Ekvator este indicat ca terapie de substituţie la pacienţii adulţi a căror tensiune arterială este controlată corespunzător prin administrarea asociată de lisinopril şi amlodipină, în aceeaşi doză. **Doze şi mod de administrare:** Doze: Doza recomandată este de un comprimat pe zi. Doza zilnică maximă este de un comprimat. În general, medicamentele care conţin combinaţii de doze fixe nu sunt potrivite pentru iniţierea tratamentului. Ekvator este indicat doar pentru pacienţii a căror doză optimă de întreţinere de lisinopril şi amlodipină a fost stabilită treptat la 10 mg şi respectiv 5 mg. În cazul administrării Ekvator 10 mg / 5 mg - 20 mg şi 10 mg în cazul administrării Ekvator 20 mg/10 mg - 20 mg şi 5 mg în cazul administrării Ekvator 20 mg/5 mg comprimate – respectiv. Dacă este necesară ajustarea dozei, poate fi luată în considerare stabilirea treptată a dozei pentru fiecare component în parte. **Mod de administrare:** Administrare orală, înainte, în timpul sau după masă. **Contraindicaţii:** Legate de lisinopril: Hipersensibilitate la lisinopril sau la oricare alt inhibitor al enzimei de conversie a angiotensinei (ECA); Antecedente de angioedem asociat cu o terapie anterioară cu inhibitori ECA; Angioedem ereditar sau idiopatic; Al doilea şi al treilea trimestru de sarcină. Administrarea concomitentă a Ekvator cu medicamente care conţin aliskiren este contraindicată la pacienţii cu diabet zaharat sau insuficienţă renală (RFG < 60 ml/min şi 1,73 m²) Administrarea concomitentă a tratamentului cu sacubitril/valsartan. Ekvator nu trebuie iniţiat mai devreme de 36 de ore după ultima doză de sacubitril/valsartan. Legate de amlodipină: Hipersensibilitate la amlodipină sau la orice alt derivat al dihidropiridinei; Hipotensiune arterială severă; Şoc (incluzând şoc cardiogen); Obstrucţie a fluxului sanguin de la nivelul ventriculului stâng (de exemplu, stenoză aortică severă); Insuficienţă cardiacă instabilă hemodinamic, după un infarct miocardic acut. **Atenţionări şi precauţii speciale pentru utilizare:** Hipotensiune arterială simptomatică. Hipotensiunea arterială în caz de infarct miocardic acut. Stenoză de valvă aortică şi mitrală, cardiomiopatie hipertrofică. Insuficienţă renală.Hipersensibilitate, angioedem. Reacţii anafilactoide la pacienţi hemodializaţi. Reacţii anafilactoide în timpul aferezei lipoproteinelor cu densitate mică (LDL). Desensibilizare. Pacienţii cărora li s-au administrat inhibitori ai ECA în timpul tratamentului de desensibilizare (de exemplu, cu venin de himenoptere) au prezentat reacţii anafilactoide susţinute. La aceşti pacienţi aceste reacţii au putut fi evitate prin întreruperea temporară a tratamentului cu inhibitori ai ECA, dar au reapărut la readministrarea accidentală a acestor medicamente. Insuficienţă hepatică. Blocarea dublă a sistemului renină-angiotensină-aldosteron (SRAA). Tuse: Hiperkaliemie. Pacienţi cu diabet zaharat. În cazul pacienţilor cu diabet zaharat trataţi cu antidiabetice orale sau cu insulină, trebuie monitorizată strict glicemia în timpul primei luni de tratament cu inhibitor ECA. Legate de amlodipină: Nu au fost stabilite siguranţa şi eficacitatea administrării amlodipinei în criza hipertensivă. Pacienţi cu insuficienţă cardiacă: Utilizarea la pacienţii cu funcţie hepatică deteriorată. Utilizarea la pacienţii vârstnici. Utilizarea în insuficienţă renală. **Reacţii adverse:** În cadrul unui studiu clinic controlat (n=195), frecvenţa de apariţie a reacţiilor adverse nu a fost mai mare la subiecţii trataţi concomitent cu ambele substanţe active decât la subiecţii trataţi în monoterapie. Reacţiile adverse au fost corespunzătoare cu cele raportate anterior pentru amlodipină şi/sau lisinopril. Reacţiile adverse au fost în general uşoare, tranzitorii şi rareori au necesitat întreruperea tratamentului cu Ekvator. Cele mai frecvente reacţii adverse în cazul combinaţiei au fost cefalee (8%), tuse (5%) şi ameţeala (3%). **STATUTUL LEGAL:** cu prescriere medicală. **DEŢINĂTORUL CERTIFICATULUI DE ÎNREGISTRARE:** Gedeon Richter Plc. Gyömrői út 19-21. 1103 Budapest, Ungaria. **NUMĂRUL(ELE) CERTIFICATULUI DE ÎNREGISTRARE:** 10/5 21514 din 22.01.2015, 20/10 22193 din 21.12.2015, **DATA REVIZUIRII TEXTULUI:** februarie 2016.

Informaţii detaliate privind acest medicament sunt disponibile pe site-ul Agenţiei Medicamentului şi Dispozitivelor Medicale (AMDM) http://nomenclator.amed.md/

Acest material publicitar este destinat persoanelor calificate să prescrie, să distribuie şi/sau să elibereze medicamente.

Societatea pe Acţiuni de Tip Deschis Fabrica de Produse Chimice "GEDEON RICHTER" Budapesta, Sucursala Chişinău, str. A. Puşkin, 47/1, bl. A, of.1; Tel./Fax: 022-22-14-49; 022-22-26-71; www.gedeonrichter.md
Pentru mesaje de siguranţă şi informaţii medicale: e-mail: drugsafety.md@gedeonrichter.com sau tel.: (022) 20-21-90.

GEDEON RICHTER